OPTIMAL EXPERIMENTAL DESIGNS FOR THE ESTIMATION OF THERMAL PROPERTIES OF COMPOSITE MATERIALS

An Annual Report
for Contract No. NAG-1-1507

to

NASA Langley Research Center
Hampton, VA

by

Elaine P. Scott
Assistant Professor

and

Deborah A. Moncman
Graduate Research Assistant

Department of Mechanical Engineering
Virginia Polytechnic Institute and State University
Blacksburg, VA 24061-0238

May 5, 1994

Optimal Experimental Designs for the Estimation of Thermal Properties of Composite Materials

by

Deborah A. Moncman

Committee Chairman: Dr. Elaine P. Scott
Mechanical Engineering

(ABSTRACT)

Reliable estimation of thermal properties is extremely important in the utilization of new advanced materials, such as composite materials. The accuracy of these estimates can be increased if the experiments are designed carefully. The objectives of this study are to design optimal experiments to be used in the prediction of these thermal properties and to then utilize these designs in the development of an estimation procedure to determine the effective thermal properties (thermal conductivity and volumetric heat capacity).

The experiments were optimized by choosing experimental parameters that maximize the temperature derivatives with respect to all of the unknown thermal properties. This procedure has the effect of minimizing the confidence intervals of the resulting thermal property estimates. Both one-dimensional and two-dimensional experimental designs were optimized. A heat flux boundary condition is required in both analyses for the simultaneous estimation of the thermal properties. For the one-dimensional experiment, the parameters optimized were the heating time of the applied heat flux, the temperature sensor location, and the experimental time. In addition to these parameters, the optimal location of the heat flux was also determined for the two-

dimensional experiments.

Utilizing the optimal one-dimensional experiment, the effective thermal conductivity perpendicular to the fibers and the effective volumetric heat capacity were then estimated for an IM7-Bismaleimide composite material. The estimation procedure used is based on the minimization of a least squares function which incorporates both calculated and measured temperatures and allows for the parameters to be estimated simultaneously.

dimensional experiments.

Utilizing the optimal one-dimensional experiment, the effective thermal conductivity perpendicular to the fibers and the effective volumetric heat capacity were then estimated for an IM7-Bismaleimide composite material. The estimation procedure used is based on the minimization of a least squares function which incorporates both calculated and measured temperatures and allows for the parameters to be estimated simultaneously.

Table of Contents

List of Tables

List of Figures

Nomenclature

A	Scalar used in the Box-Kanemasu method
$\overline{b}_i$	Mean of the parameter estimates
$\boldsymbol{b}$	Estimated parameter vector containing effective thermal conductivity (W/m°C) and effective volumetric heat capacity (MJ/kg°C) values
C_{eff}	Effective volumetric heat capacity (MJ/m^3°C)
c_p	Specific Heat (J/kg°C)
D	Determinant of $\boldsymbol{X}^T\boldsymbol{X}$
$d_{i,j}$	Time average of the sensitivity coefficients (i,j = 1,2)
D_{max}	Maximum determinant value
G	Scalar Used in the Box-Kanemasu method
h	Scalar interpolation function used in the Box-Kanemasu method
$k_{x\text{-}eff}$	Effective thermal conductivity in the x direction (W/m°C)
$k_{y\text{-}eff}$	Effective thermal conductivity in the y direction (W/m°C)
k_f	Thermal conductivity of the fibers (W/m°C)
k_m	Thermal conductivity of the matrix (W/m°C)
L_p	Thickness on the y axis where the heat flux is applied (m)
L_x	Thickness in the x direction (m)
L_y	Thickness in the y direction (m)
L_{xy}	Ratio of the composite thicknesses (L_x/L_y)

m	Counter on a summation
M	Number of temperature sensors used
n	Counter on a summation
N	Number of experimental temperature measurements
p	Number of parameters estimated
$\boldsymbol{P}$	Vector equal to $(\boldsymbol{X}^T\boldsymbol{X})^{-1}$
q_x	Heat flux (W/m^2)
s	Standard deviation of the parameter estimates
S	Least Squares function
S_o	Sum of squares value at zero
S_α	Sum of squares value at α
t	Time (sec)
t_h	Total heating time (sec)
$t_{h,opt}$	Optimal heating time (sec)
t_N	Total experimental time (sec)
T	Temperature (°C)
T_i	Initial temperature (°C)
T_{max}	Maximum temperature between the beginning and end of the experiment (°C)
$T_{o,x}$	Temperature at the boundary where $x = L_x$ (°C)
$T_{o,y1}$	Temperature at the boundary where $y = 0$ (°C)

$T_{o,y2}$	Temperature at the boundary where $y = L_y$ (°C)
$\boldsymbol{T}$	Calculated temperature vector (°C)
V	Measured thermocouple voltages (volts)
V_f	Fiber volume fraction
V_m	Matrix volume fraction
x	Position along the x axis (m)
$\boldsymbol{X}$	Sensitivity coefficient matrix
$X^+_{k_{x\text{-}eff}}$	Sensitivity coefficient for the effective thermal conductivity in the x direction
$X^+_{C_{eff}}$	Sensitivity coefficient for the effective volumetric heat capacity
$X^+_{k_{y\text{-}eff}}$	Sensitivity coefficient for the effective thermal conductivity in the y direction
y	Position along the y axis (m)
$\boldsymbol{Y}$	Measured temperature vector (°C)
α	Scalar used in the Box-Kanemasu method
α_{eff}	Effective thermal diffusivity (m^2/s)
$\alpha_{x\text{-}eff}$	Thermal diffusivity in the x direction (m^2/s)
$\alpha_{y\text{-}eff}$	Thermal diffusivity in the y direction (m^2/s)
β_n	Eigenvalues
$\underline{\beta}$	Parameter vector containing thermal conductivity (W/m°C) and volumetric heat capacity (MJ/m^3°C) values

κ_{xy}	Effective thermal conductivity ratio ($k_{y\text{-}eff}/k_{x\text{-}eff}$)
ρ	Density (kg/m^3)
Δt	Time step size
∇	Matrix derivative operator

Superscripts

k	Iteration number
T	Transpose
+	Dimensionless

Chapter 1

Introduction

A composite material is composed of two or more materials joined together to form a new medium with properties superior to those of its individual constituents. There are many potential advantages of these materials including higher strength-to-weight ratios, better corrosion and wear resistance, and an increased service life over standard metals. Because of these improved characteristics, the use of composite materials has become quite extensive in the past twenty years, with the most widespread use being in the aerospace and aeronautic industries for the design of aircraft structural components. For example, composites are used in applications such as aircraft tail sections, wing skins, and brake linings. The F-111 horizontal stabilizer was the first flight-worthy composite component and in 1986, an all-composite airplane (the Voyager), set a world record in nonstop flight around the world, revealing amazing toughness and rigidity against harsh environmental conditions. However, the use of composites is not limited to the aerospace industry. Composite technology has also gained the attention of the automotive, tooling and sporting goods industries. Everything from car bodies and brake linings to tennis

rackets, golf clubs, bicycles, and fishing rods have been successfully manufactured from composite materials.

Composites are typically classified according to their reinforcement forms; these include particulate, fiber, laminar, flake, and filled/skeletal (Vinson and Sierakowski, 1987). Fiber-reinforced composites can be further classified as continuous or discontinuous. The major types of reinforcing fibers used in composites include glass, carbon/graphite, organic, boron, silicon carbide and ceramic fibers, while the major matrix resins consist of epoxy, polyimide, polyester, and thermoplastic, with epoxy resins being the most versatile of the commercially available matrices. The composite materials focused on in this study consist of continuous carbon fiber-epoxy matrix combinations.

With the increased use of composite materials in aerospace structures and other applications, it is important that the properties of these advanced materials be known for design purposes. Many studies on the mechanical properties of composites have been conducted; however, limited analyses have been made regarding the thermal properties. Knowledge of the thermal properties becomes important when the composite is subjected to a non-isothermal environment which creates thermal loads on the component. These thermal loads induce temperature variations within the structure, which in turn results in the development of thermal stresses and possible structural failure. In order to accurately predict these thermal stresses and prevent component damage, the temperature response of the structure must first be known. However, to determine this response, the thermal properties of the composite sample, which can be thermally or directionally dependent, are required. The prediction of these thermal properties has provided the motivation for

this study. This information will then aid designers in estimating thermal stresses existing in a structural component and in turn, allow them to prevent component failure.

1.1 Goals and Objectives

The main goal of this research is to predict the thermal properties of composite materials. This prediction requires temperature measurements, and therefore, experiments must be conducted. The overall objectives of this study are to

1) develop optimal experimental designs to be used in the prediction of these thermal properties

and

2) utilize these optimal designs in the development of an estimation procedure to determine the effective thermal properties, namely the thermal conductivity and volumetric heat capacity.

Optimal experiments were designed for both isotropic and anisotropic composite materials by selecting optimal experimental parameters that maximize the sensitivity of the temperature response with respect to changes in the unknown thermal properties. An isotropic material has identical properties in every direction while materials exhibiting directional characteristics are called anisotropic. For the anisotropic composite material, the effective thermal conductivity both parallel and perpendicular to the fiber axis direction can be estimated. This optimization procedure was performed because it increases the accuracy in the resulting thermal property estimates by minimizing the

confidence intervals of the estimated parameters.

The experimental designs that were optimized not only depend on the boundary conditions used, but also on what variability is permitted. An imposed heat flux at one boundary, resulting in conductive heat transfer through the composite sample, is required in the design to allow for the simultaneous estimation of the thermal properties. Therefore, optimal experimental parameters, such as the duration of the applied heat flux, should be determined. The optimal experimental parameters determined for the isotropic case include the heating time, sensor location, and experimental duration. For the anisotropic case, two different experimental designs were used. Both designs had a uniform heat flux applied over a portion of one boundary. However, this portion varied for the two configurations. Therefore, in addition to the parameters optimized for the one-dimensional case, the optimal position of the heat flux was also found in the two-dimensional analysis.

Utilizing the optimal experimental design determined for the isotropic composite material, the effective thermal conductivity perpendicular to the fiber axis and the effective volumetric heat capacity were then estimated for a composite consisting of continuous IM7 graphite fibers and a Bismaleimide (5260) epoxy matrix. Note that this is actually an anisotropic composite material; however, since the thermal conductivity is only estimated in one direction, this is equivalent to using an isotropic material. The estimation procedure used in this investigation was the Gauss linearization method and is based on the minimization of a least-squares function, containing experimental and calculated temperatures, with respect to the unknown thermal properties. This method not

only allows for the effective thermal conductivity and effective volumetric heat capacity to be estimated simultaneously, but also enables validation of the transient heat conduction equation.

Chapter 2

Literature Review

2.1 Determination of Thermal Properties of Composite Materials

This chapter summarizes the present state of knowledge pertaining to the estimation of thermal properties of composite materials. Due to their anisotropic nature, the estimation of the thermal properties of composites has proved to be a challenging task. This estimation problem is further complicated because a composite consists of at least two different materials, each with different thermal properties. Many methods, both experimental and analytical, have been proposed for estimating these properties with the thermal conductivity being most frequently estimated. In the following two sections, these estimation techniques are reviewed, describing the methods and procedures used. The experimental techniques utilized include both steady-state and transient heat conduction processes, while the analytical methods estimate the effective thermal properties using proposed mathematical models. These models assume prior knowledge of the thermal properties of the fiber and matrix themselves, along with the void fraction

of the fibers. The third section describes a minimization procedure based on the Gauss method used to estimate the thermal properties. The advantage of this procedure over previous techniques is that it allows thermal properties, such as thermal conductivity and volumetric heat capacity, to be estimated simultaneously. The thermal properties are found by minimizing an objective function containing calculated and measured temperatures. The last section discusses optimal experimental designs to be used with this minimization procedure which provide more accurate parameter estimates. Optimal experimental parameters to be used in these designs are found by maximizing the sensitivity of the temperature response with respect to changes in the thermal properties.

2.1.1 Experimental Determination of the Thermal Properties of Composite Materials

Experimental methods have been one of the main areas for determining the thermal properties of composite materials. These methods can be classified as either steady-state or transient. Ziebland (1977) described some steady-state experiments used to calculate the thermal conductivity that used both absolute measurements, where the thermal conductivity is determined directly from the measured quantities, and relative methods, in which the thermal conductivity is determined by reference to a substance of known thermal conductivity. The absolute methods are accurate but require expensive instrumentation and are generally time consuming and thus, expensive. One steady-state, absolute technique frequently used is the guarded hot-plate method. In this method, the specimen is heated by a hot metal plate attached to it and the resulting temperature is measured at the interface to estimate the thermal conductivity (Ziebland, 1977). Although

this method is quite accurate, substantial time is required to reach steady-state; therefore, the experiment is both expensive and time consuming.

Dickson (1973) has also described a simple steady-state method for measuring the thermal conductivity of insulation materials using heat flow sensors. This method requires the measurement of a heat flux and the temperature difference across a test specimen of known thickness. Penn, et al. (1986) extended this method to composite materials and developed a thermal conductivity measuring apparatus that uses heat flow sensors. This steady-state device used smaller sample sizes and as a result, reached thermal equilibrium in only a few hours. In addition, Harris, et al. (1982) used a two plate apparatus to experimentally determine the thermal conductivities of Kevlar 49 fibers in directions parallel and perpendicular to their lengths as functions of temperature, while Havis, et al. (1989) experimentally investigated the effect of fiber direction on the effective thermal conductivity of fibrous composite materials.

The evaluation of thermal conductivity from steady-state experiments is mathematically simple but frequently lengthy; it was for this reason that transient methods were developed. One transient method used to determine the thermal diffusivity, heat capacity, and thermal conductivity of materials is the laser-flash method which was first introduced by Parker, et al. (1961). In this method, the front face of a small sample is subjected to a short, radiant energy pulse. The resulting temperature rise on the rear surface of the sample is measured and the thermal diffusivity is then determined from the time required for the back surface to reach one half of the maximum temperature rise. This can be mathematically expressed as

$$\alpha = \frac{KL^2}{t_{1/2}} \tag{2.1}$$

where K is the constant corresponding to one-half of the maximum temperature rise, L is the sample thickness, and $t_{1/2}$ is the time taken for the back surface to reach one-half of the maximum temperature rise. The heat capacity is found from the maximum temperature rise of the specimen, and the thermal conductivity is then calculated from the product of the thermal diffusivity, heat capacity, and density ($k=\alpha\rho c_p$). The advantage of this technique over steady-state methods is that smaller sample sizes and shorter experimental durations could be used. Taylor, et al. (1985) studied the applicability of the laser-flash technique for measuring the thermal diffusivity of fiber-reinforced composites and found that the technique is appropriate for examining the transient heat flow in these materials.

Lee and Taylor (1975) used the laser-flash method along with an absolute method to directly measure the thermal diffusivity of graphite/carbon fiber in unidirectionally fiber-reinforced composites. The thermal diffusivity of graphite fiber-reinforced composites (Morganite II and Thronal 50 S) was also calculated from the effective thermal conductivity of composite samples measured by an absolute method. Taylor and Kelsic (1986) also used the laser-flash method to measure the thermal diffusivity of unidirectional fiber-reinforced composites. They then investigated the effects of the thermal conductivity ratio, fiber fraction, fiber orientation, and specimen length on the thermal diffusivity. Their results indicated that the fiber-matrix thermal conductivity ratio

was the major factor governing the thermal behavior followed by the fiber volume fraction. In addition, the thermal diffusivity of both silica and carbon fiber-phenolic resin composites was measured as a function of temperature using the laser-flash technique (Mottram and Taylor, 1987a). This work was extended (1987b) and the effective thermal conductivity parallel and perpendicular to the fiber axis was calculated using specific heat and density data.

The composite method was used by Brennan, et al. (1982) to measure the thermal conductivity and diffusivity of silicon carbide fibers. This method consists of measuring the thermal diffusivity of the composite and the matrix itself (without the fibers) using the laser-flash technique. From the definition of thermal diffusivity and the Rule-of-Mixtures (discussed in the next section), the thermal properties of the fiber can then be determined. It was found that the accuracy of the thermal conductivity values determined for the fibers could be increased by using a matrix material with a thermal conductivity as close as possible to that of the fibers. Furthermore, for this method to yield reliable data, it is essential that the scale of the microstructure and the size of the composite sample behave as a continuum in its transient response (Brennan, et al., 1982).

The laser-flash method also served as the basis for the techniques developed by Welsh, et al. (1987, 1990). In these studies, a pulsed heat flux was imposed on the surface of a material and the resulting thermal response at the same surface was then recorded. This method differs from the traditional laser-flash method in that the temperature response is observed at the heated surface rather than on the surface opposite to the flux. One disadvantage of this method is that the heat capacity and thermal

conductivity cannot be estimated independently, only the thermal diffusivity can be determined.

In addition, Fukai, et al. (1991) also conducted transient experiments using a periodic hot-wire heating method to simultaneously estimate the thermal conductivity and diffusivity. In this method, the thermal conductivity and diffusivity were determined from the amplitude and phase lag of the temperature response. The calculated properties agree well with those measured by conventional methods. Beck and Al-Araji (1974) also used a transient experiment to estimate thermal conductivity and volumetric heat capacity independently.

2.1.2 Mathematical Determination of the Thermal Properties of Composite Materials

Mathematical models that are functions of the components of a composite have also been used to determine the effective thermal properties, particularly thermal conductivity. These models are based on the original theories by Maxwell and Rayleigh (Hasselman and Johnson, 1987), with the effective properties being direct functions of the thermal properties of the constituents, namely the fiber and the matrix. Therefore, it is assumed that the thermal properties of the matrix and fiber are known, along with the void fraction of the fibers. Typically, results of the mathematical model approach are expressed as the ratio of the effective conductivity of the composite to the matrix conductivity. This ratio depends on the ratio of the volume of the fiber to the total volume and the fiber-matrix conductivity ratio (Han and Cosner, 1981). Hasselman (1987) also found that if an interfacial thermal barrier resistance was present in a

composite system, the effective thermal conductivity not only depends on the volume fraction of the fibers but also on the fiber size.

One mathematical model, known as the Rule-of-Mixtures, to describe the effective thermal conductivity (k_{eff}) of a composite with heat flow parallel to the axis of the fiber is given by

$$k_{eff} = k_f V_f + (1 - V_f)k_m \tag{2.2}$$

where k_f is the thermal conductivity of the fibers, k_m is the thermal conductivity of the matrix, and V_f is the fiber volume fraction.

A unit-cell approach was presented by Ziebland (1977) to describe the thermal conductivity of a composite perpendicular to the fiber axis; this can be mathematically expressed as

$$k_{eff} = \frac{k_m k_f}{k_m V_f + (1 - V_f)k_f} \tag{2.3}$$

The Rule-of-Mixtures has also been used to calculate the effective thermal diffusivity (Taylor and Kelsic, 1986).

$$\alpha_{eff} = \frac{V_f k_f + V_m k_m}{V_f(\rho c)_f + V_m(\rho c)_m} \tag{2.4}$$

Here, V_m is the matrix volume fraction and $(\rho c)_f$ and $(\rho c)_m$ are the volumetric heat capacities of the fiber and matrix, respectively.

As indicated by Progelhof, et al. (1976), none of the correlations developed accurately predict the thermal properties of all types of composites. A review of additional models used to predict the thermal conductivity of composite systems is given

by Progelhof, et al. (1976). Beran and Silnutzer (1971) presented upper and lower bounds for the effective thermal conductivity of a fiber-reinforced composite in terms of volume fractions and a geometric factor. They found that the effective thermal conductivity could be significantly increased by changing the packing geometry.

In addition to the analytical models used to estimate thermal properties, numerical methods have also been incorporated. Havis, et al. (1989) developed a numerical model using the finite difference method that calculated the effective thermal conductivity of aligned fiber composites when the fiber to matrix conductivity ratio was greater than one. James and Harrison (1992) extended this finite difference method to enable the calculation of the temperature distribution and effective thermal conductivity in composite materials made from anisotropic materials. The standard finite difference equations were modified on a node-by-node basis to take into account anisotropy by local re-orientation of the grid. A finite difference method has also been used by James and Keen (1985) to calculate the thermal conductivity of uniaxial fiber composites. The effective thermal conductivity was then found from the fiber-matrix ratio for a range of fiber volume fractions. This finite difference approach was modified by James, et al. (1987) to calculate the transverse thermal conductivity of continuous fiber composites in which the fibers can be at any angle to the faces of the sample.

In addition to the finite difference approach, finite elements has also been used to predict thermal properties. A finite element analysis of a unit-cell approach was used by Han and Cosner (1981) to measure the effective thermal conductivity of fibrous composites for two different geometrical arrangements of the fibers, rectangular and

staggered. Their analysis assumed prior knowledge of the geometry and thermal conductivities of the composite constituents. Veyret, et al. (1993) also used a finite element formulation to determine the effective thermal conductivity of a composite material using the Laplace equation.

Other methods have also been used to determine thermal properties. One such method is based on the analogy between the response of a unidirectional composite to longitudinal shear loading and to transverse heat transfer (Springer and Tsai, 1967). In this approach, the thermal conductivities of unidirectional composites were predicted by replacing the composite stiffness with the thermal conductivity and the shear modulus ratio with the thermal conductivity ratio of the components in the numerical solutions obtained for the shear loading problem. Ishikawa (1980) used a method that was equivalent to that used by Springer and Tsai. His method was again based on the longitudinal shear problem and measured the thermal conductivities of unidirectional, carbon-epoxy composite systems using an apparatus based on the infra-red radiation method. These analytical results were obtained using a Fourier series analysis and required knowledge of the thermal conductivity of the matrix and the fiber volume fraction.

Another technique presented by Behrens (1968) used the method of long waves to obtain the average thermal conductivity. By calculating the thermal waves damping coefficients in the principal directions of the medium, Behrens was able to develop explicit expressions for the average thermal conductivity. In addition, Mottram (1992) developed design charts to estimate the effective longitudinal and transverse thermal

conductivities of continuous composites using only the fiber and matrix properties.

2.2 Minimization Methods Used for the Estimation of Thermal Properties

An alternate procedure for estimating the thermal properties of composite materials is to use a minimization technique. One minimization technique frequently used is the Gauss linearization method. This is an iterative procedure that involves the minimization of the least squares function. Beck (1963) was the first to use this minimization procedure to estimate thermal properties, namely thermal diffusivity.

2.2.1 Gauss Linearization Method

The Gauss Linearization method, which is based on the least squares function, is one of the more popular estimation methods used. This method not only allows for the simultaneous estimation of the thermal properties, but also enables validation of the transient heat conduction equation. A least squares function, as given by Beck and Arnold (1977), is

$$S = [\boldsymbol{Y} - \boldsymbol{T}(\underline{\beta})]^T[\boldsymbol{Y} - \boldsymbol{T}(\underline{\beta})] \tag{2.5}$$

where $\boldsymbol{Y}$ is a vector containing measured temperatures, $\boldsymbol{T}(\underline{\beta})$ is a vector containing calculated temperatures, and $\underline{\beta}$ is the true parameter vector. Here, the thermal properties are found by minimizing the square of the difference between the measured temperatures and the calculated temperatures. For continuous, transient temperature measurements, the

sum of squares function is minimized with respect to the parameters using the Taylor series approach. This is done by differentiating S with respect to $\underline{\beta}$, setting the resulting equation equal to zero, and then solving for $\boldsymbol{b}$, the estimated parameter vector for $\underline{\beta}$. This method, as described by Beck and Arnold (1977), is one of the simplest and most effective methods for seeking minima which are reasonably well-defined provided that the initial estimates are in the general region of the minimum. However, as explained by Box and Kanemasu (1972), if poor initial estimates for the parameters are used or severe non-linearity in the model exists, this method may cause large oscillations to occur from one iteration to another which leads to non-convergence of the estimates. In an attempt to improve the Gauss method, Box and Kanemasu (1972) modified it by changing the step size used in seeking the minimum. However, this method still did not include a check that the sum of squares function, S, decreased from iteration to iteration. Bard (1970) modified the Box-Kanemasu method to include this check; if the function was not decreasing, the step size is reduced by one-half.

The Gauss estimation procedure was used by Beck when he determined the thermal conductivity and specific heat of nickel simultaneously from transient temperature measurements (1966a) and the thermal contact conductance for both steady-state and transient conditions with a periodic contact (1988). Scott and Beck (1992a) also used this method to simultaneously estimate the thermal conductivity and volumetric heat capacity of carbon composites as functions of temperature and fiber orientation. They found that the thermal properties increased with temperature over the range studied and different stacking orientations resulted in significantly different thermal conductivity values. This

method was also used by Scott and Beck (1992b) to develop an estimation methodology for thermoset composite materials during curing, and by Xu and Bao (1990) to simultaneously estimate thermal conductivity and diffusivity.

Loh and Beck (1991) performed a two-dimensional analysis using this estimation procedure to simultaneously determine the effective thermal conductivities of anisotropic thermoset carbon composites parallel and perpendicular to the fiber axis. They found that the conductivity parallel to the fibers is about seven times higher than transverse to the fibers. In addition, Jurkowski, et al. (1992) used this method to simultaneously estimate the thermal conductivity and thermal contact resistance, as did Garnier, et al. (1992) to simultaneously estimate thermal conductivity and volumetric heat capacity without internal temperature measurements. Instead, temperature measurements were made with thin resistance thermometers and thermocouples. Using finite differences to describe the heat transfer model, Pfahl and Mitchel (1970) used this minimization technique to estimate six thermal properties of a charring carbon-phenolic material. The calculated property values were shown to be in good agreement with values from conventional tests.

2.3 Optimal Experimental Designs

Reliable estimation of thermal properties is extremely important in the utilization of composite materials. The accuracy of these estimates can be increased if the experiments are designed carefully. A carefully designed experiment is one in which there is minimum correlation between the estimated properties, as well as maximum

sensitivity of the measured experimental variables to changes in the properties being estimated (Beck and Arnold, 1977). To create such optimal experimental designs, optimal experimental parameters should first be determined. Many criteria have been proposed for the design of optimal experiments. Beck and Arnold (1977) have listed some of these criteria that are all in terms of the product of the sensitivity coefficients and their transpose ($\boldsymbol{X}^T\boldsymbol{X}$). These coefficients are the derivative of temperature with respect to the parameters being estimated. The proposed criteria are (1) maximization of the determinant of $\boldsymbol{X}^T\boldsymbol{X}$, (2) maximization of the minimum eigenvalue of $\boldsymbol{X}^T\boldsymbol{X}$, and (3) maximization of the trace of $\boldsymbol{X}^T\boldsymbol{X}$. The first method was chosen in this study because it has the effect of minimizing the confidence intervals of the resulting estimates.

This optimization method was used by Beck to determine the optimal experiments for the simultaneous estimation of thermal conductivity and specific heat (1969) and to determine the optimal transient experimental design for estimating the thermal contact conductance (1966b). Taktak, et al. (1991) also used this technique to determine the optimal heating time of an applied heat flux, optimal number of temperature sensors, and the optimal temperature sensor location for the estimation of thermal conductivity and volumetric heat capacity of a semi-infinite and a finite thickness composite material.

As explained, several methods for estimating the thermal properties of composite materials have been proposed. These include both experimental methods and the use of mathematical models. The procedure used in this study to estimate the thermal properties is a modification of the Gauss Linearization method discussed in Section 2.2.1. This method was chosen because it allows for the effective thermal conductivity and effective

volumetric heat capacity to be estimated simultaneously. Also, when using this technique, optimal experiments can be designed resulting in more accurate parameter estimates.

Chapter 3

Theoretical Analysis

In this chapter, the theoretical development used to determine the optimal experimental designs for both isotropic and anisotropic composite materials is presented. The minimization procedure used to estimate the effective thermal conductivity perpendicular to the fiber axis and the effective volumetric heat capacity of a carbon fiber-epoxy matrix composite is also discussed. Recall that this estimation procedure requires both experimental and calculated temperatures. In this study, both exact analytical temperature solutions and numerical temperature solutions were obtained, with the two results being compared to determine the accuracy of the numerical results. The numerical solutions were calculated using a finite element program called Engineering Analysis Language (EAL, Whetstone, 1983). This finite element software was utilized because of the need for future analyses of complex structures, typical in aerospace components, for which exact solutions are either complicated or unavailable.

The first section of this chapter focuses on the mathematical models used to describe one-dimensional (isotropic) and two-dimensional (anisotropic) heat conduction

processes. The second section describes the mathematical details of the parameter estimation technique used in both the exact and numerical analyses to estimate the thermal properties. Note that in both cases, the thermal properties estimated were the effective properties of the composite, not of the individual fiber and matrix components. In the final section, the mathematical criterion used to design optimal experiments, resulting in greater accuracy of the thermal properties, is discussed.

3.1 Mathematical Models Used in Estimating the Thermal Properties of Composite Materials

The formulation of a mathematical model is based on the experimental system being analyzed. In this investigation, formulating mathematical models, either exact or numerical, to describe the conductive heat transfer occurring within the composite sample will allow for the temperature distribution to be calculated. This distribution is required for the estimation of the thermal properties. As mentioned, both one-dimensional and two-dimensional heat conduction analyses have been conducted. The mathematical formulation behind both are defined in the following two subsections.

3.1.1 One-Dimensional Analysis - Isotropic Composite Material

For the isotropic situation, one-dimensional heat conduction through a carbon-epoxy composite was investigated. Note that this isotropic situation is equivalent to analyzing the properties in one direction of an anisotropic composite, as was the case in

this study. The samples used consisted of a thin, flat disk with an aspect ratio such that the two-dimensional effects at the edges can be ignored. One plane boundary had an imposed heat flux perpendicular to the fiber axis, and a known, constant temperature existed at the second boundary, as shown in Fig. 3.1. Since composite materials tend to have low thermal conductivities in directions perpendicular to the fibers, this isothermal boundary condition is readily available. The heat flux boundary condition is required for the independent estimation of the thermal properties. This requirement occurs because this type of boundary condition introduces a new equation into the model which contains only the thermal conductivity and not the volumetric heat capacity. This equation is known as Fourier's Law and is given by

$$q_x = -k_{x\text{-}eff}\frac{\partial T}{\partial x} \tag{3.1}$$

where q_x is the applied heat flux. If this boundary condition was not used, and instead, a constant temperature or insulated condition was used, then only the thermal diffusivity ($k/\rho c_p$) could be estimated.

The formulation to describe this problem can be found from an energy balance and is expressed as

$$\frac{\partial}{\partial x}\left(k_{x\text{-}eff}\frac{\partial T}{\partial x}\right) = C_{eff}\frac{\partial T}{\partial t} \qquad 0 < x < L_x \qquad t > 0 \tag{3.2}$$

where T is temperature, $k_{x\text{-}eff}$ and x are the effective thermal conductivity and position, respectively, in the direction of heat transfer, C_{eff} is the effective volumetric heat capacity

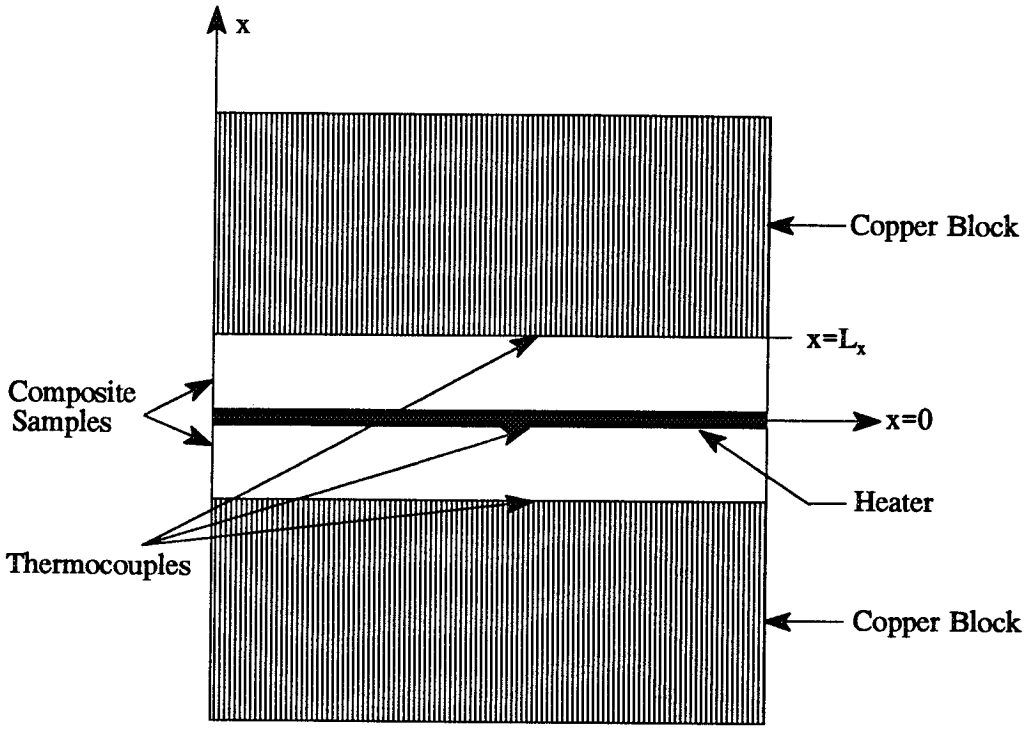

Figure 3.1. Experimental Set-Up for the Estimation of the Effective Thermal Conductivity and Volumetric Heat Capacity of an Isotropic Material.

(or product of density and specific heat), and t is time. The heat flux and constant temperature boundary and initial conditions can be described as

$$-k_{x-eff}\frac{\partial T}{\partial x} = q_x \qquad x = 0 \qquad 0 < t < t_h$$

$$= 0 \qquad x = 0 \qquad t > t_h \qquad (3.3a,b)$$

$$T(x,t) = T_{o,x} \qquad x = L_x \qquad t > 0 \qquad (3.4)$$

$$T(x,t) = T_i \qquad 0 \le x \le L_x \qquad t = 0 \qquad (3.5)$$

where t_h is the time that the heat flux is applied to the sample. After this time, the boundary condition becomes insulated, as seen by Eqs. (3.3a,b). The heat flux, q_x, the temperature at $x = L_x$ ($T_{o,x}$), and the initial temperature, T_i, are assumed to be known without errors. Note that two solutions were required for this analytical problem; one while the heat flux was applied and one after the duration of the heat flux. Also, since the experiments were conducted at room temperature, it was assumed that the temperature at $x = L_x$ was equal to the initial temperature; i.e. $T_{o,x} = T_i$. Using these assumptions, the exact solutions to describe the temperature distributions were obtained using Green's function (Beck, et al., 1992). The Green's function required for this solution is given by

$$G_x(x,t|x',\tau) = \frac{2}{L_x}\sum_{n=1}^{\infty}\cos\left(\frac{\beta_n x}{L_x}\right)\cos\left(\frac{\beta_n x'}{L_x}\right)\exp\left(\frac{-\beta_n^2 k_{x-eff}(t-\tau)}{L_x^2 C_{eff}}\right) \qquad (3.6)$$

where β_n is an eigenvalue represented by

$$\beta_n = \pi\left(n - \frac{1}{2}\right) \qquad (3.7)$$

(Beck, et al., 1992). Using Eq. (3.6), the one-dimensional temperature distribution was solved for, resulting in the following:

$$T(x,t) = T_{o,x} + \frac{q_x L_x}{k_{x-eff}}\left[1 - \frac{x}{L_x} - 2\sum_{n=1}^{\infty}\frac{1}{\beta_n^2}\cos\left(\frac{\beta_n x}{L_x}\right)\exp\left(\frac{-\beta_n^2\, k_{x-eff}\, t}{C_{eff} L_x^2}\right)\right] \tag{3.8}$$

for $0 < t < t_h$, and

$$T(x,t) = T_{o,x} - 2\frac{q_x L_x}{k_{x-eff}}\sum_{n=1}^{\infty}\frac{1}{\beta_n^2}\cos\left(\frac{\beta_n x}{L_x}\right)\left[\exp\left(\frac{-\beta_n^2 k_{x-eff} t}{C_{eff} L_x^2}\right) - \exp\left(\frac{-\beta_n^2 k_{x-eff}(t-t_h)}{C_{eff} L_x^2}\right)\right] \tag{3.9}$$

for $t > t_h$.

The temperature solution was also obtained numerically from the finite element software, EAL, using an implicit transient analysis. In EAL, the weighted residual method is used to derive the implicit time integration equations. During each time step, the temperature vector is approximated by

$$(\boldsymbol{C} + \Delta t\boldsymbol{K})\boldsymbol{T}_{i+1} = (\boldsymbol{C} - \Delta t\boldsymbol{K})\boldsymbol{T}_i + \boldsymbol{F}\Delta t + \dot{\boldsymbol{F}}\Delta t^2 \tag{3.10}$$

where $\boldsymbol{T}_i$ is the temperature vector at time t_i, $\boldsymbol{T}_{i+1}$ is the temperature vector at time t_{i+1}, Δt is the time step size, $\boldsymbol{C}$ is the capacitance matrix, $\boldsymbol{K}$ is the stiffness matrix, and $\boldsymbol{F}$ is the matrix containing the boundary conditions. (Whetstone, 1983). Again, a numerical approach was utilized for the future need to analyze complex structures which do not have exact solutions available.

3.1.2 Two-Dimensional Analysis - Anisotropic Composite Material

The two-dimensional analysis is similar to the one-dimensional analysis, only now,

two-dimensional heat conduction through an anisotropic composite sample is considered. Two different experimental configurations were used in this analysis. The first consists of an imposed heat flux perpendicular to the fiber axis over a portion of one boundary (with the remainder of the boundary insulated) and known constant temperatures at the remaining three boundaries, as shown in Fig. 3.2. The second configuration also has a heat flux imposed over a portion of one boundary, only now, the boundary opposite to the heat flux is maintained at a constant temperature, while the remaining two boundaries are insulated, as shown in Fig. 3.3. For both experimental assemblies, the heat flux boundary condition will allow for the determination of thermal conductivity in two directions. However, the actual estimation of these thermal conductivities will not be performed in this study; only the experimental designs required for this estimation process will be analyzed (Section 3.3).

The temperature distribution within the material for both configurations can be determined from conservation of energy

$$\frac{\partial}{\partial x}\left(k_{x\text{-}eff}\frac{\partial T}{\partial x}\right)+\frac{\partial}{\partial y}\left(k_{y\text{-}eff}\frac{\partial T}{\partial y}\right)=C_{eff}\frac{\partial T}{\partial t}\qquad 0<x<L_x\quad 0<y<L_y\quad t>0 \tag{3.11}$$

where, in this case, $k_{y\text{-}eff}$ and y are the effective thermal conductivity and position, respectively, perpendicular to the direction of heat transfer. The temperature solutions obtained for both configurations are discussed in the following two subsections.

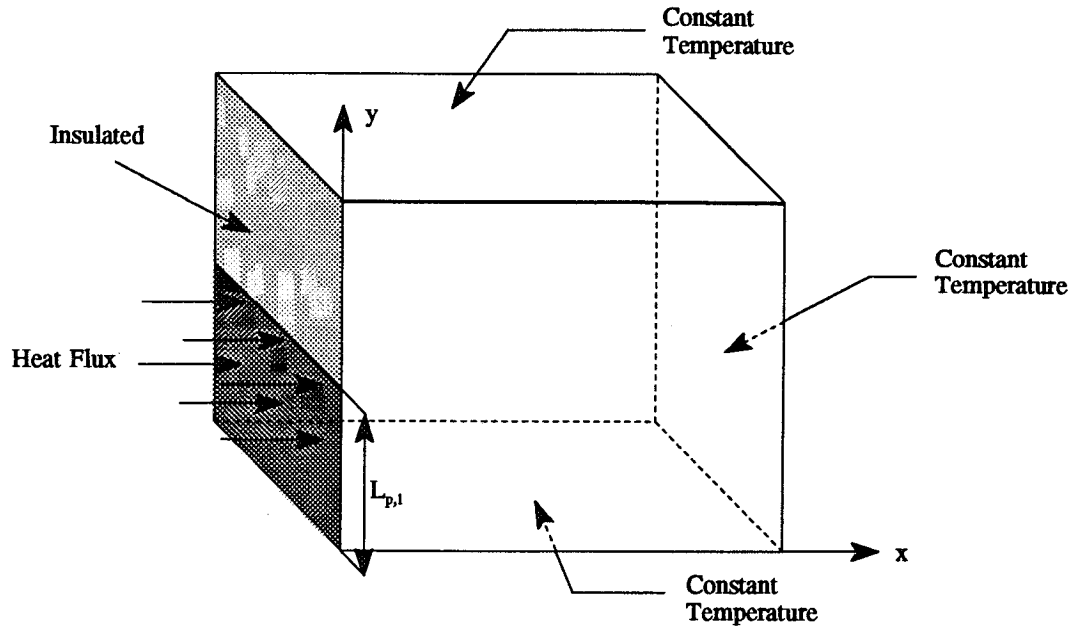

Figure 3.2. Experimental Set-up Used for Configuration 1 in the Estimation of the Effective Thermal Conductivities in Two Orthogonal Planes.

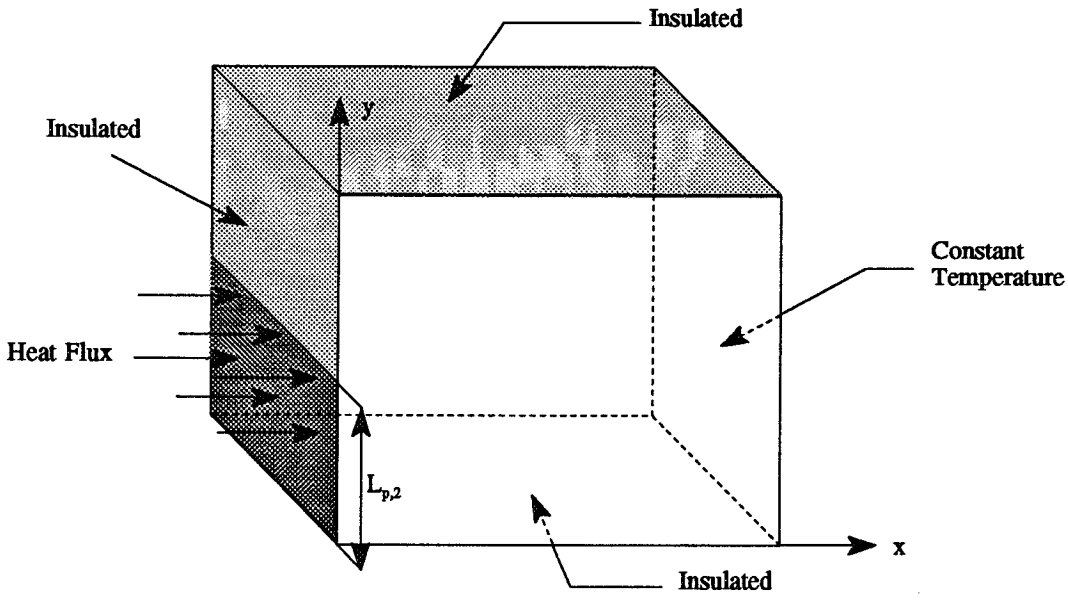

Figure 3.3. Experimental Set-up Used for Configuration 2 in the Estimation of the Effective Thermal Conductivities in Two Orthogonal Planes.

3.1.2.1 Configuration 1 - Isothermal Boundary Conditions

The heat flux and isothermal boundary conditions and the initial temperature condition for Configuration 1 (Fig. 3.2) can be described as

$$-k_{x-eff}\frac{\partial T}{\partial x} = q_x \qquad x = 0 \qquad 0 < y < L_{p,1} \qquad 0 < t < t_h$$

$$= 0 \qquad x = 0 \qquad 0 < y < L_{p,1} \qquad t > t_h \qquad (3.12a,b)$$

$$\frac{\partial T}{\partial x} = 0 \qquad x = 0 \qquad L_{p,1} < y < L_y \qquad t > 0 \qquad (3.13)$$

$$T(x,y,t) = T_{o,x} \qquad x = L_x \qquad 0 < y < L_y \qquad t > 0 \qquad (3.14)$$

$$T(x,y,t) = T_{o,y1} \qquad 0 < x < L_x \qquad y = 0 \qquad t > 0 \qquad (3.15)$$

$$T(x,y,t) = T_{o,y2} \qquad 0 < x < L_x \qquad y = L_y \qquad t > 0 \qquad (3.16)$$

$$T(x,y,t) = T_i \qquad 0 < x < L_x \qquad 0 < y < L_y \qquad t = 0 \qquad (3.17)$$

where q_x is the applied heat flux, $T_{o,x}$, $T_{o,y1}$, and $T_{o,y2}$ are the known temperature boundary conditions, L_x is the thickness of the plate in the x direction, L_y is the thickness of the plate in the y direction, $L_{p,1}$ is the portion of the plate where the heat flux is imposed, and T_i is the initial temperature. The specific value for $L_{p,1}$ will be found using the optimization procedure discussed in Section 3 of this chapter. Note that once again, two solutions are required for this analytical case; one while the heat flux is applied and one after the duration of the heat flux. Also, since the experiments were again conducted at room temperature, it is assumed that $T_{o,x} = T_{o,y1} = T_{o,y2} = T_i$. Using these assumptions, the solutions to describe the temperature distribution within the composite sample were

obtained using Green's functions. For the two-dimensional case, two Green's functions are required for the temperature solution; one for both the x and y direction boundary conditions. The Green's function for the heat transfer along the x axis is provided in Eq. (3.6), and the Green's function along the y axis is given by (Beck, et al., 1992).

$$G_y(y,t|y',\tau) = \frac{2\kappa_{xy}^{1/2}}{L_y}\sum_{m=1}^{\infty}\sin\left(\frac{m\pi y}{L_y}\right)\sin\left(\frac{m\pi y'}{L_y}\right)\exp\left(\frac{-m^2\pi^2 k_{y\text{-}eff}(t-\tau)}{L_y^2 C_{eff}}\right) \tag{3.18}$$

where κ_{xy} is the effective thermal conductivity ratio, $(k_{y\text{-}eff}/k_{x\text{-}eff})$. Using these Green's functions, the temperature solutions for Configuration 1 are represented by

$$T(x,y,t) = T_{o,x} + \frac{4q_x L_x}{k_{x\text{-}eff}\pi}\sum_{m=1}^{\infty}\sum_{n=1}^{\infty}\sin\left(\frac{m\pi y}{L_y}\right)\cos\left(\frac{\beta_n x}{L_x}\right)\left[1-\cos\left(\frac{m\pi L_{p,1}}{L_y}\right)\right] \cdot\left(\frac{1}{mB}\right)\left[1-\exp(-At)\right] \tag{3.19}$$

for $0 < t < t_h$, and

$$T(x,y,t) = T_{o,x} + \frac{4q_x L_x}{k_{x\text{-}eff}\pi}\sum_{m=1}^{\infty}\sum_{n=1}^{\infty}\sin\left(\frac{m\pi y}{L_y}\right)\cos\left(\frac{\beta_n x}{L_x}\right)\left[1-\cos\left(\frac{m\pi L_{p,1}}{L_y}\right)\right] \cdot\left(\frac{1}{mB}\right)\left[\exp[-A(t-t_h)]-\exp(-At)\right] \tag{3.20}$$

for $t > t_h$, where

$$A = \left(\frac{m^2\pi^2 k_{y\text{-}eff}}{L_y^2 C_{eff}} + \frac{\beta_n^2 k_{x\text{-}eff}}{L_x^2 C_{eff}}\right) \tag{3.21}$$

$$B = m^2\pi^2 L_{xy}^2\kappa_{xy} + \beta_n^2 \tag{3.22}$$

and L_{xy} is the ratio of the composite dimensions (L_x/L_y).

3.1.2.2 Configuration 2 - Isothermal and Insulated Boundary Conditions

The heat flux and isothermal boundary conditions and the initial temperature condition for Configuration 2 (Fig. 3.3) can be described as

$$-k_{x\text{-}eff}\frac{\partial T}{\partial x} = q_x \qquad x = 0 \qquad 0 < y < L_{p,2} \qquad 0 < t < t_h$$

$$= 0 \qquad x = 0 \qquad 0 < y < L_{p,2} \qquad t > t_h \qquad (3.23a,b)$$

$$\frac{\partial T}{\partial x} = 0 \qquad x = 0 \qquad L_{p,2} < y < L_y \qquad t > 0 \qquad (3.24)$$

$$T(x,y,t) = T_{o,x} \qquad x = L_x \qquad 0 < y < L_y \qquad t > 0 \qquad (3.25)$$

$$\frac{\partial T}{\partial y} = 0 \qquad 0 < x < L_x \qquad y = 0 \qquad t > 0 \qquad (3.26)$$

$$\frac{\partial T}{\partial y} = 0 \qquad 0 < x < L_x \qquad y = L_y \qquad t > 0 \qquad (3.27)$$

$$T(x,y,t) = T_i \qquad 0 < x < L_x \qquad 0 < y < L_y \qquad t = 0 \qquad (3.28)$$

where $L_{p,2}$ is the portion of the plate where the heat flux is imposed. Again, the specific value for $L_{p,2}$ will be found using the optimization procedure discussed in Section 3 of this chapter. Due to the different boundary conditions used in the two configurations, $L_{p,2}$ will be different than $L_{p,1}$ (the heat flux position calculated for Configuration 1). Since the experiments were again conducted at room temperature, the same assumption was used as for Configuration 1; i.e., $T_{o,x} = T_i$. The solutions to describe the temperature distribution within the composite sample were then obtained using Green's functions. Two Green's functions are again required for this configuration, one for both the x and y direction boundary conditions. The Green's function along the x axis is provided in Eq.

(3.6), and the Green's function along the y axis is given by (Beck, et al., 1992)

$$G_y(y,t|y',\tau) = \frac{\kappa_{xy}^{1/2}}{L_y}\left[1 + 2\sum_{m=1}^{\infty}\cos\left(\frac{m\pi y}{L_y}\right)\cos\left(\frac{m\pi y'}{L_y}\right)\exp\left(\frac{-m^2\pi^2 k_{y\text{-}eff}(t-\tau)}{L_y^2 C_{eff}}\right)\right] \tag{3.29}$$

Using these Green's functions, the temperature solutions for Configuration 2 are represented by

$$T(x,y,t) = T_{o,x} + \frac{2q_x L_x}{k_{x\text{-}eff}}\frac{L_{p,2}}{L_y}\sum_{n=1}^{\infty}\frac{1}{\beta_n^2}\cos\left(\frac{\beta_n x}{L_x}\right)\left[1 - \exp(-Ct)\right]$$

$$+ \frac{4q_x(t)L_x}{\pi k_{x\text{-}eff}}\sum_{m=1}^{\infty}\sum_{n=1}^{\infty}\cos\left(\frac{\beta_n x}{L_x}\right)\cos\left(\frac{m\pi y}{L_y}\right)\sin\left(\frac{m\pi L_{p,2}}{L_y}\right)\left(\frac{1}{mB}\right)\left[1 - \exp(-At)\right] \tag{3.30}$$

for $0 < t < t_h$, and

$$T(x,y,t) = T_{o,x} + \frac{2q_x L_x}{k_{x\text{-}eff}}\frac{L_{p,2}}{L_y}\sum_{n=1}^{\infty}\frac{1}{\beta_n^2}\cos\left(\frac{\beta_n x}{L_x}\right)\left[e^{[-C(t-t_h)]} - e^{(-Ct)}\right]$$

$$+ \frac{4q_x(t)L_x}{\pi k_{x\text{-}eff}}\sum_{m=1}^{\infty}\sum_{n=1}^{\infty}\cos\left(\frac{\beta_n x}{L_x}\right)\cos\left(\frac{m\pi y}{L_y}\right)\sin\left(\frac{m\pi L_{p,2}}{L_y}\right)\left(\frac{1}{mB}\right)\left[e^{[-A(t-t_h)]} - e^{(-At)}\right] \tag{3.31}$$

for $t > t_h$, where A and B are given by Eqs. (3.21) and (3.22), respectively, and C is represented by

$$C = \frac{\beta_n^2 k_{x\text{-}eff}}{L_x^2 C_{eff}} \tag{3.32}$$

In determining these temperature distributions as functions of time, one should note that there are steady state terms which need to be calculated only once since they are time

invariant. This is important since these series are slow to converge and require hundreds of terms, whereas the time varying terms of the summation converge rather quickly. An alternate solution method involves the use of time partitioning (Beck, et al., 1992). In this method, the solution is partitioned into two regions and both large-time and small-time Green's functions are used to find the temperature. For example, at early times, the solution is the same as that for a semi-infinite body, and therefore, the overall solution can be divided up into early and steady state solutions.

3.2 Minimization Procedure Used in Estimating the Thermal Properties

The method used to estimate the thermal properties is based on the minimization of an objective function with respect to the unknown parameters, effective thermal conductivity and effective volumetric heat capacity. This procedure is called the Gauss method and allows for the simultaneous estimation of the thermal properties. A modification of the Gauss method that allows for nonlinearities in the model to exist is the Box-Kanemasu method, which is utilized in this investigation. In this method, the objective function used is the least-squares function, S, and is given by

$$S = [\boldsymbol{Y} - \boldsymbol{T}(\underline{\beta})]^T [\boldsymbol{Y} - \boldsymbol{T}(\underline{\beta})] \tag{3.33}$$

(Beck and Arnold, 1977). Here, $\boldsymbol{Y}$ is the measured temperature vector, $\boldsymbol{T}(\underline{\beta})$ is the calculated temperature vector found using a transient mathematical model (as given in Eqs. (3.8-9), (3.19-20), and (3.30-31)) and the parameter estimates, and $\underline{\beta}$ is the exact

parameter vector that contains the unknown thermal properties. The objective function, S, is minimized with respect to the unknown parameters, $\underline{\beta}$. This is done by differentiating S with respect to $\underline{\beta}$ and setting the resulting equation equal to zero, giving

$$\nabla_{\underline{\beta}} S = 2[-\boldsymbol{X}^T(\underline{\beta})]\,[\boldsymbol{Y} - \boldsymbol{T}(\underline{\beta})] = 0 \tag{3.34}$$

(Beck and Arnold, 1977). Here, the sensitivity coefficient matrix, $\boldsymbol{X}(\underline{\beta})$ is defined as

$$\boldsymbol{X}(\underline{\beta}) = [\nabla_{\underline{\beta}} \boldsymbol{T}^T(\underline{\beta})]^T \tag{3.35}$$

These coefficients are the derivatives of temperature with respect to the parameters being estimated and represent the sensitivity of the temperature response with respect to changes in the unknown parameters. In order for the parameters to be estimated simultaneously, the determinant of the sensitivity coefficients and their transpose, $|\boldsymbol{X}^T\boldsymbol{X}|$, cannot equal zero. That is, any one column of $\boldsymbol{X}$ cannot be expressed as a linear combination of any other column.

Because the heat conduction process in this study is a non-linear problem, the estimator, $\underline{\beta}$, cannot easily be solved for. Therefore, two approximations are used in Eq. (3.34) to prevent this difficulty; (1) Replace $\boldsymbol{X}(\underline{\beta})$ by $\boldsymbol{X}(\boldsymbol{b})$, where $\boldsymbol{b}$ is an estimate of $\underline{\beta}$, and (2) Use the first two terms of a Taylor series for $\boldsymbol{T}(\underline{\beta})$ about $\boldsymbol{b}$ to approximate $\boldsymbol{T}(\underline{\beta})$ (Beck and Arnold, 1977). Using these approximations and implementing an iterative scheme, Eq. (3.34) can be solved for $\boldsymbol{b}$, the estimated parameter vector, resulting in the following expression for $\boldsymbol{b}^{(k+1)}$:

$$\boldsymbol{b}^{(k+1)} = \boldsymbol{b}^{(k)} + \boldsymbol{P}^{(k)}[\boldsymbol{X}^{T(k)}\,(\boldsymbol{Y} - \boldsymbol{T}^{(k)})] \tag{3.36}$$

where

$$\boldsymbol{P}^{(k)} = [\boldsymbol{X}^{(k)T}\boldsymbol{X}^{(k)}]^{-1} \tag{3.37}$$

This is known as the Gauss linearization equation Here, k is the iteration number, $\boldsymbol{b}^{(k+1)}$ is the new parameter estimate, $\boldsymbol{b}^{(k)}$ is the estimate at the previous iteration, and $\boldsymbol{T}(\boldsymbol{b})^{(k)}$ contains temperatures calculated using $\boldsymbol{b}^{(k)}$.

For a nonlinear problem, Eq. (3.36) is altered and becomes

$$\boldsymbol{b}^{(k+1)} = \boldsymbol{b}^{(k)} + h^{(k+1)}\Delta_g\boldsymbol{b}^{(k)} \tag{3.38}$$

where

$$\Delta_g\boldsymbol{b}^{(k)} = \boldsymbol{P}^{(k)}[\boldsymbol{X}^{T(k)}\ (\boldsymbol{Y} - \boldsymbol{T}^{(k)}\ )] \tag{3.39}$$

and $h^{(k+1)}$ is a scalar interpolation function. To use this nonlinear estimation procedure, an initial estimate, $\boldsymbol{b}^{(o)}$, is required. This estimate is then used to calculate $\boldsymbol{T}^{(o)}$ and $\boldsymbol{X}^{(o)}$ which are used to obtain the improved parameter vector, $\boldsymbol{b}^{(1)}$. This procedure continues until all parameters in $\boldsymbol{b}$ do not change significantly (Beck and Arnold, 1977).

Equation (3.38) represents the Box-Kanemasu method which is a modification of the Gauss method. In the Box-Kanemasu method, the sum of squares, S, is approximated at each iteration by a quadratic function in h. The minimum S is located where the derivative of S with respect to h is equal to zero, or at an h value of (Beck and Arnold, 1977)

$$h^{(k+1)} = G^{(k)}\alpha^2[S_\alpha^{(k)} - S_o^{(k)} + 2G^{(k)}\alpha]^{-1} \tag{3.40}$$

where

$$G^{(k)} = [\Delta_g\boldsymbol{b}^{(k)}]^T\ (\boldsymbol{X}^{T(k)}\boldsymbol{X}^{(k)})[\Delta_g\boldsymbol{b}^{(k)}] \tag{3.41}$$

The parameter for α is initially set equal to one and $S_\alpha^{(k)}$ and $S_o^{(k)}$ are the values of S at α and zero, respectively. If $S_\alpha^{(k)}$ is not less than $S_o^{(k)}$, α is reduced by one-half and the inequality is checked again. This is a modification over the original Box-Kanemasu method. A flow chart illustrating the modified Box-Kanemasu estimation procedure, as presented by Beck and Arnold (1977), is shown in Fig. 3.4. Note that if the investigation requires α to become less than 0.01, the calculations are terminated. One reason why this may occur is that correlation (or linear dependence) between the sensitivity coefficients exists, causing the sum of squares function not to have a unique minimum. It is therefore very important to calculate and analyze the sensitivity coefficients for possible correlation to ensure reliable parameter estimates.

A parameter estimation program was written using the modified Box-Kanemasu method and is called *MODBOX*; this program is based on the original program *NLINA*, by Beck (1993). This program uses sequential in-time estimation to calculate the parameters at each time step. The exact mathematical models given in Eqs. (3.8) and (3.9) were used in this program as well as the derived sensitivity coefficients, allowing for the estimation of the effective thermal conductivity perpendicular to the fibers and the effective volumetric heat capacity of a composite consisting of IM7 graphite fibers and a Bismaleimide epoxy matrix. The modified Box-Kanemasu method was also implemented into EAL where the temperature solution was obtained numerically. Again, the same effective thermal properties were estimated. The advantage of this sequential estimation technique is that it allows the user to observe the effects of additional data on the sequential estimates and study the validity of the proposed mathematical model and

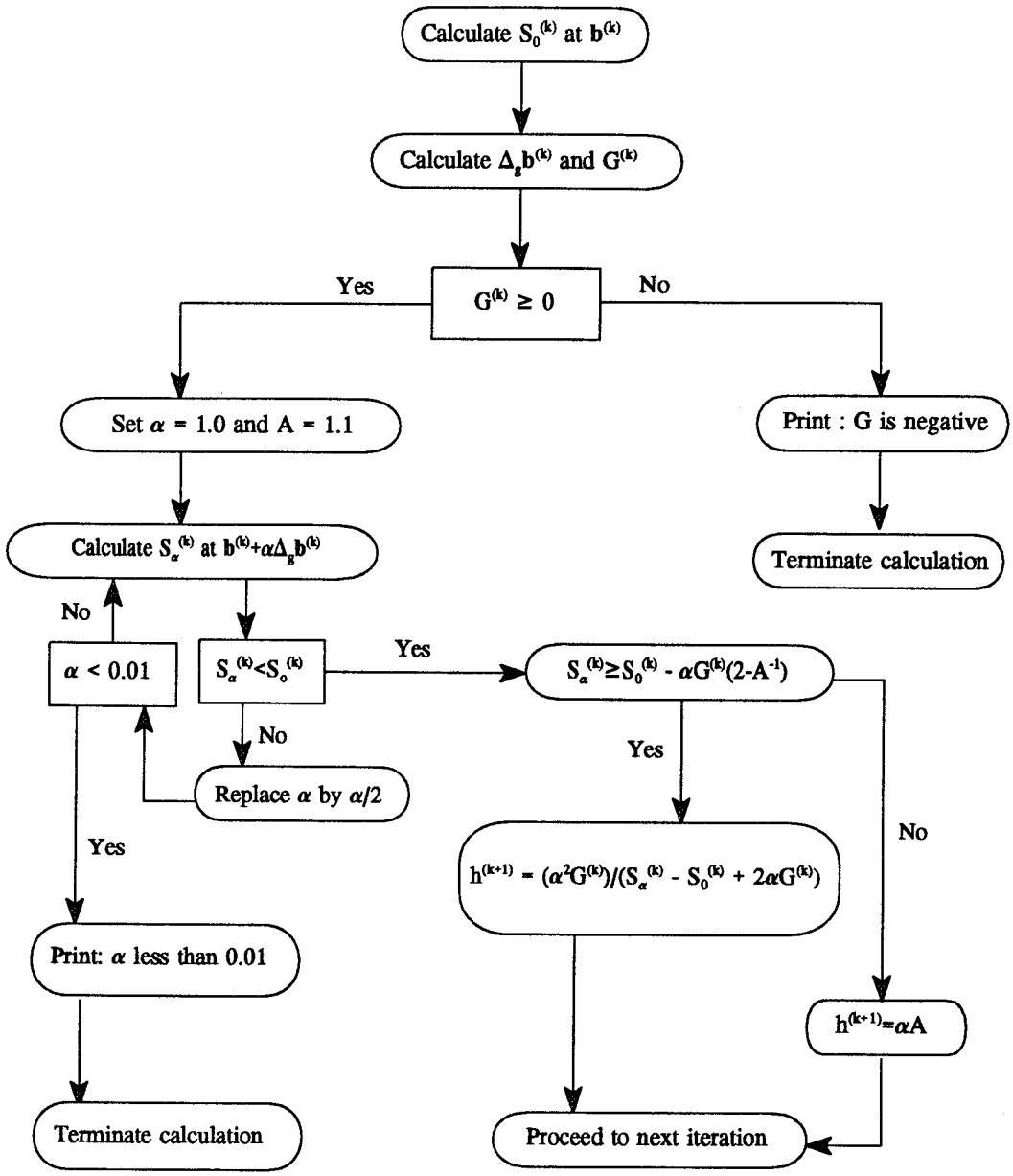

Figure 3.4 Flow Chart for the Modified Box-Kanemasu Estimation Procedure

experimental design. Ideally, at the conclusion of an experiment, any additional data should not affect the parameter estimates.

3.3 Optimal Experimental Designs Used in Estimating Thermal Properties of Composite Materials

Since the Gauss method requires experimental temperatures of the composite system to be measured, the accuracy of the thermal properties estimated can be greatly increased if these experiments are designed carefully. To create such optimal experimental designs, optimal experimental parameters must first be determined. The focus of this section is on the criterion used in obtaining these optimal parameters. For the one-dimensional analysis, the experimental design consisted of a thin plate with an imposed heat flux applied for a finite duration at one boundary and a known, constant temperature at the second boundary. For this design, the optimal experimental parameters that were determined are the heating time, temperature sensor location, and total experimental time.

For the two-dimensional heat conduction analysis, two different configurations were used, allowing for the effective thermal conductivity in two directions and the effective volumetric heat capacity to be determined simultaneously. Both designs had a heat flux imposed over a portion of one boundary, with the remainder of the boundary insulated. In addition, Configuration 1 had known, constant temperatures at the remaining three boundaries, while Configuration 2 had a constant temperature at the boundary

opposite to the heat flux, and insulated conditions at the remaining two boundaries. Therefore, in addition to the optimal experimental parameters found for the one-dimensional case, the optimal position of the heat flux was also determined for both configurations used in the two-dimensional case. Note, however, that this optimal heat flux location will not be the same for both configurations due to the different boundary conditions used.

3.3.1 Design Criterion Used for Optimal Experimental Designs

Many criterion have been proposed for the design of optimum experiments. As mentioned previously, the sensitivity coefficients indicate the sensitivity of temperature to changes in the thermal properties and optimal experiments are those which maximize these coefficients for each property. Therefore, the criterion chosen for this analysis is the maximization of the determinant (D^+) of $\boldsymbol{X}^{+T}\boldsymbol{X}^+$, which contains the product of the dimensionless sensitivity coefficients and their transpose (Beck and Arnold, 1977). This criterion is subject to a maximum temperature rise, a fixed number of measurements, and the following seven standard statistical assumptions: additive, zero mean, constant variance, uncorrelated normal errors with errorless independent variables, and no prior information. It is recommended by Beck and Arnold because it has the effect of minimizing the confidence intervals of the resulting parameter estimates. Note, it was desired to perform the optimization procedure in non-dimensional terms so the results could be applicable for any material, not just composite materials.

For the one-dimensional analysis where two properties are estimated ($k_{x\text{-}eff}$ and C_{eff}),

$| X^{+T}X^{+} |$ is a 2 x 2 matrix. Therefore, the dimensionless determinant is given as

$$D_{1\text{-}D}^{+} = \begin{vmatrix} d_{11}^{+} & d_{12}^{+} \\ d_{12}^{+} & d_{22}^{+} \end{vmatrix} = d_{11}^{+}d_{22}^{+} - (d_{12}^{+})^2 \qquad (3.42a,b)$$

where d_{11}^{+}, d_{12}^{+}, and d_{22}^{+} are found from (Beck and Arnold, 1977)

$$d_{ij}^{+} = \left[\frac{1}{T_{\max}^{+2}}\right]\left[\frac{1}{Mt_N^{+}}\right]\sum_{p=1}^{M}\int_0^{t_N^{+}} X_i^{+}(t^{+})X_j^{+}(t^{+})\, dt^{+} \qquad (3.43)$$

In this equation, M is the number of temperature sensors used and t^{+}, t_N^{+}, and T_{max}^{+} are defined as

$$T_{\max}^{+} = \frac{(T_{\max}-T_{o,x})}{q_x L_x / k_{x\text{-}eff}}, \qquad t^{+} = \frac{k_{x\text{-}eff}t}{C_{eff}L_x^2}, \qquad t_N^{+} = \frac{k_{x\text{-}eff}t_N}{C_{eff}L_x^2} \qquad (3.44a\text{-}c)$$

where t_N is the total experimental time, T_{max} is the maximum temperature reached between the start and end of the experiment, and $T_{o,x}$ is the surface (and in this case, initial) temperature. It should be noted that this definition of T_{max}^{+} was used to verify previous optimal experimental parameter results by Taktak, et al. (1991) and is not the best representative choice.

The integral in Eq. (3.43) was calculated numerically, being approximated by a summation. From Eq. (3.43), it is evident that the matrix in Eq. (3.42a) is symmetric; i.e., $d_{12}^{+} = d_{21}^{+}$. This simplifies the problem by decreasing the number of equations that must be numerically integrated.

When extending this analysis to the two-dimensional case, three properties ($k_{x\text{-}eff}$, $k_{y\text{-}eff}$ and C_{eff}) can now be estimated simultaneously for both configurations. Therefore,

$| X^{+T}X^{+} |$ is a 3 x 3 symmetric matrix and the dimensionless determinant is given by

$$D^{+}_{2\text{-}D} = \begin{vmatrix} d^{+}_{11} & d^{+}_{12} & d^{+}_{13} \\ d^{+}_{12} & d^{+}_{22} & d^{+}_{23} \\ d^{+}_{13} & d^{+}_{23} & d^{+}_{33} \end{vmatrix}$$

$$D^{+}_{2\text{-}D} = d^{+}_{11}(d^{+}_{22}d^{+}_{33} - d^{+2}_{23}) - d^{+}_{12}(d^{+}_{12}d^{+}_{33} - d^{+}_{13}d^{+}_{23}) + d^{+}_{13}(d^{+}_{12}d^{+}_{23} - d^{+}_{13}d^{+}_{22}) \qquad (3.45a,b)$$

Again, the d_{ij}^{+} values were found from Eq. (3.43), where the integral was calculated numerically. To compare both configurations used in the two-dimensional analysis, the value for T_{max}^{+} was redefined as the temperature reached at steady-state conditions. This is a more accurate choice than the T_{max}^{+} selected for the one-dimensional design, used by Taktak, et al. (1991), because it represents the true maximum temperature that can be attained for the defined problem.

From Eqs. (3.42) and (3.43), it is seen that the dimensionless sensitivity coefficients are required for this optimization procedure; these coefficients are given by

$$X^{+}_{k_{x\text{-}eff}} = \frac{k_{x\text{-}eff}}{q_x L_x / k_{x\text{-}eff}} \frac{\partial T}{\partial k_{x\text{-}eff}} \qquad (3.46)$$

$$X^{+}_{C_{eff}} = \frac{C_{eff}}{q_x L_x / k_{x\text{-}eff}} \frac{\partial T}{\partial C_{eff}} \qquad (3.47)$$

and

$$X^{+}_{k_{y\text{-}eff}} = \frac{k_{y\text{-}eff}}{q_x L_x / k_{x\text{-}eff}} \frac{\partial T}{\partial k_{y\text{-}eff}} \qquad (3.48)$$

where $X^{+}_{k_{x\text{-}eff}}$ and $X^{+}_{C_{eff}}$ are used in the one-dimensional analysis and $X^{+}_{k_{x\text{-}eff}}$, $X^{+}_{k_{y\text{-}eff}}$, and $X^{+}_{C_{eff}}$ are used in the two-dimensional analysis.

3.3.2 One-Dimensional Optimal Experimental Design Formulation

In performing this optimization procedure, a mathematical model, either exact or numerical, is required to represent the experimental process. An exact model for the one-dimensional analysis is given by the temperature solutions in Eqs. (3.8) and (3.9). Using the following dimensionless variables

$$x^+ = \frac{x}{L_x}, \quad t^+ = \frac{k_{x\text{-}eff}t}{C_{eff}L_x^2}, \quad t_h^+ = \frac{k_{x\text{-}eff}t_h}{C_{eff}L_x^2}, \quad T^+ = \frac{T-T_{o,x}}{q_xL_x/k_{x\text{-}eff}} \tag{3.49a-d}$$

these temperature distributions can be expressed in dimensionless form as

$$T^+(x,t) = 1 - x^+ - 2\sum_{n=1}^{\infty}\frac{1}{\beta_n^2}\cos(\beta_n x^+)\exp\left(-\beta_n^2 t^+\right) \tag{3.50}$$

for $0 < t^+ < t_h^+$, and

$$T^+(x,t) = -2\sum_{n=1}^{\infty}\frac{1}{\beta_n^2}\cos(\beta_n x^+)\left[\exp(-\beta_n^2 t^+) - \exp[-\beta_n^2(t^+-t_h^+)]\right] \tag{3.51}$$

for $t^+ > t_h^+$, where β_n is given by Eq. (3.7). This temperature distribution, which is calculated using a dimensionless heating time, t_h^+, equal to the total experimental time, is shown in Fig. 3.5 for several x^+ locations.

The dimensionless sensitivity coefficients, $X_{k_{x\text{-}eff}}^+$ and $X_{C_{eff}}^+$, were then found by differentiating Eqs. (3.50) and (3.51) with respect to $k_{x\text{-}eff}$ and C_{eff}. The effective thermal conductivity sensitivity coefficients are given by

$$X_{k_{x\text{-}eff}}^+ = (x^+ - 1) + 2\sum_{n=1}^{\infty}\left(\frac{1}{\beta_n^2} + t^+\right)\cos(\beta_n x^+)\exp(-\beta_n^2 t^+) \tag{3.52}$$

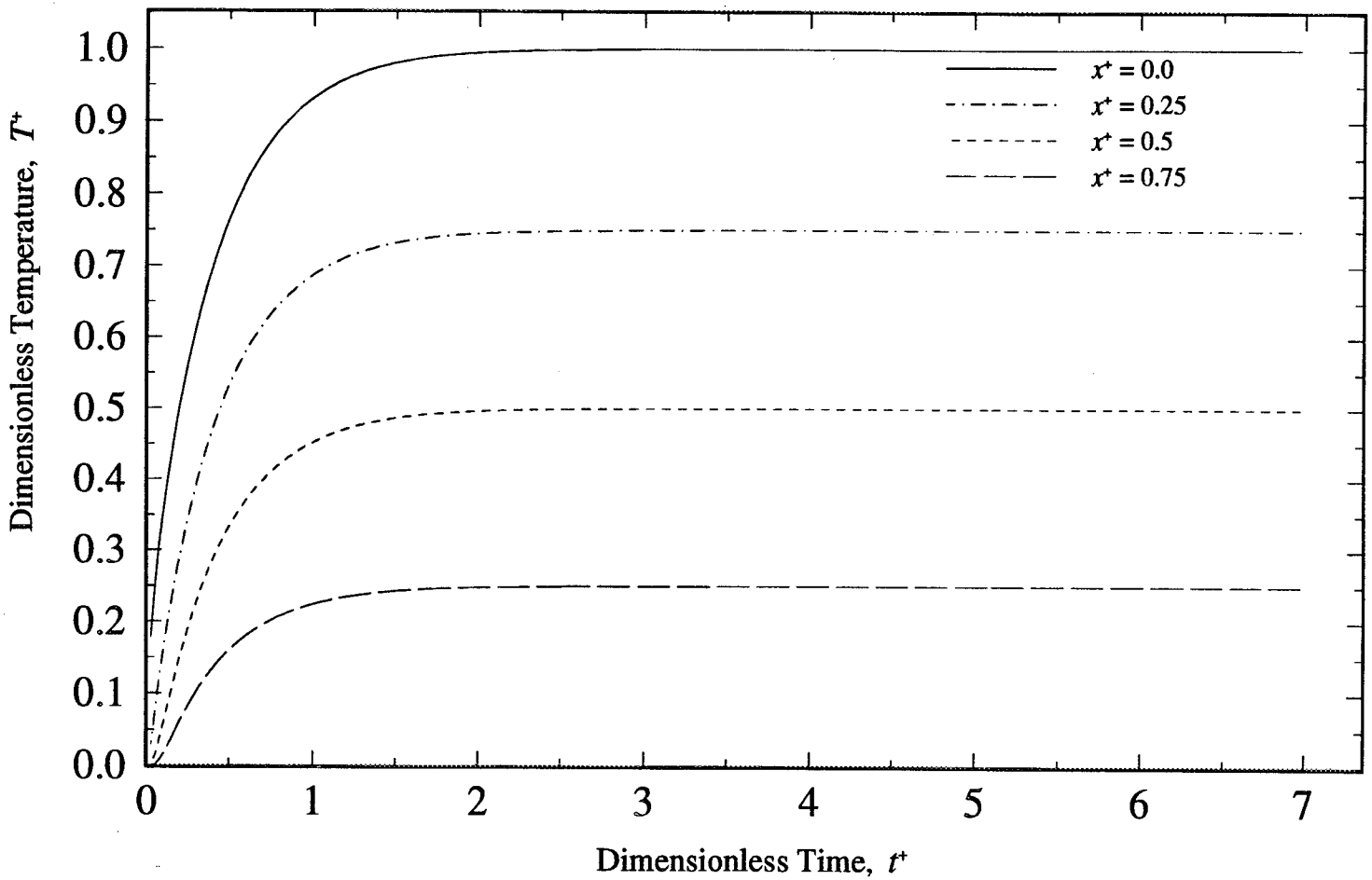

Figure 3.5. Dimensionless Temperature Distribution (T^+) for One-Dimensional Heat Conduction Using a Dimensionless Heating Time, t_h^+, Equal to the Total Experimental Time for Several x^+ (x/L_x) Locations.

for $0 < t^+ < t_h^+$, and

$$X_{k_{x-eff}}^+ = 2\sum_{n=1}^{\infty} \cos(\beta_n x^+) \left[\left(\frac{1}{\beta_n^2} + t^+ \right) e^{(-\beta_n^2 t^+)} - \left(\frac{1}{\beta_n^2} + (t^+ - t_h^+) \right) e^{[-\beta_n^2 (t^+ - t_h^+)]} \right] \tag{3.53}$$

for $t^+ > t_h^+$, while the effective volumetric heat capacity sensitivity coefficients can be expressed as

$$X_{C_{eff}}^+ = -2\sum_{n=1}^{\infty} t^+ \exp(-\beta_n^2 t^+) \cos(\beta_n x^+) \tag{3.54}$$

for $0 < t^+ < t_h^+$, and

$$X_{C_{eff}}^+ = -2\sum_{n=1}^{\infty} \left[t^+ \exp(-\beta_n^2 t^+) - (t^+ - t_h^+) \exp[-\beta_n^2 (t^+ - t_h^+)] \right] \cos(\beta_n x^+) \tag{3.55}$$

for $t^+ > t_h^+$.

These dimensionless sensitivity coefficients are then used in the optimization procedure to determine the maximum determinant value, as given by Eqs. (3.42) and (3.43), and the corresponding optimal experimental parameters. Viewing these coefficients as functions of experimental time will also give insight into the experimental design, as will be shown in Chapter 5. The sensitivity coefficients in dimensional form are also required in the program, *MODBOX*, to estimate the effective thermal conductivity and effective volumetric heat capacity simultaneously, as shown in Eqs. (3.36) and (3.37).

3.3.3 Two-Dimensional Optimal Experimental Design Formulation

The exact model used to describe the temperature distribution for two-dimensional heat transfer in an anisotropic composite material is given in Eqs. (3.19) and (3.20) for

Configuration 1 and Eqs. (3.30) and (3.31) for Configuration 2. The derived sensitivity coefficients for both configurations required for the optimization procedure are discussed in the following two subsections.

3.3.3.1 Optimal Experimental Design Formulation for Configuration 1

Using the dimensionless variables already given in Eq. (3.49) along with the following non-dimensional variables

$$y^+ = \frac{y}{L_y}, \qquad L_{p,i}^+ = \frac{L_{p,i}}{L_y}, \quad i=1,2 \tag{3.56a,b}$$

(i corresponds to the configuration number) the temperature distributions for Configuration 1 can be expressed in dimensionless form as

$$T^+(x^+,y^+,t^+) = \frac{4}{\pi}\sum_{m=1}^{\infty}\sum_{n=1}^{\infty} \sin(m\pi y^+)\cos(\beta_n x^+)\left[1 - \cos(m\pi L_{p,1}^+)\right] \cdot \left(\frac{1}{mB}\right)\left[1 - \exp(-Bt^+)\right] \tag{3.57}$$

for $0 < t^+ < t_h^+$, and

$$T^+(x^+,y^+,t^+) = \frac{4}{\pi}\sum_{m=1}^{\infty}\sum_{n=1}^{\infty} \sin(m\pi y^+)\cos(\beta_n x^+)\left[1 - \cos(m\pi L_{p,1}^+)\right]\left(\frac{1}{mB}\right) \cdot \left[\exp\left[-B(t^+ - t_h^+)\right] - \exp(-Bt^+)\right] \tag{3.58}$$

for $t^+ > t_h^+$, where L_{xy} (L_x/L_y) and κ_{xy} ($k_{y\text{-}eff}/k_{x\text{-}eff}$) are the dimension and effective thermal conductivity ratios, respectively, and B is given in Eq. (3.22).

The sensitivity coefficients for all three effective parameters, thermal conductivity

perpendicular to the fibers ($k_{x\text{-}eff}$), thermal conductivity parallel to the fibers ($k_{y\text{-}eff}$), and volumetric heat capacity (C_{eff}), were then calculated by differentiating the above temperature distribution with respect to each property. The sensitivity coefficients for the thermal conductivity perpendicular to the fiber axis are given by

$$X^+_{k_{x\text{-}eff}} = \frac{4}{\pi}\sum_{m=1}^{\infty}\sum_{n=1}^{\infty} \sin(m\pi y^+)\cos(\beta_n x^+)\,[1 - \cos(m\pi L^+_{p,1})]\left(\frac{1}{mB}\right) \cdot \left[\beta_n^2 t^+ \exp(-Bt^+) + (D-1)(1-\exp(-Bt^+))\right] \tag{3.59}$$

for $0 < t^+ < t_h^+$, and

$$X^+_{k_{x\text{-}eff}} = \frac{4}{\pi}\sum_{m=1}^{\infty}\sum_{n=1}^{\infty} \sin(m\pi y^+)\cos(\beta_n x^+)\,[1 - \cos(m\pi L^+_{p,1})]\left(\frac{1}{mB}\right) \cdot \left[(D-1)\left(e^{[-B(t^+-t_h^+)]} - e^{(-Bt^+)}\right) + \beta_n^2 t^+ e^{(-Bt^+)} - \beta_n^2 (t^+ - t_h^+) e^{[-B(t^+-t_h^+)]}\right] \tag{3.60}$$

for $t^+ > t_h^+$ where D is equal to

$$D = \left(\frac{m^2\pi^2 L_{xy}^2 \kappa_{xy}}{m^2\pi^2 L_{xy}^2 \kappa_{xy} + \beta_n^2}\right) \tag{3.61}$$

The dimensionless sensitivity coefficients for $X^+_{C_{eff}}$ and $X^+_{k_{y\text{-}eff}}$ were also calculated; the solutions for $0 < t^+ < t_h^+$ are given by

$$X^+_{C_{eff}} = \frac{4}{\pi}\sum_{m=1}^{\infty}\sum_{n=1}^{\infty} \sin(m\pi y^+)\cos(\beta_n x^+)\,[1 - \cos(m\pi L^+_{p,1})]\left(\frac{1}{mB}\right)\left(-Bt^+\exp(-Bt^+)\right) \tag{3.62}$$

and

$$X^{+}_{k_{y-eff}} = \frac{4}{\pi}\sum_{m=1}^{\infty}\sum_{n=1}^{\infty} \sin(m\pi y^{+}) \cos(\beta_n x^{+}) \left[1 - \cos(m\pi L^{+}_{p,1})\right] \cdot \left(\frac{1}{mB}\right)\left[m^2\pi^2 L^2_{xy}\kappa_{xy} t^{+}\exp(-Bt^{+}) - D\left(1 - \exp(-Bt^{+})\right)\right] \tag{3.63}$$

and for $t^{+} > t_h^{+}$, by

$$X^{+}_{C_{eff}} = \frac{4}{\pi}\sum_{m=1}^{\infty}\sum_{n=1}^{\infty} \sin(m\pi y^{+}) \cos(\beta_n x^{+}) \left[1 - \cos(m\pi L^{+}_{p,1})\right]\left(\frac{1}{mB}\right) \cdot \left[B(t^{+} - t_h^{+})\exp\left[-B(t^{+} - t_h^{+})\right] - Bt^{+}\exp(-Bt^{+})\right] \tag{3.64}$$

and

$$X^{+}_{k_{y-eff}} = \frac{4}{\pi}\sum_{m=1}^{\infty}\sum_{n=1}^{\infty} \sin(m\pi y^{+}) \cos(\beta_n x^{+}) \left[1 - \cos(m\pi L^{+}_{p,1})\right]\left(\frac{1}{mB}\right) \cdot \left[D\left(e^{(-Bt^{+})} - e^{[-B(t^{+} - t_h^{+})]}\right) + m^2\pi^2 L^2_{xy}\kappa_{xy}\left(t^{+}e^{(-Bt^{+})} - (t^{+} - t_h^{+})e^{[-B(t^{+} - t_h^{+})]}\right)\right] \tag{3.65}$$

where B and D are given in Eqs. (3.22) and (3.61), respectively.

3.3.3.2 Optimal Experimental Design Formulation for Configuration 2

Using the dimensionless variables given in Eqs. (3.49) and (3.56), the temperature distribution obtained for Configuration 2 (Eqs. (3.30) and (3.31)) can be expressed in dimensionless form as

$$T^{+}(x^{+},y^{+},t^{+}) = 2L^{+}_{p,2}\sum_{n=1}^{\infty}\frac{1}{\beta_n^2}\cos(\beta_n x^{+})\left[1 - e^{-\beta_n^2 t^{+}}\right]$$

$$+ \frac{4}{\pi}\sum_{m=1}^{\infty}\sum_{n=1}^{\infty}\cos(\beta_n x^{+})\cos(m\pi y^{+})\sin(m\pi L^{+}_{p,2})\left(\frac{1}{mB}\right)\left[1 - e^{(-Bt^{+})}\right] \tag{3.66}$$

for $0 < t^+ < t_h^+$, and

$$T^+(x^+,y^+,t^+) = 2L_{p,2}^+ \sum_{n=1}^{\infty} \frac{1}{\beta_n^2} \cos(\beta_n x^+) \left[e^{[-\beta_n^2(t^+ - t_h^+)]} - e^{(-\beta_n^2 t^+)} \right]$$

$$+ \frac{4}{\pi} \sum_{m=1}^{\infty} \sum_{n=1}^{\infty} \cos(\beta_n x^+) \cos(m\pi y^+) \sin(m\pi L_{p,2}^+) \left(\frac{1}{mB} \right) \left[e^{[-B(t^+ - t_h^+)]} - e^{(-Bt^+)} \right] \tag{3.67}$$

for $t^+ > t_h^+$.

Again, the sensitivity coefficients for all three effective parameters, thermal conductivity perpendicular to the fibers ($k_{x\text{-}eff}$), thermal conductivity parallel to the fibers ($k_{y\text{-}eff}$), and volumetric heat capacity (C_{eff}), were then calculated by differentiating the above temperature distributions with respect to each property. The sensitivity coefficients for the thermal conductivity perpendicular to the fiber axis are given by

$$X_{k_{x-eff}}^+ = 2L_{p,2}^+ \sum_{n=1}^{\infty} \cos(\beta_n x^+) \left[\frac{-1}{\beta_n^2} + \left(t^+ + \frac{1}{\beta_n^2} \right) e^{(-\beta_n^2 t^+)} \right] + \frac{4}{\pi} \sum_{m=1}^{\infty} \sum_{n=1}^{\infty} \cos(\beta_n x^+)$$

$$\cdot \cos(m\pi y^+) \sin(m\pi L_{p,2}^+) \left(\frac{1}{mB} \right) \left[(D-1)(1 - e^{(-Bt^+)}) + \beta_n^2 t^+ e^{(-Bt^+)} \right] \tag{3.68}$$

for $0 < t^+ < t_h^+$, and

$$X_{k_{x-eff}}^+ = 2L_{p,2}^+ \sum_{n=1}^{\infty} \cos(\beta_n x^+) \left[\left(\frac{1}{\beta_n^2} + t^+ \right) e^{(-\beta_n^2 t^+)} - \left(\frac{1}{\beta_n^2} + (t^+ - t_h^+) \right) e^{[-\beta_n^2(t^+ - t_h^+)]} \right]$$

$$+ \frac{4}{\pi} \sum_{m=1}^{\infty} \sum_{n=1}^{\infty} \cos(\beta_n x^+) \cos(m\pi y^+) \sin(m\pi L_{p,2}^+) \left(\frac{1}{mB} \right)$$

$$\cdot \left[(D - 1)(e^{[-B(t^+ - t_h^+)]} - e^{(-Bt^+)}) + \beta_n^2 t^+ e^{(-Bt^+)} - \beta_n^2 (t^+ - t_h^+) e^{[-B(t^+ - t_h^+)]} \right] \tag{3.69}$$

for $t^+ > t_h^+$. The dimensionless sensitivity coefficients for $X_{C_{eff}}^+$ and $X_{k_{y-eff}}^+$ were also calculated; the solutions for $0 < t^+ < t_h^+$ are given by

$$X_{C_{eff}}^+ = -2L_{p,2}^+ \sum_{n=1}^{\infty} t^+ \cos(\beta_n x^+)\ e^{(-\beta_n^2 t^+)} + \frac{4}{\pi} \sum_{m=1}^{\infty} \sum_{n=1}^{\infty} \cos(\beta_n x^+)$$

$$\cdot \left[\cos(m\pi y^+)\ \sin(m\pi L_{p,2}^+) \left(\frac{1}{mB} \right) \left(-Bt^+ e^{(-Bt^+)} \right) \right] \tag{3.70}$$

and

$$X_{k_{y-eff}}^+ = \frac{4}{\pi} \sum_{m=1}^{\infty} \sum_{n=1}^{\infty} \cos(\beta_n x^+)\ \cos(m\pi y^+)\ \sin(m\pi L_{p,2}^+) \left(\frac{1}{mB} \right)$$

$$\cdot \left[-D\left(1 - e^{(-Bt^+)}\right) + m^2 \pi^2 L_{xy}^2 \kappa_{xy} t^+ e^{(-Bt^+)} \right] \tag{3.71}$$

and for $t^+ > t_h^+$, by

$$X_{C_{eff}}^+ = 2L_{p,2}^+ \sum_{n=1}^{\infty} \cos(\beta_n x^+) \left[(t^+ - t_h^+) e^{[-\beta_n^2 (t^+ - t_h^+)]} - t^+ e^{(-\beta_n^2 t^+)} \right] + \frac{4}{\pi} \sum_{m=1}^{\infty} \sum_{n=1}^{\infty}$$

$$\left[\cos(\beta_n x^+)\ \cos(m\pi y^+)\ \sin(m\pi L_{p,2}^+) \left(\frac{1}{mB} \right) \left[B(t^+ - t_h^+) e^{[-B(t^+ - t_h^+)]} - Bt^+ e^{(-Bt^+)} \right] \right] \tag{3.72}$$

and

$$X_{k_{y-eff}}^+ = \frac{4}{\pi} \sum_{m=1}^{\infty} \sum_{n=1}^{\infty} \cos(\beta_n x^+)\ \cos(m\pi y^+)\ \sin(m\pi L_{p,2}^+) \left(\frac{1}{mB} \right)$$

$$\cdot \left[-D \left(e^{[-B(t^+ - t_h^+)]} - e^{(-Bt^+)} \right) + m^2 \pi^2 L_{xy}^2 \kappa_{xy} \left(t^+ e^{(-Bt^+)} - (t^+ - t_h^+) e^{[-B(t^+ - t_h^+)]} \right) \right] \tag{3.73}$$

where B and D are given in Eqs. (3.22) and (3.61), respectively.

Again, as in the one-dimensional analysis, the dimensionless sensitivity coefficients for both configurations will be used in the optimization procedure to determine the maximum determinant and the corresponding optimal experimental parameters.

Chapter 4

Experimental Procedures

This chapter describes the experimental procedure used to estimate the thermal properties of a continuous IM7 graphite fiber - Bismaleimide epoxy matrix composite material. Although optimal experiments were designed for both one-dimensional (isotropic) and two-dimensional (anisotropic) heat conduction, only the one-dimensional experiment was conducted, allowing for the effective thermal conductivity perpendicular to the fibers and the effective volumetric heat capacity to be estimated simultaneously.

As discussed previously in Section 3.2, the estimation procedure used in this study is the modified Box-Kanemasu method. Recall that when using this method, experimental temperatures must be recorded. To estimate the thermal properties independently, the experiments must be transient and one of the boundary conditions must be a heat flux (Beck and Arnold, 1977). With these required conditions, the experimental assemblies were designed accordingly. Discussed next are the experimental set-up and procedure utilized.

4.1 One-Dimensional Experiment for the Estimation of Thermal Properties

The experimental assembly for the one-dimensional analysis used to estimate the thermal properties of the given composite material consists of a thin composite sample subjected to a heat flux perpendicular to the fiber axis at one boundary and a known constant temperature at the other boundary. Temperature measurements were then taken at the flux boundary and were used in the estimation procedure. These experiments are described in detail in the following subsections.

4.1.1 One-Dimensional Experimental Set-Up

The experimental design for one-dimensional heat conduction was composed of two composite disks of approximately equal size, a resistance heater, eight thermocouples, and two copper cylinders. The assembly was symmetrical consisting of, from the center to the top, a thin resistance heater, two thermocouples, the composite sample, two additional thermocouples, and a copper block. The composite sample was 4.77 cm in diameter and 0.678 cm thick. The copper blocks, each with a height of 6.35 cm and a diameter of 5.08 cm, were used as heat sinks to attempt to attain the constant temperature boundary condition while the resistance heater was used to provide the heat flux boundary condition. All of the experiments were conducted at the National Aeronautics and Space Administration - Langley Research Center, Aircraft Structures Branch (NASA-LaRC,ASB) using the equipment available in their testing lab. All supplies required in the experiment, such as the resistance heater and heat sink compound, were also supplied by NASA-

LaRC. The carbon fiber-epoxy matrix composites were prepared and the thermocouples (Type K) were fabricated by NASA-LaRC personnel. The data acquisition hardware and software used in taking temperature, voltage, and current measurements had been previously programmed. Therefore, only the assembly of the experimental apparatus remained to be completed, with the details given next.

4.1.1.1 Experimental Set-Up Assembly

The one-dimensional experimental apparatus involved the following procedure:

1) Measure the thickness and diameter of two composite samples (Samples 1 and 2), and the height and diameter of two copper blocks.

2) Coat one surface of a copper block with a thin layer of silicon heat sink compound. Make sure the compound is smooth and evenly distributed. A flat edge the width of the sample is useful to apply the coating with.

3) Place (2) thermocouples on top of the copper block layered with the heat sink. The junction should be in the center of the samples and the two wires should be parallel to each other and equidistance approximately 0.635 cm from the center of the second axis. To keep the thermocouples in place, tape them down either to the table or to the sides of the sample. Be sure to number the thermocouples so that their position can be recorded (see Fig. 4.1).

4) Coat one surface of Sample 1 with a thin layer of silicon heat sink compound. Again, be sure the compound is smooth and evenly distributed. Carefully place the composite sample (coated surface down) on top of the copper block over the thermocouples (see Fig. 4.2). Do not slide the composite sample on the block or

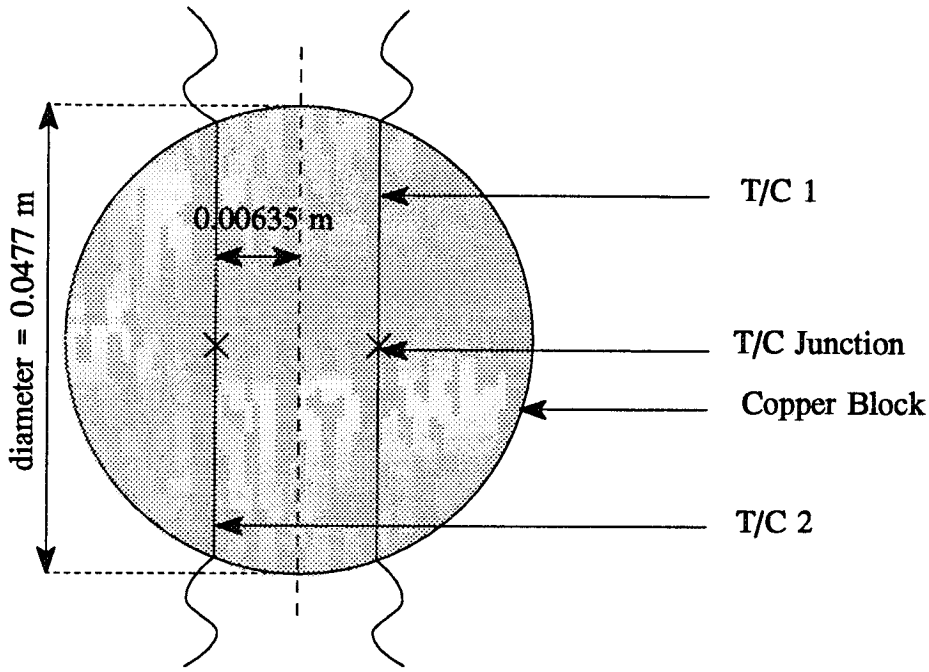

Figure 4.1. Position of Thermocouples (T/C's) on Copper Block for the One-Dimensional Experimental Design.

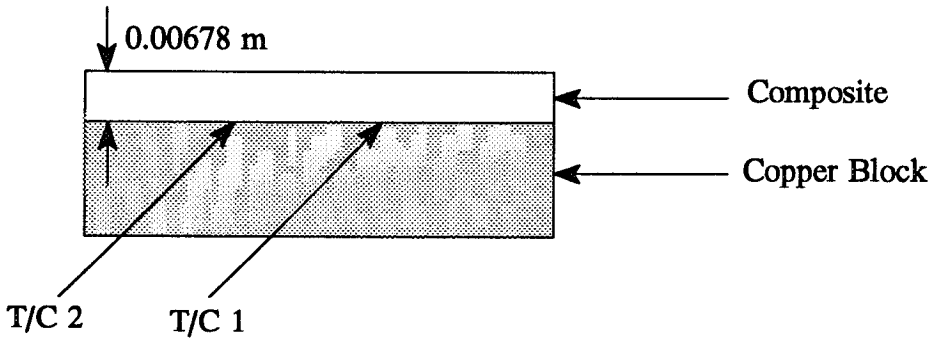

Figure 4.2. Sample 1 Placed on Top of the Copper Block for the One-Dimensional Experimental Design.

the thermocouples will be moved. Make sure that the contact is good.

5) Coat the other side of Sample 1 and again, place two thermocouples at this surface in the same manner as discussed previously.

6) Apply silicon grease to the heater on one side and place it on top of Sample 1. Be sure the heater is placed symmetrically over the sample so the same magnitude of heat flux is being distributed (see Fig. 4.3).

7) Coat the exposed top surface of the heater with the heat sink compound as before and place two more thermocouples at this surface, as described previously.

8) Coat Sample 2 (of approximately the same thickness as Sample 1) with silicon grease and place it on top of the exposed heater surface, over the thermocouples.

9) Coat the opposite side of Sample 2, place two more thermocouples as before on the surface, and finally, place a coated copper block over the composite sample (see Fig. 4.4).

10) Wrap the exposed sides of the composite material with rope insulation. Four pieces were used, two on each composite. If any thermocouple wire is exposed, tuck it inside of the insulation (see Fig. 4.5).

11) Carefully place the stacked samples between two plates and apply pressure evenly over the surface, taking care not to break the thermocouples. If thermocouples break, use less pressure. (Note, pressure was applied through threaded rods which ran through the corners of the plates).

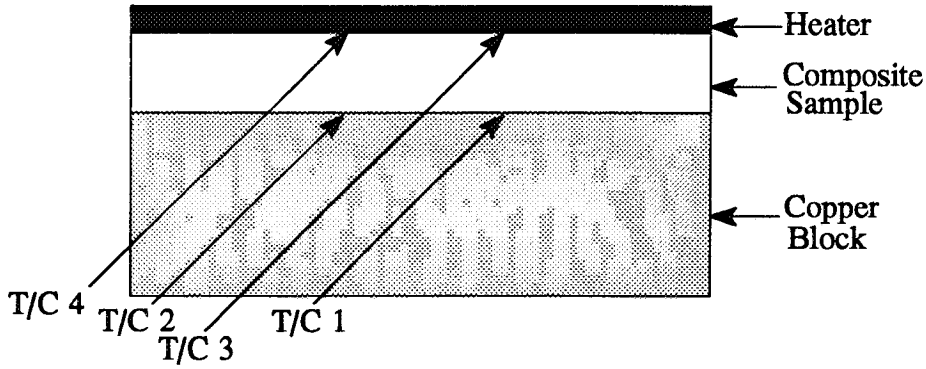

Figure 4.3. Position of the Heater and Thermocouples (T/C's) at the Heat Flux Boundary Condition for the One-Dimensional Experimental Design.

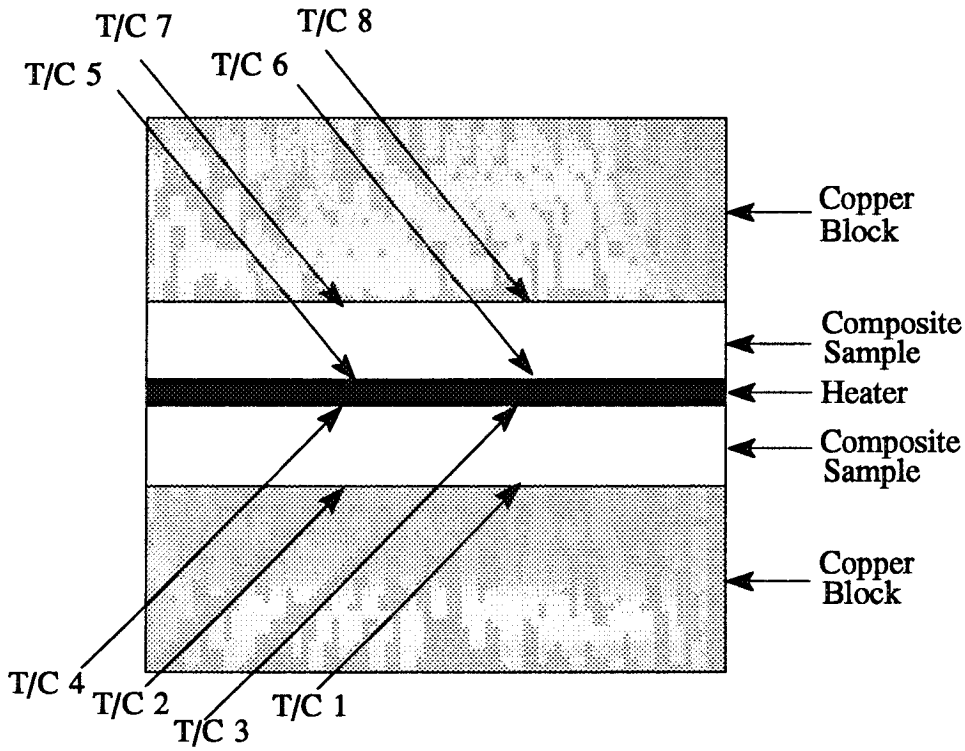

Figure 4.4. Final Assembly of the Experimental Apparatus for the One-Dimensional Experimental Design with Eight Thermocouples (T/C's).

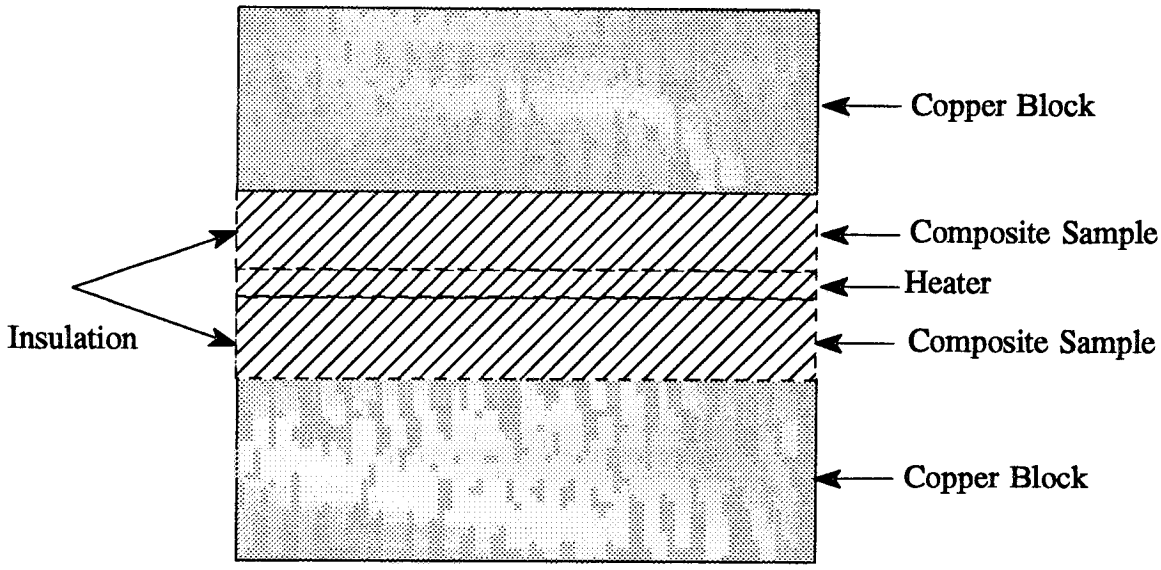

Figure 4.5. Insulation Wrapped Around the Heater and Composite Samples for the One-Dimensional Experimental Design.

4.1.1.2 Experimental Procedure

The experimental procedure consisted of applying a heat flux to a composite sample already at steady-state and then measuring the resulting temperatures using the data acquisition system. The process used for these experiments is given as follows:

1) Place the press containing the experimental set-up inside a temperature controlled oven. Connect the thermocouple wire to leads leading to a temperature compensator and data acquisition system. Heat the oven to the desired ambient temperature and allow the instrumented samples to equilibrate.
2) Activate the data acquisition system. Turn on the heater and simultaneously record temperature (mvolts) from thermocouples, and measured voltage and current to the heater. Turn the heater off after a pre-determined heating time and continue recording measurements until a pre-determined experimental time has elapsed.
3) If desired, the experiment can be repeated after the samples have again come to equilibrium with the oven temperature or the oven temperature can be changed and steps 1 and 2 can be repeated.

In these experiments, temperatures were recorded using eight Type K thermocouples at 0.5 second intervals up to a predetermined experimental time. All experiments were conducted at room temperature with the heater being applied for a predetermined heating time. (These times were determined using the optimal design criterion discussed previously). Experiments were conducted using three different voltage

inputs to the heater; 4.9V, 6.1V, and 7.3V. These resulted in maximum temperature rises of approximately 2°C, 3°C, and 4.5°C, respectively, over the initial temperature.

As mentioned, a one-dimensional heat conduction process through the composite sample was assumed. This assumption may introduce experimental error into the problem. However, to verify the validity of this assumption, the resistance to heat transfer was calculated both parallel and perpendicular to the direction of heat transfer. For one-dimensional heat conduction to be assumed, the parallel resistance should be much smaller than the perpendicular resistance, indicating that most of the heat will be conducted in one direction. To calculate the resistance in the direction of heat transfer, where only conduction through the sample is considered, the following equation was used:

$$R_{cond} = \frac{L_x}{k_{x\text{-}eff} A_x} \tag{4.1}$$

where A_x is the cross-sectional area normal to the direction of heat transfer, $k_{x\text{-}eff}$ is the effective thermal conductivity parallel to the direction of heat transfer and L_x is the thickness of the sample. For the resistance perpendicular to the direction of heat transfer, both conduction through the insulation material and convection with the air must be considered. The convective resistance is given as

$$R_{conv} = \frac{1}{hA} \tag{4.2}$$

where h is the convective heat transfer coefficient. As an extreme case, this resistance was calculated using a h of 10 W/m^2°C. This indicates that heat is lost through the insulation by convection to the surrounding air. Since the experiments were conducted

at room temperature, this h value is a good approximation for natural convection situations, as may be the case in this experiment. A thermal conductivity of 0.05 W/m°C was assumed for the insulation material used.

When performing these calculations, is was found that the resistance parallel to the direction of heat transfer is 7.3 °C/W while the resistance normal to this direction is 220 °C/W. Since the perpendicular resistance is much larger than the parallel resistance, the one-dimensional heat conduction assumption is valid.

Chapter 5

Results and Discussion

This chapter focuses on the results obtained for the optimal experimental design procedure for both the one-dimensional and two-dimensional analyses. In both cases, the experimental parameters were optimized using the technique described in Section 3.3. The thermal property estimates, effective thermal conductivity perpendicular to the fibers and effective volumetric heat capacity, obtained for the IM7 graphite fiber - Bismaleimide epoxy matrix composite are also discussed. These thermal properties were estimated using both the parameter estimation program, *MODBOX,* which requires an exact temperature solution and the finite element software, EAL, where the temperature solution is calculated numerically. In both cases, the properties were estimated using the modified Box-Kanemasu method described in Section 3.2.

The first and second sections of this chapter discuss the optimal experimental results obtained for the one-dimensional analysis and the estimated thermal properties found utilizing this design, respectively, while the last section discusses the optimal experimental results obtained for the two-dimensional configurations.

5.1 Results Obtained for the One-Dimensional Analysis (Isotropic Composite Material)

The thermal properties estimated for the one-dimensional analysis include the effective thermal conductivity perpendicular to the fiber axis, or the isotropic thermal conductivity, and the effective volumetric heat capacity. As mentioned in Section 3.2, measured temperatures were required for this estimation procedure; therefore, experiments had to be conducted. The next subsections discuss the results obtained for the optimization procedure used to determine the optimal experimental parameters utilized in these experiments. This includes an analysis of the sensitivity coefficients and the determination of the following experimental parameters: the heating time of the uniform heat flux, the temperature sensor location, and the total experimental time.

5.1.1 One-Dimensional Optimal Experimental Design

The minimization procedure used in this analysis to estimate the effective thermal properties is the Box-Kanemasu method. This method requires both measured and experimental temperatures. The experiments used to obtain the measured temperatures were optimized to provide more accurate property estimates. The optimization technique selected in this study, as discussed in Section 3.3, maximizes the determinant of the product of the dimensionless sensitivity coefficients and their transpose. Therefore, the first step in the optimization procedure is to calculate and analyze the sensitivity coefficients for each property. These coefficients are discussed next.

5.1.1.1 Sensitivity Coefficient Analysis

The first step in the optimization procedure was to calculate and plot the sensitivity coefficients. Recall that these coefficients are the derivatives of the temperature with respect to the unknown thermal properties and indicate the sensitivity of the temperature response due to changes in the parameters. In order for the thermal properties to be independently and accurately estimated, these coefficients should be large in magnitude (on the order of the temperature rise) and linearly independent. If the sensitivity coefficients are small, not enough information is available for the estimation procedure and if linear dependence exists between them, the parameters cannot be independently estimated. It is important to note, however, that the sensitivity coefficients may be linearly dependent over one range but independent over a different range. Knowing these ranges will help optimize the physical experiment.

The dimensionless sensitivity coefficients for the isotropic analysis are given by Eqs. (3.52-55). Figures 5.1 and 5.2 show the dimensionless sensitivity coefficients for the effective thermal conductivity ($X^+_{k_{x\text{-}eff}}$) and effective volumetric heat capacity ($X^+_{C_{eff}}$), respectively, at various positions within the composite. In Fig. 5.1, it is seen that after a dimensionless time of approximately three, all of the coefficients converge to a constant value. This indicates that temperature measurements taken beyond this dimensionless time supply little additional information for the estimation of $k_{x\text{-}eff}$. This same result also occurs for the effective volumetric heat capacity sensitivity coefficients (Fig. 5.2). Here, after a dimensionless time of approximately three, the coefficients converge to zero. To

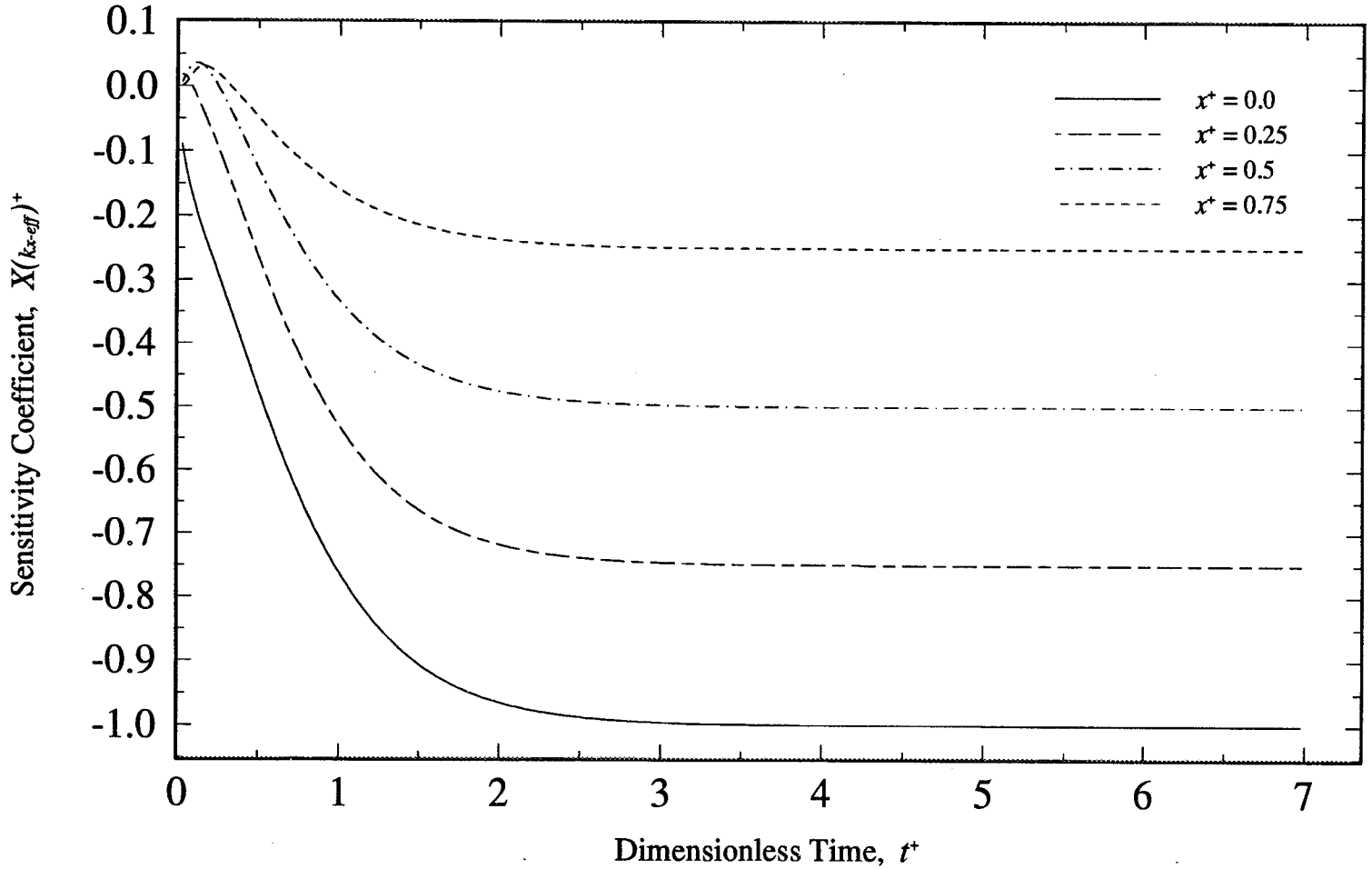

Figure 5.1. Transient Effective Thermal Conductivity Sensitivity Coefficients with the Heat Flux, $q_x(t)$, Applied for the Entire Experimental Time for Various x^+ (x/L_x) Locations.

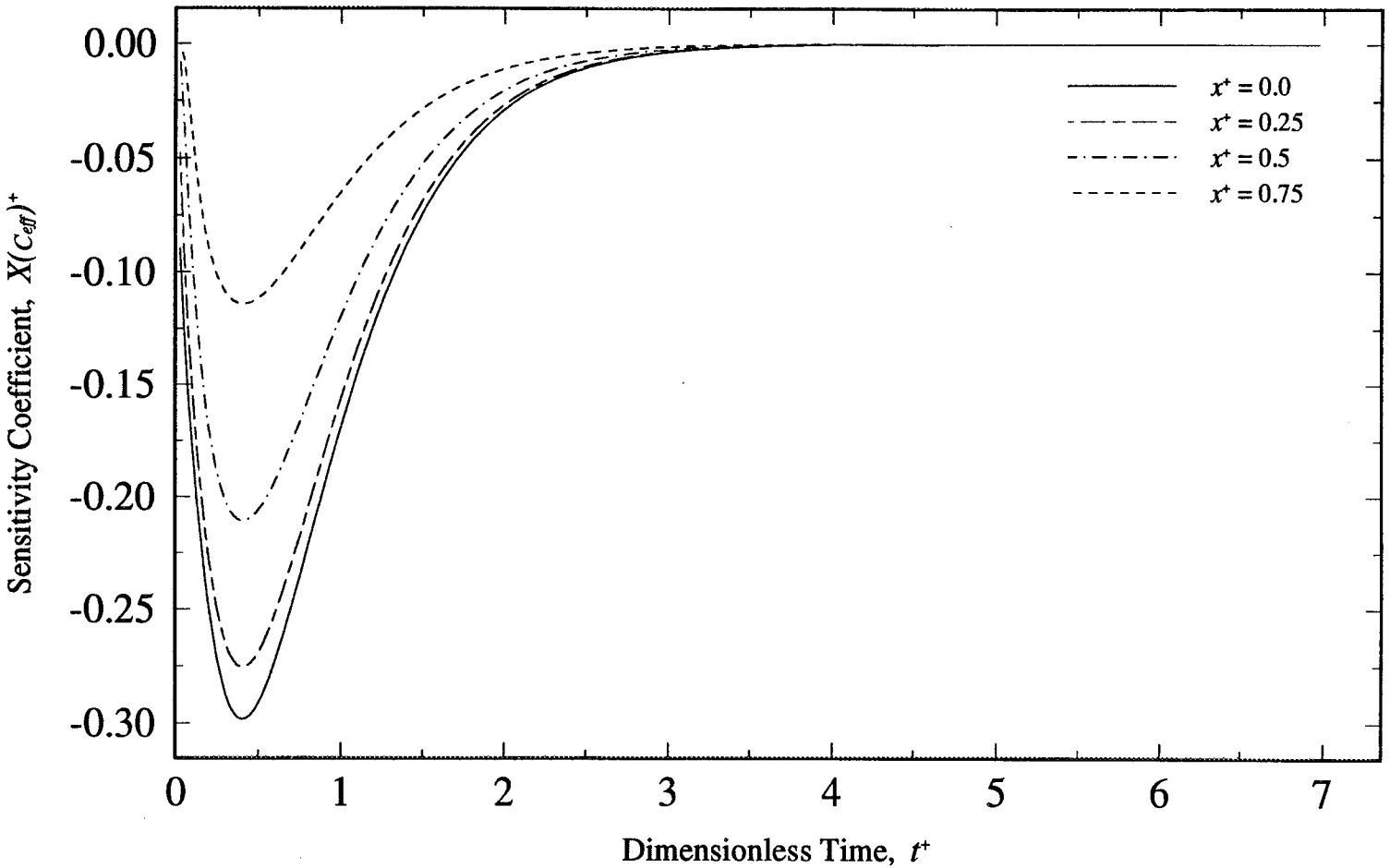

Figure 5.2. Transient Effective Volumetric Specific Heat Sensitivity Coefficients with the Heat Flux, $q_x(t)$, Applied for the Entire Experimental Time for Various x^+ (x/L_x) Locations.

more accurately estimate C_{eff}, the majority of the temperature measurements should be taken over the dimensionless time range of zero to three, where the magnitude of the sensitivity coefficients is largest. It is apparent from these figures that the coefficients with the largest magnitude occur at a dimensionless x^+ (defined as x/L_x) location of zero. This position corresponds to the heated surface in this analysis. However, it is also evident that the $X^+_{k_{x-eff}}$ have a larger magnitude than those for $X^+_{C_{eff}}$. This indicates that the temperature data provides more information about $k_{x\text{-}eff}$ than it does for C_{eff}, and therefore, the estimates of $k_{x\text{-}eff}$ will be more accurate than those for C_{eff}.

It should be noted that the sensitivity coefficients in Figs. 5.1 and 5.2 were calculated with the heat flux applied for the entire duration of the experiment. Because the volumetric heat capacity coefficients approach zero, it suggests that a better scheme may consist of applying the heat flux for a finite duration instead of for the entire experimental time. This confirms that observing the sensitivity coefficients can give insight into the accuracy of the experimental design.

As mentioned, if the sensitivity coefficients are linearly dependent, the thermal properties are correlated and cannot be simultaneously estimated. One way to determine if linear dependence exists is to plot the ratio of the sensitivity coefficients, as shown in Fig. 5.3 for an x^+ location of zero. In this figure, the ratio was plotted between the dimensionless time range of zero to three. (After this range, the volumetric heat capacity sensitivity coefficients converge to zero and the ratio becomes insignificant). If a constant curve occurs, the coefficients are linearly dependent. However, as evident from Fig. 5.3,

OPTIMAL EXPERIMENTAL DESIGNS FOR THE ESTIMATION OF THERMAL PROPERTIES OF COMPOSITE MATERIALS

An Annual Report
for Contract No. NAG-1-1507

to

NASA Langley Research Center
Hampton, VA

by

Elaine P. Scott
Assistant Professor

and

Deborah A. Moncman
Graduate Research Assistant

Department of Mechanical Engineering
Virginia Polytechnic Institute and State University
Blacksburg, VA 24061-0238

May 5, 1994

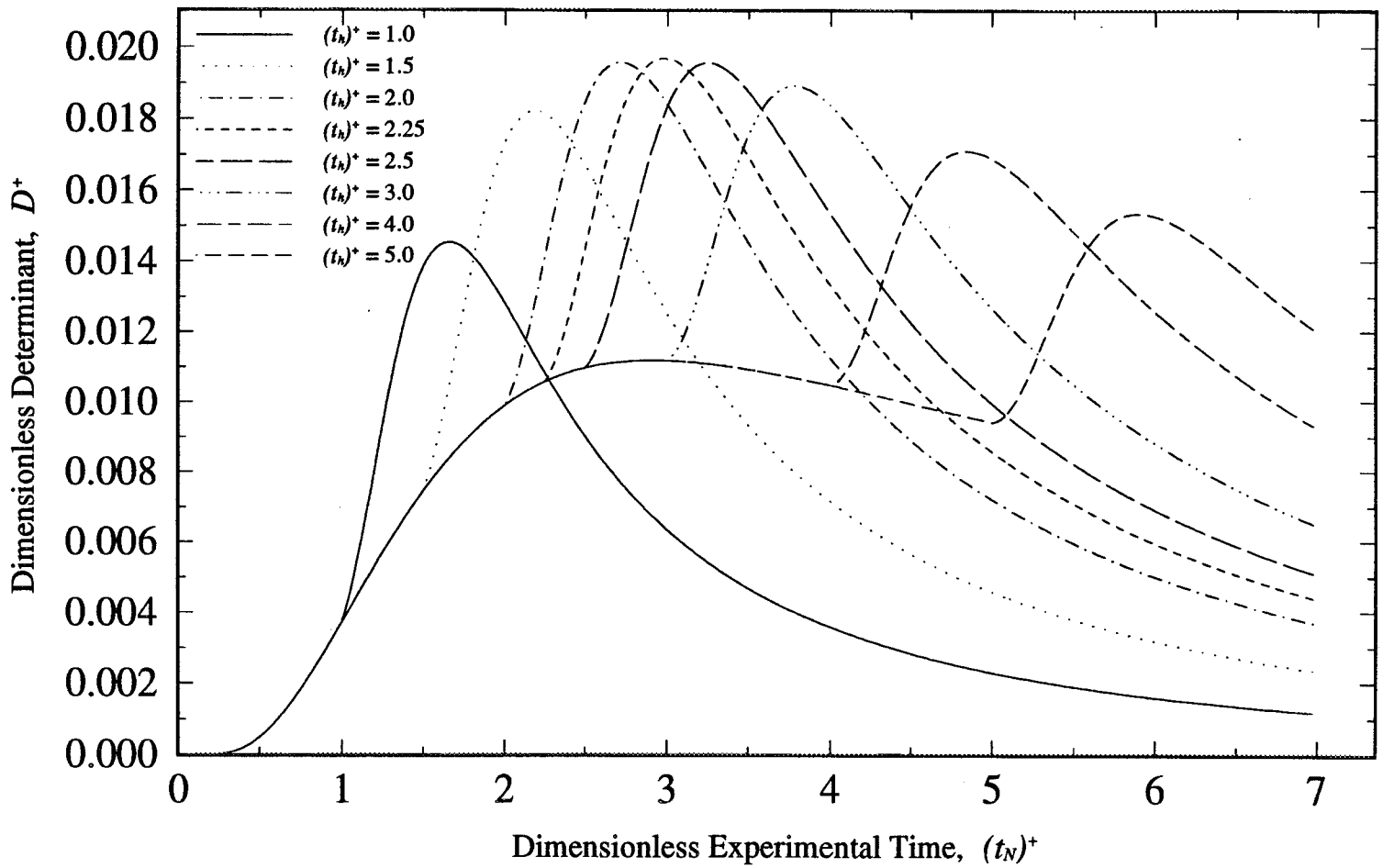

Figure 5.4. Dimensionless Determinant, D^+, for Various Dimensionless Heating Times, t_h^+, as a Function of Total Experimental Time, t_N^+.

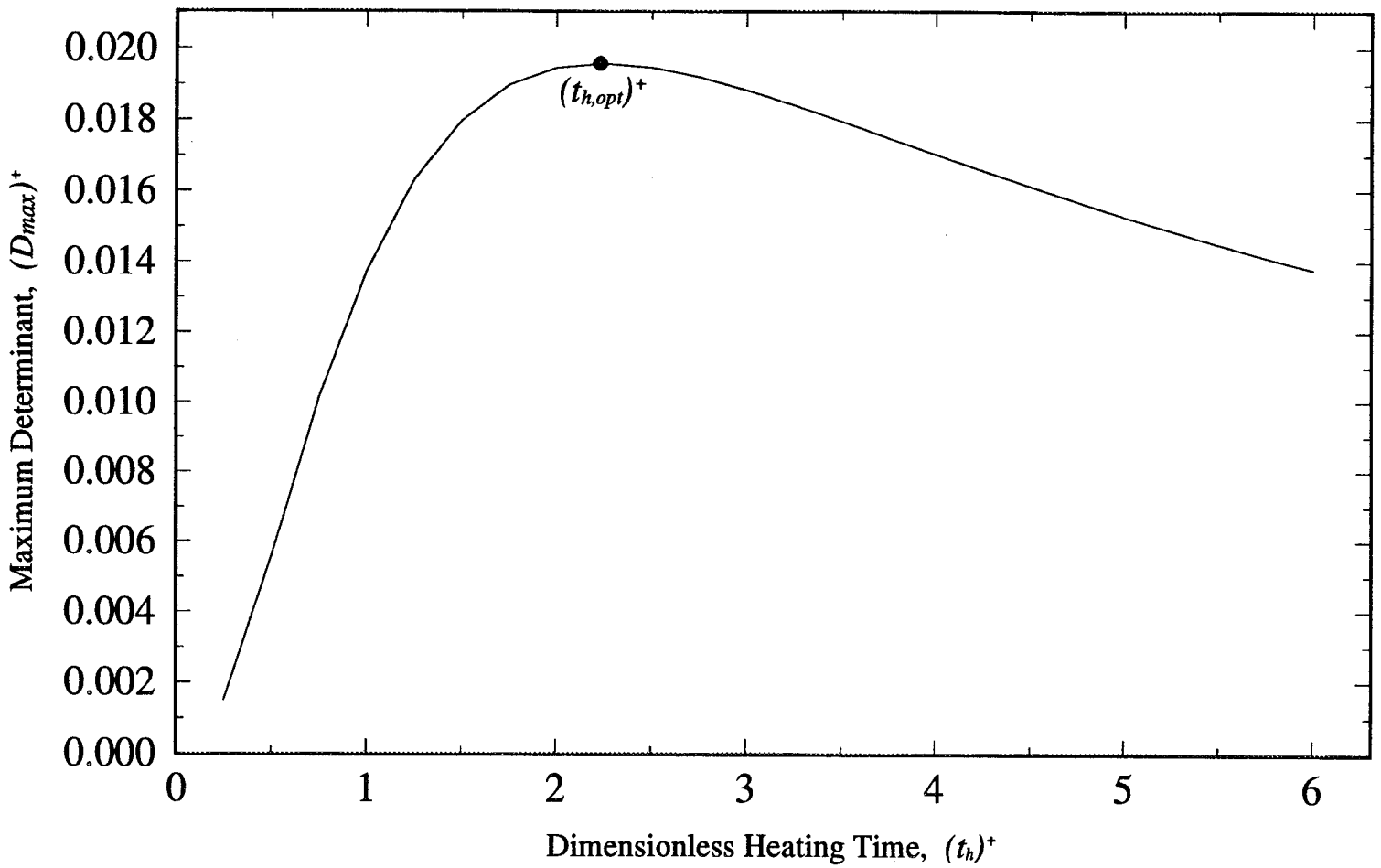

Figure 5.5. Maximum Dimensionless Determinant Curve, $D_{max}{}^+$, Used to Determine the Dimensionless Optimal Heating Time, $t_{h,opt}{}^+$.

$$t_h^+ = \frac{t_h \alpha_x}{L_x^2} \tag{5.1}$$

For this study, the thickness of the sample, L_x, was 6.78 mm. However, to determine α_x, $k_{x\text{-}eff}$ and C_{eff} are required, which are the unknown parameters being estimated. Therefore, the actual heating time can be estimated by using previous estimates of $k_{x\text{-}eff}$ and C_{eff} of other similar carbon-epoxy composite materials. The previous estimates used in this study were obtained from Scott and Beck (1992a). Using these values, the optimal heating time was calculated to be approximately 180 seconds. This value can be updated by conducting the experiments, obtaining new estimates for $k_{x\text{-}eff}$ and C_{eff}, recalculating the heating time using these new estimates, and repeating the process in an iterative procedure until the thermal properties no longer vary. However, as mentioned, a flat peak exists between heating times of 2.0 and 2.5. Therefore, the optimal heating time does not have to be precise to obtain the most accurate thermal property estimates.

5.1.1.3 Optimal Temperature Sensor Location

Next, the optimal temperature sensor location was determined by plotting the determinant as a function of heating time for various sensor locations (Fig. 5.6). It was found that the determinant is maximized when the sensor is located at the heated surface ($x^+ = 0.0$). This result is consistent with the sensitivity coefficients shown in Figs. 5.1 and 5.2, where the coefficients with the largest magnitude occurred at the heated surface. Note that by placing additional thermocouples at other positions within the composite will be redundant and will not supply more information for the estimation procedure.

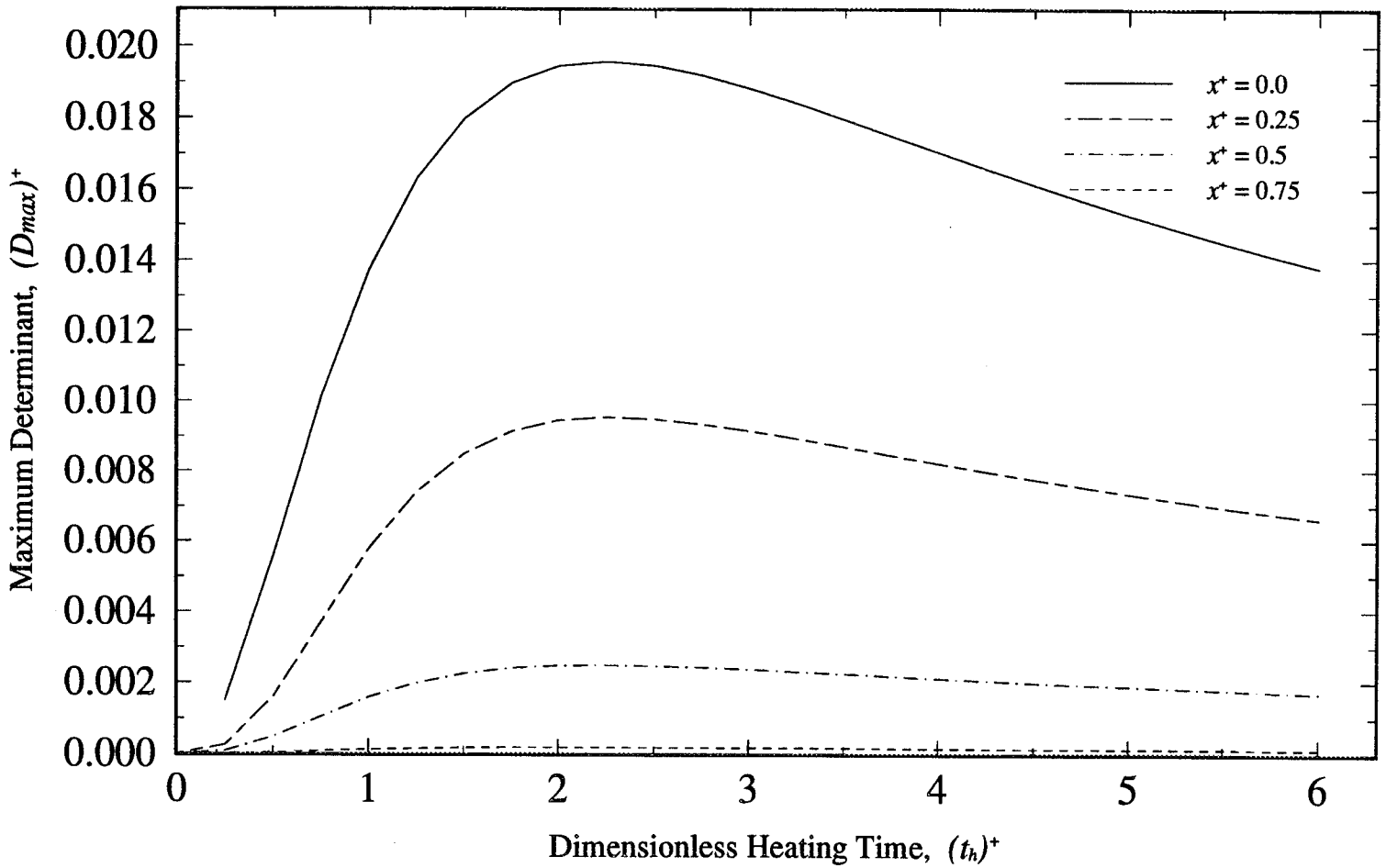

Figure 5.6. Determination of the Optimal Temperature Sensor Location, x^+ (x/L_x).

5.1.1.4 Optimal Experimental Time

The last parameter that was determined was the optimal experimental time. In order to see the effect of added data to the value of the determinant, D^+, the determinant was calculated from Eqs. (3.42) and (3.43) using the optimal heating time and sensor location previously found, but without averaging the integral contained in Eq. (3.43) over time. The results are shown in Fig. 5.7; here, it is evident that after a dimensionless time of approximately five, the determinant no longer changes significantly. This implies that after this dimensionless time, the temperature is reaching its initial state and little additional information is being provided for the estimation of the thermal properties. Therefore, the experiments can be concluded after a dimensionless time, t_N^+, of approximately five. Note that this is a conservative choice, however, and from Fig. 5.7, a smaller value, such as four, could have also been chosen. Again, the actual experimental time that t_N^+ represented was found by using the definition of t_N^+ (Eq. (3.44c)) and the previous estimates for $k_{x\text{-}eff}$ and C_{eff} (Scott and Beck, 1992a). The experimental time calculated for this study was approximately 8 minutes. However, when examining the measured temperatures obtained from the experiments, it is seen that its initial state (a dimensionless value of zero) is reached after approximately five to six minutes, indicating that no new temperature information is being supplied. This corresponds to a dimensionless experimental time of three to four, again showing that a t_N^+ of five is a conservative value.

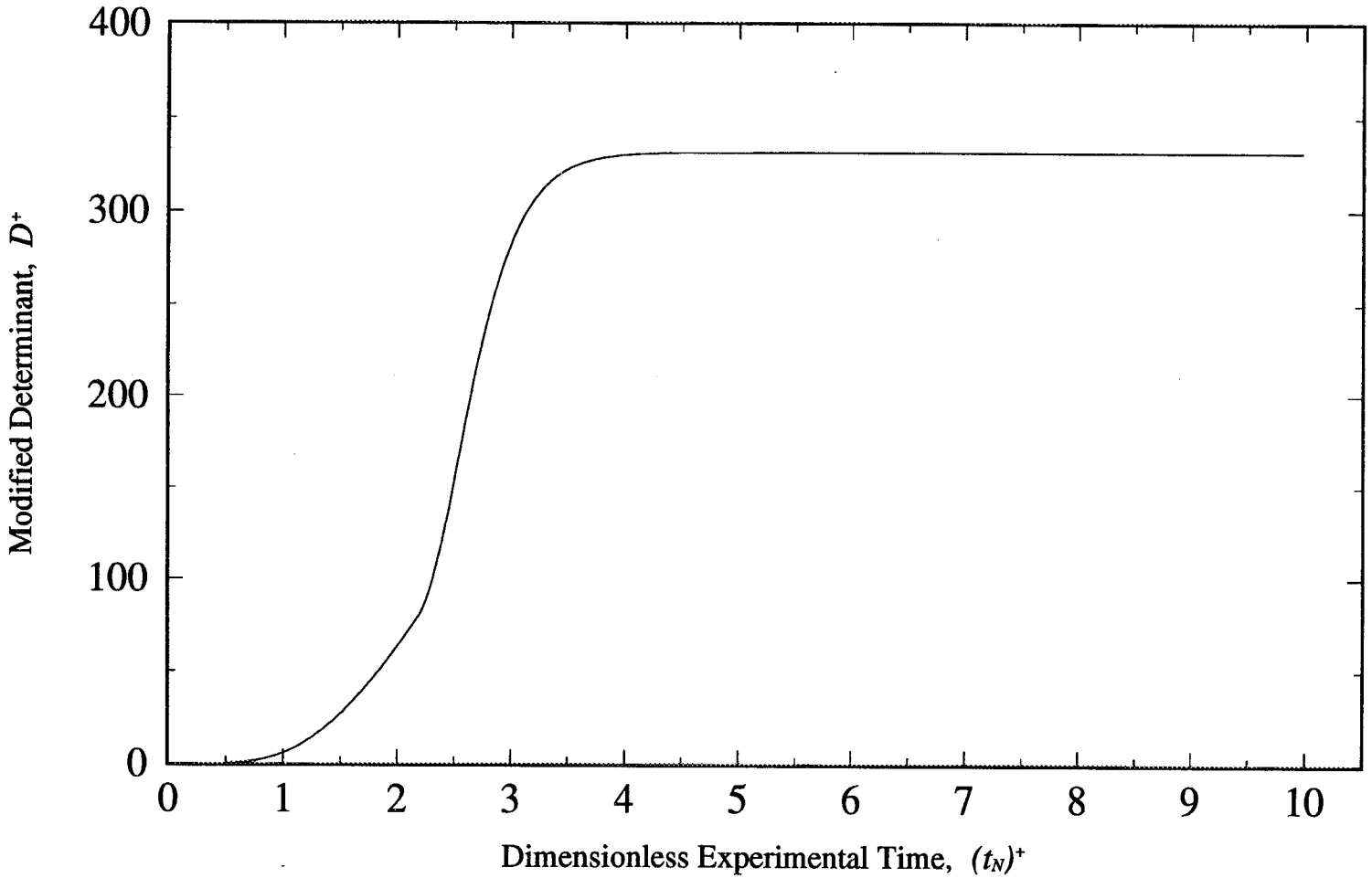

Figure 5.7. Modified Dimensionless Determinant, D^+, Used to Determine the Dimensionless Optimal Experimental Time, t_N^+.

5.1.1.5 Sensitivity Coefficient Using the Optimal Experimental Parameters

To illustrate the optimal results, the sensitivity coefficients were re-calculated using these optimal experimental parameters and are shown in Fig. 5.8 at an x^+ location of zero. As one can see from this figure, more information used to estimate the thermal properties is supplied when the heater is applied for the determined optimal heating time rather than over the entire experimental time. This occurs because when the heater is applied for the entire duration, steady-state values are reached early on and information is no longer available for the estimation of C_{eff}. However, when turning the heater off during the experiment, a new transient response is introduced which results in additional temperature information for the estimation procedure.

5.1.2 Estimation of Thermal Properties for Isotropic Materials

The thermal properties, effective thermal conductivity perpendicular to the fiber axis and effective volumetric heat capacity, were estimated for an IM7 graphite fiber - Bismaleimide epoxy matrix composite both analytically, using the program *MODBOX*, and numerically, utilizing the finite element software, EAL. In both cases, the modified Box-Kanemasu method was used in the estimation procedure. The properties were estimated using both experimental data and numerical and exact solutions so that the two could be compared and verification of the accuracy of EAL could be made. The estimated thermal properties obtained for the one-dimensional analysis are given in the following two subsections. In this analysis, the optimal experimental design previously determined was utilized to record the experimental temperatures required.

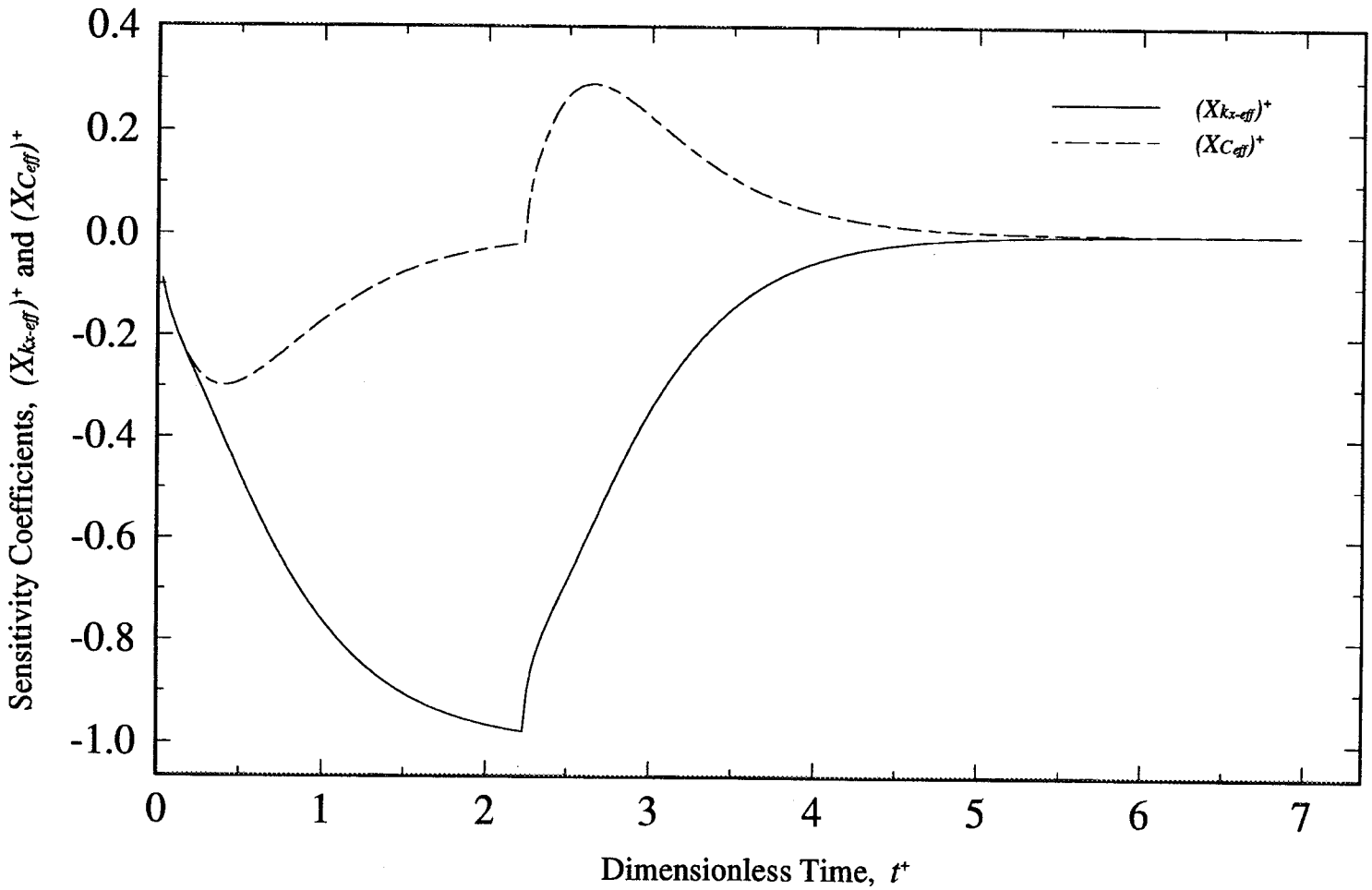

Figure 5.8. Transient Dimensionless Sensitivity Coefficients, $X^+_{k_{x\text{-}eff}}$ and $X^+_{C_{eff}}$, at an x^+ (x/L_x) Location of 0.0 Using the Dimensionless Optimal Heating Time, $t_{h,opt}{}^+$.

5.1.2.1 Estimated Thermal Properties Using an Exact Temperature Solution

The thermal properties, effective thermal conductivity perpendicular to the fiber axis and effective volumetric heat capacity, were estimated from an exact temperature model (Eqs. (3.8) and (3.9)) using the sequential, non-linear estimation program *MODBOX*. The estimates that were obtained for three repeated experiments are given in Table 5.1, along with their 95% confidence intervals. The confidence intervals for each estimated parameter, b_i, were approximated by

$$b_i \pm \left[P_{ii}\frac{S}{(N-p)}\right]^{1/2} t_{1-\alpha/2}(N-p) \tag{5.2}$$

where p is the number of parameters estimated, N is the number of data points measured, P_{ii} is the ith diagonal of the $\boldsymbol{P}$ matrix (Eq. (3.37)) which represents the variance of the parameter, S is the sum of the squared residuals, and $t_{1-\alpha/2}(N-p)$ is the value of the t distribution for $(1-\alpha/2)$ confidence region and $(N-p)$ degrees of freedom (Beck and Arnold, 1977). In this study, a considerable number of temperature measurements were taken and used in the estimation procedure; therefore, only a slight variance in the estimates would be expected. This is in fact the case, as shown by the small confidence intervals for each property estimate in Table 5.1. It is also seen that the confidence intervals for $k_{x\text{-}eff}$ were smaller than those for C_{eff}. This implies that the estimates for $k_{x\text{-}eff}$ are more accurate than for C_{eff}. This is consistent with the sensitivity coefficients (Figs. 5.1 and 5.2), where the magnitude of the effective volumetric heat capacity sensitivity coefficients is less than that of the effective thermal conductivity. Therefore, the

estimation of C_{eff} is more sensitive to experimental errors and will not be as accurate as estimates for $k_{x\text{-}eff}$.

The mean value of the thermal property estimates was also calculated, along with its 95% confidence interval. In this case, the 95% confidence intervals were obtained from

$$\bar{b}_i \pm \frac{t_{\alpha/2}\, s}{\sqrt{N}} \tag{5.3}$$

where $\bar{b}_i$ and s are the mean and standard deviation of the estimate, respectively, N is the number of data points used, and $t_{\alpha/2}$ is the value of the t distribution with $(N\text{-}1)$ degrees of freedom and $\alpha/2$ confidence region (Walpole and Myers, 1978). As seen in Table 5.1 for all three experiments, the property estimates fall within the 95% confidence intervals of the mean values.

To determine how accurately the calculated temperatures matched the measured temperatures, the Root Mean Square (*RMS*) error was also computed where

$$RMS = \sqrt{\frac{\sum_{i=1}^{n_i} (Y_i - T_i)^2}{N}} \tag{5.4}$$

Here, T_i and Y_i are the calculated and measured temperatures, respectively, at the ith time step, and N is the total number of temperature measurements. The *RMS* values were calculated two different ways. First, the measured temperatures for each individual experiment were compared with calculated values using the thermal properties estimated for that experiment; these values are indicated by RMS_1 in Table 5.1. The *RMS* values

were then determined using the experimental temperatures and calculated temperatures determined using the mean thermal property values (also shown in Table 5.1); these values are indicated by RMS_M.

To demonstrate the validity of the estimated properties, the calculated temperatures obtained using the estimated effective thermal conductivity and effective volumetric heat capacity values were compared with the measured temperatures for Experiment 3 in Fig. 5.9. As one can see, there was very good agreement between the calculated and measured temperatures which indicates that the estimated values are reliable.

The significance of the RMS_M values, or the errors resulting from using the mean

Table 5.1 Estimated effective thermal conductivity, $k_{x\text{-}eff}$, and volumetric heat capacity, C_{eff}, from Experiments 1, 2, and 3, using exact temperature solutions along with the Root Mean Square error calculated from individual and mean thermal property estimates (RMS_I and RMS_M).

	Exp. 1	Exp. 2	Exp. 3	Mean
$k_{x\text{-}eff}$ (W/m°C)	0.519 ± 0.002	0.506 ± 0.002	0.529 ± 0.003	0.518 ± 0.028
C_{eff} (MJ/m^3°C)	1.423 ± 0.013	1.505 ± 0.012	1.495 ± 0.008	1.474 ± 0.111
RMS_I (°C)	0.0526	0.0815	0.0652	
% Maximum Temperature Rise	0.24%	0.36%	0.26%	
RMS_M (°C)	0.0548	0.0908	0.0827	
% Maximum Temperature Rise	0.34%	0.40%	0.34%	

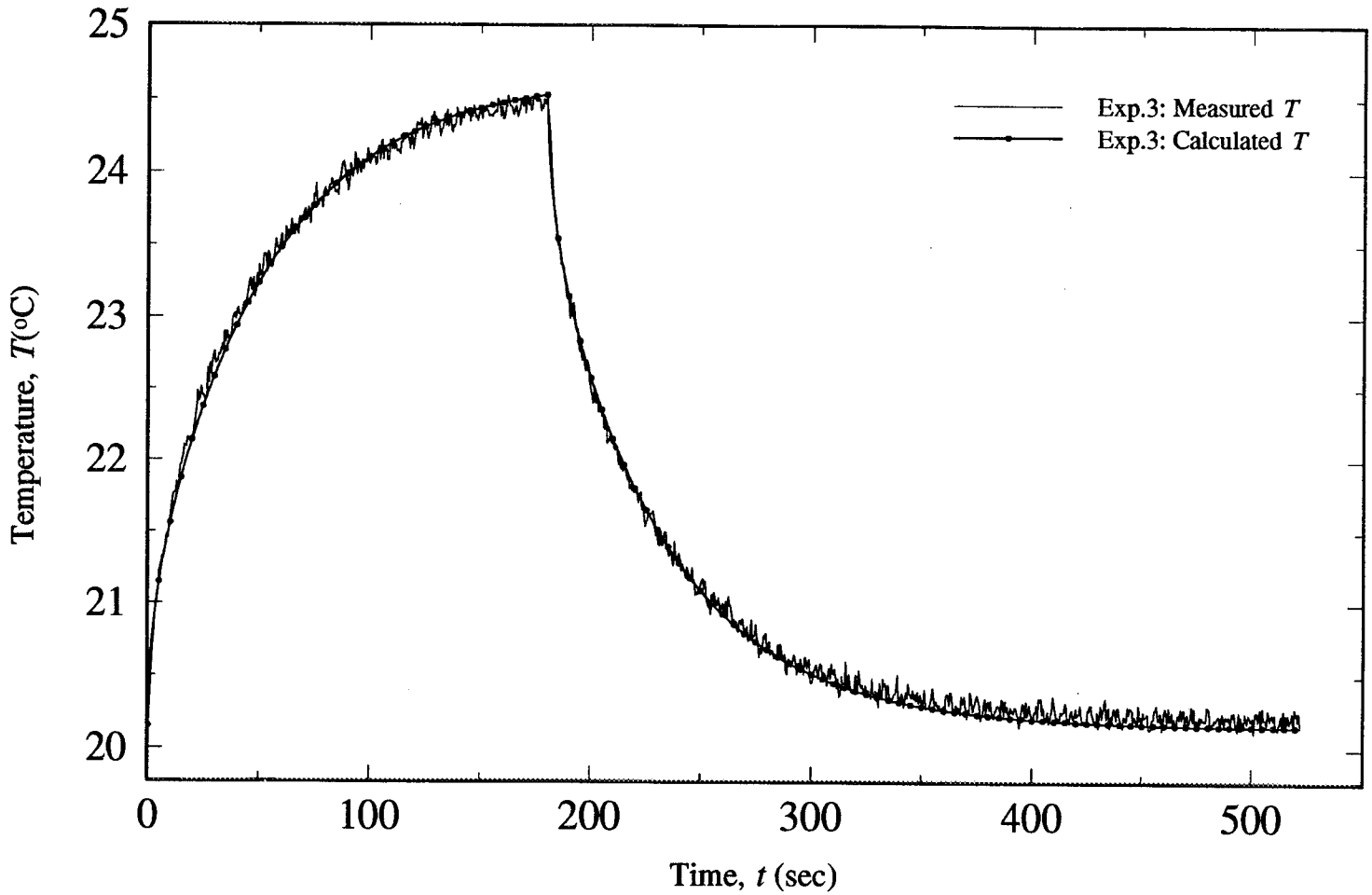

Figure 5.9. Calculated and Measured Temperature (T) Profiles for Exp. 3

thermal property estimates, was demonstrated by plotting the temperatures calculated using the mean thermal property estimates against each set of experimental data in Fig. 5.10. From this figure, it is evident that in each case, the calculated temperatures closely match the measured temperatures. Furthermore, in comparing Table 5.1 with Fig. 5.10, the slight under prediction of temperature in Experiment 2 and the slight over prediction of temperature in Experiment 3 can be attributed to the small differences between the individual estimated effective thermal conductivity and the mean value, with the thermal conductivity estimate for Experiment 2 being slightly under the mean and the value for Experiment 3 being slightly over the mean value. However, even with these slight variations, the RMS_M as a percentage of the maximum temperature rise for each run was less than 0.5%, as shown in Table 5.1. This indicated that for all three cases, the mean values provided reasonable estimates of the true thermal property values. It also indicates that the model used to describe this heat conduction process, as well as the experimental design used to obtain the temperature data, are satisfactory.

The estimate obtained for the effective thermal conductivity was compared with results obtained at NASA-LaRC using a cut-bar comparative apparatus (Dynatech, model number TCFCM-N4). This device operates by supplying a steady state heat flow in one dimension across the composite sample and the same heat flow through a known standard material. The temperature difference across the standard material allows for the determination of the heat flux, while the temperature difference across the sample gives the value of the effective thermal conductivity. Using this apparatus, experiments were conducted on three composite samples that were the same type studied in this analysis.

C-2

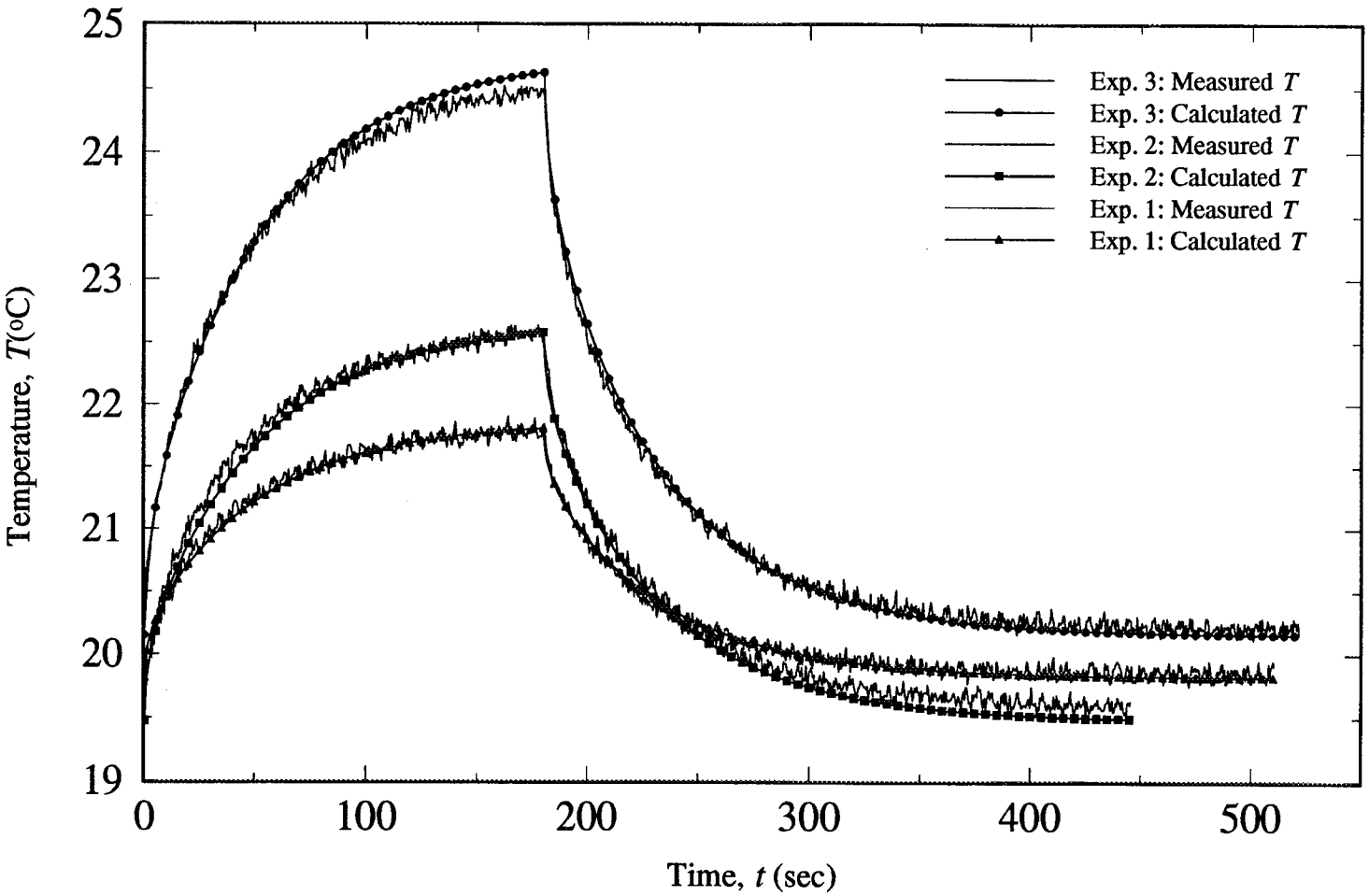

Figure 5.10. Temperature (T) Profiles for Both Experimental and Calculated Measurements Using Average Thermal Property Estimates.

The average result obtained for these three composite samples for the thermal conductivity was 0.473 ± 0.038 W/m°C. This is approximately a 9% difference from the average $k_{x\text{-}eff}$ estimated in this study. However, these experiments were conducted at 40°C, whereas in this investigation, the experiments were performed at room temperature; therefore, an exact comparison cannot be made.

5.1.2.2 Estimated Thermal Properties Using a Numerical Temperature Solution

The thermal properties were also estimated using EAL, where the temperatures were calculated numerically. Again, the modified Box-Kanemasu estimation technique was employed. The results obtained for the estimated effective thermal conductivity perpendicular to the fibers and effective volumetric heat capacity for the three experiments are shown in Table 5.2, along with the % difference from the estimates obtained using the exact temperature solutions. This % difference is defined as

$$\left(\frac{\beta_{EAL} - \beta_{Exact}}{\beta_{Exact}} \right) x\ 100\% \tag{5.5}$$

where β is the parameter being estimated. As one can see from Table 5.2, the estimates found using EAL closely match those obtained using exact temperature models with a percent difference of less than 1% occurring. The effective volumetric heat capacity estimates had the largest percent differences and resulted because this property is more difficult to estimate than the thermal conductivity. As mentioned, this occurs because the magnitude of the sensitivity coefficients for C_{eff} are less than those for $k_{x\text{-}eff}$, causing the estimation of C_{eff} to be more sensitive to experimental errors and to not be as accurately

Table 5.2 Estimated effective thermal conductivity, $k_{x\text{-}eff}$, and volumetric heat capacity, C_{eff}, from Experiments 1, 2, and 3, using numerical temperature solutions (from EAL) along with the % difference from estimates calculated using exact temperature models.

	Exp. 1	Exp. 2	Exp. 3	Mean
$k_{x\text{-}eff}$ (W/m°C)	0.518	0.503	0.527	0.516
% Difference	0.19%	0.59%	0.38%	0.39%
C_{eff}(MJ/m^3°C)	1.420	1.495	1.486	1.467
% Difference	0.21%	0.66%	0.60%	0.49%

estimated as $k_{x\text{-}eff}$.

From Table 5.2, it can be concluded that the estimated parameters found using the finite element software, EAL, are quite accurate and provide reasonable estimates of the true thermal property values.

To verify the accuracy of the temperature solution found using EAL, based on the estimated parameters, the temperature profile was plotted along with the temperature distribution calculated using an exact analytical solution, as shown in Fig. 11. Here, it is seen that the two curves are essentially equal, and therefore, using EAL provides reliable temperatures. This is also shown by calculating the *RMS* value, as given in Eq. (5.4), where Y_i is the temperature calculated from an exact solution and T_i is the temperature calculated from EAL. For the experiment shown in Fig. 5.11, the *RMS* value was only 0.27%, again indicating the accuracy of EAL.

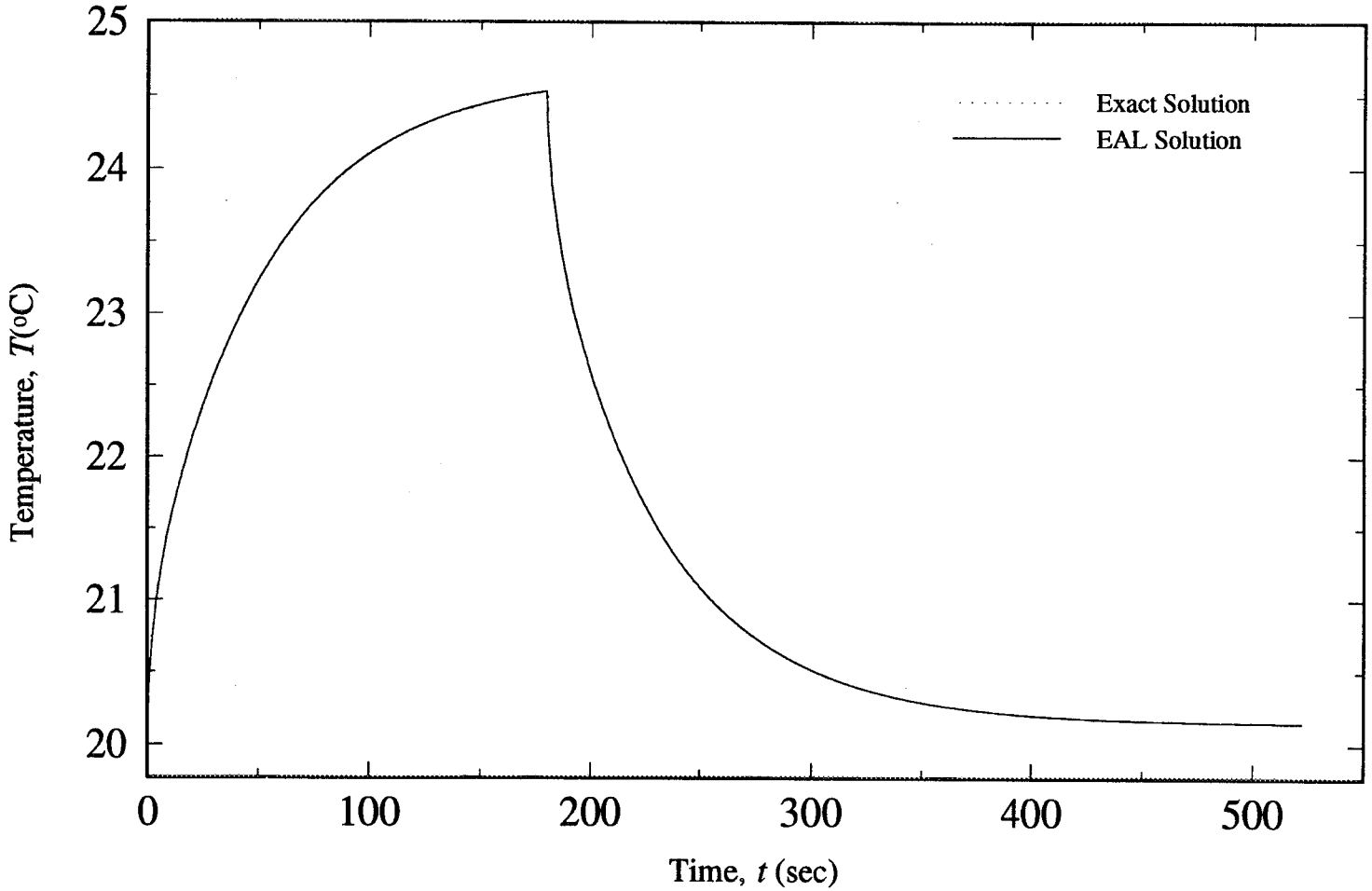

Figure 5.11. Temperature (T) Profile Using Both an Exact Solution and EAL.

5.1.2.3 Sequential Parameter Estimates

Viewing the sequential parameter estimates can give insight on the validity of the mathematical model used to represent the heat conduction process and the resulting experimental design. The sequential estimates for the converged values of the thermal conductivity and volumetric heat capacity for Experiment 3 are plotted in Fig. 5.12; these estimates were obtained using exact mathematical models. From this figure, it is evident that each estimate fluctuated greatly towards the beginning of the experiment. This occurred because the heat flux had just been activated and not enough temperature information was available for the estimation procedure. However, after approximately 400 seconds which corresponds to a dimensionless experimental time of approximately three, the estimates for both the thermal conductivity and volumetric heat capacity are constant, indicating that additional data would have provided little additional information for the estimation of these parameters. This also indicates that the heat conduction model is satisfactory and the optimal experimental time of five is indeed a conservative value, as discussed previously.

5.2 Results Obtained for the Two-Dimensional Analysis (Anisotropic Composite Material)

For the two-dimensional analysis, three properties can be estimated simultaneously: effective thermal conductivity perpendicular to the fiber axis ($k_{x\text{-}eff}$), effective thermal conductivity parallel to the fiber axis ($k_{y\text{-}eff}$), and effective volumetric heat capacity (C_{eff}).

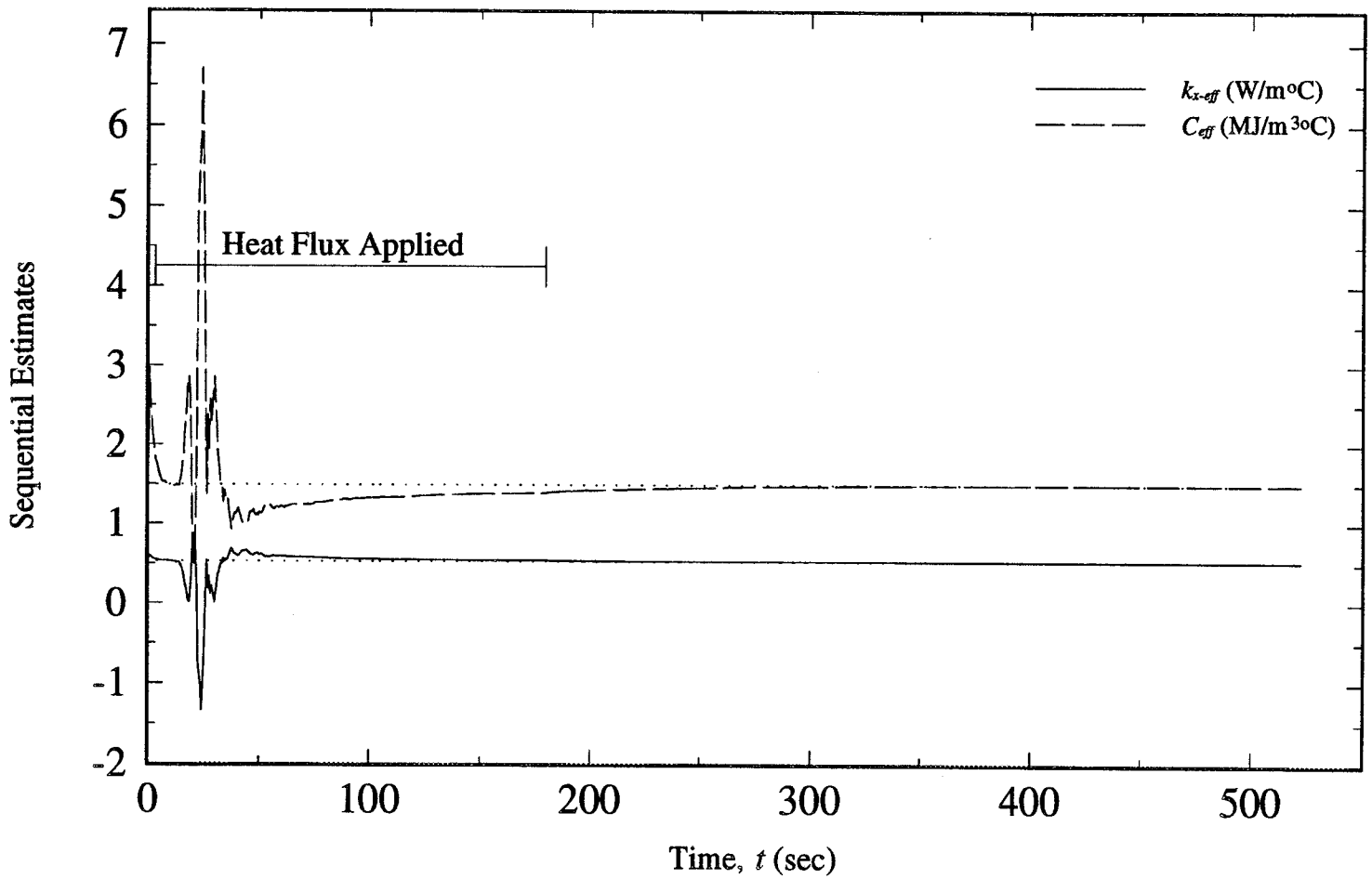

Figure 5.12. Sequential Estimates for Effective Thermal Conductivity, $k_{x\text{-}eff}$ (W/m°C) and Effective Volumetric Heat Capacity, C_{eff} (MJ/m^3°C).

In this investigation, these thermal properties are not estimated; however, the experimental designs used to obtain the temperature data required for the estimation procedure are optimized, as in the one-dimensional analysis. Discussed next are the results obtained for these optimal experiments.

5.2.1 Two-Dimensional Optimal Experimental Designs

Two different two-dimensional experimental configurations were analyzed in this study, each containing different boundary conditions. The experimental parameters for both configurations were optimized by maximizing the determinant of the product of the sensitivity coefficients and their transpose. The maximum determinant values for both configurations were then compared to determine which design would be the best choice; the configuration with the largest determinant value would give the most accurate property estimates. Recall that both configurations had a uniform heat flux imposed over a portion of one boundary with the remainder of the boundary insulated. In addition, Configuration 1 had known, constant temperatures at the remaining three boundaries, while the second configuration had a constant temperature at the boundary opposite to the flux boundary and insulated conditions at the remaining two boundaries. (For clarity, these configurations are again shown in Figs. 5.13 and 5.14). Therefore, in addition to the optimal parameters determined for the one-dimensional case, the optimal position of the heat flux was also determined for both configurations. Because of the different boundary conditions used, the optimal experimental parameters for each design will not be identical. For example, the portion of the boundary that the heat flux should cover

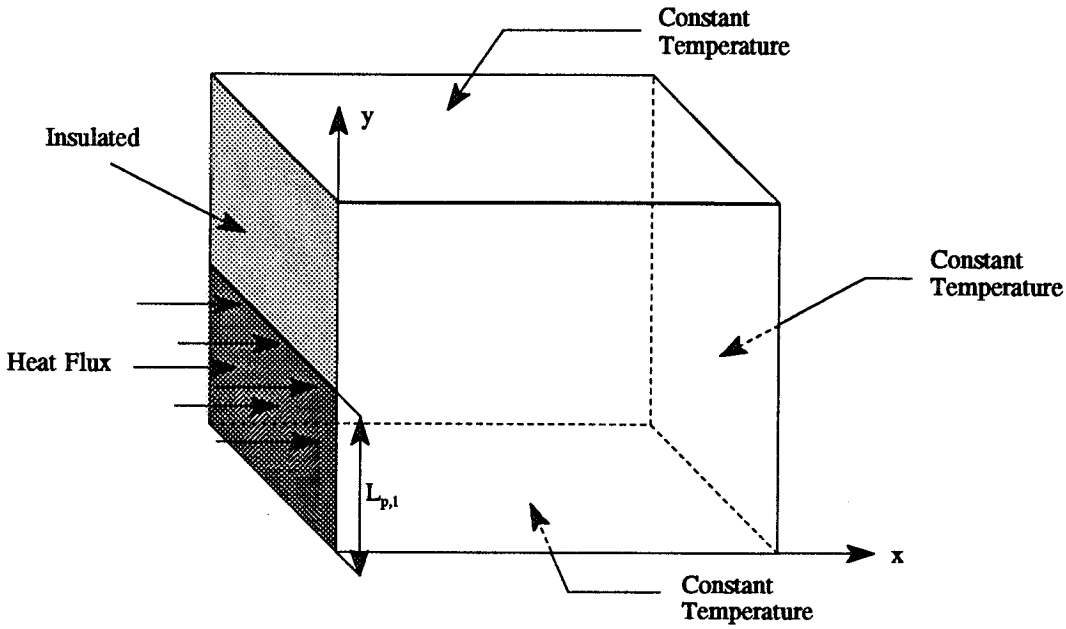

Figure 5.13. Experimental Set-up Used for Configuration 1 in the Estimation of the Effective Thermal Conductivities in Two Orthogonal Planes.

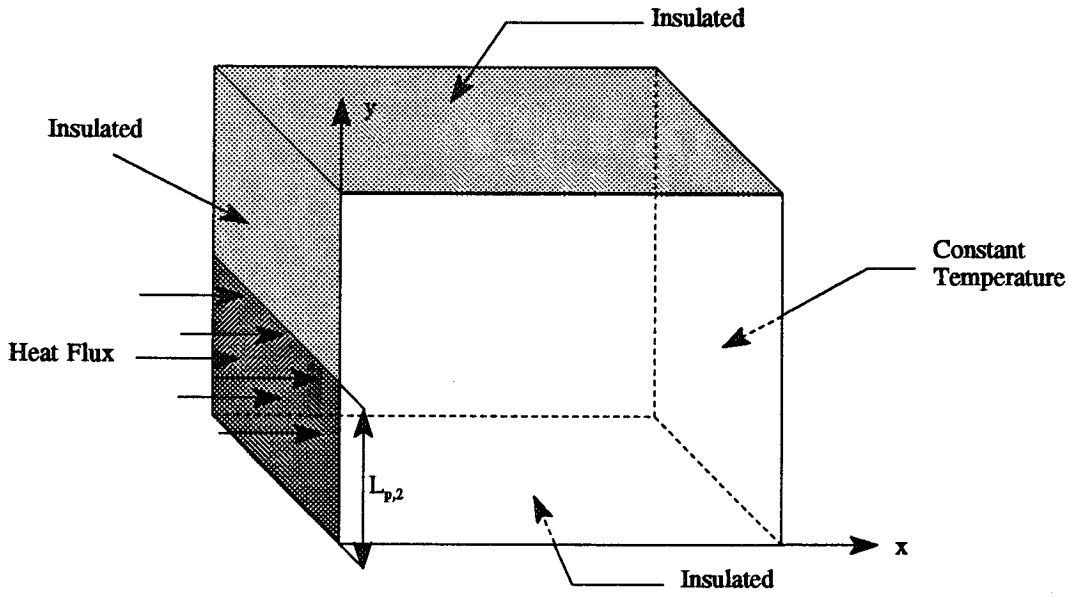

Figure 5.14. Experimental Set-up Used for Configuration 2 in the Estimation of the Effective Thermal Conductivities in Two Orthogonal Planes.

will vary between the two configurations, and therefore, must be determined for each individual design. The optimal parameter results for both configurations are discussed in the following two subsections. These include the optimal heating time, optimal temperature sensor location, optimal heat flux position, and optimal experimental time. In addition, the sensitivity coefficients for both configurations are analyzed for insight into the experimental design and to determine if possible correlation exists between the thermal properties. The two configurations are then compared to determine which will provide more accurate property estimates, and finally, the last subsection discusses the optimal values for various composite dimension (L_{xy}) and thermal conductivity (κ_{xy}) ratios.

5.2.1.1 Optimal Experimental Parameters Determined for Configuration 1

Using Configuration 1, it was desired to select the experimental parameters which maximize the sensitivity of the temperature with respect to all of the unknown thermal properties. The same technique was used as in the one-dimensional optimization procedure, only now, the required maximum temperature value (T_{max}^{+}) was redefined as the temperature attained at steady state. This T_{max}^{+} was used because it represents the actual maximum temperature that could be reached for this particular design.

To perform the optimization procedure, the temperature solutions and sensitivity coefficients require predetermined values for L_{xy} (L_x/L_y) and κ_{xy} ($k_{y\text{-}eff}/k_{x\text{-}eff}$). The value chosen for L_{xy} in this analysis corresponds to the size (0.49 cm x 10.16 cm) of an existing composite sample that can be used in the experiments to determine the temperatures needed in the estimation procedure, while the value for κ_{xy} was taken from previously

measured effective thermal conductivities parallel and perpendicular to the fiber axis of similar carbon-epoxy composite samples (Loh and Beck, 1991). The specific values used were L_{xy} = 0.048 and κ_{xy} = 7. However, to allow the optimization procedure to be applicable to other composite dimensions or effective thermal conductivity ratios, optimal experimental parameters were also calculated for all possible combinations of L_{xy}'s equal to 0.5 and 1.0, and κ_{xy}'s equal to 1 and 1/7. This results in a total of nine combinations. The results for the combination discussed above (L_{xy} = 0.048 and κ_{xy} = 7) will be examined the most thoroughly, however, since these are the actual conditions of an existing composite sample that can later be utilized in the experimental designs to estimate the thermal properties.

In performing the optimization procedure for L_{xy} = 0.048 and κ_{xy} = 7, five parameters were optimized: the dimensionless portion of the boundary that the heat flux is applied, $L_{p,1}^+$, the dimensionless location (x_s^+,y_s^+) of the temperature sensor, the dimensionless heating time, t_h^+, and the dimensionless experimental time, t_N^+. Note that the optimal experimental time is not as important as the other four parameters. Therefore, the optimal procedure used to determine x_s^+, y_s^+, $L_{p,1}^+$, and t_h^+ did not take into account the optimization of t_N^+ (this value was determined last).

The most accurate way to determine the optimal value for each parameter is to differentiate the determinant given in Eq. (3.45) with respect to each of the experimental parameters and set it equal to zero, resulting in four equations and four unknowns. These equations can then be solved simultaneously, allowing for the desired optimal parameters to be determined. However, this method is not practical due to the complexity of the

equations involved. Therefore, an iterative scheme was developed where a program was used to vary each of the four parameters individually (excluding t_N^+). This iterative procedure consists of two phases; the first phase includes determining the general range of the optimal values, while the second phase narrows this range to determine the optimal experimental parameters more precisely. In phase one, the following procedure was used:

1) Fix x_s^+, y_s^+, and $L_{p,1}^+$ to their starting values (0.0, 0.0, and 0.1, respectively).

2) Vary t_h^+ from 0.05 to 5.0 by 0.05. For each t_h^+, calculate the determinant, D^+, as a function of time, t^+.

3) Determine the maximum determinant value, D_{max}^+, for each of the determinant curves generated in step 2 for each t_h^+.

4) Compare the maximum determinant values found for each t_h^+ and record the one with the largest magnitude, along with its corresponding heating time, t_h^+.

5) Holding y_s^+ and $L_{p,1}^+$ constant at their original values, vary x_s^+ and repeat steps 2 through 4. Note, x_s^+ was varied from 0.0 to 1.0 by 0.1 increments.

6) After the x_s^+ loop is completed, change y_s^+ to its new value (increment the previous value by 0.1) holding $L_{p,1}^+$ fixed and again repeat steps 2 through 5. Note, y_s^+ was varied from 0.0 to 1.0 by 0.1 increments.

7) Finally, change $L_{p,1}^+$ to its new value (increment the previous value by 0.1) and repeat steps 2 through 6 in the designated order.

This procedure then provides a maximum determinant value for all combinations of x_s^+, y_s^+ and $L_{p,1}^+$, with the corresponding t_h^+. From this data, the general region of the actual

maximum determinant can be determined. Phase two then involves refining the grid sizes for the parameters in this region to determine the D_{max}^{+} location more precisely. Since there is more than one parameter that can vary, the procedure is more complex than the one-dimensional analysis, and must be iteratively updated.

5.2.1.1.1 Optimal Temperature Sensor Location on the x^+ Axis

The first optimal parameter determined was the temperature sensor location along the x^+ direction. Recall from the experimental configuration (Fig. 5.13) that this is the direction parallel to the heat flow. From the one-dimensional analysis, it was determined that the optimal location to place the sensor was at the heated surface. Therefore, the same result would be expected for the two-dimensional analysis. This was in fact the case, with the maximum determinant always occurring at a x_s^+ location equal to zero (or at the heat flux boundary) for all combinations of $L_{p,1}^+$ and y_s^+. This result is reasonable because the maximum determinant occurs when the sensitivity coefficients are the largest, or when the greatest temperature variation occurs. Since the temperature of the composite is initially at a dimensionless value of zero, then at the boundary where the uniform heat flux is applied would be the location where the largest temperature gradient in the x^+ direction would occur.

5.2.1.1.2 Optimal Temperature Sensor Location on the y^+ Axis

The next parameter chosen to optimize was the sensor location along the y^+ axis. After calculating the maximum determinant value for each x_s^+, y_s^+, and $L_{p,1}^+$ combination

and determining that the optimal sensor location along the x^+ axis was at the heated surface, it was found that the true maximum determinant (the largest value of all of the maximum determinants for each combination) was in the general region of y_s^+=0.1, $L_{p,1}^+$=1.0, and t_h^+=1.35. However, it should be noted that for all $L_{p,1}^+$ locations, the maximum determinant always occurred at y_s^+ equal to 0.1 with a t_h^+ of approximately 1.35. Using the optimal values of $L_{p,1}^+$=1.0 and t_h^+=1.35, the grid size for y_s^+ was refined around 0.13, using a range from 0.05 to 2.0, to determine the optimal y_s^+ location more precisely. Using this refined range, the maximum determinant occurred at a new y_s^+ location of 0.13, as shown in Fig. 5.15, where the maximum determinant values for various y_s^+ locations are plotted (again, using $L_{p,1}^+$=1.0 and t_h^+=1.35). It should be noted that when the heat flux is applied across the entire boundary ($L_{p,1}^+$=1.0), the problem becomes symmetric. Therefore, a y_s^+ of 0.87 would also be an optimal location, resulting in the same maximum determinant value as for y_s^+ equal to 0.13.

5.2.1.1.3 Optimal Heating Time

The next parameter determined was the optimal heating time. Using the optimal location for y_s^+ found above of 0.13 and the corresponding $L_{p,1}^+$ of 1.0, the dimensionless heating times were varied around the previously determined optimal value of t_h^+=1.35 (ranging from 0.05 to 2.0). The maximum determinant then occurred at a new t_h^+ of 1.4, as seen in Fig. 5.16, where the maximum determinants are plotted for various t_h^+ values. As mentioned, since more than one parameter can vary, determining the optimal

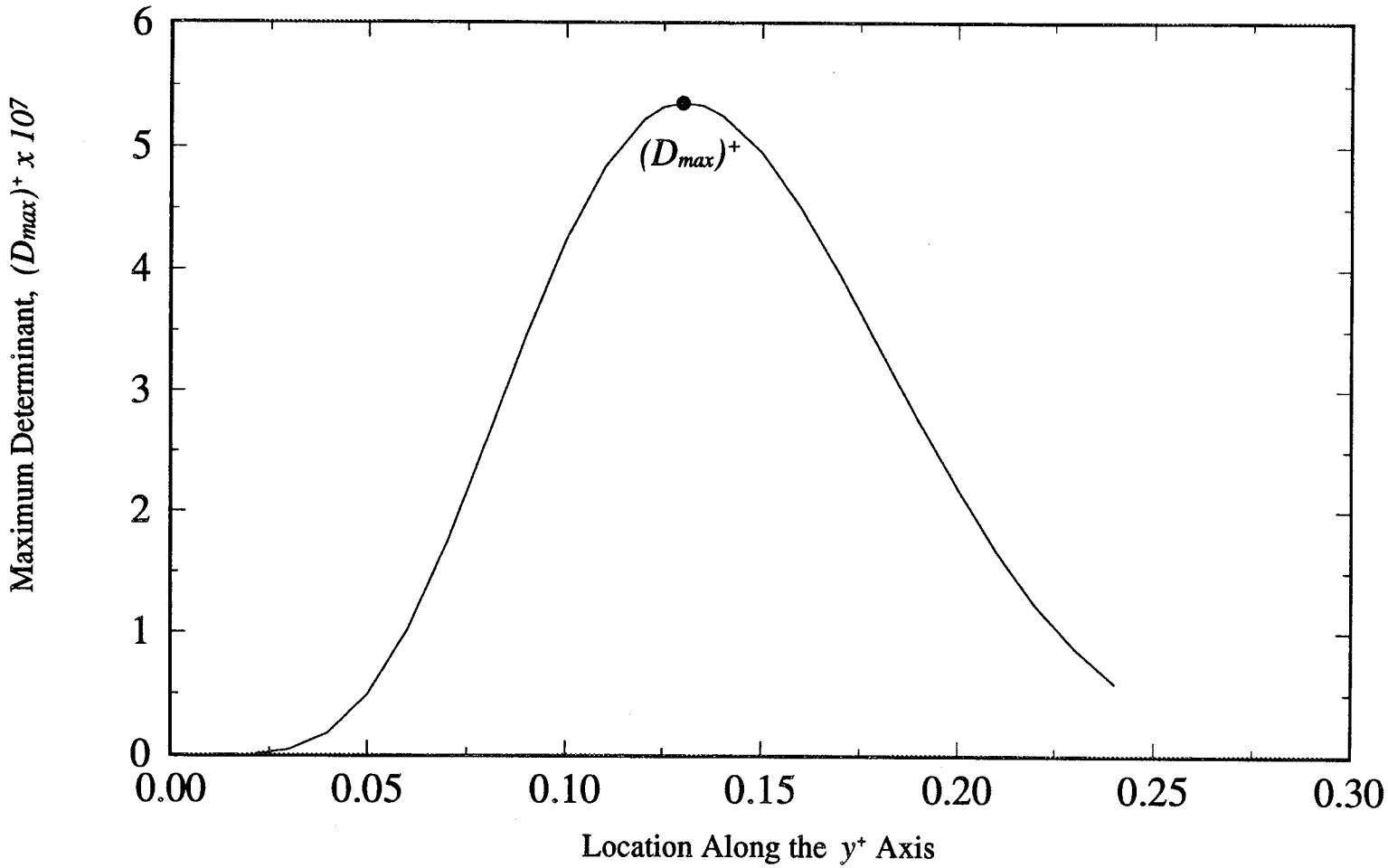

Figure 5.15. Maximum Determinant, $D_{max}{}^+$, for Various Locations Along the y^+ (y/L_y) Axis Calculated Using the Optimal Values of $x_s{}^+$=0.0, $L_{p,1}{}^+$=1.0, and $t_h{}^+$=1.35.

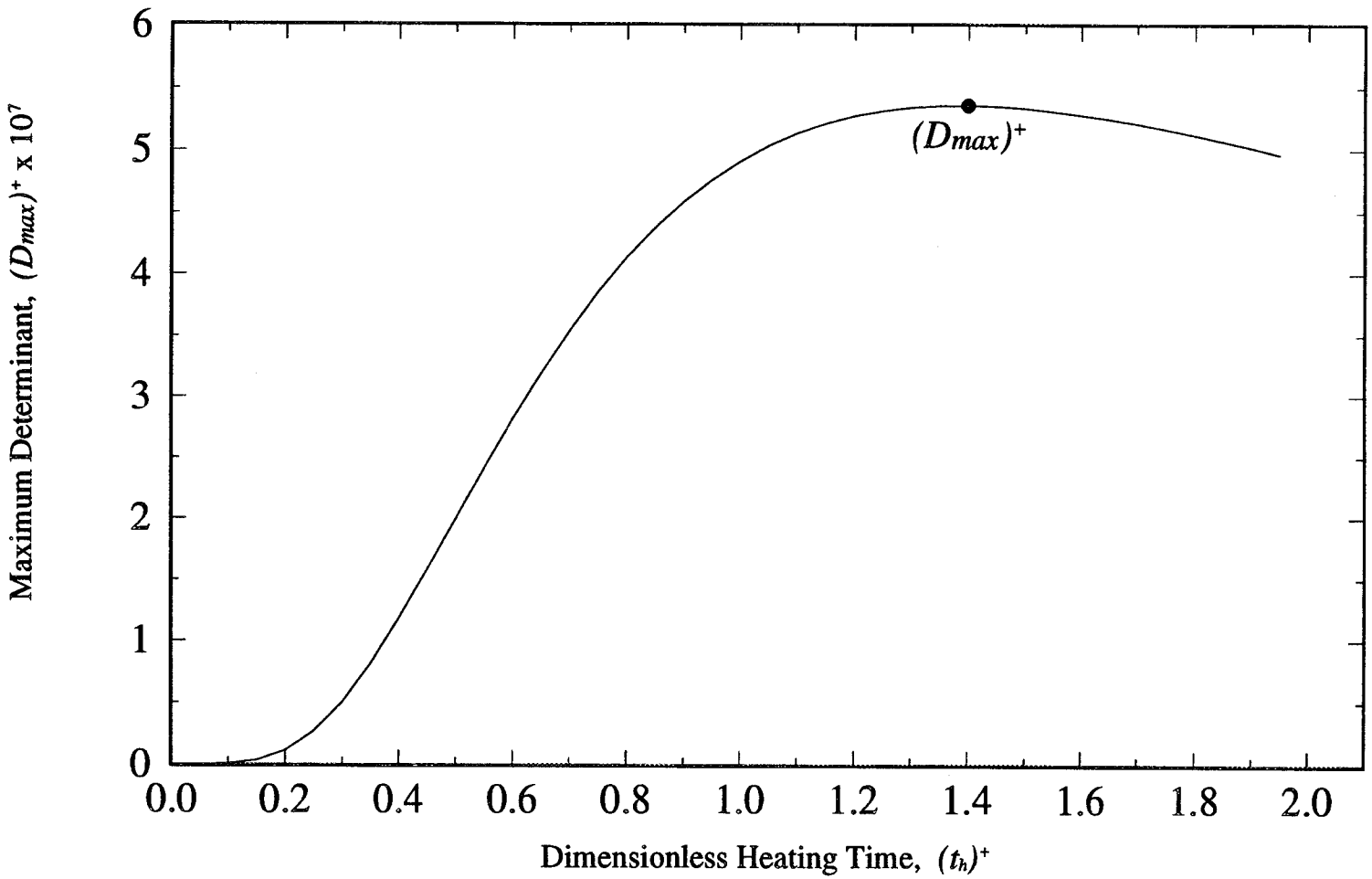

Figure 5.16. Maximum Determinant, D_{max}^+, for Various Heating Times, t_h^+, Calculated Using the Optimal Values of x_s^+=0.0, $L_{p,1}^+$=1.0, and y_s^+=0.13.

parameters for the actual maximum determinant becomes an iterative process. Therefore, since a new t_h^+ was determined, the y_s^+ values were again varied over the same range (0.05 to 2.0) using the new heating time of 1.4 (and the previously calculated optimal value for $L_{p,1}^+$ of 1.0) to see if its optimal value changed. However, as seen in Fig. 5.17, changing the heating time from 1.35 to 1.4 did not alter the optimal y_s^+ value of 0.13.

5.2.1.1.4 Optimal Heat Flux Location, $L_{p,1}^+$

Using the optimal parameters determined of x_s^+=0.0, y_s^+=0.13, and t_h^+=1.4, the position of the heat flux, $L_{p,1}^+$, was then varied from 0.6 to 1.0 to see if the previous optimal location of $L_{p,1}^+$=1.0 changed when using these new y_s^+ and t_h^+ values. This result is shown in Fig. 5.18. As seen in this figure, the maximum determinant occurred at a $L_{p,1}^+$ location of 1.0, as obtained previously. This indicates that the optimal design for Configuration 1 consists of having the heat flux applied over the entire boundary. However, it is evident that the curve in Fig. 5.18 is rather flat when the heater is applied over 70 to 100% (0.70 to 1.0) of the boundary, and therefore, any value in this range could be used to obtain the same accuracy in the property estimates.

5.2.1.1.5 Optimal Experimental Time

Finally, the last parameter determined was the optimal dimensionless experimental time, t_N^+. This was calculated using the same procedure as for the one-dimensional analysis, where the dimensionless determinant, D^+, was calculated from Eqs. (3.42) and (3.43) using the optimal parameters determined for x_s^+, y_s^+, $L_{p,1}^+$, and t_h^+, but without

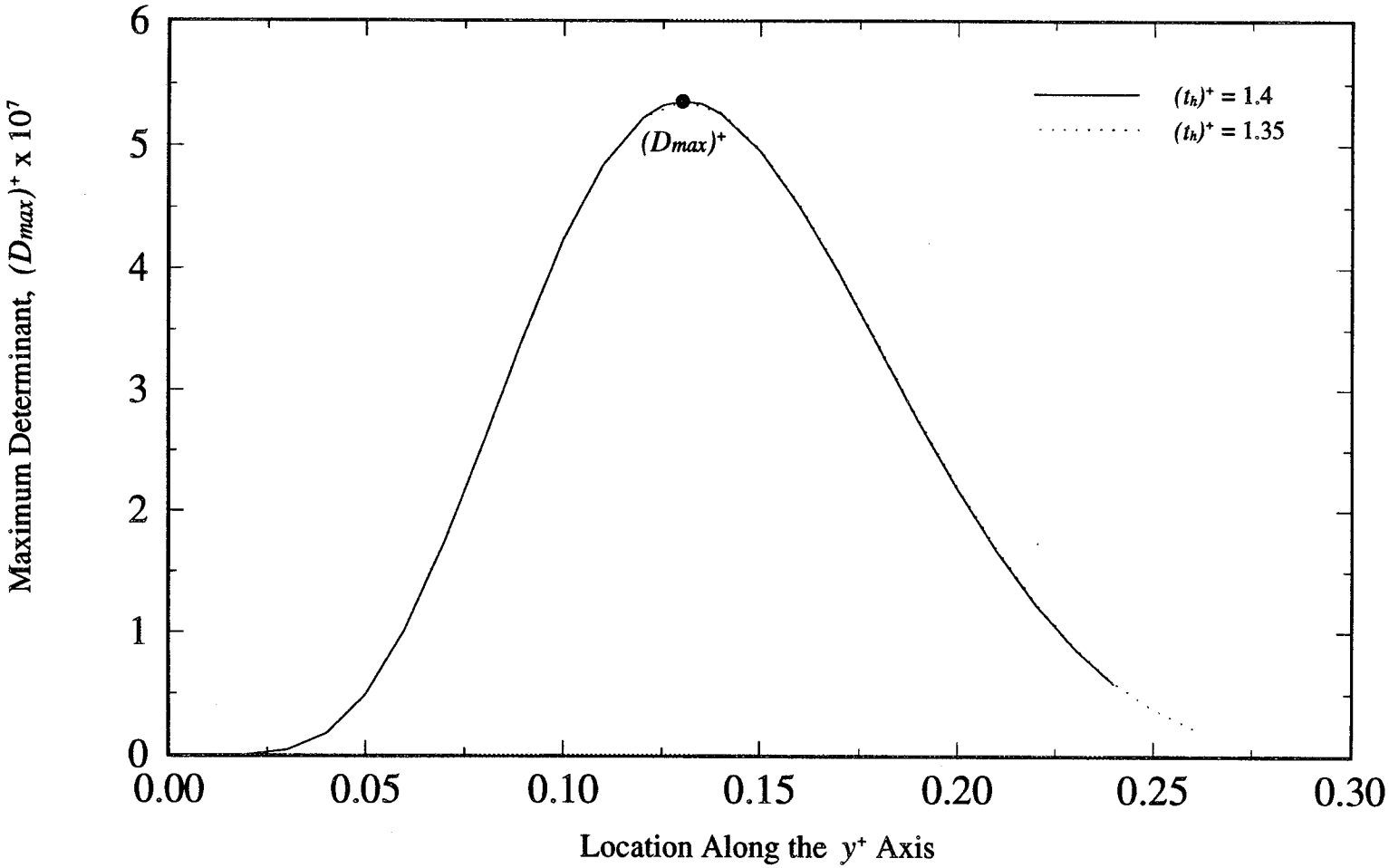

Figure 5.17. Maximum Determinant, $D_{max}{}^+$, for Various Locations Along the y^+ (y/L_y) Axis Calculated Using the Optimal Values of $x_s{}^+$=0.0, $L_{p,1}{}^+$=1.0, and $t_h{}^+$=1.35 (Second Iteration).

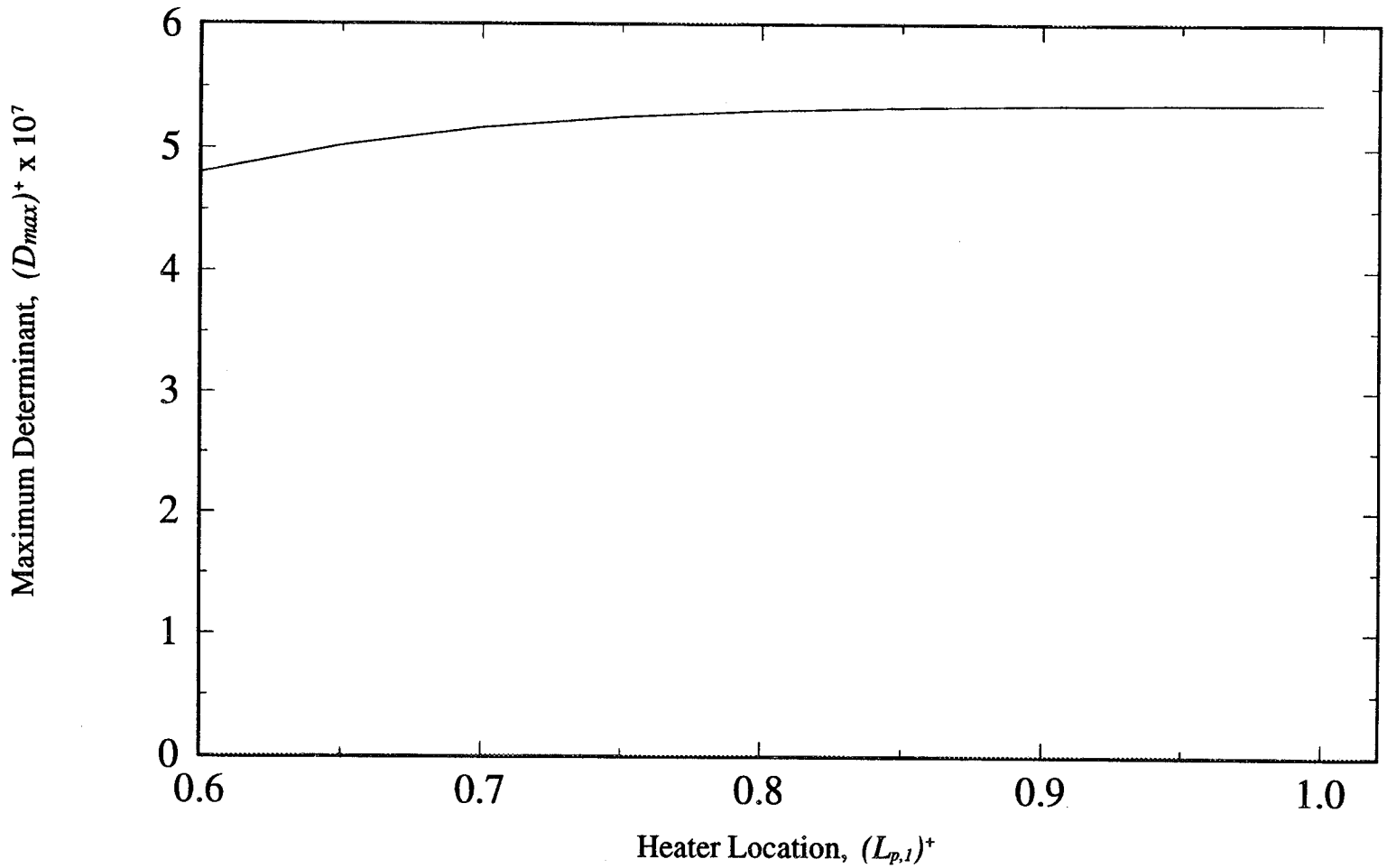

Figure 5.18. Maximum Determinant, D_{max}^+, for Various Heater Locations, $L_{p,1}^+$ ($L_{p,1}/L_y$), Calculated Using the Optimal Values of x_s^+=0.0, y_s^+=0.13, and t_h^+=1.4.

averaging the integral contained in Eq. (3.43) over time. The results are shown in Fig. 5.19; here, it is evident that after a dimensionless time of approximately 4.0, the determinant no longer changes significantly. This implies that after this dimensionless time, the temperature is returning to its initial state (a dimensionless value of zero) and little additional or no information is being provided for the estimation of the thermal properties. Therefore, the experiments can be concluded after a dimensionless time, t_N^+, of approximately 4.0. Again, however, as in the one-dimensional case, this is a conservative choice, and a smaller value, such as 3.5, could have also been chosen.

5.2.1.1.6 Verification of the Optimal Temperature Sensor Location of the x^+ Axis

To verify the optimal location of the temperature sensor along the x^+ direction, for which a value of zero was determined, the dimensionless determinant was calculated using the optimal values for y_s^+, $L_{p,1}^+$, and t_h^+ for various x_s^+ locations. The results are plotted in Fig. 5.20 against dimensionless time. As seen from this figure, the maximum determinant occurred when the sensor was at the heated surface ($x_s^+ = 0.0$), confirming the optimal result obtained for the x_s^+ location.

5.2.1.1.7 Maximum Determinant Using the Optimal Experimental Parameters

In summary, the above optimization procedure resulted in the following optimal experimental parameters for Configuration 1: x_s^+=0.0, y_s^+=0.13, $L_{p,1}^+$=1.0, and t_h^+=1.4. Using these optimal experimental parameters, the dimensionless determinant, D^+, was plotted versus dimensionless time, where a maximum of 5.36 x 10^{-7} occurred, as shown

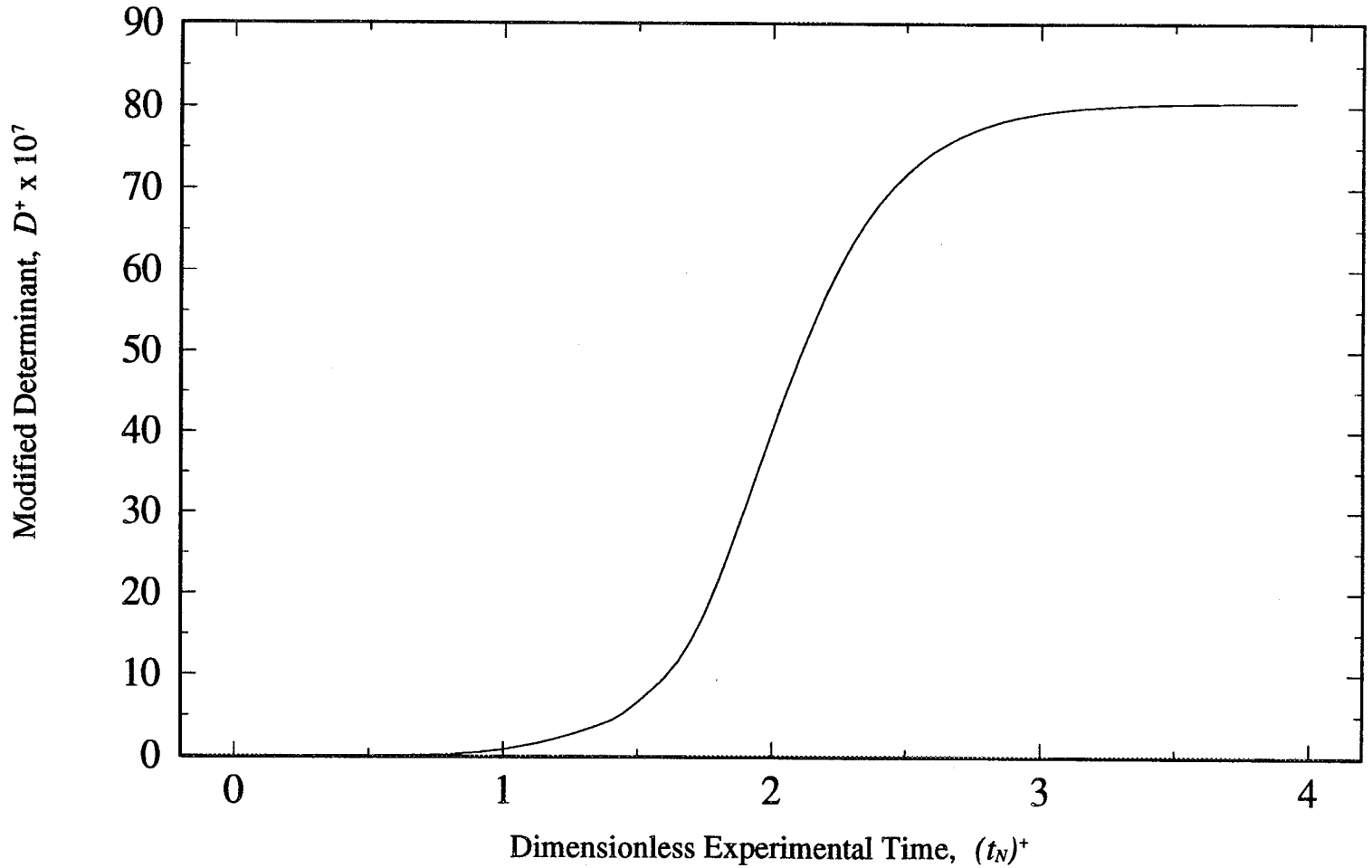

Figure 5.19. Modified Dimensionless Determinant, D^+, Used to Determine the Dimensionless Optimal Experimental Time, t_N^+.

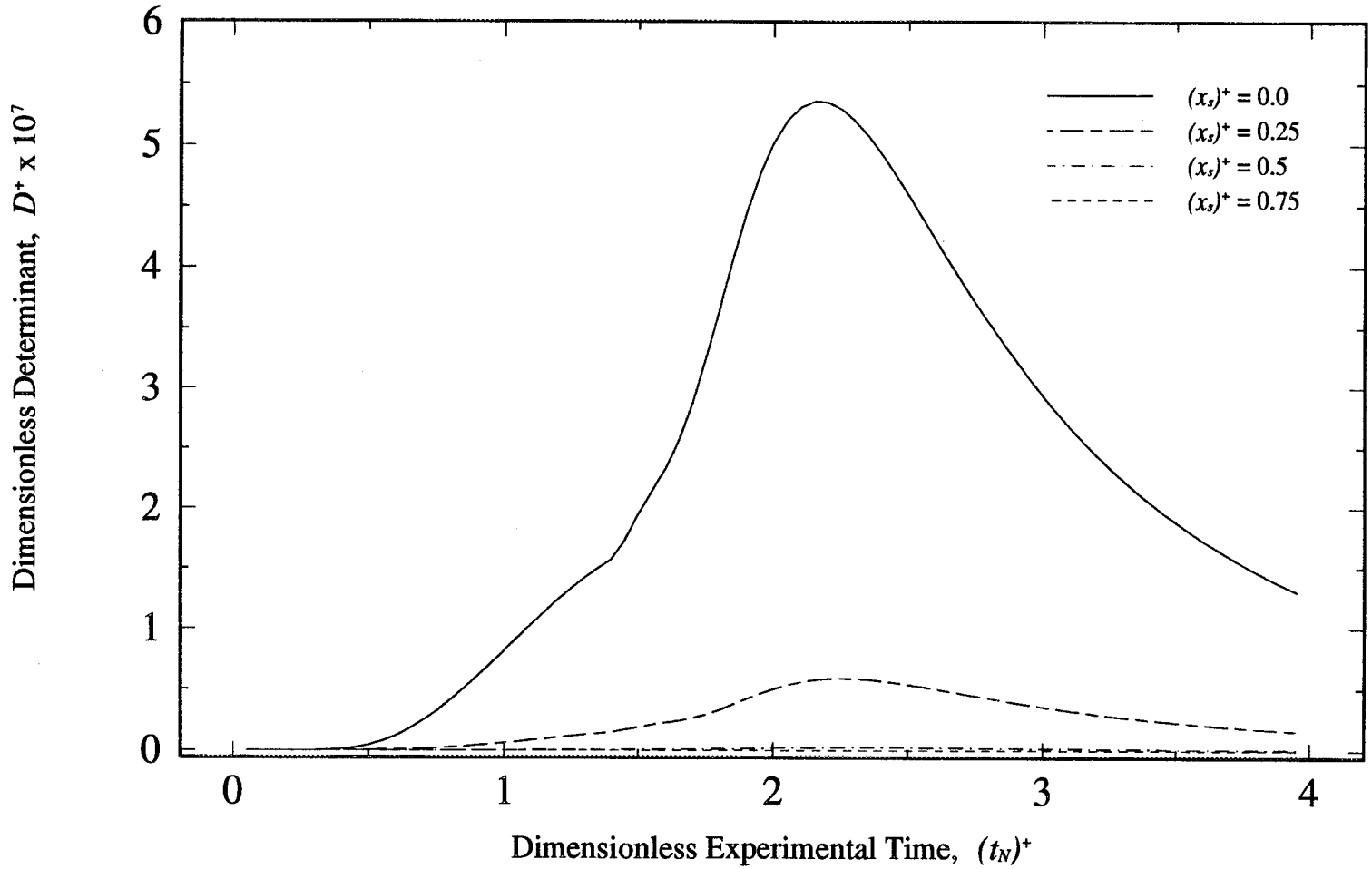

Figure 5.20. Determination of the Optimal Sensor Location on the x^+ (x/L_x) Axis.

in Fig. 5.21. The reason why these determinant values are less than those obtained for the one-dimensional case is because D^+ is now a 3 x 3 determinant, as given in Eq. (3.45). Since the sensitivity coefficients are of the same order of magnitude for both the one-dimensional and two-dimensional cases, then multiplying three coefficients together, as required in the 2-D determinant, will result in smaller maximum determinant values than multiplying only two coefficient values, as in the 1-D determinant.

5.2.1.1.8 Temperature Distributions for Configuration 1

Using the optimal values for x_s^+ and $L_{p,1}^+$, temperature was plotted for various y_s^+ locations for four different dimensionless times: early (0.1), intermediate (two at 0.5 and 1.4), and steady state (4.0) (Fig. 5.22). Note that these temperature distributions were calculated with the heat flux applied for the entire experimental time, t_N^+. The desired optimal values occur when the determinant is a maximum, or when the sensitivity coefficients are the most sensitive to temperature changes. This typically occurs when the temperature gradient is large. As seen from this figure, at and near the optimal y_s^+ location of 0.13, the temperature gradient is steep with respect to y_s^+, and therefore, the sensitivity coefficients for $k_{y\text{-}eff}$ are expected to be large in magnitude. This steep gradient occurs because the composite sample is heated, however, the temperatures at the boundaries are held constant, resulting in a large temperature variation. However, it is also seen that the optimal y_s^+ location is not at the steepest temperature gradient. This results because the maximum determinant occurs when the product of the sensitivity coefficients for all three parameters is the largest in magnitude, which is not necessarily

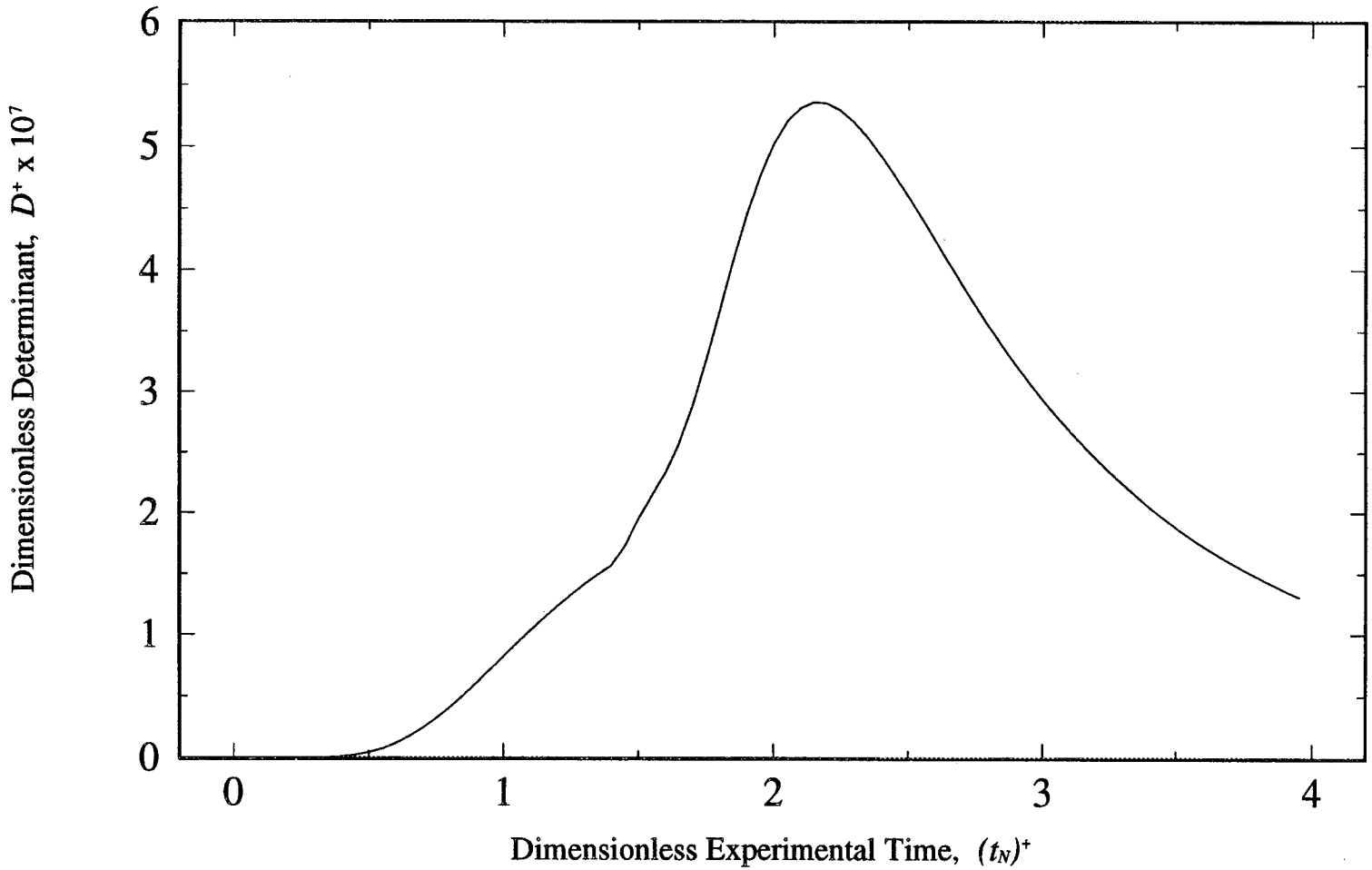

Figure 5.21. Dimensionless Determinant, D^+, Calculated Using the Optimal Experimental Parameters of x_s^+=0.0, y_s^+=0.13, $L_{p,1}^+$=1.0, and t_h^+=1.4.

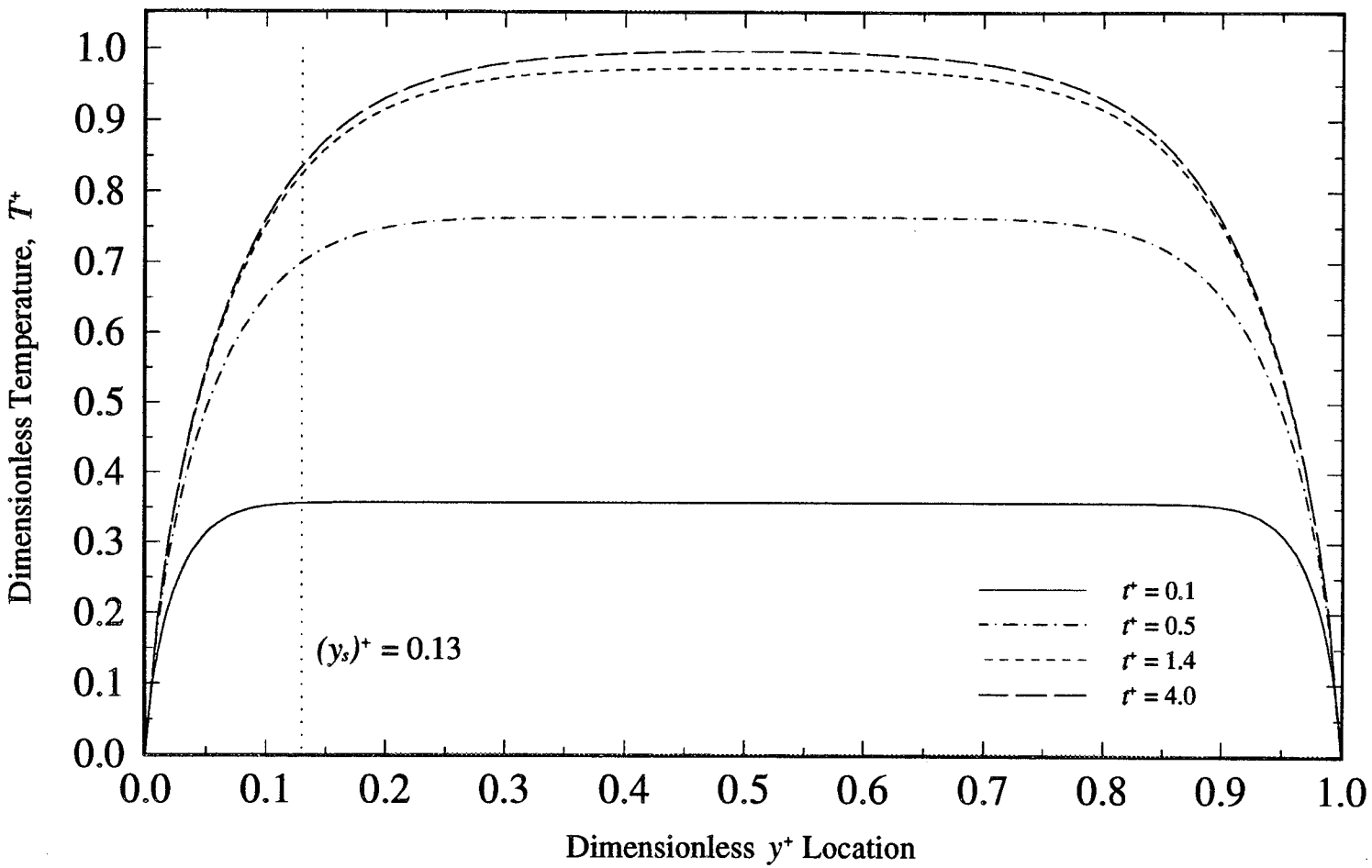

Figure 5.22 Temperature (T) Distribution for Various y_s^+ Locations Calculated Using Four Different Experimental Times.

at the largest temperature gradient in the y^+ direction.

The temperature distribution was also calculated as a function of time using the optimal experimental parameters determined above (see Fig. 5.23). As shown in Fig. 5.23, the heat flux is terminated as the temperature approaches steady state (t_h^+=1.4). This is consistent with Fig. 5.22, where applying the heat flux for the dimensionless time of 1.4 results in temperatures close to the steady state temperatures attained at t^+=4.0.

5.2.1.1.9 Sensitivity Coefficients Calculated Using the Optimal Experimental Parameters

Using the optimal experimental parameters determined, the dimensionless sensitivity coefficients for the three effective thermal properties, $k_{x\text{-}eff}$, $k_{y\text{-}eff}$, and C_{eff}, were calculated and plotted as a function of dimensionless time, as shown in Fig. 5.24. Here, it is seen that the sensitivity coefficients for $k_{x\text{-}eff}$ and C_{eff} are relatively large in magnitude, being on the same order as the temperature rise, with the $k_{x\text{-}eff}$ coefficients being the largest. The sensitivity coefficients for $k_{y\text{-}eff}$ have the smallest magnitude of all three. It is also seen that after a dimensionless time of approximately four, all of the coefficients converge to zero, indicating that temperature measurements taken beyond this time supply little additional information for the estimation procedure. This result is consistent with the temperature distribution (Fig. 5.23), where its initial state was attained after this dimensionless time. Therefore, no new temperature information is being provided and the estimation procedure is complete. This result is also consistent with the determined optimal experimental time, where after a t_N^+ of 4.0, the determinant no longer varied.

Since the sensitivity coefficients for $k_{x\text{-}eff}$ have a larger magnitude than the

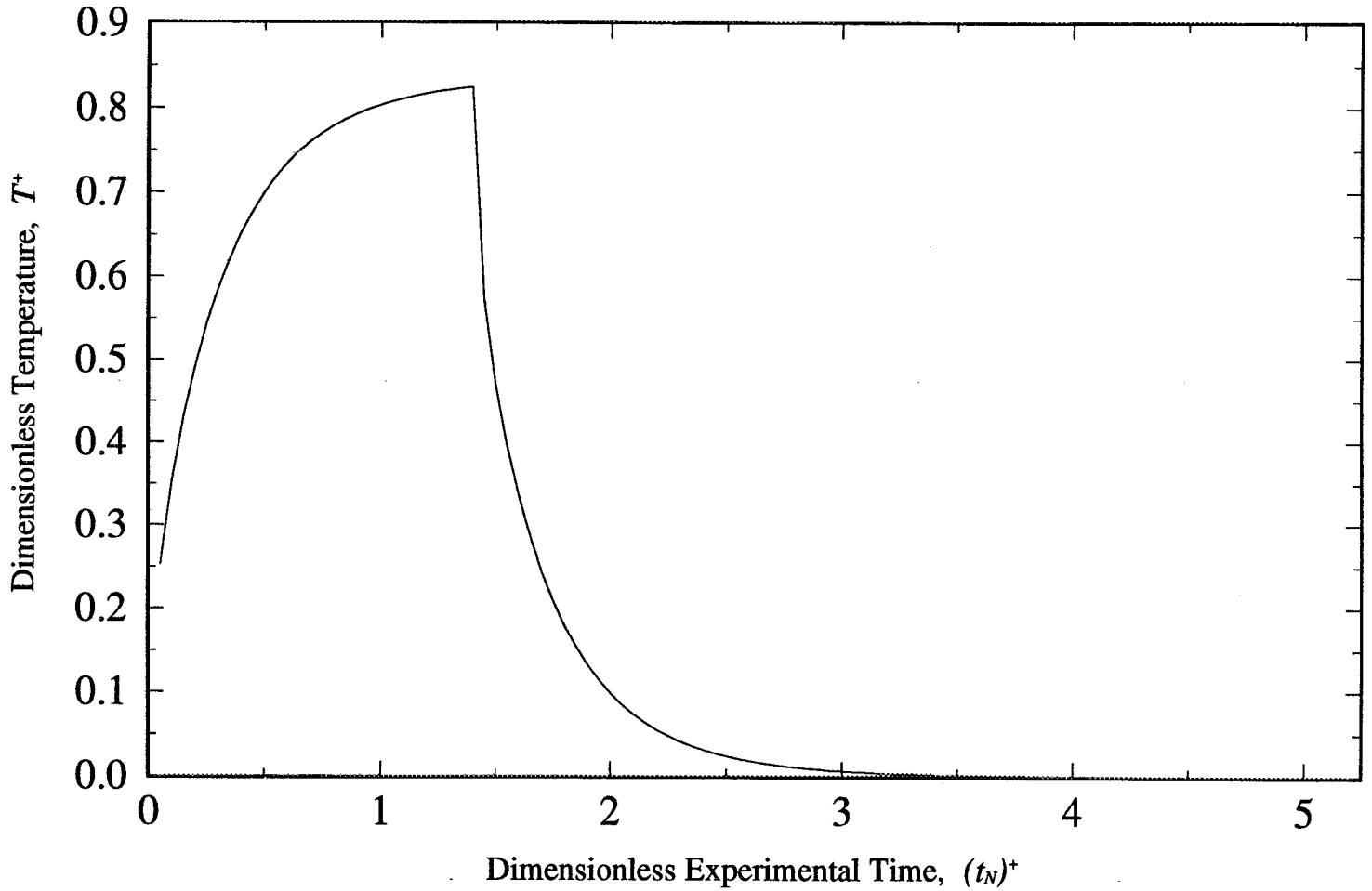

Figure 5.23. Temperature Distribution for Configuration 1 Calculated Using the Optimal Experimental Parameters of x_s^+=0.0, y_s^+=0.13, $L_{p,1}^+$=1.0, and t_h^+=1.4.

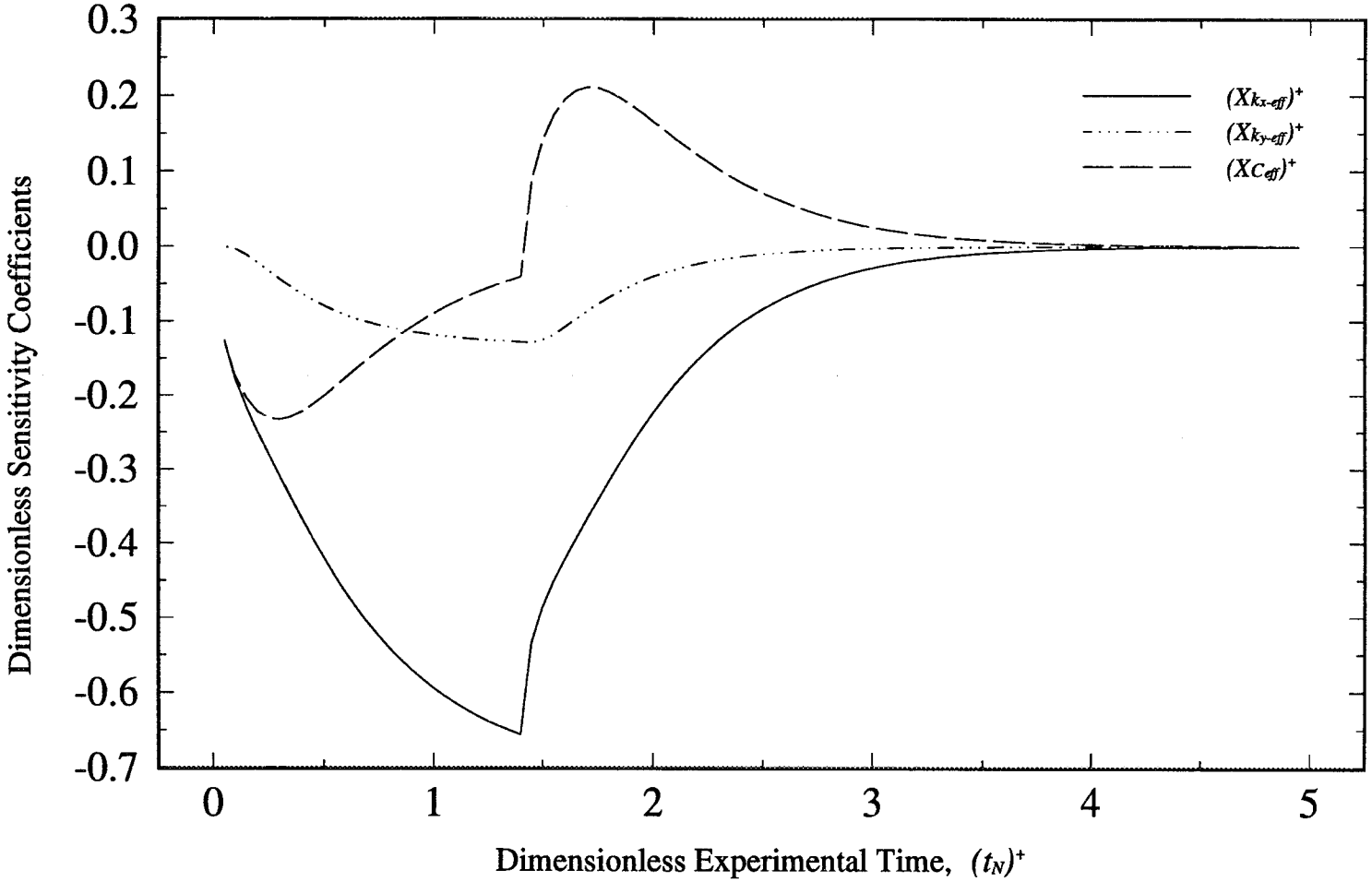

Figure 5.24. Dimensionless Sensitivity Coefficients, $X^+_{k_{x-eff}}, X^+_{k_{y-eff}}$ and $X^+_{C_{eff}}$, Calculated Using the Optimal Experimental Parameters of x_s^+=0.0, y_s^+=0.13, $L_{p,1}^+$=1.0, and t_h^+=1.4.

coefficients for $k_{y\text{-}eff}$ and C_{eff}, it implies that the temperature data are supplying more information for the estimation of $k_{x\text{-}eff}$ than $k_{y\text{-}eff}$ and C_{eff}. As a result, the estimated values obtained for $k_{x\text{-}eff}$ can be regarded as the most accurate of the three parameters, resulting in the smallest confidence intervals.

As mentioned in the one-dimensional case, it is important to plot the sensitivity coefficients to see if they are correlated. If correlation occurs, the thermal properties cannot be estimated independently. From Fig. 5.24, it is evident that the C_{eff} sensitivity coefficient, which changes from negative to positive values, is not correlated with either the $k_{x\text{-}eff}$ or $k_{y\text{-}eff}$ coefficients, which are always negative. However, this observation is not as apparent between the $k_{x\text{-}eff}$ and $k_{y\text{-}eff}$ sensitivity coefficients. If they are correlated, then only the ratio, κ_{xy}, can be estimated. Therefore, to test for possible correlation, the ratio of $X^+_{k_{y\text{-}eff}}/X^+_{k_{x\text{-}eff}}$ was calculated and plotted as a function of dimensionless time (Fig. 5.25). If a straight line occurs, the two parameters are correlated. However, as evident from Fig. 5.25, the line is far from linear, and therefore, $k_{x\text{-}eff}$ and $k_{y\text{-}eff}$ can be estimated simultaneously.

5.2.1.2 Optimal Experimental Parameters Determined for Configuration 2

Recall that Configuration 2 consisted of a uniform heat flux imposed over a portion of one boundary, with the remainder of the boundary insulated. The boundary opposite to the flux boundary was maintained at a known constant temperature, and the remaining two boundaries were insulated (Fig. 5.14). Again, for this configuration, it was

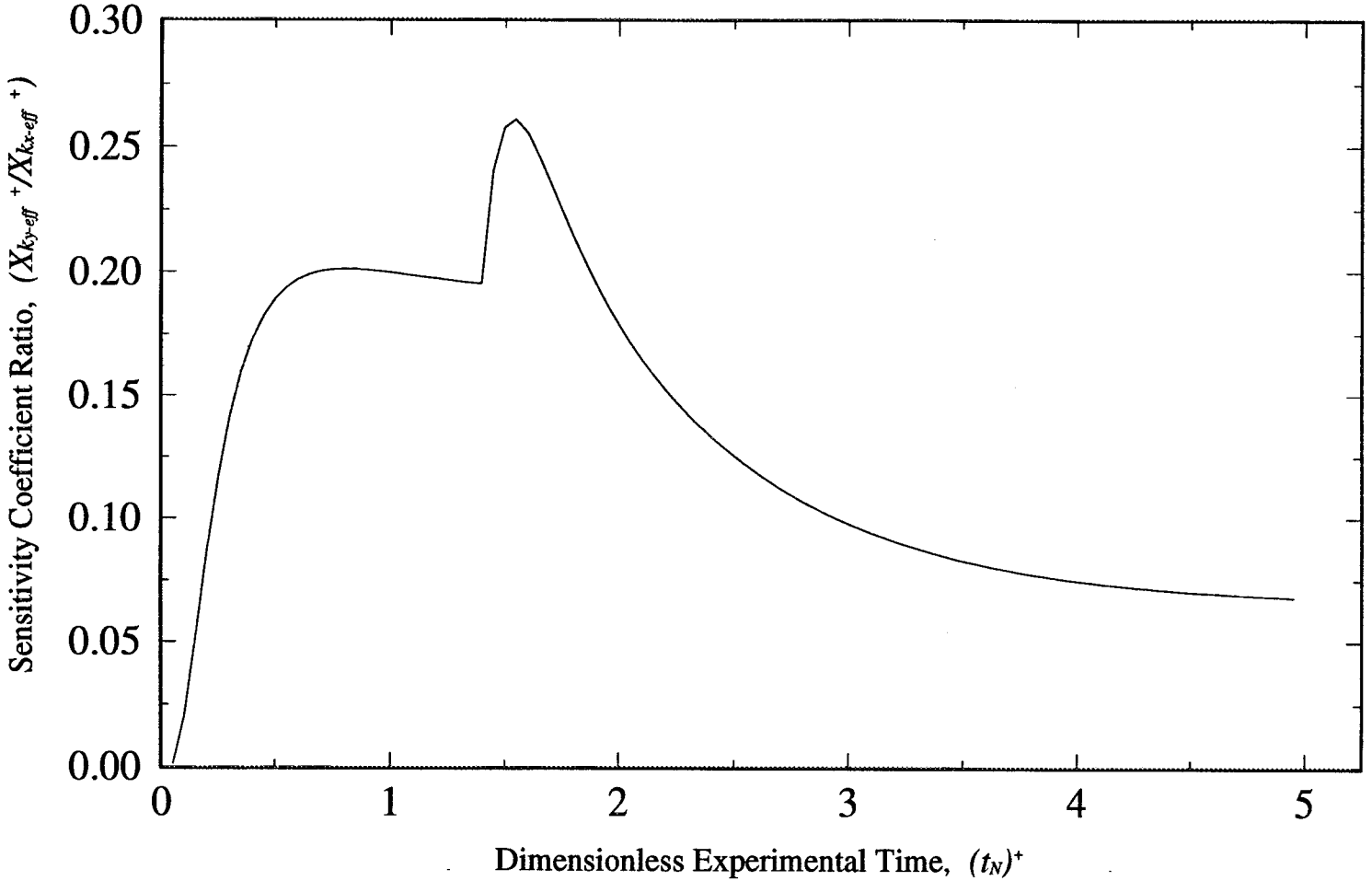

Figure 5.25. Sensitivity Coefficient Ratio, $X^{+}_{k_{y\text{-}eff}}/X^{+}_{k_{x\text{-}eff}}$ to Check for Correlation Between $k_{x\text{-}eff}$ and $k_{y\text{-}eff}$.

desired to select the experimental parameters which maximize the sensitivity of the temperature with respect to all of the unknown thermal properties. Since the same composite samples will be used in the experiments for both Configurations 1 and 2, the result for a L_{xy} of 0.048 and a κ_{xy} of 7 (Loh and Beck, 1991) will again be the most thoroughly analyzed. However, as in the Configuration 1 case, all possible combinations of κ_{xy} equal to 1 and 1/7, and L_{xy} equal to 0.048, 0.5, and 1.0 will also be performed. The same optimization procedure, as discussed in Section 5.2.1.1 for Configuration 1, was used and similar experimental parameters were optimized (x_s^+, y_s^+, $L_{p,2}^+$, t_h^+, and t_N^+). These experimental parameter results are discussed next.

5.2.1.2.1 Optimal Temperature Sensor Location on the x^+ Axis

The first optimal experimental parameter determined was the temperature sensor location along the x^+ axis. Again, as in Configuration 1, the maximum determinant always occurred at a x_s^+ location equal to zero (or at the heated surface) for all combinations of y_s^+ and $L_{p,2}^+$. This occurs for the same reason as discussed in Section 5.2.1.1.1, where the largest temperature gradient in the x^+ direction occurs at the heated surface.

5.2.1.2.2 Optimal Temperature Sensor Location on the y^+ Axis and Heat Flux Position

The next parameters that were optimized were the sensor location along the y^+ axis and the position of the applied heat flux, $L_{p,2}^+$. After calculating the maximum determinant for each x_s^+, y_s^+, and $L_{p,2}^+$ combinations, the true maximum determinant (the

largest value of all of the maximum determinants for each combination) was in the general region of $L_{p,2}^{+}$=0.9, y_s^{+}=0.8, and t_h^{+}=1.55. To determine the precise location of the actual maximum determinant, both the $L_{p,2}^{+}$ and y_s^{+} grid sizes were refined around the previously obtained values of 0.9 and 0.8 respectively, ($L_{p,2}^{+}$ was varied from 0.84 to 0.92 and y_s^{+} was varied from 0.6 to 0.9) while holding t_h^{+} constant at 1.55. For each $L_{p,2}^{+}$ value, the maximum determinant was plotted as a function of the y_s^{+} location in Fig. 5.26. As seen in this figure, the actual maximum determinant occurs at a $L_{p,2}^{+}$ of 0.89 and a corresponding y_s^{+} location of 0.77. However, it is seen that the curve is fairly flat when $L_{p,2}$ is located between 0.88 to 0.9; therefore, any value within this range could be used for $L_{p,2}$ to improve the accuracy of the property estimates. Note that $L_{p,2}^{+}$ is different than $L_{p,1}^{+}$, as expected. If $L_{p,2}^{+}$ had equalled $L_{p,1}^{+}$ the heat flux would be applied over the entire boundary. Due to the insulated boundary conditions on the sides used in this configuration, the problem would reduce to one-dimensional heat conduction and $k_{y\text{-}eff}$ could no longer be estimated.

5.2.1.2.3 Optimal Heating Time

The next parameter optimized was the heating time. Setting $L_{p,2}^{+}$ and y_s^{+} equal to their optimal values calculated in the above section, (0.89 and 0.77, respectively) the heating time was varied around its previously determined value of t_h^{+}=1.55 (from 1.45 to 1.65). At each heating time, the dimensionless determinant was calculated as a function of dimensionless time. A few of these determinant curves are shown in Fig. 5.27 for

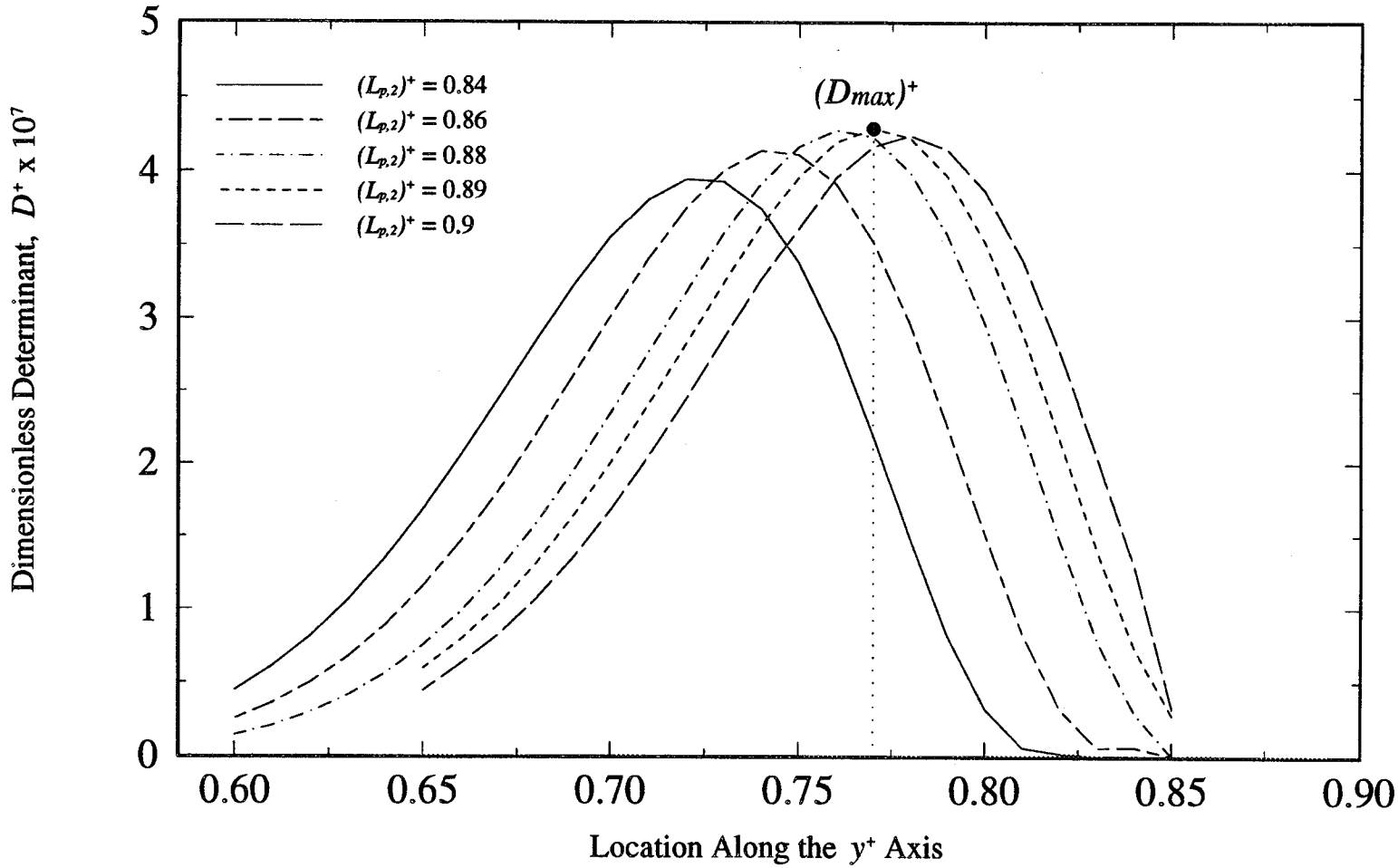

Figure 5.26. Maximum Determinant, D_{max}^+, for Various y_s^+ (y/L_y) Locations and Heater Locations, $L_{p,2}^+$ ($L_{p,2}/L_y$), Calculated at x_s^+=0.0.

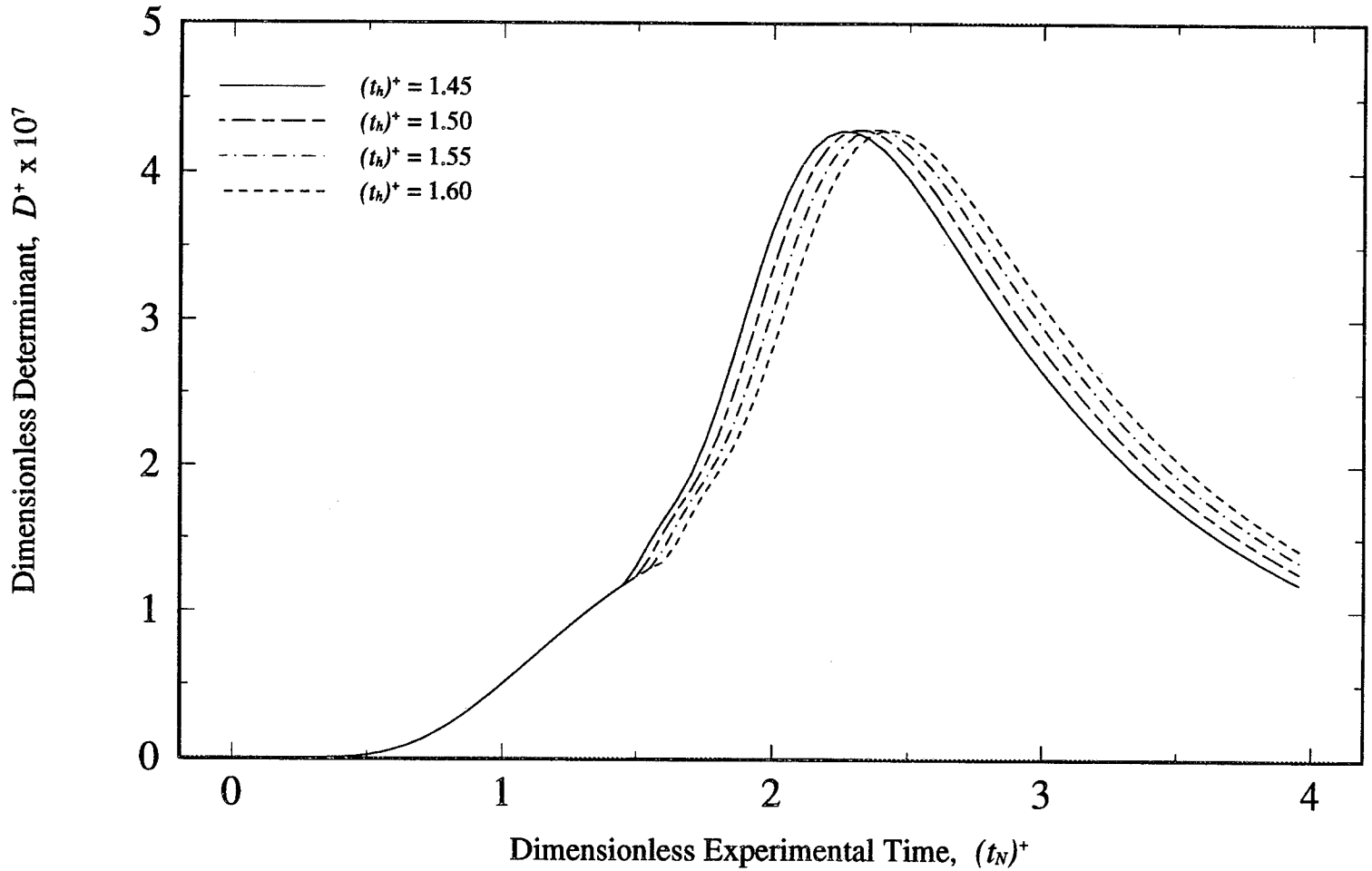

Figure 5.27. Maximum Determinant, D_{max}^+, for Various Heating Times, t_h^+, Calculated Using the Optimal Experimental Parameters of x_s^+=0.0, y_s^+=0.77, and $L_{p,2}^+$=0.89.

various heating times. The maximum determinant value of all of these curves occurred when the heating time was equal to 1.55. This is the same result obtained previously, and therefore, the optimal values calculated for $L_{p,2}^{+}$ and y_s^{+}, which were found using a t_h^{+} of 1.55, do not have to be iteratively updated. Note, however, that the maximum determinants are practically equal for all heating times between 1.45 and 1.65. Therefore, using a t_h^{+} of 1.55 does not have to be precise to provide the most accurate property estimates.

5.2.1.2.4 Optimal Experimental Time

Finally, the last parameter determined was the optimal dimensionless experimental time, t_N^{+}. This was calculated using the same procedure as in Configuration 1 (Section 5.2.1.1.5) with the modified dimensionless determinant results shown in Fig. 5.28. Here, it is evident that again, as in Configuration 1, after a dimensionless time of approximately 4.0, the determinant no longer changes. This implies that after this dimensionless time, the temperature is returning to its initial state (a dimensionless value of zero) and little additional information is being provided for the estimation of the thermal properties. Therefore, the experiments can be concluded after a t_N^{+} of 4.0. Again, however, as was the case for Configuration 1, this is a conservative choice and a smaller value, such as 3.5, could have also been chosen.

5.2.1.2.5 Verification of the Optimal Temperature Sensor Location on the x^{+} Axis

To verify the optimal location of the temperature sensor along the x^{+} direction, for

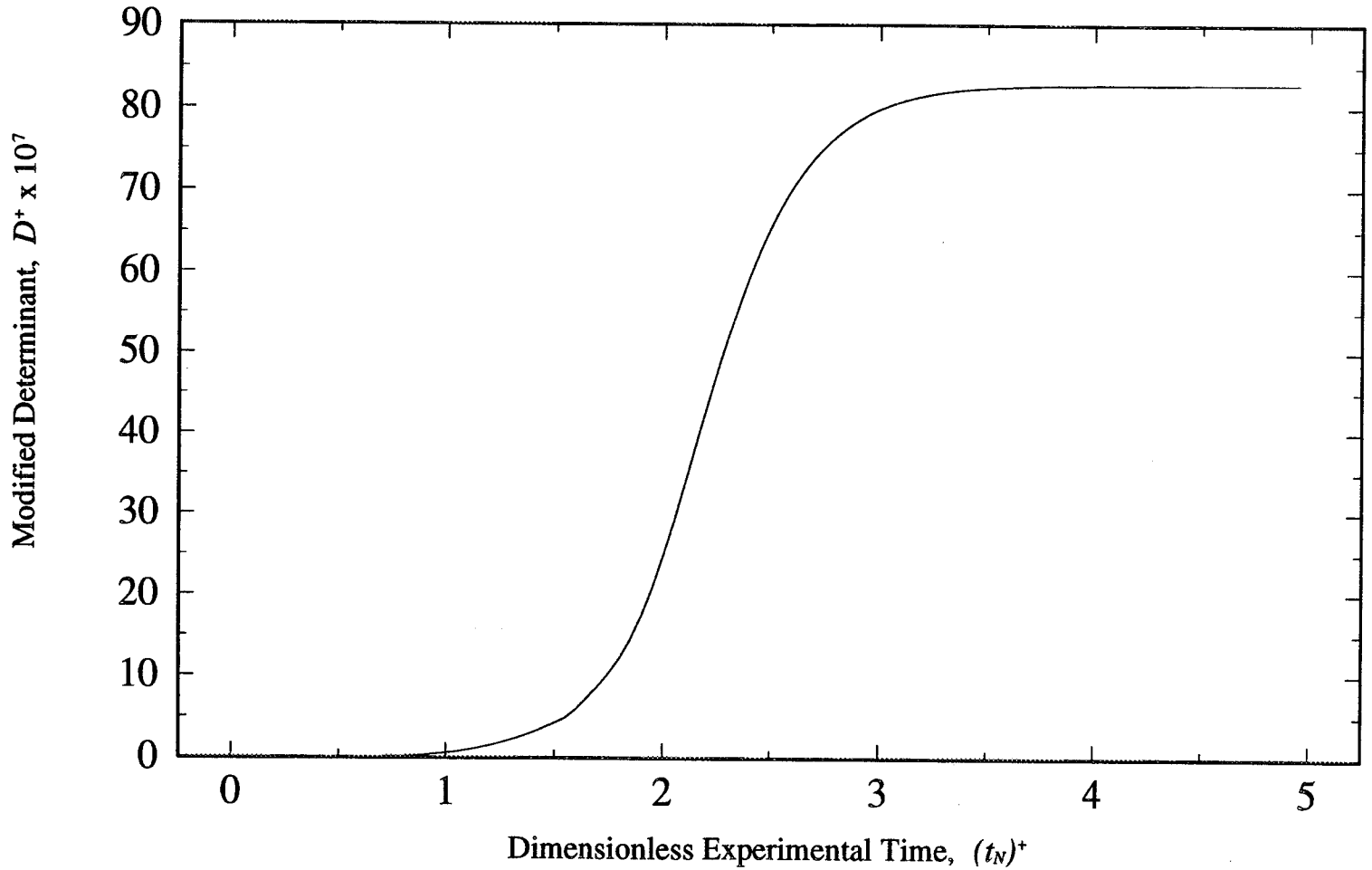

Figure 5.28. Modified Dimensionless Determinant, D^+, Used to Determine the Dimensionless Optimal Experimental Time, t_N^+.

which a value of zero was determined, the dimensionless determinant was calculated using the optimal values for y_s^+, $L_{p,2}^+$, and t_h^+ for various x_s^+ locations. The results are shown in Fig. 5.29 against dimensionless time. As seen from this figure, the maximum determinant occurred when the sensor was at the heated surface (x_s^+=0.0), confirming the optimal result obtained for the x_s^+ location.

5.2.1.2.6 Maximum Determinant Using the Optimal Experimental Parameters

In summary, the above optimization procedure resulted in the following optimal experimental parameters for Configuration 2: x_s^+=0.0, y_s^+=0.77, $L_{p,2}^+$=0.89 and t_h^+=1.55. Using these optimal parameters, the dimensionless determinant, D^+, was plotted as a function of dimensionless time, where a maximum of 4.29 x 10^{-7} occurred, as shown in Fig. 5.30. Again, the reason why these determinant values are less than those obtained for the one-dimensional case is the same as discussed in Section 5.2.1.1.7.

5.2.1.2.7 Temperature Distributions for Configuration 2

Using the optimal values for x_s^+ and $L_{p,2}^+$, the temperature was plotted for various y_s^+ locations for four different dimensionless times; initial (0.1), two intermediate (0.5 and 1.55), and steady state (4.0) (Fig. 5.31). Note that these temperature distributions were calculated with the heat flux applied for the entire experimental time, t_N^+. The desired optimal values occur when the determinant is a maximum, or when the sensitivity coefficients are the most sensitive to temperature changes. As mentioned previously, in the case of thermal conductivity, this can occur when the temperature gradient is large.

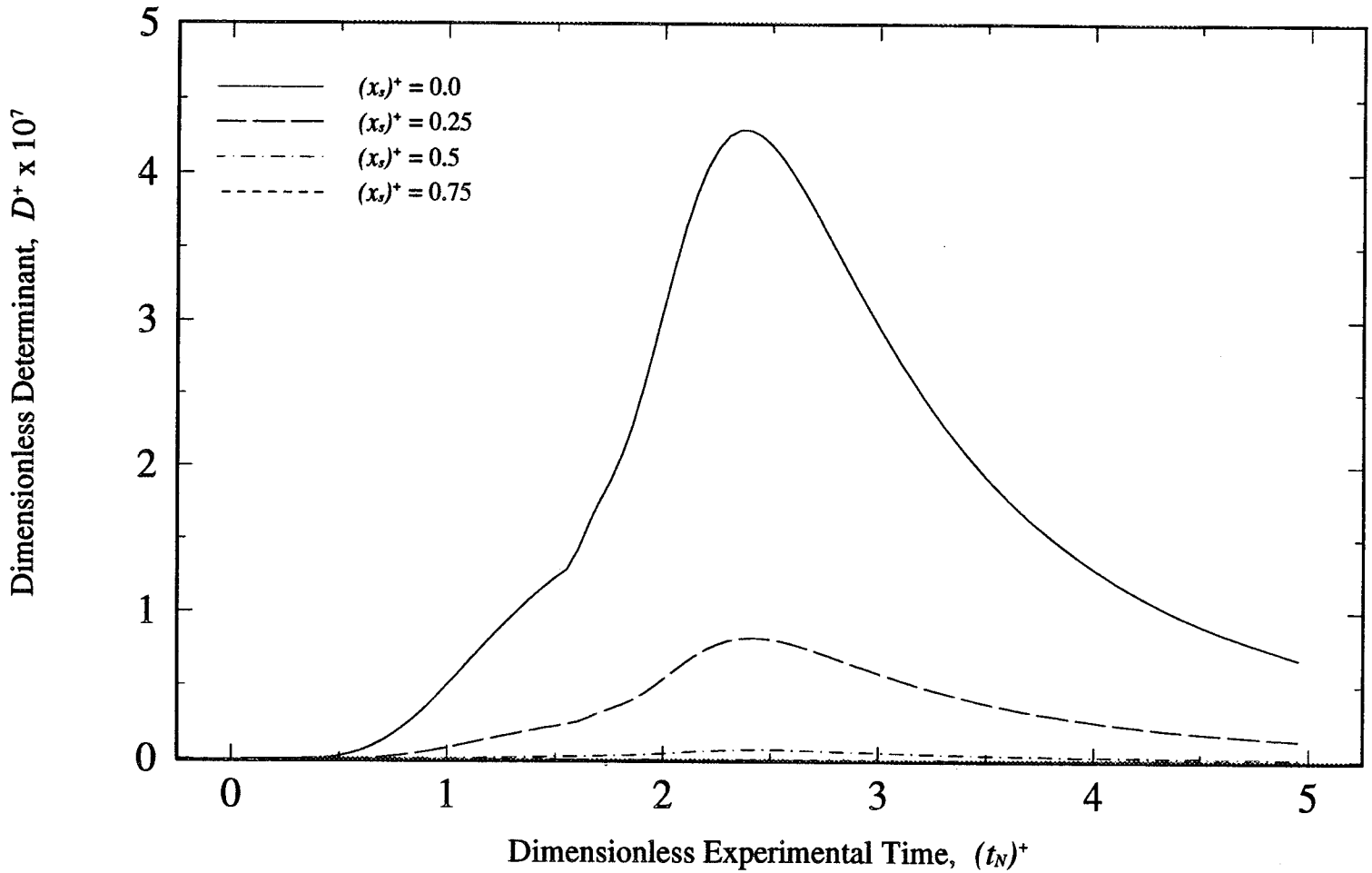

Figure 5.29. Determination of the Optimal Sensor Location on the x^+ (x/L_x) Axis.

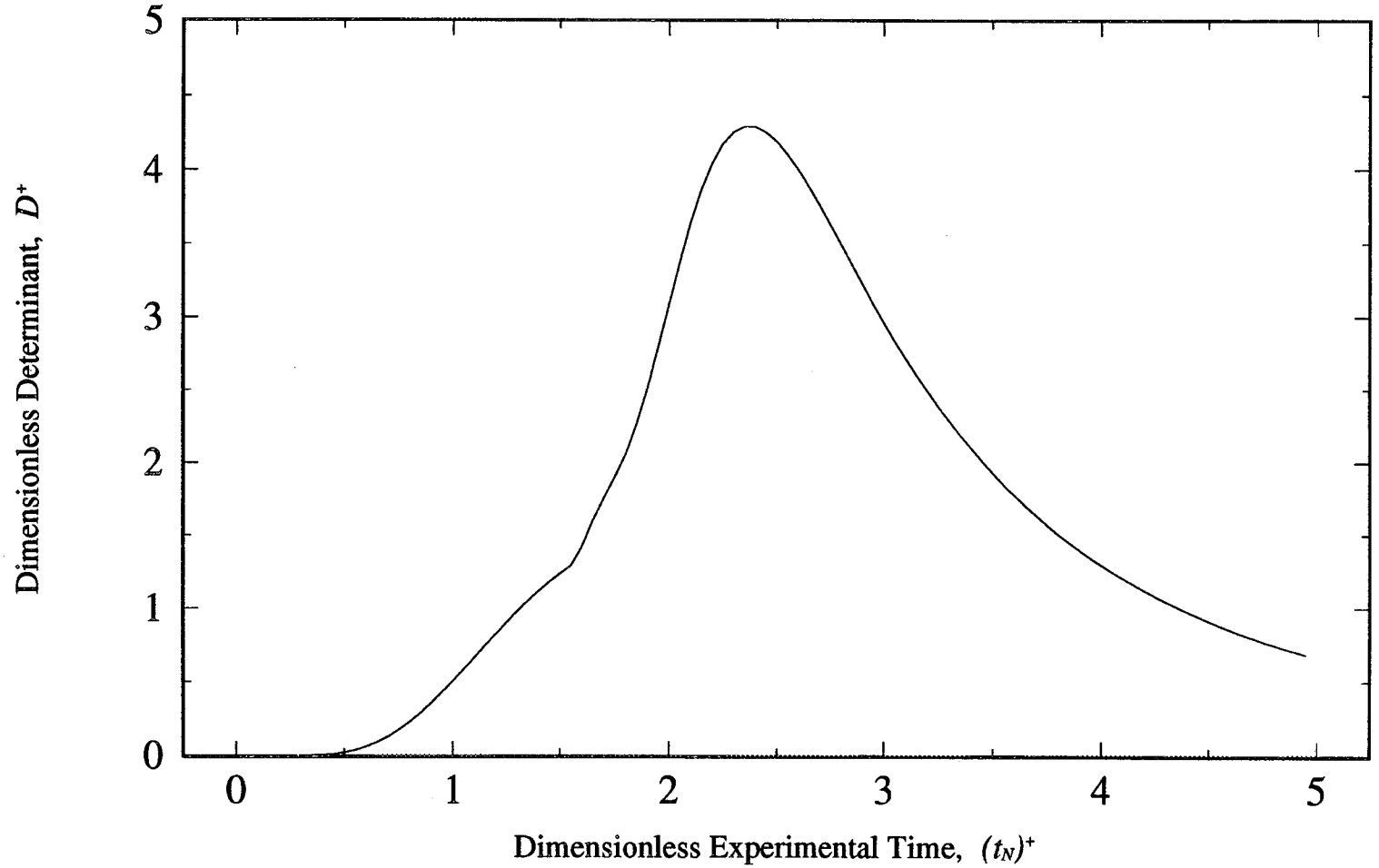

Figure 5.30. Dimensionless Determinant, D^+, Calculated Using the Optimal Experimental Parameters of x_s^+=0.0, y_s^+=0.77, $L_{p,2}^+$=0.89, and t_h^+=1.55.

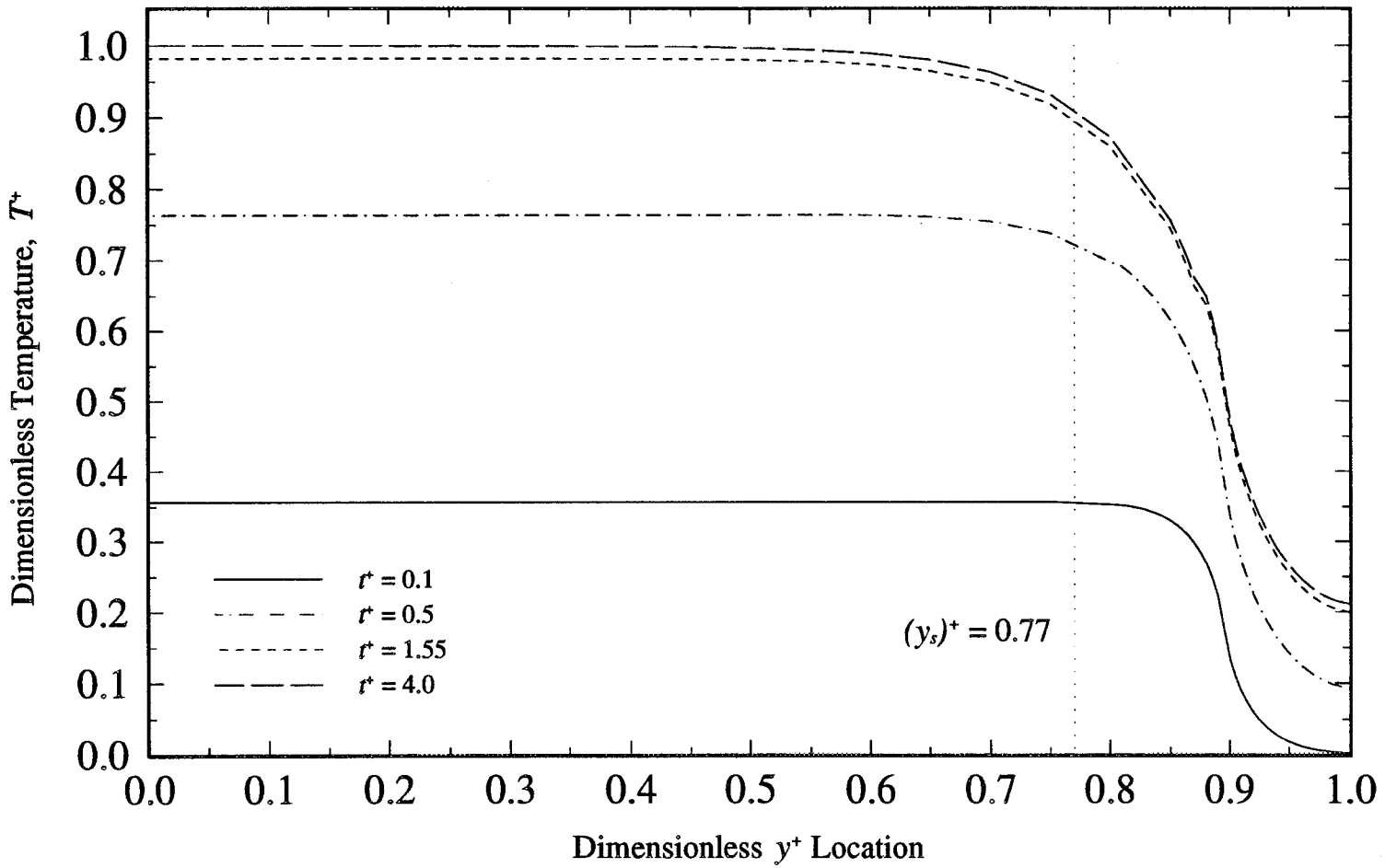

Figure 5.31 Temperature (T) Distribution for Various y_s^+ Locations Calculated Using Four Different Experimental Times.

As seen from this figure, at an optimal y_s^+ location of 0.77, the temperature gradient is steep, and therefore, it is expected that the sensitivity coefficients for $k_{y\text{-}eff}$ are large in magnitude. However, the optimal y_s^+ location for this design again does not occur at the steepest temperature gradient and results for the same reasons given in the Configuration 1 analysis.

The temperature was also calculated as a function of dimensionless time using the optimal experimental parameters determined previously (Fig. 5.32). As seen in Fig. 5.32, the temperature distribution behaves the same way as for Configuration 1, where the heat flux is terminated as the temperature approaches steady state (t_h^+=1.55). This is again consistent with Fig. 5.31, where applying the heat flux for the dimensionless time of 1.55 results in temperatures close to the steady state temperatures attained at t^+=4.0.

5.2.1.2.8 Sensitivity Coefficients Using the Optimal Experimental Parameters

Using the optimal experimental parameters determined, the dimensionless sensitivity coefficients for the three effective thermal properties, $k_{x\text{-}eff}$, $k_{y\text{-}eff}$, and C_{eff}, were calculated and plotted as a function of dimensionless time in Fig. 5.33. Here, it is seen that the sensitivity coefficients for $k_{x\text{-}eff}$ and C_{eff} are relatively large in magnitude, while for $k_{y\text{-}eff}$, the coefficients are much smaller (of the order 0.1). It is also seen that after a dimensionless time of approximately four, all of the coefficients converge to zero, indicating that temperature measurements taken beyond this time supply little additional information for the estimation procedure. This result is consistent with both the temperature distribution in Fig. 5.32, where its initial state was attained after this

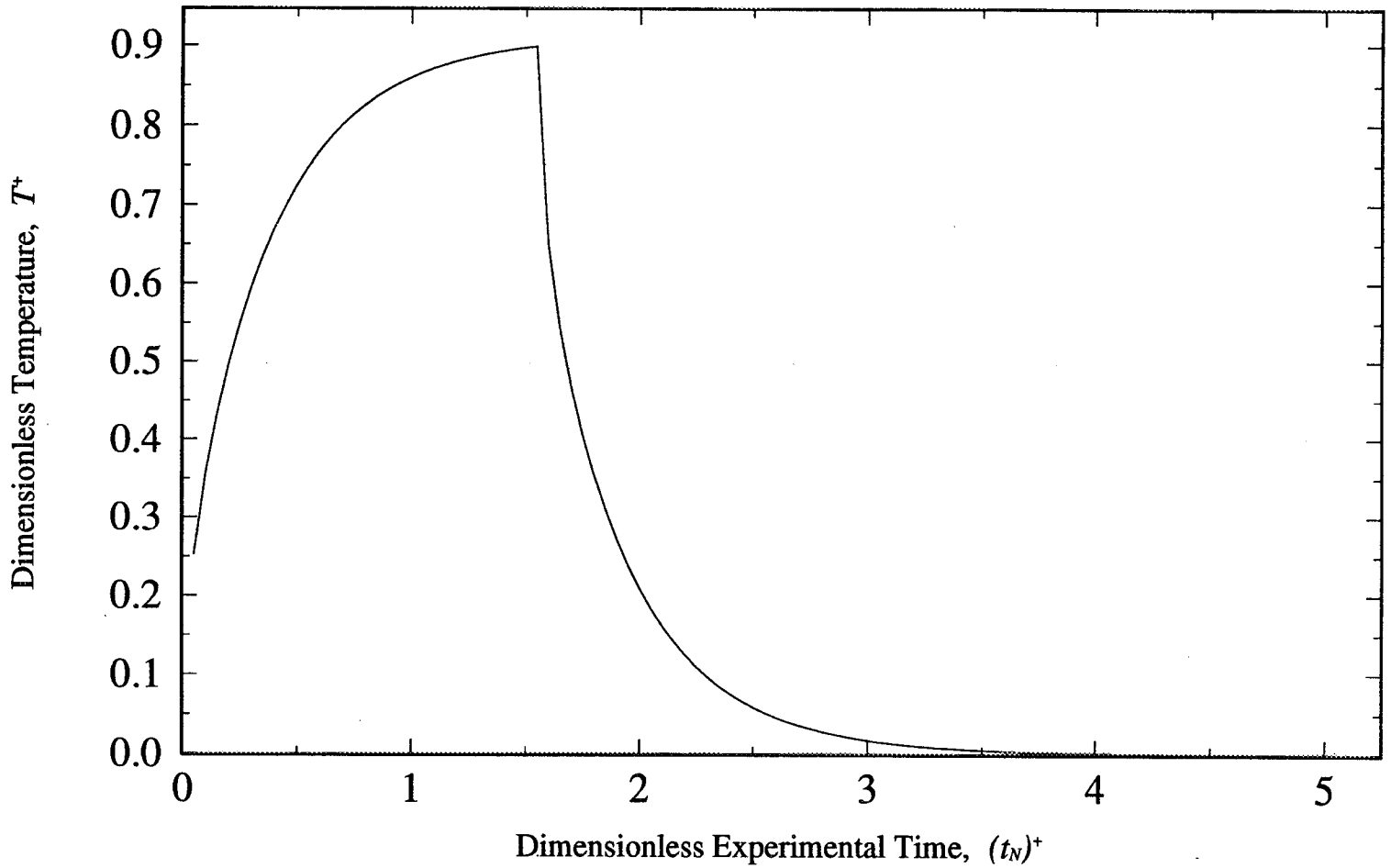

Figure 5.32. Temperature Distribution for Configuration 2 Calculated Using the Optimal Experimental Parameters of x_s^+=0.0, y_s^+=0.77, $L_{p,2}^+$=0.89, and t_h^+=1.55.

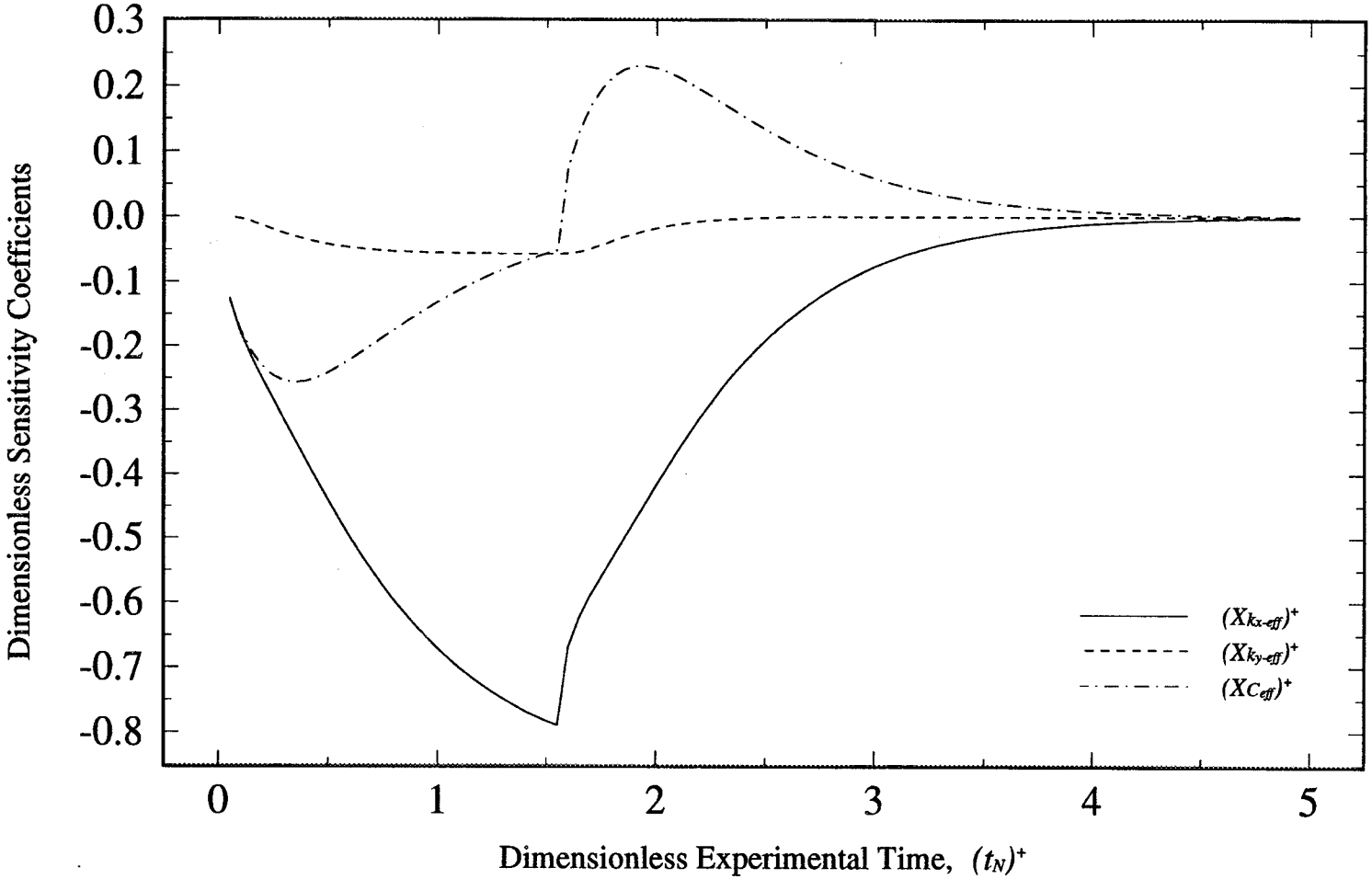

Figure 5.33. Dimensionless Sensitivity Coefficients, $X^+_{k_{x-eff}}$, $X^+_{k_{y-eff}}$, and, $X^+_{C_{eff}}$, Calculated Using the Optimal Experimental Parameters of x_s^+=0.0, y_s^+=0.77, $L_{p,2}^+$=0.89, and t_h^+=1.55.

dimensionless time, and with the determined optimal experimental time, where after a t_N^+ of 4.0, the determinant no longer varied (Fig. 5.28).

Again, the sensitivity coefficients should be analyzed to see if they are correlated. If correlation occurs, the thermal properties cannot be estimated independently. From Fig. 3.33, linear independence is again evident between C_{eff}, whose coefficient changes from negative to positive values, and both $k_{x\text{-}eff}$ and $k_{y\text{-}eff}$, where the coefficients are always negative. However, as with Configuration 1, it was desired to determine if the sensitivity coefficients for $k_{x\text{-}eff}$ and $k_{y\text{-}eff}$ are correlated. If correlation occurs, then only the ratio, κ_{xy}, can be estimated. To test for possible correlation, the ratio of $X_{k_{y\text{-}eff}}^+ / X_{k_{x\text{-}eff}}^+$ was again calculated, with the results shown in Fig. 5.34. If a straight line occurs, correlation exists. From this figure, however, it is evident that a linear line does not occur, and therefore, the coefficients are linearly independent and $k_{x\text{-}eff}$ and $k_{y\text{-}eff}$ can be estimated simultaneously.

5.2.1.3 Comparison of Configurations 1 and 2

After calculating the optimal experimental parameters for both Configurations 1 and 2, the configurations were compared to determine which one would provide the most accurate thermal property estimates. This comparison can be made by determining which configuration has the largest maximum determinant. Figure 5.35 shows the dimensionless determinants as a function of dimensionless experimental time calculated using the optimal experimental parameters found for each configuration. From this figure, it is

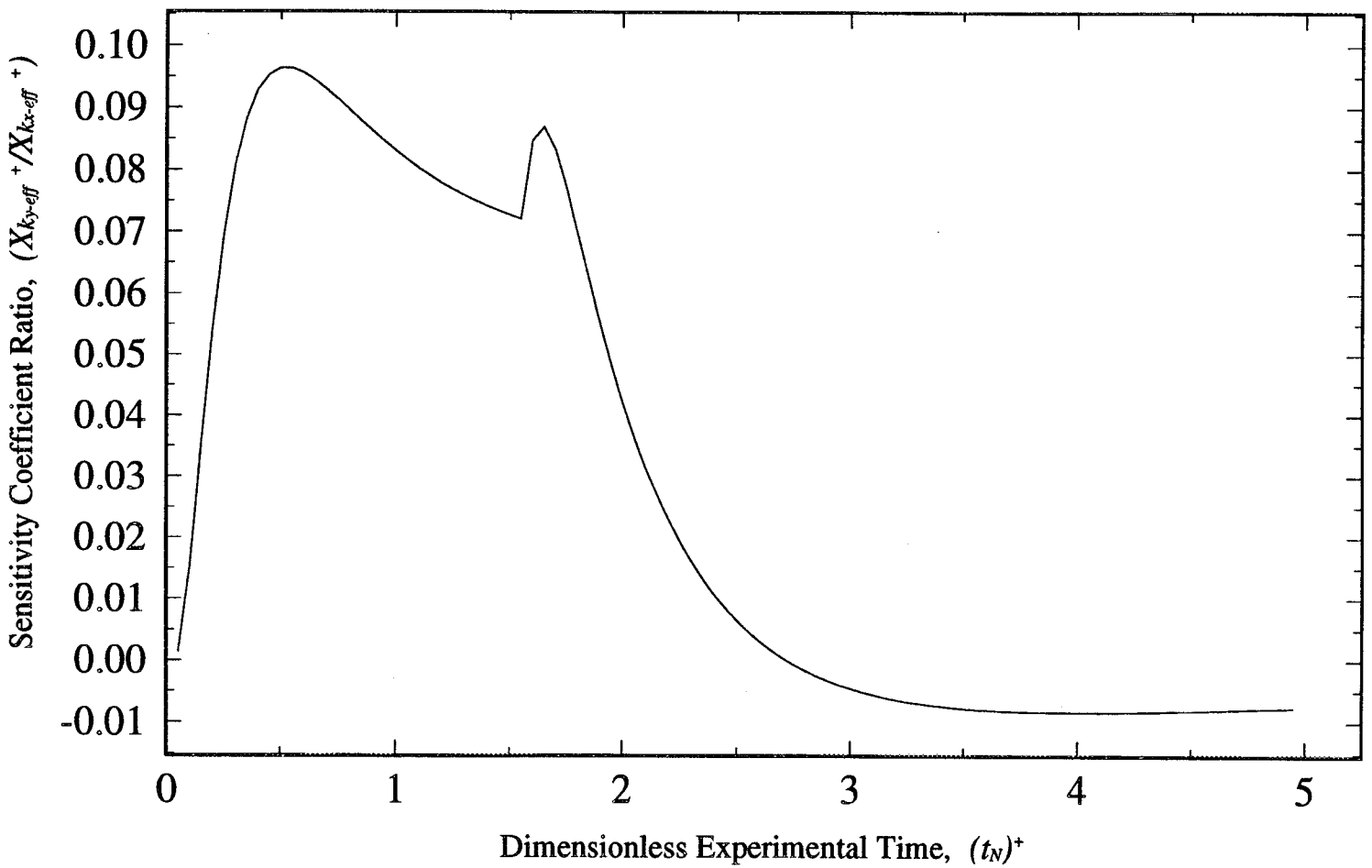

Figure 5.34. Sensitivity Coefficient Ratio, $X^{+}_{k_{y\text{-}eff}}/X^{+}_{k_{x\text{-}eff}}$ to Check for Correlation Between $k_{x\text{-}eff}$ and $k_{y\text{-}eff}$.

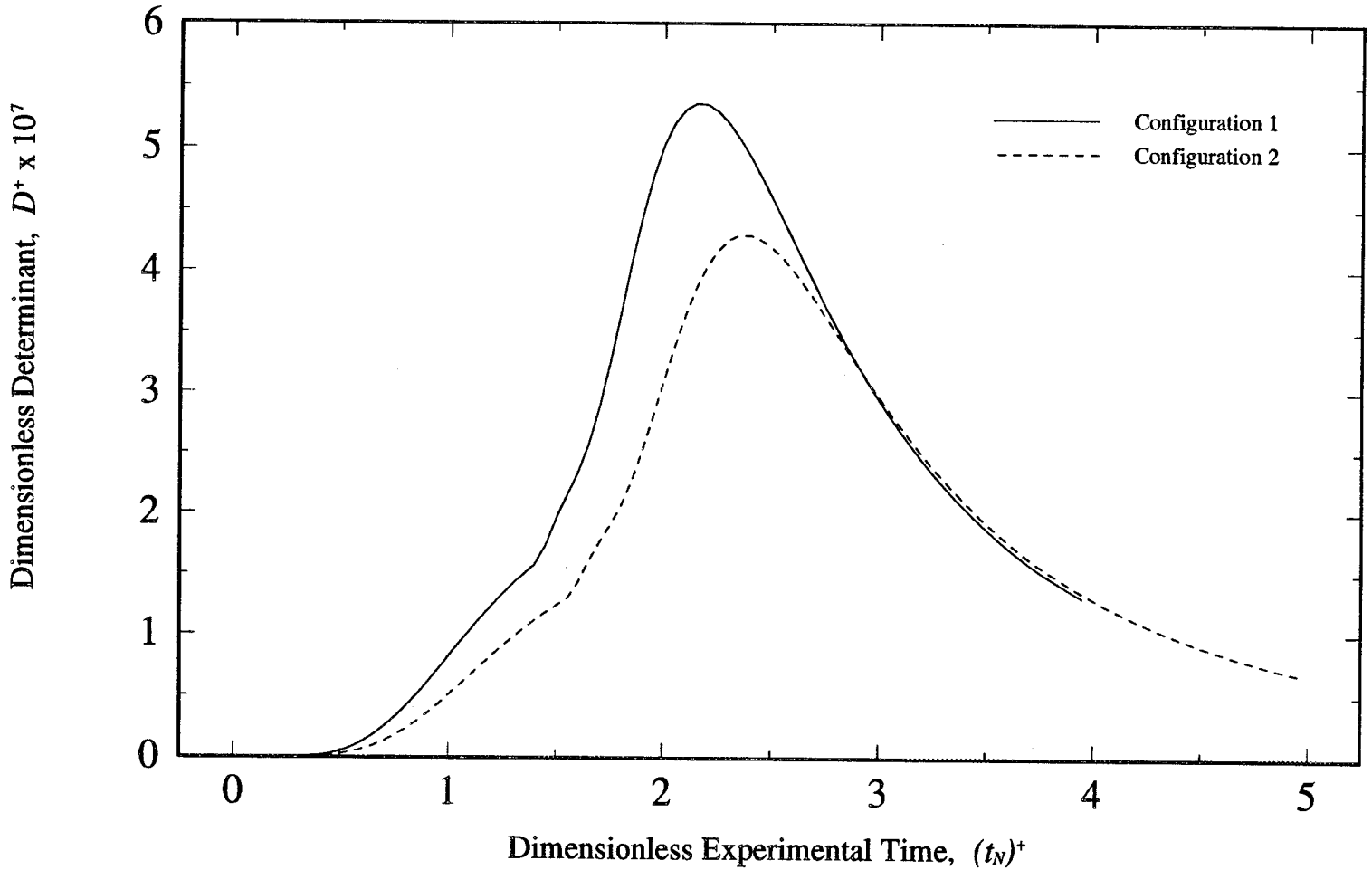

Figure 5.35. Comparison of the Dimensionless Determinant, D^+, for Configurations 1 and 2.

evident that the design with constant temperatures on the two sides (Configuration 1) will provide more accurate estimates than the design with insulated sides (Configuration 2). However, this conclusion requires further analysis by viewing the sensitivity coefficients for each configuration, as shown in Fig. 5.36. Here, it is seen that the sensitivity coefficients for $k_{x\text{-}eff}$ and C_{eff} are 20% and 9% larger in magnitude, respectively, for Configuration 2 than Configuration 1. However, the sensitivity coefficient for $k_{y\text{-}eff}$ is 136% larger in magnitude for Configuration 1 than Configuration 2. (Note, these percents were calculated using the largest point on each of the curves). This difference in $k_{y\text{-}eff}$ is much more substantial than that for $k_{x\text{-}eff}$ and C_{eff}. From viewing these sensitivity coefficients, it can be concluded that when estimating all three thermal properties simultaneously, Configuration 1 should be utilized, since it will provide approximately the same amount of information for $k_{x\text{-}eff}$ and C_{eff} that Configuration 2 would provide, but considerably more information for the estimation of $k_{y\text{-}eff}$. This result seems reasonable since a greater temperature variation would occur in the y^+ direction (the same direction as $k_{y\text{-}eff}$) when the walls are maintained at a constant temperature of zero rather than insulated, where the wall temperatures are allowed to rise (only the gradient at the wall is required to remain equal to zero). This result in consistent with comparing the maximum determinant values between the two configurations, as discussed previously.

5.2.1.4 Other Optimized Parameters

For both configurations used in the two-dimensional analysis, the optimal parameters were determined using a L_{xy} of 0.048 and a κ_{xy} of 7. A L_{xy} ratio of this

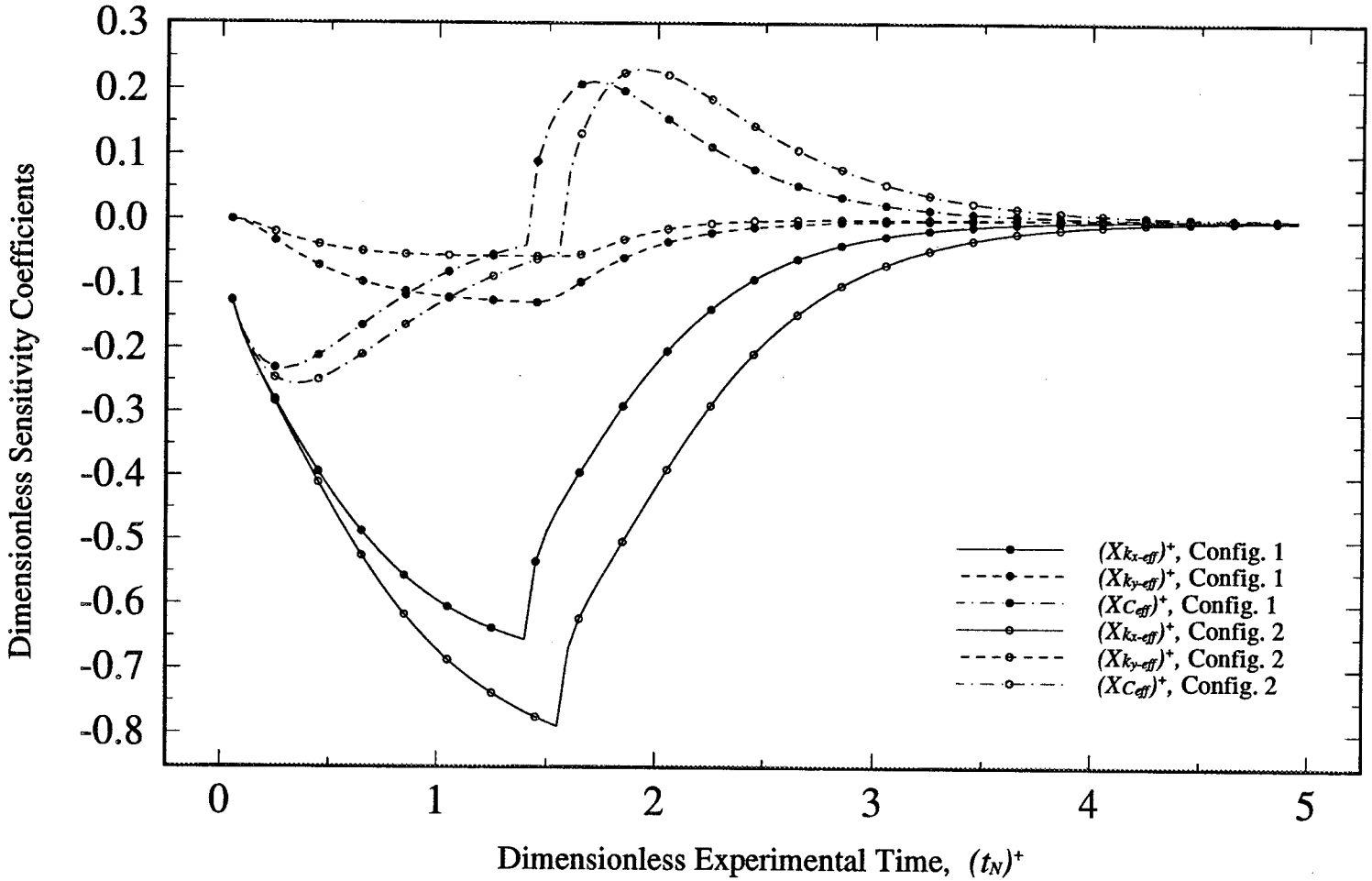

Figure 5.36. Comparison of the Dimensionless Sensitivity Coefficients, $X^+_{k_{x\text{-}eff}}$, $X^+_{k_{y\text{-}eff}}$, and, $X^+_{C_{eff}}$, for Configurations 1 and 2.

magnitude is typical of the sizes of composite samples used in experimental designs. The samples used by Loh and Beck (1991) to determine the effective thermal conductivities parallel ($k_{y\text{-}eff}$) and perpendicular ($k_{x\text{-}eff}$) to the fibers, from which they determined a thermal conductivity ratio of 7, were also of this magnitude. Since this study uses similar carbon-epoxy composite materials, a κ_{xy} of 7 was also used in this investigation. However, to demonstrate how this optimization analysis could be extended to other composite dimensions or effective thermal conductivity ratios, different values for κ_{xy} and L_{xy} were also used in the optimization procedure. These combinations include L_{xy} equal to 0.048, 0.5, and 1.0, and κ_{xy} equal to 7, 1, and 1/7. The results for all combinations are discussed in the following subsections.

5.2.1.4.1 Various L_{xy} and κ_{xy} Combinations Used for Configuration 1

The first combination investigated was $L_{xy} = 0.5$, and $\kappa_{xy} = 7$. This L_{xy} results in the composite thickness in the direction of heat transfer (the x^+ direction in this analysis) being ten times greater than when L_{xy} equalled 0.048. Using the same procedure discussed in Section 5.2.1.1, the general region of the maximum determinant was calculated. Using the optimal experimental parameters found for this region, the sensitivity coefficients were calculated and plotted, as shown in Fig. 5.37. From this figure, it is seen that the coefficients reach steady state very quickly. This occurs because of the significant increase in the thickness in the x^+ direction, creating more material to absorb the heat produced from the applied heat flux. Therefore, it can be concluded that using this L_{xy} and κ_{xy} combination provides inadequate information for the estimation

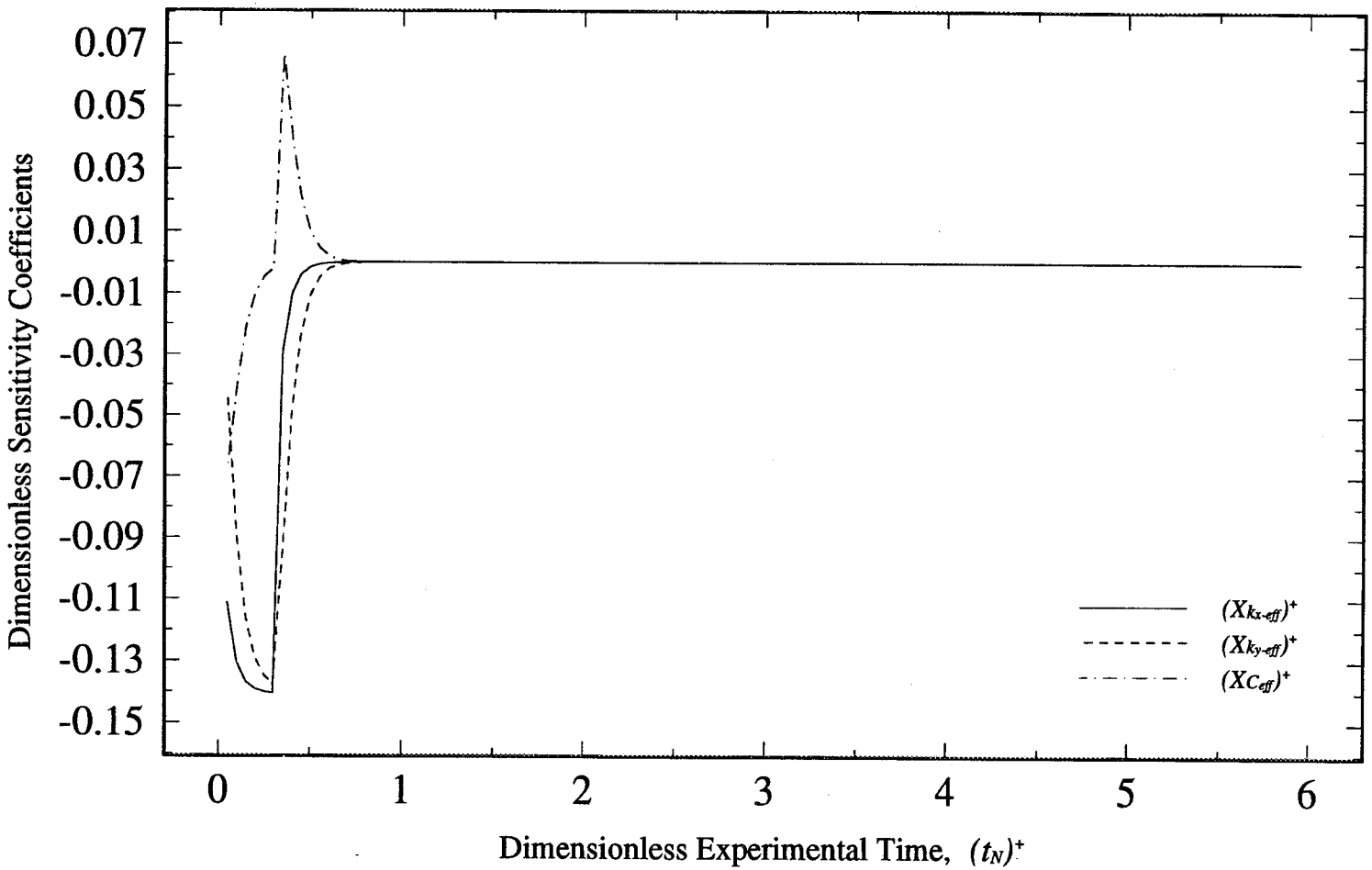

Figure 5.37. Sensitivity Coefficients for Configuration 1 Using a L_{xy} (L_x/L_y) of 0.5 and κ_{xy} ($k_{y\text{-}eff}/k_{x\text{-}eff}$) of 7.

procedure and is not recommended as an experimental design. Based on this result, it is evident that raising L_{xy} to 1.0, where the thickness in the x^+ direction is additionally increased, will provide similar results, and therefore, should also not be used as an experimental design. When comparing these two results to the case previously analyzed in Section 5.2.1.1.9 ($L_{xy} = 0.048$, $\kappa_{xy} = 7$), it is seen that when using a thin sample for this thermal conductivity ratio, more information is available for the estimation of the thermal properties. This is shown by the larger sensitivity coefficients that result for all three parameters (Fig. 5.24).

Next, to determine the effects of different effective thermal conductivity ratios, κ_{xy} was decreased to 1, and again, combinations for L_{xy} equal to 0.048, 0.5, and 1.0 were analyzed. Note that a κ_{xy} of 1 implies that the resistance to heat flow is equal in both the x^+ and y^+ directions (due to equal effective thermal conductivities).

For all three L_{xy}-κ_{xy} combinations, the sensitivity coefficients were plotted using experimental parameters around the maximum determinant region. These results are shown in Figs. 5.38, 5.39, and 5.40 for L_{xy} values of 0.048, 0.5, and 1.0, respectively. From Fig. 5.38, it is seen that when L_{xy} equals 0.048, sufficient information is provided for the estimation of $k_{x\text{-}eff}$ and C_{eff}, where the sensitivity coefficients are large in magnitude. However, the coefficients for $k_{y\text{-}eff}$ are quite small, remaining practically zero for the entire experimental time. This implies that the estimation of $k_{y\text{-}eff}$ will be difficult, and most likely, inaccurate.

For L_{xy} equal to 1.0 (Fig. 5.40), it is again seen that the sensitivity coefficients

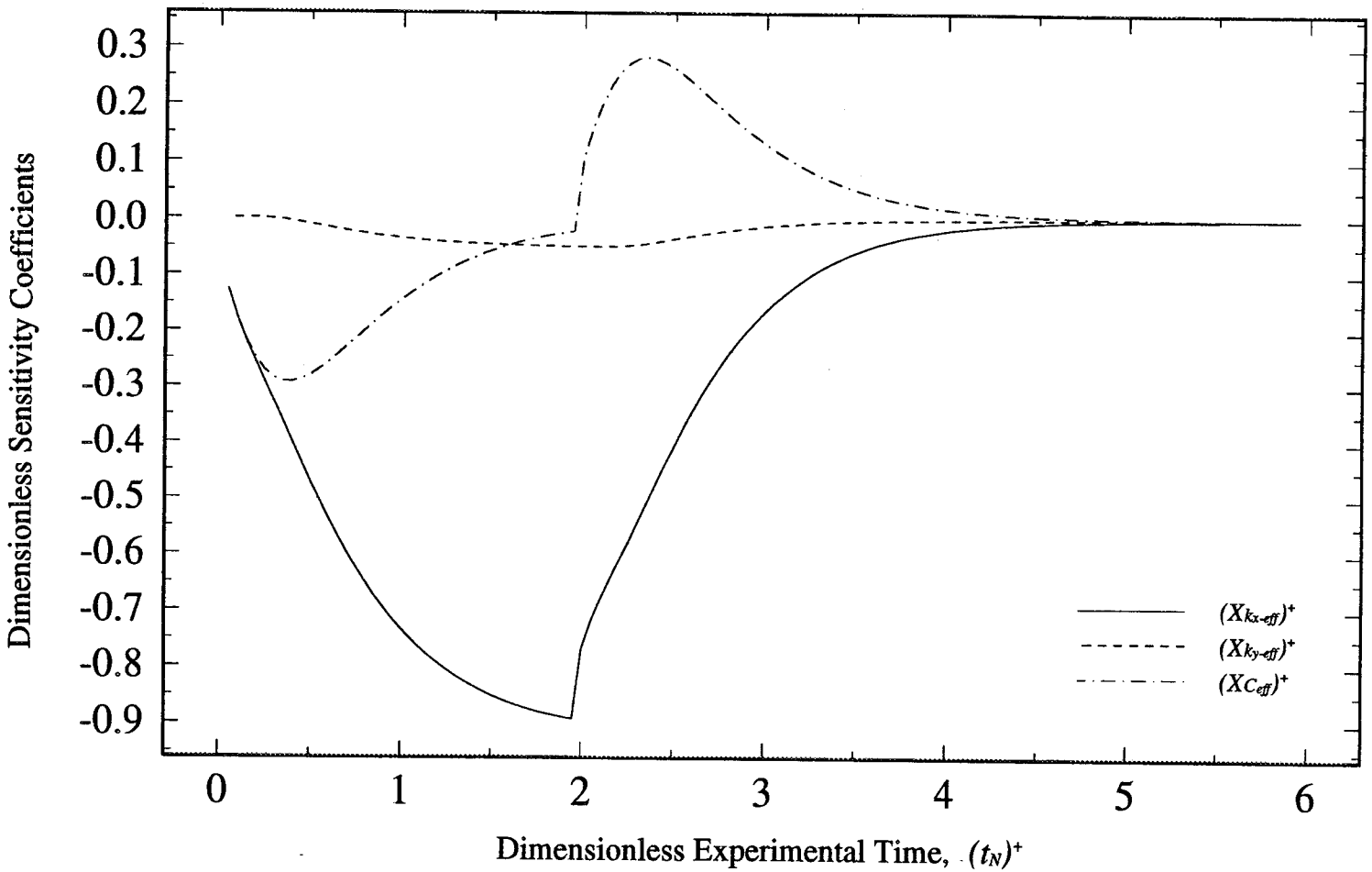

Figure 5.38. Sensitivity Coefficients for Configuration 1 Using a L_{xy} (L_x/L_y) of 0.048 and κ_{xy} ($k_{y\text{-}eff}/k_{x\text{-}eff}$) of 1.

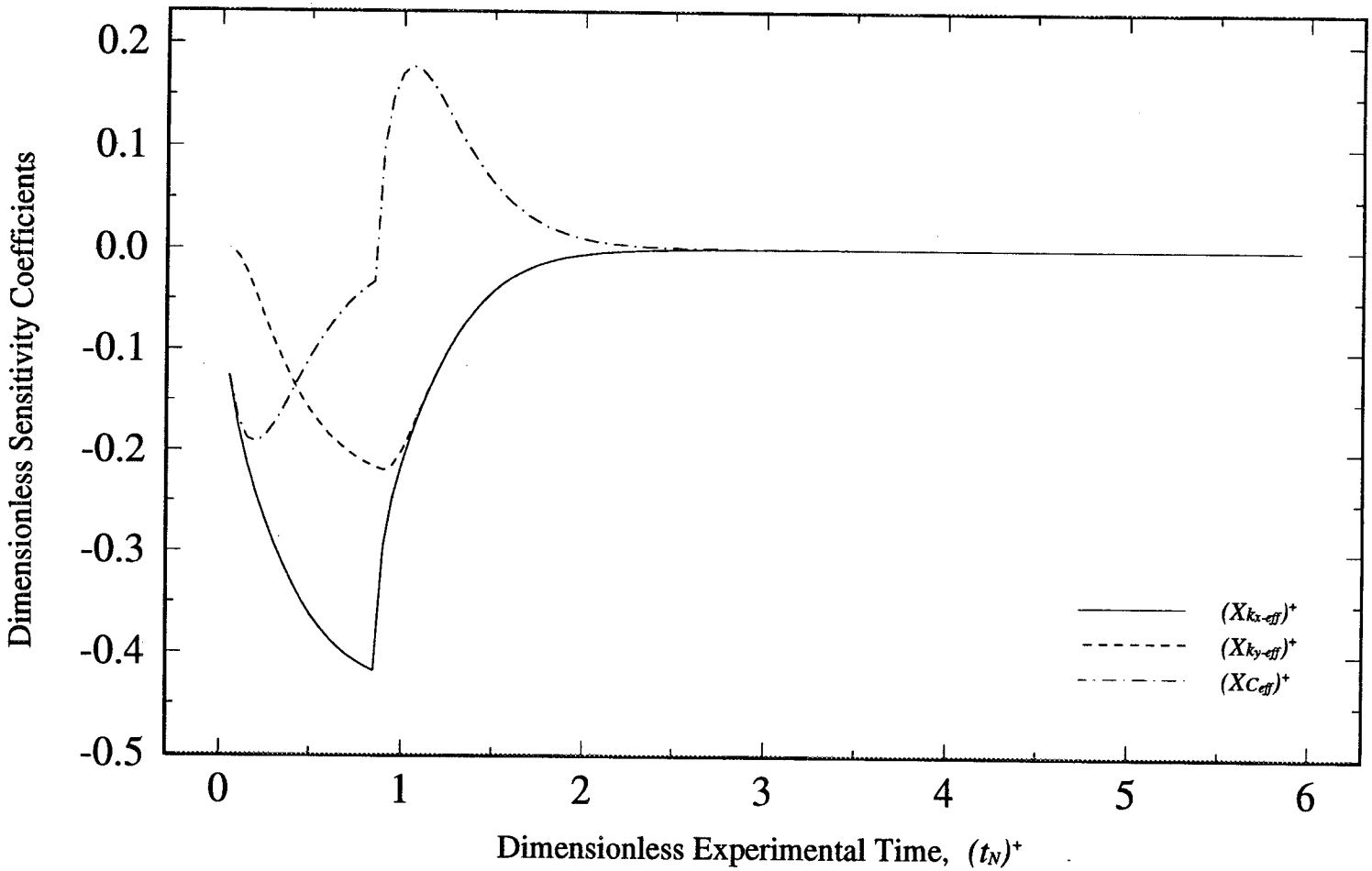

Figure 5.39. Sensitivity Coefficients for Configuration 1 Using a L_{xy} (L_x/L_y) of 0.5 and κ_{xy} ($k_{y\text{-}eff}/k_{x\text{-}eff}$) of 1.

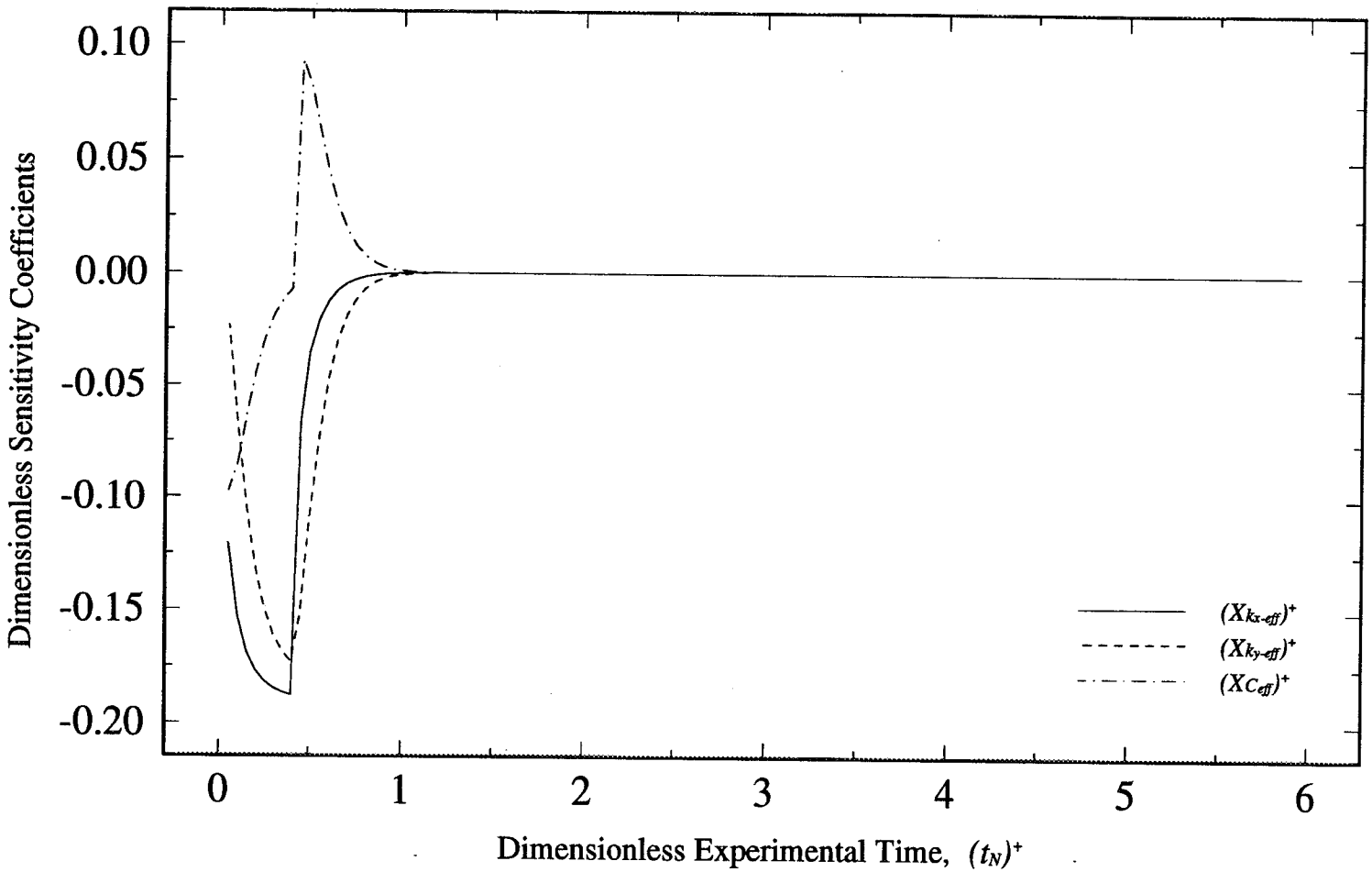

Figure 5.40. Sensitivity Coefficients for Configuration 1 Using a L_{xy} (L_x/L_y) of 1.0 and κ_{xy} ($k_{y\text{-}eff}/k_{x\text{-}eff}$) of 1.

reach steady state fairly rapidly, and therefore, little information is being supplied for the estimation of the thermal properties.

The sensitivity coefficients calculated using a L_{xy} of 0.5 (Fig. 5.39), however, are all relatively large in magnitude. This implies that when using this L_{xy} ratio, difficulty in the estimation of the thermal parameters will not be encountered.

In conclusion, when a composite has equal effective thermal conductivities parallel and perpendicular to the fibers, the optimal L_{xy} ratio is not for either a real small or real large thickness in the direction of heat flow, but instead, falls somewhere in between. An L_{xy} of 0.5 may perhaps be the optimal ratio; however, this conclusion would require further analysis.

The last combination of L_{xy}'s and κ_{xy} for Configuration 1 were again, L_{xy} equal to 0.048, 0.5, and 1.0, with κ_{xy} equal to 1/7. Now, the effective thermal conductivity perpendicular to the fibers (in the direction of the heat flow) is 7 times larger than the thermal conductivity parallel to the fibers. The sensitivity coefficients for all three combinations, L_{xy} equal to 0.048, 0.5, and 1.0, were calculated using the optimal experimental parameters determined around the maximum determinant region. These are shown in Figs. 5.41, 5.42, and 5.43, respectively. From Fig. 5.41, where L_{xy} = 0.048, it is seen that $k_{y\text{-}eff}$ cannot be estimated since the sensitivity coefficient is zero. This occurs because the larger thermal conductivity ($k_{x\text{-}eff}$) is parallel to the heat flow (in the x^+ direction). Since the sample is so thin in this direction, the majority of heat is conducted along this path, causing very small temperature variations to occur perpendicular to the heat flow, along the y^+ axis.

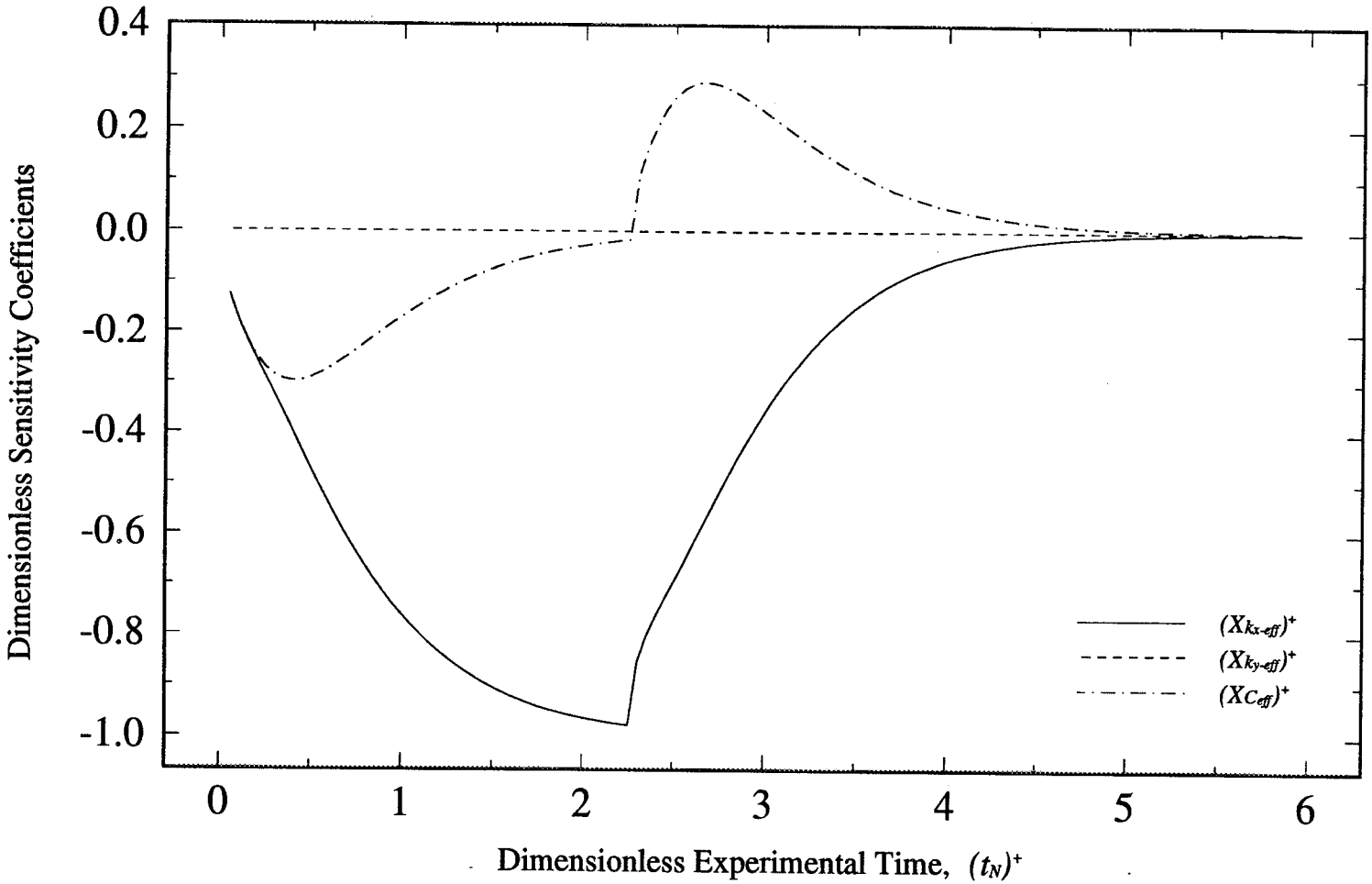

Figure 5.41. Sensitivity Coefficients for Configuration 1 Using a L_{xy} (L_x/L_y) of 0.048 and κ_{xy} ($k_{y\text{-}eff}/k_{x\text{-}eff}$) of 1/7.

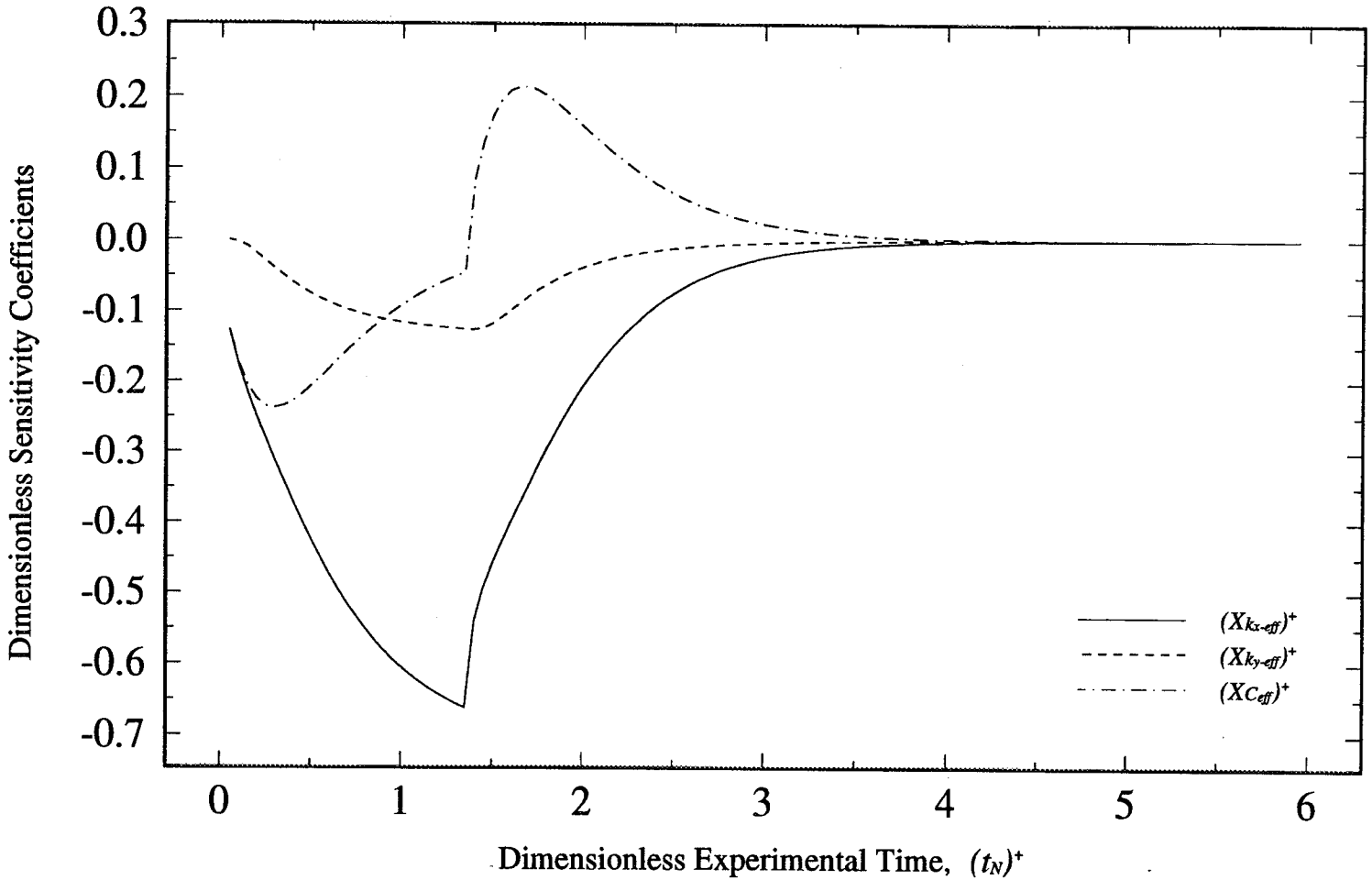

Figure 5.42. Sensitivity Coefficients for Configuration 1 Using a L_{xy} (L_x/L_y) of 0.5 and κ_{xy} ($k_{y\text{-}eff}/k_{x\text{-}eff}$) of 1/7.

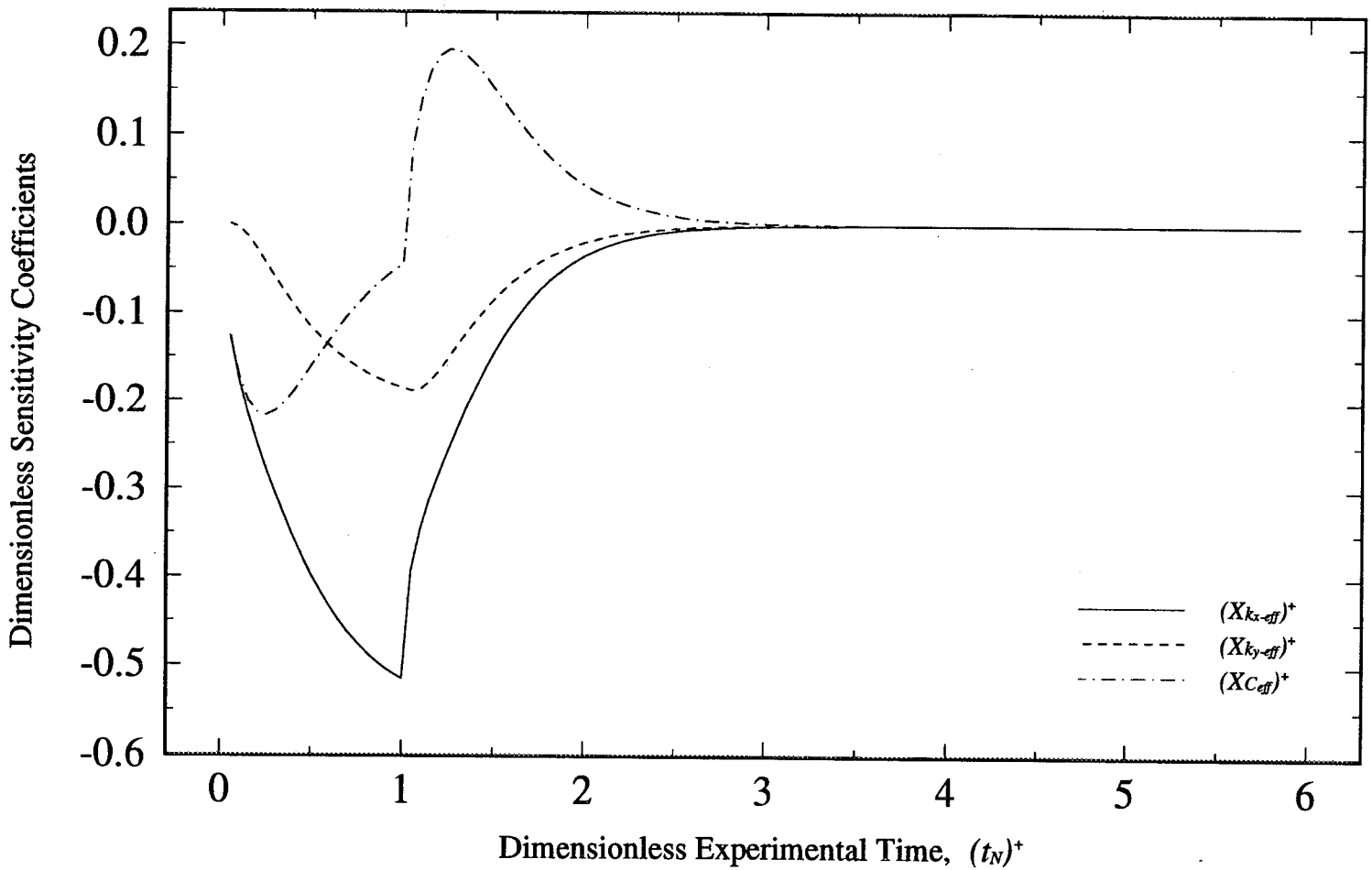

Figure 5.43. Sensitivity Coefficients for Configuration 1 Using a L_{xy} (L_x/L_y) of 1.0 and κ_{xy} ($k_{y\text{-}eff}/k_{x\text{-}eff}$) of 1/7.

From Fig. 5.42, is seen that increasing L_{xy} to 0.5 provides better results for the estimation of $k_{y\text{-}eff}$, where the sensitivity coefficient is larger in magnitude. This occurs because the thickness in the direction of heat flow, x^+, increases. Therefore, the conduction process is slowed, allowing more heat to be dissipated in the y^+ direction.

This result is even more significant when increasing L_{xy} to 1.0 (Fig. 5.43), where the largest magnitude for the $k_{y\text{-}eff}$ sensitivity coefficient out of all three combinations occurs.

It can be concluded from these results that when the effective thermal conductivity in the direction of heat flow is much larger than the thermal conductivity in the direction perpendicular, a better experimental design would consist of a larger thickness in the x^+ direction, allowing more heat to be dissipated in the direction perpendicular to the heat flow.

5.2.1.4.2 Various L_{xy} and κ_{xy} Combinations Used for Configuration 2

Again, the first combination investigated was $L_{xy} = 0.5$ and $\kappa_{xy} = 7$. The sensitivity coefficients calculated using the optimal experimental parameters in the region of the maximum determinant are shown in Fig. 5.44. Here, it is seen that not much information is being supplied for the estimation of $k_{y\text{-}eff}$, where the sensitivity coefficient is small. This occurs because of the increased thickness in the x^+ direction. Raising L_{xy} to 1.0 will further increase this thickness, and therefore, similar results are expected. Therefore, it can be concluded that when the thermal conductivity in the direction of heat flow is much smaller than the thermal conductivity perpendicular to the direction of heat flow, a

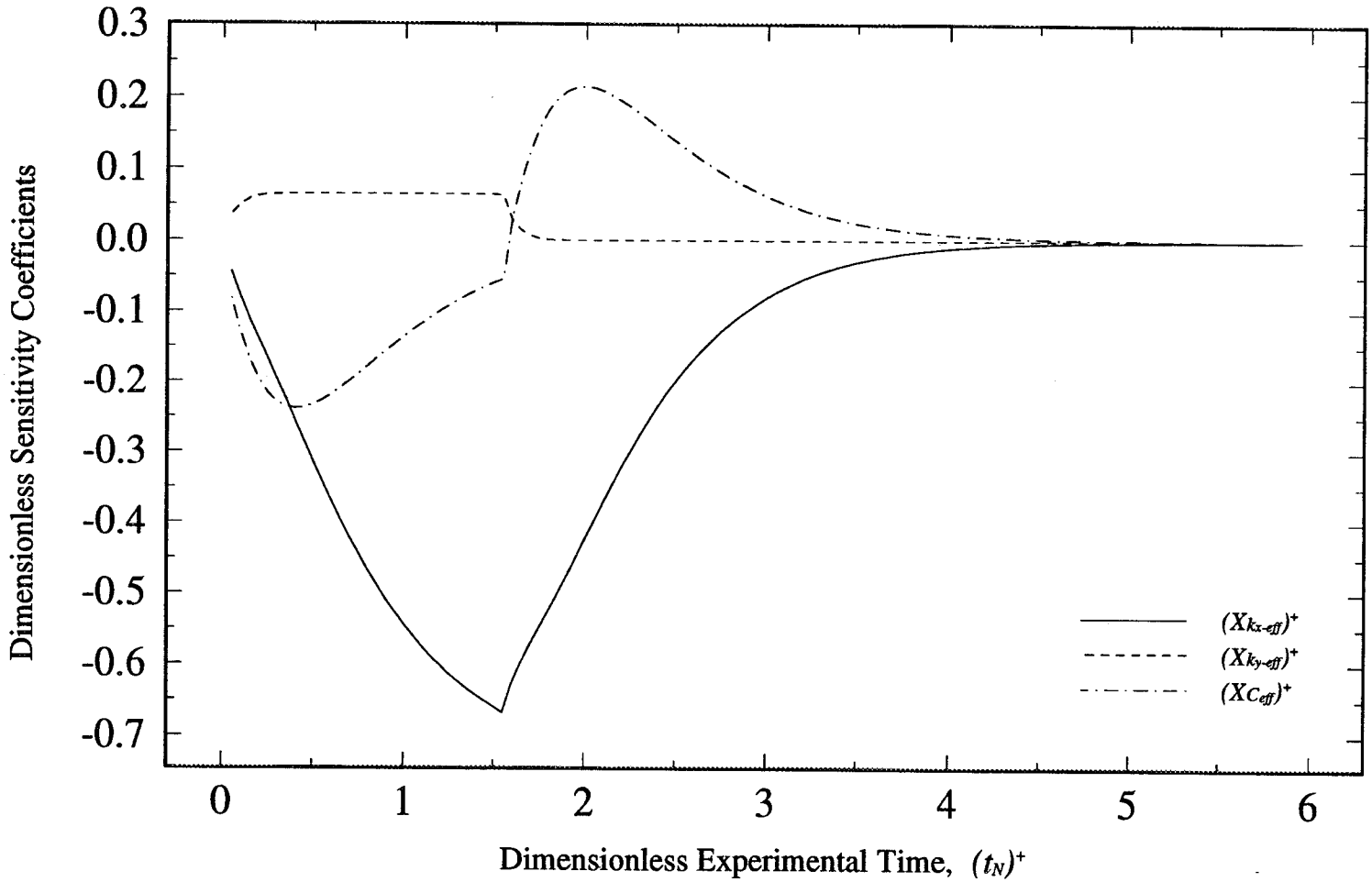

Figure 5.44. Sensitivity Coefficients for Configuration 2 Using a L_{xy} (L_x/L_y) of 0.5 and κ_{xy} ($k_{y\text{-}eff}/k_{x\text{-}eff}$) of 7.

composite sample with a small thickness should be used for the best results. This result is consistent with the case previously analyzed ($L_{xy} = 0.048$, $\kappa_{xy} = 7$), where the sensitivity coefficients for all three parameters are slightly larger than when $L_{xy} = 0.5$.

Next, κ_{xy} was decreased to 1 and similar combinations for L_{xy} were analyzed. Again, note that this κ_{xy} implies that the resistance to heat flow is equal in both the x^+ and y^+ directions. The sensitivity coefficients calculated using the experimental parameters around the maximum determinant region for all three L_{xy}-κ_{xy} combinations are shown in Figs. 5.45, 5.46, and 5.47. In Fig. 5.45 (L_{xy} = 0.048), it is seen that having a small thickness in the x^+ direction creates difficulty in the estimation of $k_{y\text{-}eff}$, where the sensitivity coefficient is essentially zero for the entire experimental time. This result is consistent with that obtained for Configuration 1 at a similar L_{xy} ratio. However, when L_{xy} is increased to 0.5 or 1.0 (Figs. 5.46 and 5.47, respectively), the $k_{y\text{-}eff}$ sensitivity coefficients are of approximately the same magnitude, only different in sign. However, this magnitude is still small and therefore, neither an L_{xy} of 0.5 or 1.0 is the optimal value. The optimal L_{xy} may lie between these values, but the exact determination would require further analysis.

The last combinations of L_{xy}'s and κ_{xy} for Configuration 2 were again, L_{xy} equal to 0.048, 0.5, and 1.0, with κ_{xy} equal to 1/7. Now, the effective thermal conductivity perpendicular to the fibers (in the direction of heat flow), $k_{x\text{-}eff}$, is 7 times larger than the thermal conductivity parallel to the fibers, $k_{y\text{-}eff}$. The sensitivity coefficients for all three combinations, L_{xy} equal to 0.048, 0.5, and 1.0, were calculated using the optimal

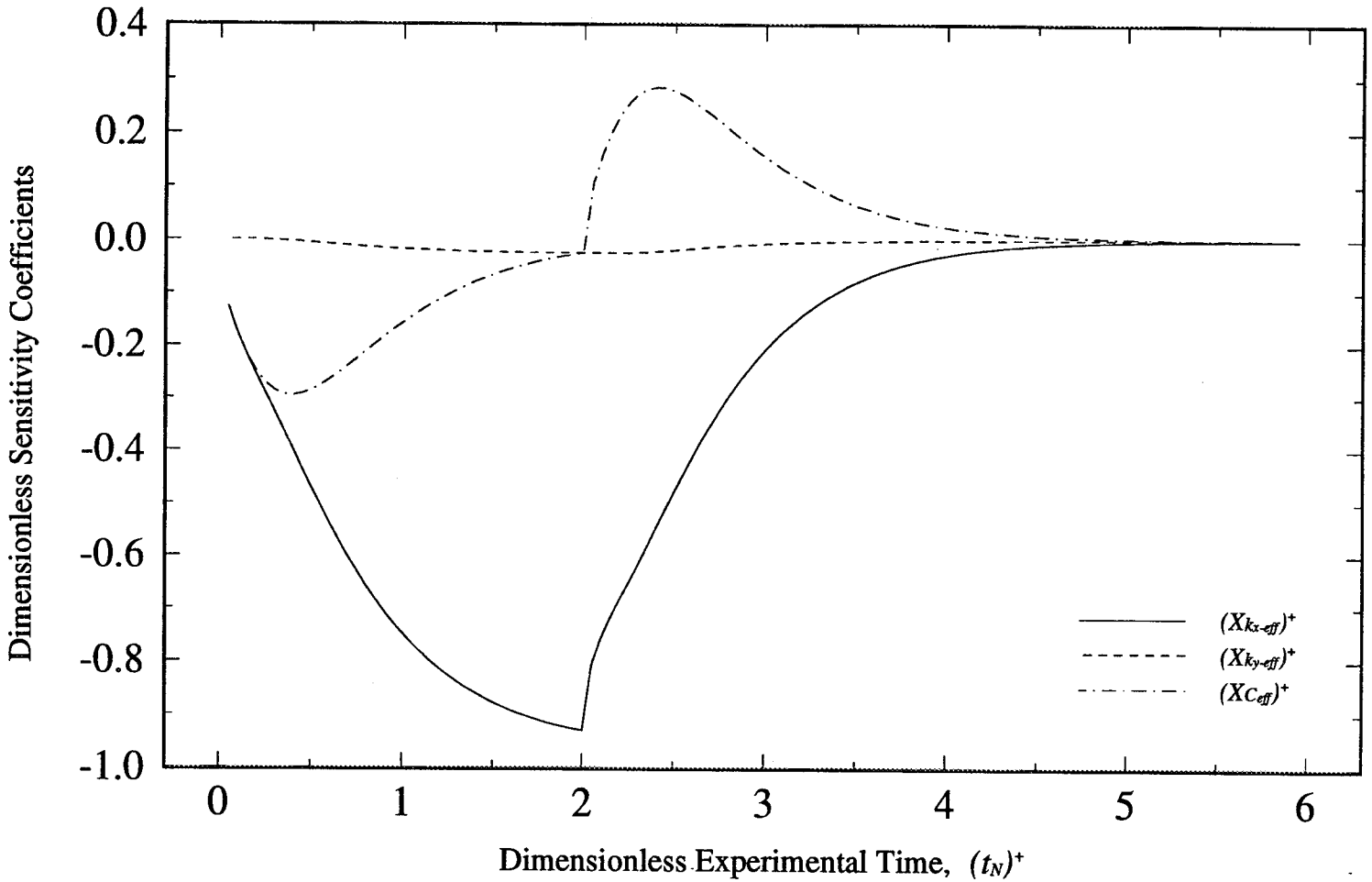

Figure 5.45. Sensitivity Coefficients for Configuration 2 Using a L_{xy} (L_x/L_y) of 0.048 and κ_{xy} ($k_{y\text{-}eff}/k_{x\text{-}eff}$) of 1.

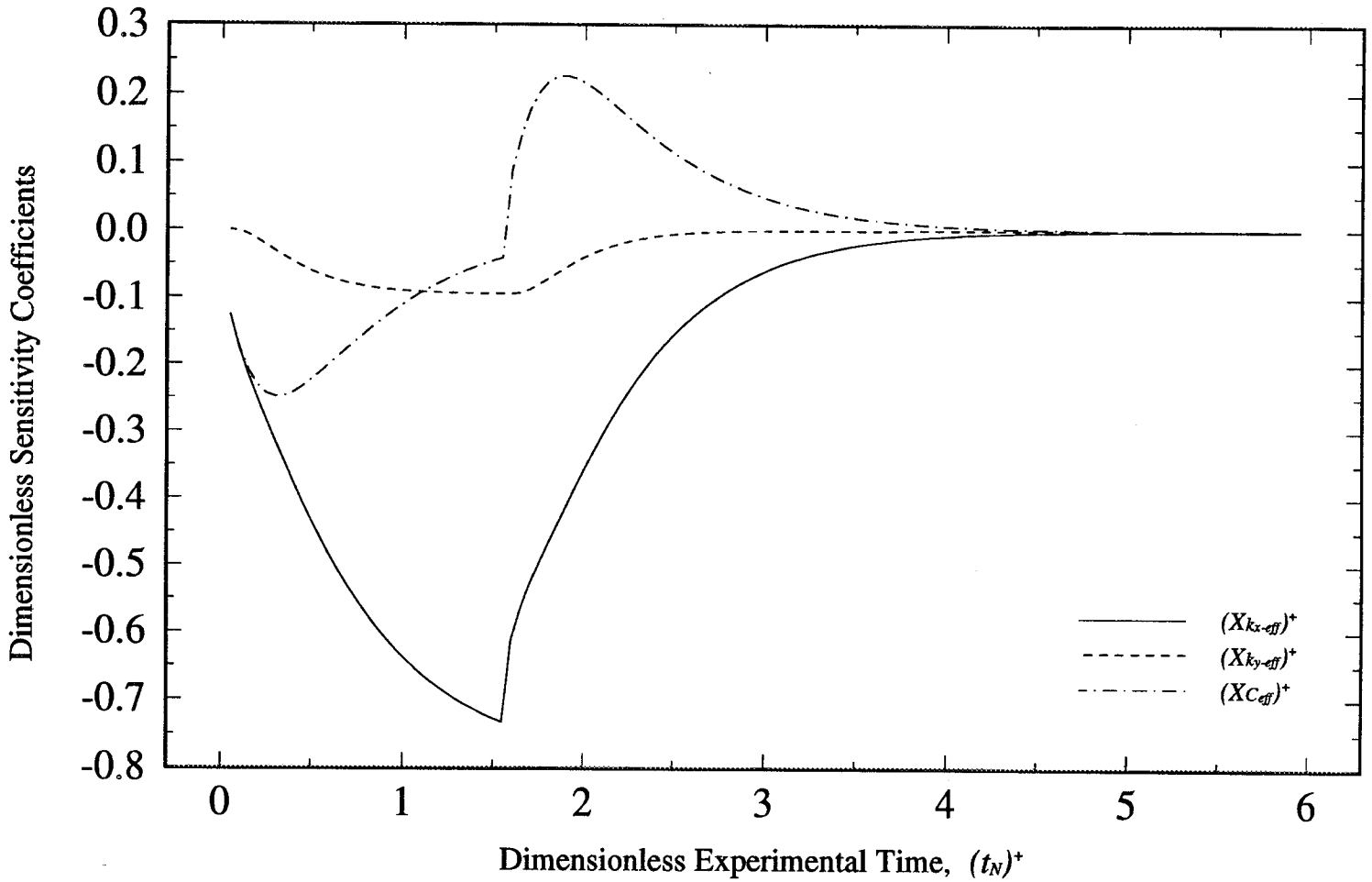

Figure 5.46. Sensitivity Coefficients for Configuration 2 Using a L_{xy} (L_x/L_y) of 0.5 and κ_{xy} ($k_{y\text{-}eff}/k_{x\text{-}eff}$) of 1.

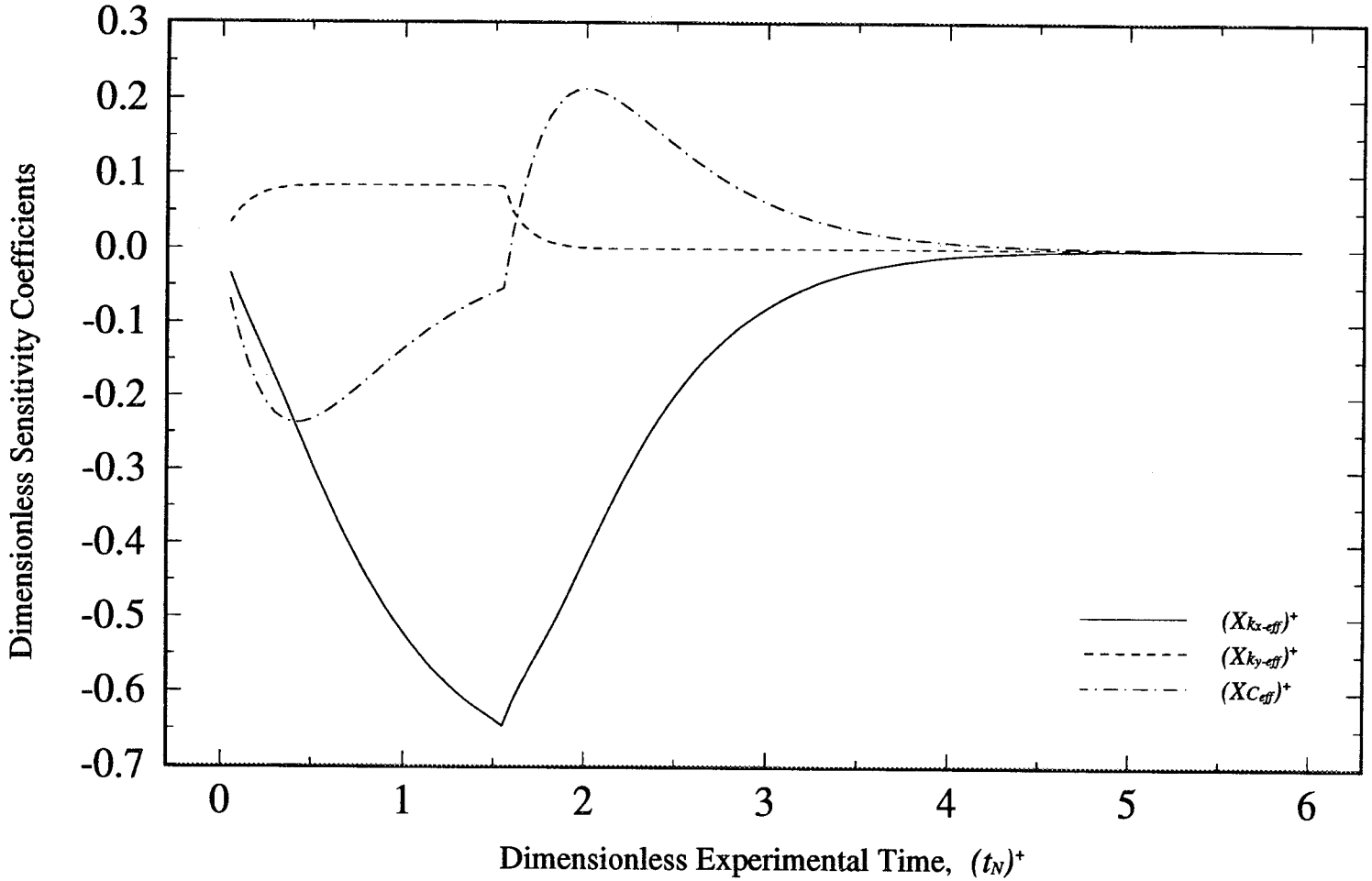

Figure 5.47. Sensitivity Coefficients for Configuration 2 Using a L_{xy} (L_x/L_y) of 1.0 and κ_{xy} ($k_{y\text{-}eff}/k_{x\text{-}eff}$) of 1.

experimental parameters determined around the maximum determinant region. These results are shown in Figs. 5.48, 5.49, and 5.50, respectively. From each of these figures, the same results are seen as for Configuration 1, where the best experimental design consisted of a larger thickness in the x^+ direction (a L_{xy} of 1.0), allowing more heat to be dissipated in the direction perpendicular to the applied heat flux. This is evident by the larger sensitivity coefficient for $k_{y\text{-}eff}$ when $L_{xy} = 1.0$ (Fig. 5.50) than when L_{xy} equals either 0.5 (Fig. 5.49), where the magnitude of the coefficient is 0.1, or 0.048 (Fig. 5.48), where the coefficients are essentially zero. Recall that this zero coefficient results for L_{xy} = 0.048 because the sample is very thin in the direction of heat transfer, x^+ (and the direction of the larger effective thermal conductivity). Therefore, the majority of the heat is conducted along the x^+ axis, causing very small temperature variations to occur along the y^+ axis, and as a result, the estimation of $k_{y\text{-}eff}$ becomes difficult.

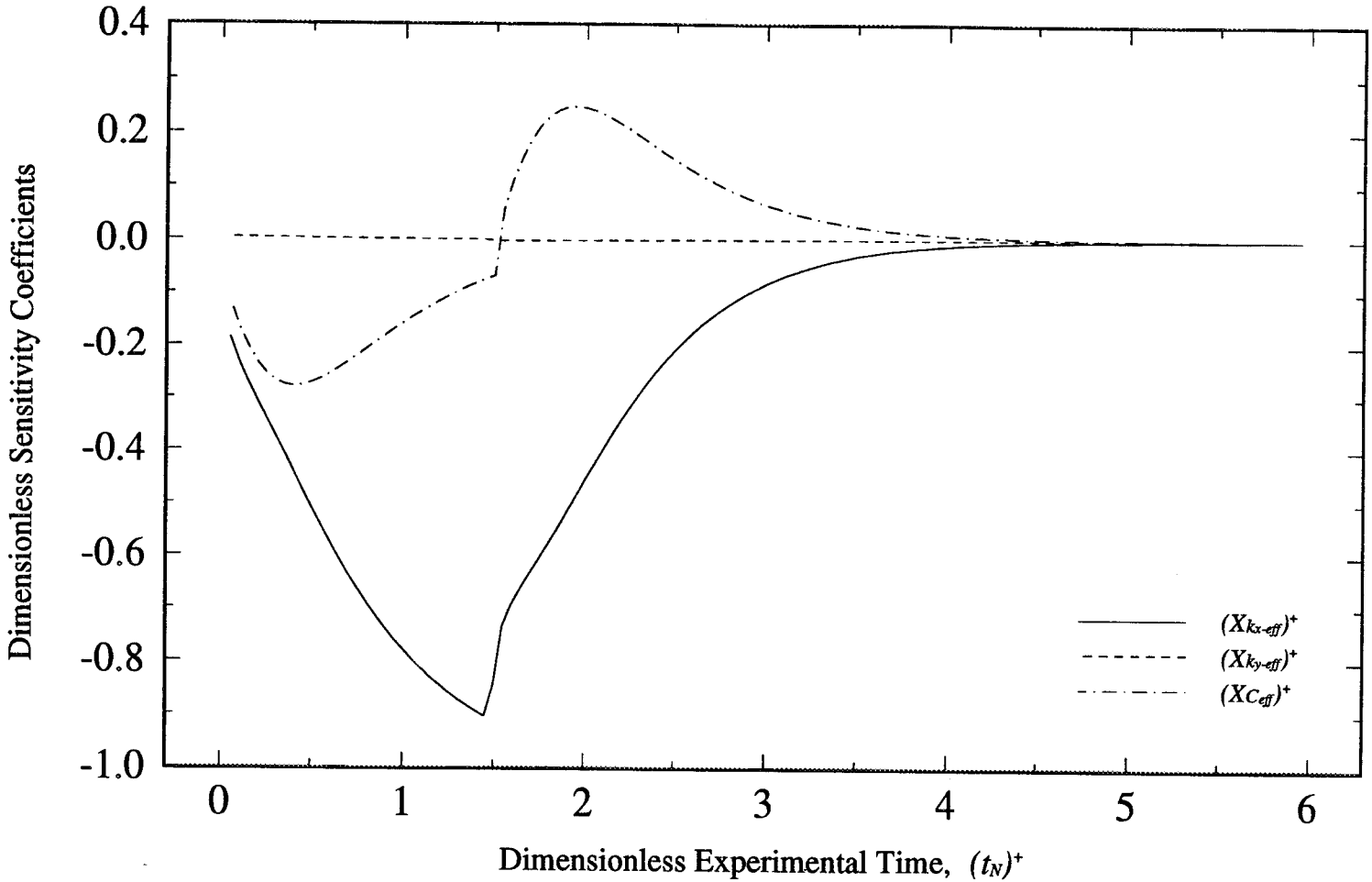

Figure 5.48. Sensitivity Coefficients for Configuration 2 Using a L_{xy} (L_x/L_y) of 0.048 and κ_{xy} ($k_{y\text{-}eff}/k_{x\text{-}eff}$) of 1/7.

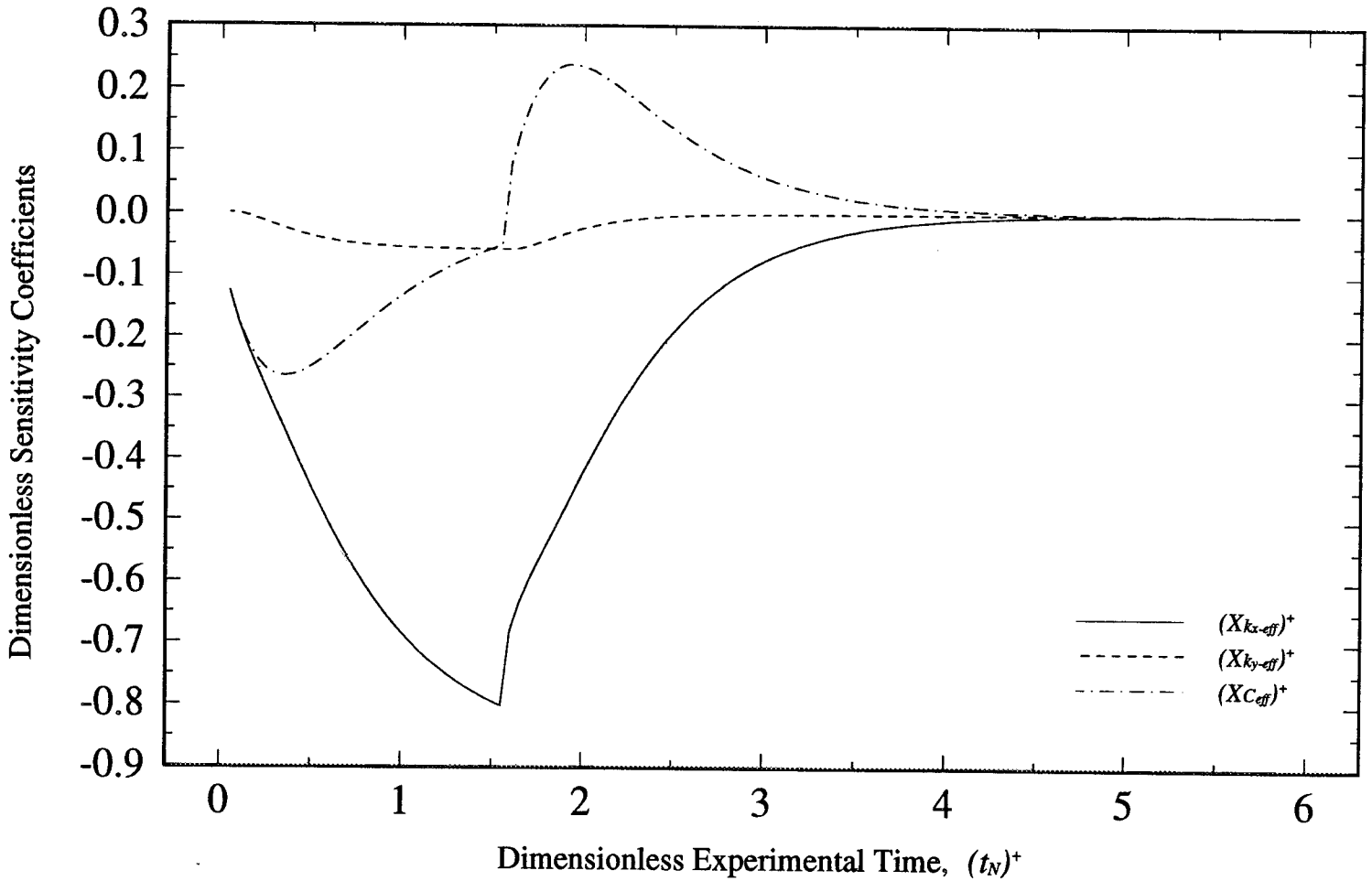

Figure 5.49. Sensitivity Coefficients for Configuration 2 Using a L_{xy} (L_x/L_y) of 0.5 and κ_{xy} ($k_{y\text{-}eff}/k_{x\text{-}eff}$) of 1/7.

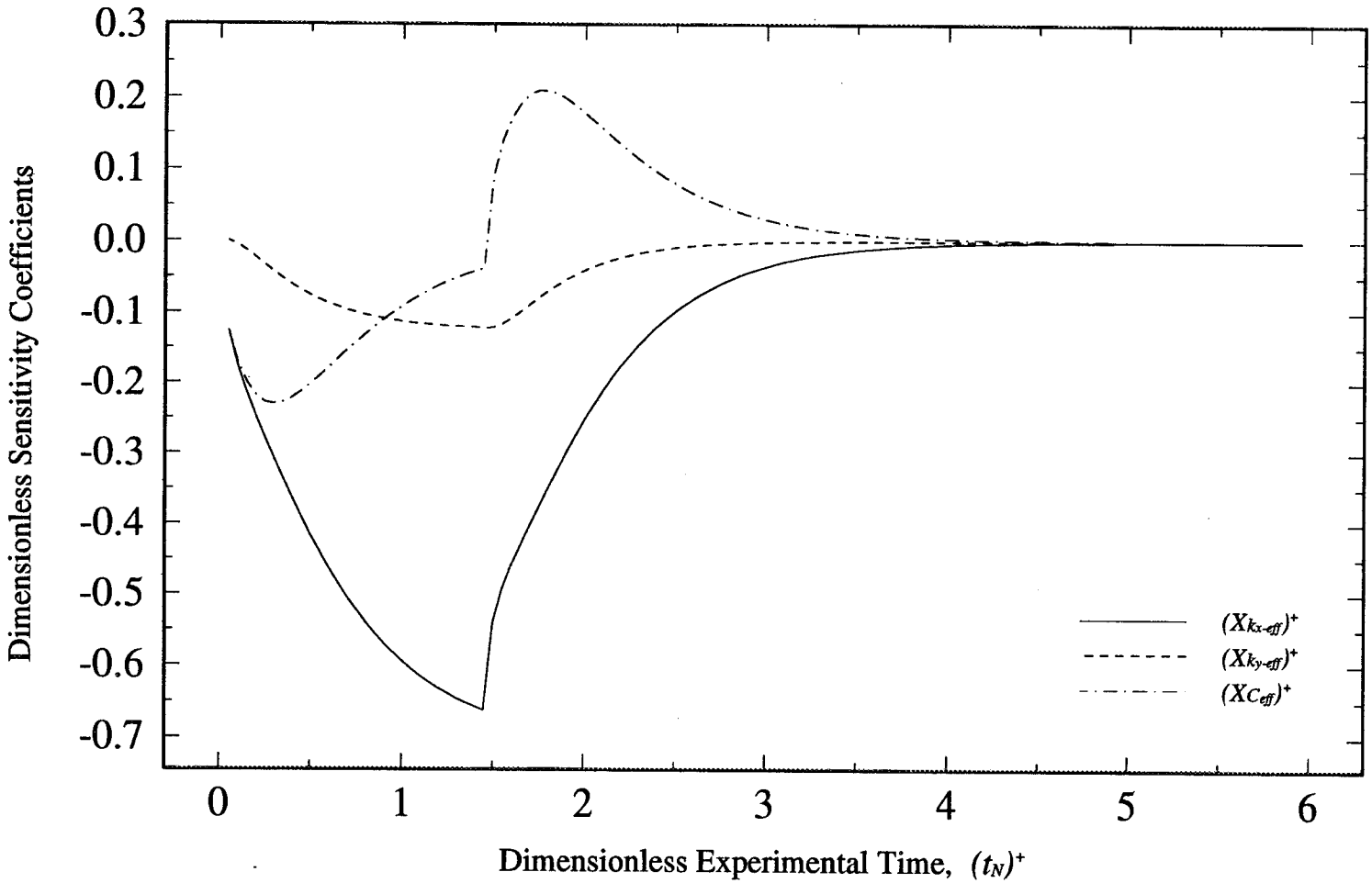

Figure 5.50. Sensitivity Coefficients for Configuration 2 Using a L_{xy} (L_x/L_y) of 1.0 and κ_{xy} ($k_{y\text{-}ff}/k_{x\text{-}eff}$) of 1/7.

Chapter 6

Conclusions and Summary

The primary objectives of this study were to develop optimal experimental designs to be used for the estimation of thermal properties of composite materials. This includes both one-dimensional (isotropic) and two-dimensional (anisotropic) analyses. Experiments were then conducted for the one-dimensional case, using the optimal design, to estimate the effective thermal conductivity perpendicular to the fibers and the effective volumetric heat capacity of a composite consisting of IM7 graphite fibers and a Bismaleimide epoxy matrix. The estimation procedure used was the modified Box-Kanemasu method. The following conclusions can be made based on the obtained results.

6.1 Optimal Experimental Designs

In this investigation, optimal experimental designs were determined for both one-dimensional and two-dimensional heat conduction processes. In the two-dimensional analysis, two different configurations were investigated, both allowing for the estimation

of the effective thermal conductivity in two directions and the effective volumetric heat capacity.

6.1.1 One-Dimensional Optimal Experimental Design

For the one-dimensional experimental design, three experimental parameters were optimized: dimensionless heating time, temperature sensor location, and dimensionless experimental time. The following conclusions can be made based on the results obtained for the specific geometry and boundary conditions used in this analysis:

1) The optimal dimensionless heating time is 2.2. However, the maximum determinant curve had a rather flat peak between heating times of 2.0 and 2.5. Therefore, any values within this range can be used.
2) The optimal temperature sensor location is at the heated surface.
3) The optimal dimensionless experimental time is approximately 5.0. Note however, that this is a conservative choice.

6.1.2 Two-Dimensional Optimal Experimental Designs

For the two-dimensional experimental design, two configurations were analyzed. Both configurations had a heat flux applied over a portion of one boundary, with the remainder of the boundary insulated. In addition, Configuration 1 had known, constant temperatures at the remaining three boundaries, while the second configuration had a known constant temperature at the boundary opposite to the heat flux and insulated conditions at the remaining two boundaries. For each configuration, the optimal

experimental parameters determined include the temperature sensor location (x_s^+,y_s^+), the dimensionless heating time, the location of the heat flux, and the dimensionless experimental time. Based on the obtained results for the specific geometry and boundary conditions used in this analysis, the following conclusions can be made:

6.1.2.1 Conclusions for Configuration 1

1) The optimal dimensionless heating time is 1.4.
2) The optimal temperature sensor location occurs at a x_s^+ of 0.0 (or at the heated surface) and a y_s^+ of 0.13 (13% of L_y from the bottom edge).
3) The optimal location of the heat flux is across the entire y^+ boundary ($L_{p,1}^+$=1.0).
4) The optimal dimensionless experimental time is approximately 4.0. Note however, that this is a conservative choice.

6.1.2.2 Conclusions for Configuration 2

1) The optimal dimensionless heating time is 1.55.
2) The optimal temperature sensor location occurs at a x_s^+ of 0.0 (or at the heated surface) and a y_s^+ of 0.77 (77% of L_y from the bottom edge).
3) The optimal location of the heat flux is across 89% of the y^+ boundary ($L_{p,2}^+$=0.89).
4) The optimal dimensionless experimental time is approximately 4.0. Again, this is a conservative value.

The following conclusion can also be made when comparing the two configurations:

1) Configuration 1 should be utilized when estimating $k_{x\text{-}eff}$, $k_{y\text{-}eff}$, and C_{eff} simultaneously, increasing the accuracy of the resulting property estimates.

6.2 Thermal Property Estimates

The estimation of the thermal properties, namely the effective thermal conductivity perpendicular to the fibers and the effective volumetric heat capacity, was conducted for the one-dimensional analysis using the modified Box-Kanemasu method. This estimation procedure requires both measured and calculated temperatures. The measured temperatures were obtained from experiments conducted using the optimal experimental parameters. The following conclusions can be made based on the results of this portion of the investigation:

1) The effective thermal conductivity perpendicular to fibers ($k_{x\text{-}eff}$) is 0.52 W/m°C.
2) The effective volumetric heat capacity (C_{eff}) is 1.48 MJ/m^3°C.
3) The estimated parameters are both reliable, as shown by the small confidence intervals and the Root Mean Square values.
4) The estimates for $k_{x\text{-}eff}$ are more accurate than for C_{eff}.
5) The sequential estimates converge to a steady value, indicating that the heat conduction model and experimental design are satisfactory.
6) No bias error in the calculated temperatures is apparent.

Chapter 7

Recommendations

The estimation procedure used in this investigation to determine the effective thermal conductivity perpendicular to the fiber axis and the effective volumetric heat capacity proved to be quite accurate. However, because the problem had been simplified by conducting the required experiments at room temperature, the actual environmental conditions that many composites, especially in aerospace vehicles, are subjected to have not been accurately described. These operating conditions usually occur over extreme temperature ranges, resulting in temperature dependent thermal properties. Therefore, in order to accurately determine the temperature distributions within these structures during actual operational conditions, it is necessary to characterize this temperature dependence. The estimation procedure can be modified to include this dependence by assuming a functional relationship between the thermal properties and temperature. For example, the thermal conductivity can be approximated by a piece-wise linear function with temperature:

$$k_{eff} = k_i + (k_{i+1} - k_i)\left(\frac{T - T_i}{T_{i+1} - T_i}\right) \tag{7.1}$$

where k_i and k_{i+1} are the coefficients to be estimated. The mathematical model can now be modified to include temperature dependent properties and the least squares function given in Eq. (3.33) can be minimized with respect to k_i and k_{i+1}.

In addition, it is also recommended that the results of the two-dimensional optimization procedure be verified. This can be done by conducting experiments for the two configurations using both the optimal experimental parameters and arbitrary experimental parameters. The measured temperatures will then be utilized in the estimation procedure to determine the thermal properties, $k_{x\text{-}eff}$, $k_{y\text{-}eff}$, and C_{eff}. The estimates obtained using the experiments conducted with the optimal parameters should provide the smallest confidence intervals. (Recall that the optimization procedure selected for this study has the effect of minimizing the confidence intervals of the estimated parameters).

The Box-Kanemasu method could also be implemented to determine the thermal properties using both configurations simultaneously. Based on the magnitude of the sensitivity coefficients, temperature measurements from Configuration 2 would be used to estimate $k_{x\text{-}eff}$ and C_{eff}, while $k_{y\text{-}eff}$ would be estimated using measurements taken from Configuration 1. Using both configurations together will then supply the most accurate estimates for all three thermal properties.

Other properties could also be estimated, such as the thermal contact resistance between composite components. Here, the least squares function would be minimized with respect to the contact resistance. Furthermore, efforts could be taken for the analysis of complex structures.

BIBLIOGRAPHY

Bard, Y., 1970, "Comparison of Gradient Methods for the Solution of Nonlinear Parameter Estimation Problems," *SIAM Journal of Numerical Analysis*, Vol. 7, pp. 157-186.

Beck, J. V., 1963, "Calculation of Thermal Diffusivity from Temperature Measurements," *Journal of Heat Transfer*, Vol. 85, pp. 181-182.

Beck, J. V., 1966a, "Transient Determination of Thermal Properties," *Nuclear Engineering and Design*, Vol. 3, pp. 373-381.

Beck, J. V., 1966b, "Analytical Determination of Optimum, Transient Experiments for Measurement of Thermal Properties," Proceedings of the 3rd International Heat Transfer Conference, Vol. 44, pp. 74-80.

Beck, J. V., 1969, "Determination of Optimum, Transient Experiments for Thermal Contact Conductance", *International Journal of Heat and Mass Transfer*, Vol. 12, pp. 621-633.

Beck, J. V., 1988, "Combined Parameter and Function Estimation in Heat Transfer with Application to Contact Conductance," *Journal of Heat Transfer*, Transactions of the ASME, Vol. 110, No. 4B, pp. 1046-1058.

Beck, J. V., 1993, *NLINA.FOR*, FORTRAN Computer Program, Department of Mechanical Engineering, Michigan State University, E. Lansing, MI.

Beck, J. V. and S. Al-Araji, 1974, "Investigation of a New Simple Transient Method of Thermal Property Measurement," *Journal of Heat Transfer*, Vol. 96, No. 1 pp. 59-64.

Beck, J. V. and K. J. Arnold, 1977, *Parameter Estimation in Engineering and Science*, John Wiley & Sons, New York.

Beck, J. V., K. D. Cole, A. Haji-Sheikh, and B. Litkouhi, 1992, *Heat Conduction Using Green's Functions*, Hemisphere Publishing Corporation, Washington, DC.

Behrens, E., 1968, "Thermal Conductivities of Composite Materials," *Journal of Composite Materials*, Vol. 2, No. 1, pp. 2-17.

Beran, M. J. and N. R. Silnutzer, 1971, "Effective Electrical, Thermal and Magnetic Properties for Fiber Reinforced Materials," *Journal of Composite Materials*, Vol. 5, pp. 246-249.

Brennan, J. J., L. D. Bentsen and D. P. H. Hasselman, 1982, "Determination of the Thermal Conductivity and Diffusivity of Thin Fibres by the Composite Method," *Journal of Materials Science*, Vol. 17, pp. 2337-2342.

Box, G. E. P. and H. Kanemasu, 1972, "Topics in Model Building, Part II, on Non-linear Least Squares," Tech. Report No. 321, University of Wisconsin, Dept. of Statistics, Madison, Wisconsin.

Dickson, D. J., 1973, "Measurement of the Thermal Conductivity of Thermal Insulations Using Miniature Heat Flow Sensors," *Journal of Physics E: Scientific Instruments*, Vol. 6, No. 11, pp. 1074-1076.

Fukai, J., H. Nogami, T. Miura and S. Ohtani, 1991, "Simultaneous Estimation of Thermophysical Properties by Periodic Hot-Wire Heating Method," *Experimental Thermal and Fluid Science*, Vol. 4, pp. 198-204.

Garnier, B., D. Delaunay and J. V. Beck, 1992, "Estimation of Thermal Properties of Composite Materials without Instrumentation Inside the Samples," *International Journal of Thermophysics*, Vol. 13, No. 6, pp. 1097-1111.

Han, L. S. and A. A. Cosner, 1981, "Effective Thermal Conductivities of Fibrous Composites," *Journal of Heat Transfer*, Vol. 103, No. 5, pp. 387-392.

Harris, J. P, B. Yates, J. Batchelor and P. J. Garrington, 1982, "The Thermal Conductivity of Kevlar Fibre-Reinforced Composites," *Journal of Materials Science*, Vol. 17, No. 10, pp. 2925-2930.

Hasselman, D. P. H., 1987, "Thermal Diffusivity and Conductivity of Composites with Interfacial Thermal Contact Resistance", *Thermal Conductivity*, Vol. 20, pp. 405-413.

Hasselman, D. P. H. and L. F. Johnson, 1987, "Effective Thermal Conductivity of Composites with Interfacial Thermal Barrier Resistance," *Journal of Composite*

Materials, Vol. 21, pp. 508-515.

Havis, C. R., G. P. Peterson and L. S. Fletcher, 1989, "Predicting the Thermal Conductivity and Temperature Distribution in Aligned Fiber Composites," *Journal of Thermophysics*, Vol. 3, No. 4, pp. 416-422.

Ishikawa, T., 1980, "Analysis and Experiments on Thermal Conductivities of Unidirectional Fiber-Reinforced Composites," *Heat Transfer - Japanese Research*, Vol. 9, No. 3, pp. 41-53.

James, B. W. and P. Harrison, 1992, "Analysis of the Temperature Distribution, Heat Flow and Effective Thermal Conductivity of Homogeneous Composite Materials with Anisotropic Thermal Conductivity," *Journal of Physics D: Applied Physics*, Vol. 25, No. 9, pp. 1298-1303.

James, B. W. and G. S. Keen, 1985, "A Nomogram for the Calculation of the Transverse Thermal Conductivity of Uniaxial Composite Lamina," *High Temperatures - High Pressures*, Vol. 17, pp. 477-480.

James, B. W., G. H. Wostenholm, G. S. Keen and S. D. McIvor, 1987, "Prediction and Measurement of the Thermal Conductivity of Composite Materials," *Journal of Physics; D: Applied Physics*, Vol. 20, No. 3, pp. 261-268.

Jurkowski, T., Y. Jarny and D. Delaunay, 1992, "Simultaneous Identification of Thermal Conductivity and Thermal Contact Resistances without Internal Temperature Measurements," *Institution of Chemical Engineers Symposium Series*, Vol. 2, No. 129, pp. 1205-1211.

Lee, H. J. and R. E. Taylor, 1975, "Thermophysical Properties of Carbon/Graphite Fibers and mod-3 Fiber-Reinforced Graphite," *Carbon*, Vol. 13, pp. 521-527.

Loh, M. H. and J. V. Beck, 1991, "Simultaneous Estimation of Two Thermal Conductivity Components from Transient Two-Dimensional Experiments," ASME Paper No. 91-WA/HT-11, ASME, NY.

Mottram, J. T., 1992, "Design Charts for the Thermal Conductivity of Continuous Fibre-Reinforced Composites," *Materials and Design*, Vol. 13, No. 5, pp. 279-284.

Mottram, J. T. and R. Taylor, 1987a, "Thermal Conductivity of Fibre-Phenolic Resin Composites. Part I: Thermal Diffusivity Measurements," *Composites Science and Technology*, Vol. 29, pp. 189-210.

Mottram, J. T. and R. Taylor, 1987b, "Thermal Conductivity of Fibre-Phenolic Resin

Composites. Part II: Numerical Evaluation," *Composites Science and Technology*, 29:211-232.

Parker, W. J., R. J. Jenkins, C. P. Butler and G. L. Abbott, 1961, "Flash Method of Determining Thermal Diffusivity, Heat Capacity, and Thermal Conductivity," *Journal of Applied Physics*, Vol. 32, No. 9, pp. 1679-1684.

Penn, B. G., F. E. Ledbetter III, W. T. White and J. M. Clemons, 1986, "Measurement of the Thermal Conductivity of Composites Using Heat Flow Sensors," *Polymer Composites*, Vol. 7, No. 6, pp. 426-430.

Pfahl, R. C., and B. J. Mitchel, 1970, "Simultaneous Measurement of Six Thermal Properties of a Charring Plastic," *International Journal of Heat and Mass Transfer*, Vol. 13, pp. 275-286.

Progelhof, R. C., J. L. Throne and R. R. Ruetsch, 1976, "Methods for Predicting the Thermal Conductivity of Composite Systems: A Review," *Polymer Engineering and Science*, Vol. 16, No. 9, pp. 615-625.

Scott, E. P. and J. V. Beck, 1992a, "Estimation of Thermal Properties in Epoxy Matrix/Carbon Fiber Composite Materials," *Journal of Composite Materials*, Vol. 26, No. 1, pp. 132-149.

Scott, E. P. and J. V. Beck, 1992b, "Estimation of Thermal Properties in Carbon/Epoxy Composite Materials during Curing," *Journal of Composite Materials*, Vol. 26, No. 1, pp. 20-36.

Springer, G. S. and S. W. Tsai, 1967, "Thermal Conductivities of Unidirectional Materials," *Journal of Composite Materials*, Vol. 1, pp. 166-173.

Taktak, R., E. P. Scott and J. V. Beck, 1991, "Optimal Experimental Designs for Estimating the Thermal Properties of Composite Materials," Proceedings of the 3rd ASME - JSME Thermal Engineering Joint Conference, ASME.

Taylor, R. E. and B. H. Kelsic, 1986, "Parameters Governing Thermal Diffusivity Measurements of Unidirectional Fiber-Reinforced Composites," *Journal of Heat Transfer*, Vol. 108, pp. 161-165.

Taylor, R. E., J. Jortner and H. Groot, 1985, "Thermal Diffusivity of Fiber-Reinforced Composites Using the Laser Flash Technique," *Carbon*, Vol. 23, No. 2, pp. 215-222.

Vinson, J. R. and R. L. Sierakowski, 1987, *The Behavior of Structures Composed of*

Composite Materials, Martinus Nijhoff Publishers, Hingham, MA.

Walpole, R. E. and R. H. Myers, 1978, *Probability and Statistics for Engineers and Scientists*, 2nd Edition, Macmillan Publishing Co., NY.

Welsh, C. S., D. M. Heath and W. P. Winfree, 1987, "Remote Measurement of In-Plane Diffusivity Components in Plates," *Journal of Applied Physics*, Vol. 61, No. 3, pp. 895-898.

Welsh, C. S., W. P. Winfree, D. M. Heath and E. Cramer, 1990, "Material Property Measurements with Post-Processed Thermal Image Data," *SPIE* Vol. 1313 Thermosense XII, pp. 124-132.

Whetstone, W. D., 1983, *EISI-EAL Engineering Analysis Language*, Engineering Information Systems, Inc., San Jose, CA.

Xu, G. and B. Zhonghao, 1990, "Research on Measuring Thermophysical Properties Using Parameter Estimation," *Journal of Thermal Analysis*, Vol. 36, pp. 1049-1056.

Ziebland, H., 1977, "The Thermal and Electrical Transmission Properties of Polymer Composites," in Chapter 7, *Polymer Engineering Composites*, M. O. W. Richardson, ed., Applied Science Publishers, LTD., London.

Appendix A

The FORTRAN program 1DOPT.FOR

This program, 1DOPT.FOR, is used to calculate the maximum determinant value for the one-dimensional analysis, and to determine the corresponding optimal experimental parameters.

```
      PROGRAM ONEDOPT
C     Written by Debbie Moncman, 1993
      DOUBLE PRECISION BETAM,BETA2M,SUMT,SUMC,SUMK
      DOUBLE PRECISION FF1,FF2,BETA2(0:1000),M,TIME,TIMEH
      DOUBLE PRECISION BETA(0:1000),TT,X1T,X2T,INCRX2,PI
      DOUBLE PRECISION Xi,T1,X1,X2,TTIME,DELTA,INCRET
      DOUBLE PRECISION TMAX,D,XTX11,XTX12,XTX22,INCRX1
      COMMON Xi,TIME,TIMEH
      OPEN(UNIT = 15, FILE ='T.DAT', STATUS='UNKNOWN')
      OPEN(UNIT = 20, FILE ='X1.DAT', STATUS='UNKNOWN')
      OPEN(UNIT = 25, FILE ='X2.DAT', STATUS='UNKNOWN')
      OPEN(UNIT = 30, FILE ='Dx1.DAT', STATUS ='UNKNOWN')
      OPEN(UNIT = 35, FILE = 'DMAX.DAT', STATUS='UNKNOWN')
      PI =DACOS(-1.D0)
      DELTA = 0.0250D0
      TTIME = 6.d0
      Xi = 0.0D+0
      DO 7 TIMEH = DELTA, TTIME, DELTA
          TMAX = 0.0D0
          DMAX = 0.0D0
          XTX11 = 0.0D0
          XTX12 = 0.0D0
          XTX22 = 0.0D0
          TT = 0.0D+0
          X1T = 0.0D+0
          X2T = 0.0D+0
```

```
      DO 20, TIME = DELTA, TTIME , DELTA
           CALL MODEL(TT)
           CALL SENS(X1T,X2T)
           XTX11=XTX11+ X1T * X1T
           XTX12=XTX12+ X1T * X2T
           XTX22=XTX22+ X2T * X2T
C     FIND TMAX
           IF(TT.GT.TMAX)TMAX = TT
           D=(1.0D0/(TMAX*TMAX*TIME/DELTA))**2*
     +       (XTX11*XTX22-XTX12*XTX12)
C     FIND DMAX
           IF(D.GE.DMAX) THEN
             DMAX = D
         ENDIF
         WRITE(15,12)TIME/DELTA,TIME,TT
         WRITE(20,12)TIME,X1T
         WRITE(25,12)TIME,X2T
         WRITE(30,40) TIME,D
40       FORMAT(1X, D10.5, 4X, D12.5)
12       FORMAT(2(1X,D12.4),4X,D12.5)
14       FORMAT(1X,D12.4,3(4X,D12.5))
20       CONTINUE
         WRITE(35,8)DMAX,TIMEH
8        FORMAT(1X,2D15.6)
7        CONTINUE
         CLOSE(15)
         CLOSE(20)
         CLOSE(25)
         CLOSE(30)
         CLOSE(35)
         STOP
         END

C*************************************************************************
C    Subroutine to calculate the dimensionless temperature

         SUBROUTINE MODEL(TT)
         DOUBLE PRECISION FF1,BETA2M,TIME,TIMEH,T1,PI
         DOUBLE PRECISION FF2,INCRET,SUMT,Xi,BETAM,M,TT
         DOUBLE PRECISION BETA2(0:1000), BETA(0:1000)
         COMMON Xi,TIME,TIMEH
         PI =DACOS(-1.D0)
         SUMT = 0.0D0
         DO 10, M = 1, 1000, 1
              BETA(M) = (M - 0.5D0)*PI
              BETA2(M) = BETA(M)**2.0D+0
              BETAM = BETA(M)
              BETA2M = BETA2(M)
              FF1 = EXP(-BETA2M * TIME)
              IF (TIME.LE.TIMEH) THEN
```

```
            T1 = FF1
            ELSE
            FF2 = EXP(-BETA2M *(TIME - TIMEH))
            T1 = FF1-FF2
        ENDIF
        INCRET = T1*COS(BETAM*Xi)/BETA2M
        IF(M.NE.1) THEN
            IF(ABS(INCRET/SUMT).LT.1.0D-20) THEN
            GO TO 15
            ENDIF
        ENDIF
        SUMT = SUMT + INCRET
10      CONTINUE
15      IF(TIME.LE.TIMEH) THEN
            TT = 1.0D+0 - Xi - 2.0D+0*SUMT
        ELSE
            TT = -2.0D+0*SUMT
        ENDIF
        RETURN
        END

C*************************************************************************
C  Subroutine to Calculate the dimensionless Sensitivity Coefficients

        SUBROUTINE SENS(X1T,X2T)
        DOUBLE PRECISION TIME,TIMEH,BETAM,BETA2M, SUMK,Xi,M
        DOUBLE PRECISION SUMC,FF1,FF2,X1,X2,INCRX1,INCRX2
        DOUBLE PRECISION BETA(0:1000),BETA2(0:1000),PI
        DOUBLE PRECISION X1T, X2T
        COMMON Xi,TIME,TIMEH
        PI =DACOS(-1.D0)
        SUMK = 0.0D+0
        SUMC = 0.0D+0
        DO 30, M = 1, 1000, 1
            BETA(M) = (M - 0.5D0)*PI
            BETA2(M) = BETA(M)**2.0D+0
            BETAM = BETA(M)
            BETA2M = BETA2(M)
            FF1 = EXP(-BETA2M * TIME)
            IF(TIME.LE.TIMEH) THEN
            X1 = FF1 * (1/BETA2M + TIME)
            X2 = TIME*FF1
            ELSE
            FF2 = EXP(-BETA2M *(TIME - TIMEH))
            X1 = (1/BETA2M+TIME)*FF1-(1/BETA2M+(TIME-TIMEH))*FF2
            X2 = TIME*FF1 - (TIME-TIMEH)*FF2
            END IF
        INCRX1 = X1*COS(BETAM * Xi)
        INCRX2 = X2*COS(BETAM * Xi)
        IF(M.NE.1) THEN
```

```
            IF(ABS(INCRX1/SUMK).LT.1.0D-20.AND.
     +       ABS(INCRX2/SUMC).LT.1.0D-20) THEN
            GO TO 16
            END IF
          END IF
          SUMK = SUMK + INCRX1
          SUMC = SUMC + INCRX2
30      CONTINUE
16      IF(TIME.LE.TIMEH) THEN
          X1T = -(1.0D0 - Xi) + 2.0D0*SUMK
          X2T = -2.0D0 * SUMC
        ELSE
          X1T =  2.0D0*SUMK
          X2T = -2.0D0 * SUMC
        END IF
        RETURN
        END
```

Appendix B

The FORTRAN program 2DC1OPT.FOR

This program, 2DC1OPT.FOR, is used to calculate the maximum determinant value for Configuration 1 of the two-dimensional analysis, and to determine the corresponding optimal experimental parameters.

```
      PROGRAM CFONEOPT
C     Written by Debbie Moncman, 1994
      DOUBLE PRECISION PI,SUMC,SUMKX,SUMKY
      DOUBLE PRECISION Lr,K,BETAN,BETAN2,EXPON,TERM1,TX
      DOUBLE PRECISION FF1,XKX,XKY,XC,FF2,CONST,INCRKX,INCRKY,INCRC
      DOUBLE PRECISION TERM2,TERM3,SUMT,TEMP,INCRT
      DOUBLE PRECISION EXPONTM,EXPONTH,SSSUMT, SSINCRT
      DOUBLE PRECISION SSSUMKX,SSINCRKX,SSSUMKY,SSINCRKY
      DOUBLE PRECISION TERM4,X,Y,Yp,TERM5,TMAX
      DOUBLE PRECISION X1T,X2T,X3T,XTX11,XTX12,XTX13,XTX22
      DOUBLE PRECISION XTX23,XTX33,DET,D,DMAX,THOPT
      DOUBLE PRECISION TIME,TIMEH,TTIME,DELTA,TIMET
      INTEGER M,N
C     OPEN(UNIT=40,FILE='TCTL1K17.DAT',STATUS='UNKNOWN')
C     OPEN(UNIT=65,FILE='d.DAT',STATUS='UNKNOWN')
      PI = DACOS(-1.0D0)
      DELTA = 0.05D0
      TTIME = 6.0D0
      K = 7.0d0
      Lr = 0.048276D0
      SSSUMT = 0.D0
       DO 2, M = 1, 3000
         Y = 0.5D0
         Yp = 1.0D0
         X = 0.D0
         TERM1 = DSIN(M*PI*Y)
         TERM2 = 1.D0 - DCOS(M*PI*Yp)
```

```
            IF(TERM1.EQ.0..OR.TERM2.EQ.0.) GOTO 2
          TERM3 = M**2*PI**2*Lr**2*K
          DO 3, N = 1, 3000
               BETAN = PI*(N-0.5D0)
               BETAN2 = BETAN*BETAN
               TERM4 = TERM3 + BETAN2
               TERM5 = DCOS(BETAN*X)
                    IF(TERM5.EQ.0.) GOTO 3
               SSINCRT=TERM1*TERM2*TERM5*(1.D0/(M*TERM4))
               SSSUMT = SSSUMT + SSINCRT
3       CONTINUE
2       CONTINUE
        TMAX = SSSUMT*(4.D0/PI)
        DO 150, Yp = 0.1D0, 1.0D0, 0.05D0
        DO 125, X = 0.0D0, 1.0D0, 0.05D0
        DO 100, Y = 0.0D0, 1.0D0, 0.05D0
          DMAX = 0.D0
          SSSUMT = 0.0D0
          SSSUMKX = 0.0D0
          SSSUMKY = 0.D0
        DO 400, M = 1, 3000
          TERM1 = DSIN(M*PI*Y)
          TERM2 = 1.D0 - DCOS(M*PI*Yp)
               IF(TERM1.EQ.0..OR.TERM2.EQ.0.) GOTO 400
          TERM3 = M**2*PI**2*Lr**2*K
        DO 300, N = 1, 3000
          BETAN = PI*(N-0.5D0)
          BETAN2 = BETAN*BETAN
          TERM4 = TERM3 + BETAN2
          TERM5 = DCOS(BETAN*X)
               IF(TERM5.EQ.0.) GOTO 300
          SSINCRT=TERM1*TERM2*TERM5*(1.D0/(M*TERM4))
          SSINCRKX = TERM1*TERM2*DCOS(BETAN*X)*(1.D0/(M*TERM4))
     +                    *((TERM3/TERM4)-1.D0)
          SSINCRKY = TERM1*TERM2*DCOS(BETAN*X)*(1.D0/(M*TERM4))
     +                    *(-TERM3/TERM4)
          SSSUMT = SSSUMT + SSINCRT
          SSSUMKX = SSSUMKX + SSINCRKX
          SSSUMKY = SSSUMKY + SSINCRKY
300     CONTINUE
400     CONTINUE
        DO 650, TIMEH = DELTA, TTIME, DELTA
          XTX11 = 0.D0
          XTX12 = 0.D0
          XTX13 = 0.D0
          XTX22 = 0.D0
          XTX23 = 0.D0
          XTX33 = 0.D0
          SUMT = 0.0D0
          SUMC = 0.D0
```

```
      SUMKX = 0.D0
      SUMKY = 0.D0
    DO 200, TIME = DELTA, TTIME, DELTA
      DO 500, M = 1, 10000,1
          TERM1 = DSIN(M*PI*Y)
          TERM2 = 1.D0 - DCOS(M*PI*Yp)
              IF(TERM1.EQ.0..OR.TERM2.EQ.0.)GOTO 500
          TERM3 = M**2*PI**2*Lr**2*K
      DO 600, N = 1, 1000, 1
          BETAN = PI*(N-0.5D0)
          BETAN2 = BETAN*BETAN
          TERM4 = TERM3 + BETAN2
          TERM5 = DCOS(BETAN*X)
              IF(TERM5.EQ.0.)GOTO 600
          EXPON = TERM4
          EXPONTM = EXPON*TIME
          IF(TIME.LE.TIMEH) THEN
              IF(EXPONTM.LT.225.) THEN
              FF1 = DEXP(-EXPONTM)
              ELSE
              FF1 = 0.D0
              ENDIF
              TX = FF1
              XKX = BETAN2*TIME*FF1-((TERM3/EXPON)-1.D0)*FF1
              XKY = TERM3*TIME*FF1 + ((TERM3/EXPON)*FF1)
              XC = -EXPON*TIME*FF1
      ELSE
          EXPONTH = (EXPON*(TIME-TIMEH))
              IF(EXPONTH.LT.225..AND.EXPONTM.LT.225.)THEN
              FF1 = DEXP(-EXPONTM)
              FF2 = DEXP(-EXPONTH)
              ELSE IF(EXPONTH.LT.225..AND.EXPONTM.GE.225.) THEN
              FF2 = DEXP(-EXPONTH)
              FF1 = 0.D0
              ELSE IF(EXPONTH.GE.225..AND.EXPONTM.LT.225.) THEN
              FF1 = DEXP(-EXPONTM)
              FF2 = 0.D0
              ELSE
              FF1 = 0.D0
              FF2 = 0.D0
              ENDIF
          TX = FF2 - FF1
          XKX = ((TERM3/EXPON)-1.D0)*(FF2-FF1) +
     +          BETAN2*TIME*FF1 - BETAN2*(TIME-TIMEH)*FF2
          XKY = (-TERM3/EXPON)*(FF2-FF1) + TERM3*TIME*FF1
     +        - TERM3*(TIME-TIMEH)*FF2
          XC = EXPON*(TIME-TIMEH)*FF2 - EXPON*TIME*FF1
      ENDIF
      CONST = TERM1*TERM2*TERM5*(1.D0/(M*TERM4))
      INCRT = TX*CONST
```

```
          INCRC = XC*CONST
          INCRKX = XKX*CONST
          INCRKY = XKY*CONST
          IF(SUMT.NE.0..AND.SUMKX.NE.0..AND.SUMKY.NE.0..AND.
     +       SUMC.NE.0.)THEN
             IF(ABS(INCRT/SUMT).LT.1.D-20.AND.ABS(INCRKX/SUMKX).LT.
     +          1.D-20.AND.ABS(INCRKY/SUMKY).LT.1.D-20.AND.ABS
     +          (INCRC/SUMC).LT.1.D-20) THEN
             GO TO 410
           ENDIF
          ENDIF
          SUMT = SUMT + INCRT
          SUMC = SUMC + INCRC
          SUMKX = SUMKX + INCRKX
          SUMKY = SUMKY + INCRKY
600       CONTINUE
410       IF(N.EQ.1)THEN
            IF(ABS(INCRKX).LT.1.D-20.AND.ABS(INCRKY).LT.1.D-20
     +        .AND.ABS(INCRC).LT.1.D-20.AND.ABS(INCRT).LT.
     +        1.D-20)THEN
            GO TO 450
            ENDIF
          ENDIF
500       CONTINUE
450       IF(TIME.LE.TIMEH) THEN
            TEMP = (4.D0/PI)*(SSSUMT-SUMT)
            X3T = (4.0D0/PI)*SUMC
            X1T = (4.D0/PI)*(SSSUMKX + SUMKX)
            X2T = (4.D0/PI)*(SUMKY + SSSUMKY)
          ELSE
            TEMP = (4.0D0/PI)*SUMT
            X3T = (4.D0/PI)*SUMC
            X1T = (4.D0/PI)*SUMKX
            X2T = (4.D0/PI)*SUMKY
          ENDIF
          WRITE(40,14)y,TIME,TEMP,x1t,x2t,x3t
14        FORMAT(1x,f5.2,5e13.5)
          X1T = X1T/TMAX
          X2T = X2T/TMAX
          X3T = X3T/TMAX
          XTX11 = XTX11 + X1T*X1T
          XTX12 = XTX12 + X1T*X2T
          XTX13 = XTX13 + X1T*X3T
          XTX22 = XTX22 + X2T*X2T
          XTX23 = XTX23 + X2T*X3T
          XTX33 = XTX33 + X3T*X3T
          DET = XTX11*(XTX22*XTX33 - XTX23*XTX23) - XTX12*(XTX12*XTX33
     +        - XTX13*XTX23) + XTX13*(XTX12*XTX23 - XTX13*XTX22)
          D = (1.D0/(TIME/DELTA))**3*DET
          IF(D.GE.DMAX) THEN
```

```
            DMAX = D
            THOPT = TIMEH
            TIMET = TIME
          ENDIF
          SUMT = 0.0D0
          SUMC = 0.D0
          SUMKX = 0.D0
          SUMKY = 0.D0
200       CONTINUE
650       CONTINUE
          WRITE(65,110)X,Y,Yp,DMAX,THOPT,TIMET
110       FORMAT(1X,3(2X,F6.3),3E13.6)
100       CONTINUE
125       CONTINUE
150       CONTINUE
          STOP
          END
```

Appendix C

The FORTRAN program 2DC2OPT.FOR

This program, 2DC2OPT.FOR, is used to calculate the maximum determinant value for Configuration 2 of the two-dimensional analysis, and to determine the corresponding optimal experimental parameters.

```
      PROGRAM CFTWOOPT
C     Written by Debbie Moncman, 1994
      DOUBLE PRECISION PI,SUMC,SUMKX,SUMKY
      DOUBLE PRECISION Lr,K,BETAN,BETAN2,TERM1,T1
      DOUBLE PRECISION FF1,XKX,XKY,XCP,FF2,CONST,INCRKX,INCRKY,INCRC
      DOUBLE PRECISION TERM2,TERM3,SUMT,TEMP,INCRT,KYN,CPN
      DOUBLE PRECISION EXPONTM,EXPONTH,SSSUMT, SSINCRT
      DOUBLE PRECISION SSSUMKX,SSINCRKX,SSSUMKY,SSINCRKY,SSTEMP2
      DOUBLE PRECISION TERM4,X,Y,Xp,TMAX,TEMP1,TEMP2,SSTEMP1
      DOUBLE PRECISION X1T,X2T,X3T,XTX11,XTX12,XTX13,XTX22
      DOUBLE PRECISION XTX23,XTX33,DET,D,DMAX,THOPT,SSUMTN
      DOUBLE PRECISION TIME,TIMEH,TTIME,DELTA,timet,term5
      INTEGER M,N
      OPEN(UNIT=40,FILE='TIL1K17.DAT',STATUS='UNKNOWN')
      OPEN(UNIT=65,FILE='DIVARYY.DAT',STATUS='UNKNOWN')
      PI = DACOS(-1.0D0)
      DELTA = 0.05D0
      TTIME = 6.0D0
      K = 7.0d0
      Lr = 0.048276D0
      SSSUMT = 0.D0
      SSUMTN = 0.D0
      DO N = 1, 3000,1
        Y = 0.0D0
        Xp = 1.0D0
        X = 0.5D0
```

```
            BETAN = PI*(N-0.5D0)
            BETAN2 = BETAN*BETAN
            INCRT = DCOS(BETAN*Y)/BETAN2
            SSUMTN = SSUMTN + INCRT
          ENDDO
          SSTEMP1 = 2.D0*Xp*SSUMTN
          DO 2, M = 1, 3000
            Y = 0.0D0
            Xp = 1.0D0
            X = 0.5D0
            TERM1 = DCOS(M*PI*X)
            TERM2 = DSIN(M*PI*Xp)
            IF(TERM1.EQ.0..OR.TERM2.EQ.0.) GOTO 2
            TERM3 = M**2*PI**2*Lr**2*K
            DO 3, N = 1, 3000, 1
                 BETAN = PI*(N-0.5D0)
                 BETAN2 = BETAN*BETAN
                 TERM4 = TERM3 + BETAN2
                 TERM5 = DCOS(BETAN*Y)
              IF(TERM5.EQ.0.) GOTO 3
                 SSINCRT = TERM1*TERM2*term5*(1.D0/(M*TERM4))
            SSSUMT = SSSUMT + SSINCRT
3         CONTINUE
2         CONTINUE
          SSTEMP2 = 4.0D0/PI*SSSUMT
          TMAX = SSTEMP2 + SSTEMP1
          DO 150, Xp = 0.1D0, 1.05D0, 0.05D0
          DO 125, Y = 0.0D0, 1.0D0, 0.05D0
          DO 100, X = 0.0D0, 1.0D0, 0.05D0
          DMAX = 0.D0
          SSSUMT = 0.0D0
          SSSUMKX = 0.0D0
          SSSUMKY = 0.D0
           DO 400, M = 1, 3000
            TERM1 = DCOS(M*PI*X)
            TERM2 = DSIN(M*PI*Xp)
            IF(TERM1.EQ.0..OR.TERM2.EQ.0.) GOTO 400
            TERM3 = M**2*PI**2*Lr**2*K
                 DO 300, N = 1, 3000, 1
                      BETAN = PI*(N-0.5D0)
                      BETAN2 = BETAN*BETAN
                      TERM4 = TERM3 + BETAN2
                      TERM5 = DCOS(BETAN*Y)
                      IF(TERM5.EQ.0.) GOTO 300
                      SSINCRT = TERM1*TERM2*term5*(1.D0/(M*TERM4))
                      SSINCRKX = TERM1*TERM2*term5*(1.D0/(M*TERM4))
     +               *(-TERM3/TERM4)
                      SSINCRKY = TERM1*TERM2*term5*(1.D0/(M*TERM4))
     +                *((TERM3/TERM4)-1.D0)
                      SSSUMKX = SSSUMKX + SSINCRKX
```

```
                SSSUMKY = SSSUMKY + SSINCRKY
                SSSUMT = SSSUMT + SSINCRT
300     CONTINUE
400     CONTINUE
        DO 650, TIMEH = DELTA, TTIME, DELTA
        XTX11 = 0.D0
        XTX12 = 0.D0
        XTX13 = 0.D0
        XTX22 = 0.D0
        XTX23 = 0.D0
        XTX33 = 0.D0
        SUMT = 0.0D0
        SUMC = 0.D0
        SUMKX = 0.D0
        SUMKY = 0.D0
        DO 200, TIME = DELTA, TTIME, DELTA
        DO N = 1, 500,1
          BETAN = PI*(N-0.5D0)
          BETAN2 = BETAN*BETAN
          EXPONTM = BETAN2*TIME
          IF(TIME.LE.TIMEH) THEN
               IF(EXPONTM.LE.225.) THEN
               FF1 = DEXP(-EXPONTM)
               ELSE
               FF1 = 0.D0
               ENDIF
          T1 = (1.D0 - FF1)
          XCP = TIME*FF1
          XKY = (-1.D0/BETAN2) + (TIME +(1.D0/BETAN2))*FF1
          ELSE
          EXPONTH = BETAN2*(TIME-TIMEH)
               IF(EXPONTH.LE.225..AND.EXPONTM.LE.225.) THEN
               FF1 = DEXP(-EXPONTM)
               FF2 = DEXP(-EXPONTH)
               ELSE IF(EXPONTH.GT.225..AND.EXPONTM.LE.225.)THEN
               FF1 = DEXP(-EXPONTM)
               FF2 = 0.D0
               ELSE IF(EXPONTH.LE.225..AND.EXPONTM.GT.225.) THEN
               FF1 = 0.D0
               FF2 = DEXP(-EXPONTH)
               ELSE IF(EXPONTH.GT.225..AND.EXPONTM.GT.225.) THEN
               FF1 = 0.D0
               FF2 = 0.D0
               ENDIF
          T1 = FF2 - FF1
          XKY = ((1.D0/BETAN2)+TIME)*FF1 - ((TIME-TIMEH)
     +           + (1.D0/BETAN2))*FF2
          XCP = TIME*FF1 - (TIME-TIMEH)*FF2
          ENDIF
          INCRT = T1*DCOS(BETAN*Y)/BETAN2
```

```
          INCRKY = DCOS(BETAN*Y)*XKY
          INCRC = XCP*DCOS(BETAN*Y)
          IF(SUMT.NE.0..AND.SUMKY.NE.0..AND.SUMC.NE.0.)THEN
               IF(ABS(INCRT/SUMT).LE.1.D-10.AND.ABS(INCRKY/SUMKY)
     +              .LE.1.D-10.AND.ABS(INCRC/SUMC).LE.1.D-10) THEN
               GOTO 13
               ENDIF
          ENDIF
          SUMT = SUMT + INCRT
          SUMKY = SUMKY + INCRKY
          SUMC = SUMC + INCRC
        ENDDO
13      TEMP1 = 2.D0*Xp*SUMT
        KYN = 2.D0*Xp*SUMKY
        CPN = -2.D0*Xp*SUMC
        SUMT = 0.D0
        SUMC = 0.D0
        SUMKY = 0.D0
        DO 500, M = 1, 10000,1
          TERM1 = DCOS(M*PI*X)
          TERM2 = DSIN(M*PI*Xp)
               IF(TERM1.EQ.0..OR.TERM2.EQ.0.) GOTO 500
          TERM3 = M**2*PI**2*Lr**2*K
          DO 600, N = 1, 1000, 1
               BETAN = PI*(N-0.5D0)
               BETAN2 = BETAN*BETAN
               TERM4 = TERM3 + BETAN2
               TERM5 = DCOS(BETAN*Y)
                    IF(TERM5.EQ.0.) GOTO 600
               EXPONTM = TERM4*TIME
               IF(TIME.LE.TIMEH) THEN
                    IF(EXPONTM.LT.225.) THEN
                    FF1 = DEXP(-EXPONTM)
                    ELSE
                    FF1 = 0.D0
                    ENDIF
               T1 =  FF1
               XKX = (TERM3/TERM4)*FF1 + TERM3*TIME*FF1
               XKY = ((TERM3/TERM4)-1.D0)*(-FF1)+BETAN2*TIME*FF1
               XCP = -(TERM4*TIME*FF1)
               ELSE
               EXPONTH = TERM4*(TIME-TIMEH)
                    IF(EXPONTH.LE.225..AND.EXPONTM.LE.225.) THEN
                    FF1 = DEXP(-EXPONTM)
                    FF2 = DEXP(-EXPONTH)
                    ELSE IF(EXPONTH.GT.225..AND.EXPONTM.LE.225.)THEN
                    FF2 = 0.D0
                    FF1 = DEXP(-EXPONTM)
                    ELSE IF(EXPONTH.LE.225..AND.EXPONTM.GT.225.) THEN
                    FF1 = 0.D0
```

```
                FF2 = DEXP(-EXPONTH)
                ELSE IF(EXPONTH.GT.225..AND.EXPONTM.GT.225.) THEN
                FF1 = 0.D0
                FF2 = 0.D0
                ENDIF
            T1 = FF2 - FF1
            XKX = (-TERM3/TERM4)*(FF2-FF1) + TERM3*TIME*FF1
     +            - TERM3*(TIME-TIMEH)*FF2
            XKY = ((TERM3/TERM4)-1.D0)*(FF2-FF1) + BETAN2*TIME*FF1
     +            - BETAN2*(TIME-TIMEH)*FF2
            XCP = TERM4*(TIME-TIMEH)*FF2 - TERM4*TIME*FF1
            ENDIF
        CONST = TERM1*TERM2*TERM5*(1.D0/(M*TERM4))
        INCRT = T1*CONST
        INCRKX = XKX*CONST
        INCRKY = XKY*CONST
        INCRC = XCP*CONST
        IF(SUMT.NE.0..AND.SUMKX.NE.0..AND.SUMKY.NE.0..AND.
     +    SUMC.NE.0.)THEN
          IF(ABS(INCRT/SUMT).LT.1.D-20.AND.ABS(INCRKX/SUMKX).LT.
     +     1.D-20.AND.ABS(INCRKY/SUMKY).LT.1.D-20.AND.ABS
     +    (INCRC/SUMC).LT.1.D-20) THEN
          GO TO 410
          ENDIF
        ENDIF
      SUMT = SUMT + INCRT
      SUMC = SUMC + INCRC
      SUMKX = SUMKX + INCRKX
      SUMKY = SUMKY + INCRKY
600   CONTINUE
410   IF(N.EQ.1)THEN
        IF(ABS(INCRKX).LT.1.D-20.AND.ABS(INCRKY).LT.1.D-20
     +      .AND.ABS(INCRC).LT.1.D-20.AND.ABS(INCRT).LT.
     +      1.D-20)THEN
        GO TO 450
        ENDIF
      ENDIF
500   CONTINUE
450   IF(TIME.LE.TIMEH) THEN
        TEMP2 = (4.D0/PI)*(SSSUMT - SUMT)
        X1T = (4.D0/PI)*(SSSUMKX + SUMKX)
        X2T = KYN + (4.D0/PI)*(SSSUMKY + SUMKY)
        X3T = CPN + (4.D0/PI)*SUMC
      ELSE
        TEMP2 = (4.D0/PI)*SUMT
        X1T = (4.D0/PI)*SUMKX
        X2T = KYN + (4.D0/PI)*SUMKY
        X3T = CPN + (4.D0/PI)*SUMC
      ENDIF
      TEMP = TEMP1 + TEMP2
```

```
      WRITE(40,14)y,TIME,TEMP,x1t,x2t,x3t
14    format(1x,f5.2,5e13.5)
      X1T = X1T/TMAX
      X2T = X2T/TMAX
      X3T = X3T/TMAX
      XTX11 = XTX11 + X1T*X1T
      XTX12 = XTX12 + X1T*X2T
      XTX13 = XTX13 + X1T*X3T
      XTX22 = XTX22 + X2T*X2T
      XTX23 = XTX23 + X2T*X3T
      XTX33 = XTX33 + X3T*X3T
      DET = XTX11*(XTX22*XTX33 - XTX23*XTX23) - XTX12*(XTX12*XTX33
     +          - XTX13*XTX23) + XTX13*(XTX12*XTX23 - XTX13*XTX22)
      D = (1.D0/(TIME/DELTA))**3*DET
      IF(D.GE.DMAX) THEN
        DMAX = D
        THOPT = TIMEH
        TIMET = TIME
      ENDIF
      SUMT = 0.0D0
      SUMC = 0.D0
      SUMKX = 0.D0
      SUMKY = 0.D0
200   CONTINUE
650   CONTINUE
      WRITE(65,110)Xp,Y,X,DMAX,THOPT,TIMET
110   FORMAT(1X,3(2X,F6.3),3E13.6)
100   CONTINUE
125   CONTINUE
150   CONTINUE
      STOP
      END
```

Appendix D

The FORTRAN program MODBOX.FOR

This program, MODBOX.FOR, uses the modified Box-Kanemasu method to estimate the thermal properties.

```
      PROGRAM NLINA
CCCCCCCCC            PROGRAM DESCRIPTION            CCCCCCCCC
C     THIS PROGRAM USES THE MATRIX INVERSION LEMMA (BASED ON   C
C     THE GAUSS LINEARIZATION METHOD) AND THE BOX-KANEMASU     C
C     METHOD TO ESTIMATE THE PARAMETERS OF A GIVEN MODEL.      C
C************************************************************C
C
C  Written by Debbie Moncman, 1993
C  Based on the program, NLINA.FOR, by J. V. Beck (1993)
CCCCCCCCC            DIMENSION BLOCK                CCCCCCCCC
      IMPLICIT DOUBLE PRECISION (A-H,O-Z)
        DIMENSION T(1500,5),Y(1500),SIG2(1500),B(5),SC(5),A(5),BS(5),
     +   VINV(5,5),BSS(5),SUMG(5),R(5,5),EXTRA(20),ERR(1500),
     + PS(5,5),P(5,5),XTX(5,5),XTY(5),SUM(5),VALUEK(5),BSV(5)
      CHARACTER*40 INFILE, OUTFIL
C************************************************************C
C                    COMMON BLOCK                           C
      COMMON T,N,SC,BS,I,ETA,PS,P,B,A,Y,SIG2,MODL,VINV,NP,EXTRA
      COMMON/ERROR/ERR
      COMMON/MOD/AA,TL,SUM
C************************************************************C
C                    DATA BLOCK                             C
      DATA EPSDEN,CRITER/1.0D-30,0.0001D+0/
C************************************************************C
C                    INITIALIZATION BLOCK                   C
      WRITE(*,*)'ENTER THE NAME OF THE INPUT DATA FILE'
      READ(*,'(A40)')INFILE
      OPEN(8,FILE=INFILE)
```

```
      WRITE(*,*)'ENTER THE NAME OF THE OUTPUT FILE'
      READ(*,'(A40)')OUTFIL
      OPEN(7,FILE=OUTFIL)
C*****************************************************************C
C                    PROCESS BLOCK                              C
C -- START READING INPUT VALUES
C    BLOCK 1
      WRITE(7,*)'INPUT QUANTITIES'
      READ(8,*) N, NP, NI, MAXIT, MODL, IPRINT
      WRITE(7,*)
      WRITE(7,*)'BLOCK 1'
      WRITE(7,*)
      WRITE(7,*)'N - NUMBER OF DATA POINTS (MEASUREMENTS)'
      WRITE(7,*)'NP - NUMBER OF PARAMETERS'
      WRITE(7,*)'NI - NUMBER OF INDEPENDENT VARIABLES'
      WRITE(7,*)'MAXIT - MAXIMUM NUMBER OF ITERATIONS'
      WRITE(7,*)'MODL - MODEL NO.(NEEDED IF SEVERAL MODELS ARE USED)'
      WRITE(7,*)'IPRINT - 1 FOR USUAL PRINTOUTS, 0 FOR LESS'
      WRITE(7,*)
      IF(N.LE.0)THEN
        STOP
      END IF
      WRITE(7,'(/,9X,''N'',8X,''NP'',8X,''NI'',5X,''MAXIT'',5X,
     +''MODL'',4X,''IPRINT'')')
      WRITE(7,'(7I10)')N,NP,NI,MAXIT,MODL,IPRINT
C    BLOCK 2 (INITIAL PARAMETER ESTIMATES)
      WRITE(7,*)
      WRITE(7,*)'BLOCK 2'
      WRITE(7,*)
      WRITE(7,*)'B(1),...,B(NP) ARE THE INITIAL PARAMETER ESTIMATES.'
      WRITE(7,*)
      READ(8,*)(B(I),I=1,NP)
      WRITE(7,'(10X,''B('',I1,'') ='',F16.5)')(I,B(I),I=1,NP)
C    BLOCK 3 (INPUT MEASUREMENTS)
      WRITE(7,*)
      WRITE(7,*)'BLOCK 3'
      WRITE(7,*)
      WRITE(7,*)'J - DATA POINT INDEX'
      WRITE(7,*)'Y(J) - MEASURED TEMPERATURE VALUE'
      WRITE(7,*)'SIGMA(J) - STANDARD DEVIATION OF Y(J)'
      WRITE(7,*)'T(J,1) - FIRST INDEPENDENT VARIABLE'
      WRITE(7,*)
      WRITE(7,'(/,9X,''J'',6X,''Y(J)'',3X,''SIGMA(J)'',6X,
     +      ''T(J,1)'',6X,''T(J,2)'')')
      DO I1=1,N
        READ(8,*)J,Y(J),SIG2(J),(T(J,KT),KT=1,NI)
        WRITE(7,'(I10,7F10.5)')J,Y(J),SIG2(J),(T(J,KT),KT=1,NI)
        SIG2(J) = SIG2(J)*SIG2(J)
      END DO
C    BLOCK 4 (INPUT ANY EXTRA DATA NEEDED IN THE MODEL)
```

```
      READ(8,*)IEXTRA
C     IEXTRA is the number of constants used in the model such as
C     initial temperatures, surface temperatures, or a heat flux.
C     It equals 0 for no extra input.
      WRITE(7,*)
      WRITE(7,*)'BLOCK 4'
      WRITE(7,*)
      WRITE(7,*)'IEXTRA - NUMBER OF EXTRA(I) PARAMETERS (0 IF NONE)'
      WRITE(7,*)
      WRITE(7,'(10X,''IEXTRA ='',I10)')IEXTRA
      IF(IEXTRA.GE.1) THEN
        WRITE(7,*)
        WRITE(7,*)'EXTRA(1),... ARE EXTRA CONSTANTS USED IN THE MODEL'
        WRITE(7,*)
        READ(8,*)(EXTRA(I),I=1,IEXTRA)
        WRITE(7,'(''EXTRA('',I2,'') ='',F16.5)')
     +  (I,EXTRA(I),I=1,IEXTRA)
      ENDIF
C     End input, begin calculations
      WRITE(7,*)
      WRITE(7,*)'END INPUT QUANTITIES, BEGIN OUTPUT CALCULATIONS'
      WRITE(7,*)
      WRITE(7,*)'SSY  - SUM OF SQUARES FOR PRESENT PARAMETER VALUES'
      WRITE(7,*)'SSYP - SUM OF SQUARES FOR BOX-KANEMASU PARAMETER VAL.'
      WRITE(7,*)'       SSYP DECREASES TOWARDS A POSITIVE CONSTANT'
      WRITE(7,*)'       AND SHOULD BE LESS THAN SSY'
      WRITE(7,*)'G    - MEASURE OF THE SLOPE, IT SHOULD APPROACH ZERO'
      WRITE(7,*)'       AT CONVERGENCE'
      WRITE(7,*)'H    - SCALAR INTERPOLATION FACTOR; ITS A FRACTION OF'
      WRITE(7,*)'       THE GAUSS STEP GIVEN BY THE BOX-KANEMASU METHOD'
      WRITE(7,*)
      WRITE(7,*)
CCCCCCCC          PART I OF PROGRAM (GAUSS METHOD)     CCCCCCCCC
CCCCCCCC**************************************************CCCCCCCCC
C -- Set the P matrix equal to zero
      DO I2=1,NP
        DO K2=1,NP
          PS(K2,I2)=0
          P(K2,I2)=0
        ENDDO
      ENDDO
      DO I3=1,NP
        PS(I3,I3)=B(I3)*B(I3)*1.0D+7
       ENDDO
      DO K = 1, NP
        BS(K)=B(K)
        BSV(K)=BS(K)
        SUMG(K) = 0.0D+0
      ENDDO
C -- Set XTX and XTY sums equal to 0
```

```
      DO K = 1, NP
        XTY(K) = 0.0D+0
        DO J = 1, NP
          XTX(J,K) = 0.0D+0
        ENDDO
      ENDDO

C -- I and MAX are counters
      I = 0
      MAX = 0
100    MAX = MAX + 1
      SSY = 0.0D+0
      DO I3 = 1, N
        I=I3
        CALL MODEL
          CALL SENS
        RESID = Y(I) - ETA
        SSY = SSY + RESID*RESID/SIG2(I)
C -- Calculate XTX, XTY, and SUMG (used in the Box-Kanemasu method)
      DO K = 1, NP
        XTY(K) = XTY(K) + SC(K)*RESID/SIG2(I)
        SUMG(K) = SUMG(K) + SC(K)*RESID/SIG2(I)
          DO L = 1, NP
            XTX(K,L) = XTX(K,L) + SC(K)*SC(L)/SIG2(I)
          ENDDO
      ENDDO
      DO K = 1, NP
        A(K) = 0.0D+0
      ENDDO
C -- Calculate 'A' used in the MIL method
      DO K = 1, NP
        DO J = 1, NP
          A(K) = A(K) + SC(J)*P(K,J)
        ENDDO
      ENDDO
      DELSUM = 0.0D+0
C -- Calculate 'DELTA' used in the MIL method
      DO K = 1,NP
        DELSUM = DELSUM + SC(K)*A(K)
      ENDDO
      DELTA = SIG2(I) + DELSUM
C -- Calculate 'K' used in the MIL method
      DO K = 1, NP
        VALUEK(K) = A(K)/DELTA
      ENDDO
      SUMH = 0.0D+0
C -- Calculate 'SUMH' used in 'HU'
      DO J = 1, NP
        SUMH = SUMH + SC(J)*(B(J) - BS(J))
      ENDDO
```

```
      HU = Y(I) - ETA - SUMH
C -- Estimated parameters found using the Gauss Method:
      DO K = 1, NP
        B(K) = B(K) + VALUEK(K)*HU
      ENDDO
C -- Calculate the new P matrix
      DO U = 1,NP
        DO V = 1,NP
          P(U,V) = PS(U,V) - VALUEK(U)*A(V)
        ENDDO
      ENDDO
C -- Make the P matrix symmetrical
      DO J = 2, NP
        JK = J - 1
          DO K = 1, JK
            P(K,J)=P(J,K)
          ENDDO
      ENDDO
      DO J = 1,NP
        DO K = 1,NP
          PS(K,J) = P(K,J)
        ENDDO
      ENDDO
C*************************************************************************
C -- Done with Gauss calculations, Print results
      IF(IPRINT.GT.0) THEN
        IF(I.EQ.1) THEN
          WRITE(7,*)
          WRITE(7,*)'SEQUENTIAL ESTS. OF THE PARAMETERS GIVEN BELOW'
          WRITE(7,*)'(THESE EST. ARE FOUND USING THE GAUSS METHOD)'
          WRITE(7,'(//,3X,''I'',6X,''ETA'',5X,''RESIDUALS'',7X,
     +          ''B(1)'',8X,''B(2)'',6X,''SC(1)'', 6X,''SC(2)'')')
        END IF
      WRITE(7,'(I4,6E12.5)')I, ETA, RESID, (B(IP),IP=1,NP),SC(1)*B(1),
     + SC(2)*B(2)
      ENDIF
      ENDDO
      WRITE(7,*)
      WRITE(*,*)'END BASIC LOOP'
      WRITE(7,*)'THE FINAL SEQUENTIAL ESTIMATES WILL NOW BE MODIFIED
     +           USING THE BOX-KANEMASU METHOD'
CCCCCCCCC        PART II: BOX-KANEMASU MODIFICATION      CCCCCCCCC
CCCCCCCCC**************************************************CCCCCCCCC
C -- Set BSS equal to the initial estimate for that iteration
      DO J = 1, NP
        BSS(J) = BS(J)
      ENDDO
      ALPHA = 2.0D+0
      AA = 1.1D+0
200    ALPHA = ALPHA/2.0D+0
```

```
C -- Calculate the parameters using the modified step-size
      DO K = 1,NP
        BS(K) = BSS(K) + ALPHA*(B(K) - BSS(K))
      ENDDO
      CHANGE = 0
      G = 0.0D+0
C -- Calculate the slope, G
      DO K = 1, NP
        DELTAB = BS(K) - BSS(K)
          G = G + DELTAB*SUMG(K)
        ENDDO

C -- By the definition of G, it should always be positive.
      IF (G.LT.0.0D+0) THEN
         WRITE(7,*)'G IS NEGATIVE, TERMINATE CALCULATIONS'
         GOTO 1000
      ENDIF
      SSYP = 0.0D+0
C -- Calculate the new sum of squares based on the modified parameters
      DO I3 = 1, N
        I = I3
        CALL MODEL
        RESID = Y(I) - ETA
        SSYP = SSYP + RESID*RESID/SIG2(I)
      ENDDO
        IF(SSYP.GT.SSY) THEN
            IF (ALPHA.LE.0.01D+0) THEN
              WRITE(7,250)ALPHA,SSYP,SSY
250             FORMAT(3X,'ALPHA IS TOO SMALL, ALPHA =',F12.6,2X,
     +              'SSYP = ', E15.6, 2X, 'SSY =', E15.6)
              GOTO 1000
            ELSE
              GOTO 200
            ENDIF
        ENDIF
C -- Calculate SUMCH, used in the following inequality to determine H
      SUMCH = SSY - ALPHA*G*(2.0D+0-(1.0D+0/AA))
      IF(SSYP.GT.SUMCH) THEN
        H = (ALPHA*ALPHA*G)/(SSYP - SSY + (2.0D+0*ALPHA*G))
      ELSE
        H = ALPHA*AA
      ENDIF
C -- Calculate the final parameter estimates using H.
      DO K = 1, NP
        B(K) = BSS(K) + H*(B(K) - BSS(K))
      ENDDO
C -- Calculate RATIO; if it is less that CRITER (0.0001), then the change
C    in the estimated parameters is insignificant and the iterative
C    process is terminated. CHANGE is used to determine when all
C    parameters stop varying.
```

```
      DO J = 1, NP
        RATIO = (B(J) - BSS(J))/( BSS(J)+EPSDEN)
        RATIO = ABS(RATIO)
            IF(RATIO.LE.CRITER)THEN
             CHANGE = CHANGE + 1
          ENDIF
      ENDDO
C -- Print out the calculated values for H, G, SSY, and SSYP
      WRITE(7,120)
      WRITE(*,120)
120    FORMAT(5X,'MAX',10X,'H',13X,'G',12X,'SSY',11X,'SSYP')
      WRITE(*,125)MAX,H,G,SSY,SSYP
      WRITE(7,125)MAX,H,G,SSY,SSYP
125    FORMAT(I8,1F13.6,4E14.6)

C -- Print out the final parameter estimates
      WRITE(7,*)'THE FINAL PARAMETER ESTIMATES FOR THIS ITERATION ARE'
      WRITE(*,'(10X,''B('',I1,'') ='',E16.6)') (I,B(I),I=1,NP)
      WRITE(7,'(10X,''B('',I1,'') ='',E16.6)') (I,B(I),I=1,NP)
C -- End the Box-Kanemasu Modification
       WRITE(7,'(/,5X,''P(1,KP)'',9X,''P(2,KP)'',9X,''P(3,KP)'',9X,
   +   ''P(7,KP)'',9X,''P(5,KP)'')')
C -- Print out the P matrix
       WRITE(7,129)
129     FORMAT(5X,'THE P MATRIX IS')
       DO IP = 1, NP
         WRITE(7,130) (P(IP,KP),KP=1,NP)
       ENDDO
130     FORMAT(5D15.7)
       WRITE(7,135)
135     FORMAT(5X,'THE CORRELATION MATRIX IS')
       DO IR=1,NP
         DO IR2 = 1, IR
           AR = P(IR,IR) * P(IR2,IR2)
           R(IR,IR2) = P(IR,IR2)/SQRT(AR)
         ENDDO
       ENDDO
       DO IR = 1, NP
         WRITE(7,'(5E15.7)')(R(IR,III),III=1, IR)
       ENDDO
       WRITE(7,*)
       WRITE(7,*)'The diagonal terms of the correlation matrix are
   +    all unity and the off-diagonal terms must be in the interval
   +    [-1,1]. Whenever all the off-diagonal terms exceed 0.9
   +    in magnitude, the estimates are highly correlated and
   +    tend to be inaccurate'
       DO K = 1, NP
         XTY(K) = 0.0D+0
         BS(K) = B(K)
         SUMG(K) = 0.0D+0
```

```
            DO J = 1, NP
              XTX(J,K) = 0.0D+0
              PS(J,K)=0.0D+0
              PS(J,J) = BSV(J)*BSV(J)*1.0D+7
            ENDDO
          ENDDO
          WRITE(7,400)
400       FORMAT(7X,'MAX',8X,'NP',5X,'IP')
          WRITE(7,'(7I10,4F10.4)')MAX, NP
           IF(NP.GT.CHANGE)THEN
            M = MAXIT
            IF(MAX.LE.M)GO TO 100
         ENDIF
         IF(IPRINT.LE.0) THEN
            IPRINT = IPRINT + 1
         ENDIF
1000     CONTINUE
         CLOSE(7)
         CLOSE(8)
         STOP
         END
CCCCCCCCC*************************************************CCCCCCCCC
      SUBROUTINE MODEL
C     THIS SUBROUTINE IS TO CALCULATE T, THE TRUE TEMPERATURE
      IMPLICIT REAL*8 (A-H,O-Z)
      DIMENSION  T(1500,5),Y(1500),SIG2(1500),B(5),Z(5),
     +A(5),BS(5),VINV(5,5),EXTRA(20)
      DIMENSION P(5,5),PS(5,5),SUM(5)
      COMMON T,N,Z,BS,I,ETA,PS,P,B,A,Y,SIG2,MODL,VINV,NP,EXTRA
      COMMON/MOD/AA,TL,SUM
      PI=4.0D+0*DATAN(1.0D+0)
      QO = EXTRA(1)
      TO = EXTRA(2)
      TIMEH = EXTRA(3)
      AL = EXTRA(4)
      AL2 = AL*AL
      X = 0.0D+0
      TIME = T(I,1)
      THCON = BS(1)
      RHOCP = BS(2)*1.D6
      TOL = 1.D-8
      XL = X/AL
C     DIMT = (ALPHA*t/L^2)
      DIMT = (THCON*TIME)/(RHOCP*AL2)
      DIMTH = (THCON*(TIME-TIMEH))/(RHOCP*AL2)
C     CONST = (QL/K)
      CONST = (QO*AL)/THCON
      SUMT = 0.0D+0
      DO 20, M = 1, 1000
        BETAM = (M - 0.5D+0)*PI
```

```
      BETA2M = BETAM*BETAM
      FF1 = DEXP(-BETA2M*DIMT)
      IF(TIME.LE.TIMEH) THEN
        T1 = FF1
      ELSE
        FF2 = DEXP(-BETA2M*DIMTH)
        T1 = FF1 - FF2
      ENDIF
      TINCR = T1*DCOS(BETAM*XL)*(1/BETA2M)
      IF(M.NE.1) THEN
        IF(ABS(TINCR/SUMT).LT.TOL) THEN
          GOTO 15
        ENDIF
      ENDIF
      SUMT = SUMT + TINCR
20    CONTINUE
15    IF(TIME.LE.TIMEH) THEN
        ETA = TO + CONST*(1.0D0 - XL - 2.0D0*SUMT)
      ELSE
        ETA = TO - 2.0D0*CONST*SUMT
      ENDIF
      GOTO 1000
1000  CONTINUE
      RETURN
      END

      SUBROUTINE SENS
C     THIS SUBROUTINE IS FOR CALCULATING THE SENSITIVITY COEFFICIENTS
      IMPLICIT REAL*8 (A-H,O-Z)
      DIMENSION T(1500,5),Y(1500),SIG2(1500),B(5),
     +Z(5),A(5),BS(5),VINV(5,5),EXTRA(20)
      DIMENSION P(5,5),PS(5,5),SUM(5)
      COMMON T,N,Z,BS,I,ETA,PS,P,B,A,Y,SIG2,MODL,VINV,NP,EXTRA
      COMMON/MOD/AA,TL,SUM
      PI=4.0D+0*DATAN(1.0D+0)
      TZ=0.0
      QO = EXTRA(1)
      TO = EXTRA(2)
      TIMEH = EXTRA(3)
      AL = EXTRA(4)
      AL2 = AL*AL
      X = 0.0D+0
      TIME = T(I,1)
      THCON = BS(1)
      RHOCP = BS(2)*1.D6
      TOL = 1.D-8
      XL = X/AL
C     DIMT = (ALPHA*t/L^2)
      DIMT = (THCON*TIME)/(RHOCP*AL2)
      DIMTH = (THCON*(TIME-TIMEH))/(RHOCP*AL2)
```

```
C     CONST = (QL/K)
      CONST = (QO*AL)/THCON
      SUMK = 0.0D+0
      SUMC = 0.0D+0
      DO 20, M = 1, 1000
        BETAM = (M - 0.5D+0)*PI
        BETA2M = BETAM*BETAM
        FF1 = DEXP(-BETA2M*DIMT)
        IF(TIME.LE.TIMEH) THEN
          X1 = FF1*((1/BETA2M) + DIMT)
          X2 = DIMT*FF1
        ELSE
          FF2 = DEXP(-BETA2M*DIMTH)
            X1 = ((1/BETA2M)+DIMT)*FF1 - ((1/BETA2M)+DIMTH)*FF2
          X2 = DIMT*FF1 - DIMTH*FF2
        ENDIF
        X1INCR = X1*DCOS(BETAM*XL)
        X2INCR = X2*DCOS(BETAM*XL)
        IF(M.NE.1) THEN
         IF(ABS(X1INCR/SUMK).LT.TOL.AND.ABS(X2INCR/SUMC).LT.TOL)THEN
           GOTO 15
         ENDIF
        ENDIF
        SUMK = SUMK + X1INCR
        SUMC = SUMC + X2INCR
20     CONTINUE
15     IF(TIME.LE.TIMEH) THEN
         Z(1) = -(CONST/THCON)*(1.0D0 - XL - 2.0D0*SUMK)
         Z(2) = -2.0D0*(CONST/RHOCP)*SUMC*1.D6
      ELSE
        Z(1) = 2.0D0*(CONST/THCON)*SUMK
        Z(2) = -2.0D0*(CONST/RHOCP)*SUMC*1.D6
      ENDIF
      GOTO 1000
1000   CONTINUE
      RETURN
      END
```

Appendix E

Input file for MODBOX.FOR

This file represents a sample input file to be used in MODBOX.FOR for the estimation of the thermal properties. The first row of numbers represents the number of data points, the number of parameters to be estimated, the number of independent variables, the maximum number of iterations to be performed, the model number, and the usual printouts, respectively. The second row represents the initial guesses for $k_{x\text{-}eff}$ and C_{eff}, which are to be estimated. The first column is the index, the second column is the values of the temperatures, the third is the standard deviation of the measurement errors, and the fourth column is the independent variable, time. At the end of the columns, the first row represents the number of extra parameters to be used in the program. These parameters are then given in the next row, and represent the magnitude of the heat flux, the initial temperature (and in this analysis, the constant temperature at the boundary), the heating time, and the composite thickness, L_x, respectively.

```
1045 2 1 2 1
0.5  1.5
1     .201515E+02  .100000E+01    .000000E+00
2     .202875E+02  .100000E+01    .500000E+00
3     .204508E+02  .100000E+01    .100000E+01
4     .205471E+02  .100000E+01    .150000E+01
```

5	.207033E+02	.100000E+01	.200000E+01
6	.207728E+02	.100000E+01	.250000E+01
7	.209213E+02	.100000E+01	.300000E+01
8	.209658E+02	.100000E+01	.350000E+01
9	.210080E+02	.100000E+01	.400000E+01
10	.211043E+02	.100000E+01	.450000E+01
.	.	.	.
.	.	.	.
.	.	.	.
1035	.201841E+02	.100000E+01	.517086E+03
1036	.202061E+02	.100000E+01	.517586E+03
1037	.202114E+02	.100000E+01	.518086E+03
1038	.202536E+02	.100000E+01	.518586E+03
1039	.201520E+02	.100000E+01	.519086E+03
1040	.202833E+02	.100000E+01	.519586E+03
1041	.202411E+02	.100000E+01	.520086E+03
1042	.202583E+02	.100000E+01	.520586E+03
1043	.201989E+02	.100000E+01	.521086E+03
1044	.202584E+02	.100000E+01	.521586E+03
1045	.201692E+02	.100000E+01	.522086E+03

4

351.05 20.1515 180.036 0.0067818

Appendix F

Finite Element (EAL) program

This is the finite element program (EAL) used to estimate the thermal properties.

```
$          EAL THERMAL ANALYSIS RESEARCH PROJECT, EXP. 3
$
$                  Debbie A. Moncman
$
$*************************************************************************
$
$   This problem solves for the temperature distribution in a 2-D plate
$   with dimensions LXm x LYm.  It then uses the Modified Box-Kanemasu
$   method to sequentially estimate the thermal properties of the material.
$   The properties of interest are the effective thermal conductivity and the
$   volumetric heat capacity. The left and right surfaces of the flat plate are
$   insulated, the bottom surface is maintained at a const. temp, and at
$   the top surface is a constant heat flux.  The assumptions
$   used are: Transient, one-dimensional conduction, constant properties,
$   and no internal heat generation.
$
$*************************************************************************
*XQT U1
*CM=200000
$
$*************************************************************************
$
$  Subroutine VARB - defines variables used in the program
$                  NOTE: Variable names can only be four
$                        letters long!
$*************************************************************************
$
*(29 VARB DEFI) VARB
$
$  Set RACM = 0 to use Fortran logic in all subroutines
*RACM = 0
```

```
$
$  Define geometry for 2-D plate
$
!LX=0.0479425      $Length of plate (m)
!LY=0.0067818      $Height of plate (m)
$
$Define number of elements and nodes in each direction
$
!NX=5            $Number of elements in X direction
!NX1=NX+1        $Number of nodes in X direction
!NX2=NX1+1       $JJUMP for meshing; start of second row
!NY=5            $Number of elements in Y direction
!NY1=NY+1        $Number of nodes in Y direction
!NT=NX1*NY1      $Total number of nodes in mesh
!NTOT=NT
!N1=1            $Beginning node for mat'l 1 (only 1 mat'l in this analysis)
!RN1=1.
!RINC=1.         $Node number increment
!CRIT = 1.E-6    $Criteria used to terminate estimation process
!IT1 = 0         $Value used in determining if ests. are still changing signific.
!IT2 = 0         $Value used in determining if ests. are still changing signific.
$
$ Define initial temperature, initial and final time, time step for
$ transient solution, total heating time, and heat flux value.
$
!TEMI=20.1515            $Initial temperature (oC)
!TIMI=0.0                $Initial (starting) time (sec)
!TIMF=522.086            $Final (stopping) time (sec)
!DELT=0.5                $Time step for transient solution
!TIMH=180.036            $Time that heat flux is applied.
!DFLX = 1.E-8            $Small value added to timeh to define heat flux value
!THDL = TIMH + DFLX      $This is needed due to the discontinuity at timeh
!FLUX = 350.05           $Heat flux value
$
!COU=TIMF-TIMI
!COU=COU/DELT            $Number of time steps used in taking temp. measms.
!NTS=IFIX(COU+0.0001)    $Number of time steps must be an integer
!NTS=NTS+1               $Total number of times from TIMI to TIMF
$
$  Enter initial parameter estimates
$
!A1I=2.0         $Initial estimate for eff. thermal conductivity
!A2I=3.0         $Initial estimate for eff. volumetric heat capacity
!LOOP=0          $Used in sequential process
*RETURN
*VARB
$
$*****************************************************************************
$
$  Subroutine NODE - defines the nodal positions
```

```
$
$*************************************************************************
$
*(29 NODE GENE)NODE
*XQT TAB
START "NT"      $ Define the total number of nodes
UPDATE=1
JLOC            $ Give the location of the nodes (set up the mesh)
$
$   In the next statement, FORMAT=1 is used for rectangular coordinates;
$   N1 is the number to start the node locations at (in this case, 1);
$   0,0,0 are the coordinates of N1; LX,0,0 are the coordinates
$   for the bottom right corner of the mesh; NX1 is the number of nodes
$   in the x direction; 1 is the increment in the node number in the x
$   direction; and NY1 is the total number of nodes in the y direction.
$   For the next line, NX1 is jjump used in the y direction; 0, LY, 0 are
$   the coordinates of the upper left node; and LX, LY, 0 are the
$   coordinates of the upper right node.
$
FORMAT = 1: "N1", 0., 0., 0.,"LX", 0., 0.,"NX1",1,"NY1"
          "NX1", 0., "LY", 0.,"LX", "LY", 0.
*RETURN
*NODE
$
$*************************************************************************
$
$  Subroutine ELEM - defines the element connectivity
$
$*************************************************************************
$
*(29 ELEM DEFI)ELMT
*XQT ELD
$
$  Define K41 elements
$  K41 signifies a conductive, 4 node element.
$
RESET NUTED=1
 K41
 GROUP = 1          $Group 1
 NMAT=1             $Material 1
!J1=N1             $J1 is the number of the bottom LF node in an element
!J2=N1+1           $J2 is the number of the bottom RT node in an element
!J3=NX2+1          $J3 is the number of the top RT node in an element
!J4=NX2            $J4 is the number of the top LF node in an element
 "J1" "J2" "J3" "J4", 1, "NX" "NY"
$
$ The above line sets up the nodal positions of each element.  1 is the
$ node increment and NX and NY signify the number of elements in the x and
$ y directions, respectively.
$
```

```
$   Define K21 elements
$   K21 is used to represent the heat flux
$   Note: since we're using this element to model the heat flux, the
$   thermal conductivities and specific heat must be zero (reason for Mat'l 2)
 K21
 GROUP = 1
 NMAT = 2
!J1=NY*NX1+1
!J2=NY*NX1+2
 "J1" "J2", 1, "NX", 1
$
*RETURN
*ELMT
$
$*****************************************************************************
$
$  Subroutine TABL - Defines the thickness of the elements
$
$*****************************************************************************
$
*(29 TABL GENE)TABL
*XQT AUS
TABLE(NI=1,NJ=1): K THIC: J=1: 1.   $The thickness of K41 elements
TABLE(NI=1,NJ=1): K AREA: J=1: 1.   $The area of K21 elements
$
*RETURN
*TABL
$
$*****************************************************************************
$
$  Subroutine UPDA - Updates thermal property values
$
$*****************************************************************************
$
*(29 TABL UPDA) UPDA
*XQT AUS
$
$ The following table gives the thermal conductivity in the x and y direc.
$ NI=9 indicates that nine variables can be entered to determine k (T, rho,
$ c, kxx, kyy, kzz, kxy, kzy, kzx) however, NJ=1 indicates that k is
$ temperature independent.  I = 4 5: correspond to kxx and kyy inputs (i.e.
$ the thermal conductivities in the x and y directions). NOTE: all non-zero
$ conductivities must be specified; there are no default values.  To define
$ isotropic properties, identical values for kxx, kyy, and kzz must be entered.
$ Note that a value of 1.0E+6 was given for the density.  This is used as a
$ scaling factor.  Therefore, the estimate for the volumetric specific heat
$ must be multiplied by (1.0E+6).
$
TABLE(NI=9,NJ=1): COND PROP 1: I = 2,3,4,5,6
OPERATION=XSUM
```

```
 J=1: 1.E+6,"A2","A1","A1","A1"
$
$ The next table sets up the 0 value properties for the K21 element
$
TABLE(NI=9,NJ=1): COND PROP 2: I = 3 4 5 6: J=1: 0.,0.,0.,0.
$
$ The next table defines the constant heat flux applied to the top surface.
$ Here, J is the number of elements.  To specify a line heat flux (W/m) along
$ prescribed line flux divided by the element's cross-sectional area.
$ A constant heat flux is applied for a timeh "TIMH", and is then removed.
$ (It is a step function)
$
 TABLE(NI=1,NJ="NX"): SOUR K21 1: BLOCK 1: J=1, "NX": "FLUX"
                                BLOCK 2: J=1, "NX": "FLUX"
                                BLOCK 3: J=1, "NX": 0.0
                                BLOCK 4: J=1, "NX": 0.0
 TABLE(NI=1,NJ=4):    SOUR TIME: J=1: "TIMI"
                               J=2: "TIMH"
                               J=3: "THDL"
                               J=4: "TIMF"
$ The next table defines the nodes that have a prescribed temperature
$ (The bottom surface in this analysis).  DDATA is a counter; Note: it must
$ be a REAL value (not an integer).  Here, J is the number of nodes, NOT
$ the node number!
$
TABLE(NI=1,NJ="NX1"): TEMP NODE: DDATA="RINC":J="N1","NX1": "RN1"
$
$ The next table defines the prescribed temperature at each of the nodes
$ specified in the previous table.  In this analysis, all specified nodes
$ are at the same temperature "TEMI" since exps. were conducted at room temp
$
 TABLE(NI=1,NJ="NX1"): APPL TEMP: BLOCK 1: J=1,"NX1": "TEMI"
$
*RETURN
*UPDA
$
$*************************************************************************
$
$  Subroutine TDAT: Builds data files for experimental temperatures, initial
$                   guesses, and sensitivity coefficients.
$                   Data format:
$                   TS AUS n3 1
$                   Specify both n3 and n4 to identify the data tables
$                   n3 = 1: measured temperatures
$                   n3 = 2: initial temperatures
$                   n3 = 3: derivative #n (the n-2th parameter)
$                   n4 - x position where temperatures are measured
$                        (only measured at one location (n4=1) for this case).
$*************************************************************************
$
```

```
*(29 BILD TS) XXXX
!NCO2 = NCOU
$
$  Bring surface temperature data from TRAN TEMP multi-block data set using
$  XSUM and TRANSFER.
$
$*************************************************************************
$
!NTN = NTOT-1          $Total number of nodes - 1.
!NCP = NCOU+1          $=NTS, the total number of times from TIMI to TIMF
!DBS = 0
*IF("N4" EQ 2):!DBS=NCOU
*XQT AUS
 DEFINE A = 1 TRAN TEMP 1 1 2 "NCP"
*IF("N3" GT 1):*JUMP 1215
*IF("N4" EQ 1):TABLE(NI=1,NJ="NCP"): 4 TS AUS "N3" 1
*IF("N4" EQ 2):TABLE,U (NI=1,NJ="NCP"):4 TS AUS "N3" 1
 TRANSFER(SOURCE=A,DBASE="DBS",SBASE="NTN",ILIM=1,OPERATION=XSUM)
*LABEL 1215
*IF("N4" EQ 1):TABLE(NI=1,NJ="NCP"): 2 TS AUS "N3" 1
*IF("N4" EQ 2):TABLE,U (NI=1,NJ="NCP"): 2 TS AUS "N3" 1
 TRANSFER(SOURCE=A,DBASE="DBS",SBASE="NTN", ILIM=1,OPERATION=XSUM)
*RETURN
*XXXX
$
$*************************************************************************
$
$  Subroutine INVH - Minimization Procedure
$
$*************************************************************************
$
*(29 INV HEAT) INVH
$
!NCOU=NTS-1     $Total number of time steps
*XQT AUS
$
TABLE(NI=1,NJ=1045): 4 TS AUS 1 1: I=1
J=1:.201515E+02
J=2:.202875E+02
J=3:.204508E+02
          .
          .
          .
J=1043:.201989E+02
J=1044:.202584E+02
J=1045:.201692E+02
!NCOU=NTS-1
!EPS=1.0E-6     $Convergence criteria used in (b-b0)/(b0-EPS)
!NEPS=1         $Used to determine is No. of iterations exceeds NEMX.
!NEMX=25        $Maximum number of iterations
```

```
*XQT AUS
!TINI=DS 1,1,1 (4,TS AUS,1,1)    $Defines the initial exp. temperature
 TABLE (NI=4,NJ="NEMX"): 4 CONV HIST 1 1   $Table that stores sequential est.
$TABLE (NI=1,NJ="NCOU"): 4 RES HIST 1 1
!A1=A1I          $Set A1 and A2 back to the initial estimates.
!A2=A2I
!AS1 = A1I       $AS1 and AS2 are previous iteration, final estimate holders.
!AS2 = A2I
*LABEL 4000      $Begins the loop process
!A10=A1
!A20=A2
$
$Derivative calculations (Used to calculate the sensitivity coefficients
!TINI = DS 1,1,1 (4,TS AUS,1,1)
!N4=1
!N3=2
!NTAB=0
*DCALL(29 TRAN ANAL)
$The above call stmt. calculates temps. at the initial parameter estimates for
$the first iteration and at the final estimates of the previous iteration for
$the 2nd, 3rd, ... NEMX iterations.
!A1=1.001*A10            $Estimate at A1+dA1
!DA1=0.001*A10           $Step used to numerically differentiate
!N3=3
*DCALL(29 TRAN ANAL)     $Calculates temps. at (A1+dA1)
!A1=A10                  $Set A1 back to initial estimate
$
!A2=1.001*A20            $Estimate at A2+dA2
!DA2=0.001*A20
!N3=4
*DCALL(29 TRAN ANAL)     $Calculates temps. at (A2+dA2)
!A2=A20                  $Set A2 back to initial estimate
$
$ **** INVERSE HEAT TRANSFER BEGINS HERE ****
$
$ The parameters are initially estimated using the Gauss Method.  These
$ estimated values are then modified using the Box-Kanemasu Method.
$
*XQT AUS
 INLIB = 2       $Identifies the source library
 OUTLIB = 2      $Identifies the destination library for output datasets
 DEFINE TM = 4 TS AUS 1 1        $Experimental Temperatures (Y)
 DEFINE TO = 2 TS AUS 2 1        $Calc. temps. at initial parameter est. (ETA)
 DEFINE TA1 = 2 TS AUS 3 1       $Temps at A1 + DA1
 DEFINE TA2 = 2 TS AUS 4 1       $Temps at A2 + D2A
$
!A1NV = 1.0/DA1       $The following 4 statements are used in finding
!A1N2 = -1.0/DA1      $the sensitivity coefficients.  (The derivative of
!A2NV = 1.0/DA2       $the temperature with respect to the parameter).
!A2N2 = -1.0/DA2
```

```
$
 D1 = SUM ("A1NV" TA1, "A1N2" TO)  $Delta Ti (TI@A1+DA1-TI@A1)
$ This statement sums the derivatives for the thermal conductivity
$Meaning:  A1NV * TA1 + A1N2 * TO
 D2 = SUM ("A2NV" TA2, "A2N2" TO)  $Delta Ti (TI@A2+DA2-TI@A2)
$This statement sums the derivatives for the volumetric heat capacity
$
 N1 = SUM (TM,-1. TO)          $Gives the matrix (Y - ETA); the Residuals
$                          Build up the X matrix using vectors containing
$                          the derivatives
$
 SENS MATRIX = UNION(D1,D2)    $Joins D1 and D2 into a new dataset
$                          D1 and D2 must have the same block length.
$
 DEFINE S=SENS MATRIX 1 1     $Defines the matrix X, i.e., the Sens. Coeffs.
 ERR = XTY(S,N1)              $Calculates XT (Y - ETA)
 STS = XTY(S,S)               $Calculates XTX
 STSI = RINV(STS)             $Calculates the INVERSE of (XTX)
 DA = RPROD(STSI,ERR)          $Calculates  INV(XTX)*(XT)*(Y - ETA)
$
 NTN = XTY(N1,N1)             $Calcs the Sum of Squares, (Y-ETA)T(Y-ETA)
 TTT = XTY(TM,TM)             $Calculates YTY
!DA1 = DS 1,1,1 (2, DA AUS, 1,1)
$DA1 is the  perturbation for the new estimate (thermal conductivity)
!DA2 = DS 2,1,1 (2, DA AUS, 1,1)
$DA2 is the perturbation for the new estimate (volumetric heat capacity)
!SYS = DS 1,1,1 (2, NTN AUS, 1, 1)    $The sum of squares value
$
$The following (A1 & A2) are the estimates obtained with only the Gauss Method
$
!A1 = DA1+A1      $New parameter estimate for the thermal conductivity
!A2 = DA2+A2      $New parameter estimate for the volumetric heat capacity
$
$ *** END BASIC LOOP-BEGIN BOX-KANEMASU MODIFICATION ***
$
$  This section of the program takes the estimated parameter values found
$  using the Gauss Method and modifies them using the Box-Kanemasu method.
$  This method may allow for convergence of the parameters when the Gauss
$  method does not.  It uses the direction provided by the Gauss method but
$  modifies the step size by introducing a scalar interpolation factor (H).
$  The final parameter values are calculated using the Box-Kanemasu method.
$  For a detailed explanation of this method, see 'Parameter Estimation' by
$  J. Beck and K. Arnold (p. 362-367).
!AG1 = A1             $Fixes the Gauss estimates
!AG2 = A2
!ASS1 = AS1           $Fixes the initial estimate for that iteration
!ASS2 = AS2
!ALPH = 2.0           $Used in finding the parameter estimates
!AA = 1.1             $Used to calculate H
*LABEL 620
```

```
*IF("ALPH" LT 0.01):*JUMP 4001  $Alpha is too small, estms. aren't converging.
!ALPH = ALPH/2.0        $Alpha starts out as 1.0.
!DIF1 = A1 - ASS1       $Diff btw. Gauss & final est. of previous iteration.
!DIF2 = A2 - ASS2
!AS1 = ASS1 + ALPH*DIF1 $Est. using the modified step-size
!AS2 = ASS2 + ALPH*DIF2
!ALPHA
 DATR = RTRAN(DA)       $Transpose (XTX)^(-1)XT(Y - ETA)
 G = RPROD(DATR,ERR)    $Used in calc. H, it's the slope of the Sum of Squares
$                       vs. H.  By defn., it should always be a positive scalar
!GVAL = DS 1,1,1 (2, G AUS, 1, 1)  $Gives the scalar value found for G
!A1 = AS1
!A2 = AS2
!N3 = 5
!N4 = 1
*DCALL(29 TRAN ANAL)
$The above call stmt. calculates the temp. at the estimates obtained using ALPH
*XQT AUS
 INLIB = 2
 OUTLIB = 2
$ EXIT
 DEFINE TOG = 2 TS AUS 5 1    $Temperatures at the Gauss est. + Step Size(alph)
 DEFINE TM = 4 TS AUS 1 1     $Experimental temperatures
 NSS = SUM(TM,-1. TOG)        $New (Y-ETA) using TOG temperatures.
 SYP = XTY(NSS,NSS)           $New sum of squares
!SSYP = DS 1,1,1 (2, SYP AUS, 1, 1)  $Gives the sum of squares value
$
*IF("SSYP" GT "SYS"):*JUMP 620
$
$ The above statement is a check to see if the sum of squares is decreasing
$ If it's not, alpha is decreased by 1/2.  This process continues until the
$ above if statement is no longer true or until alpha is < 0.01, in which
$ case the program is terminated.
$
!CHEK = SYS - ALPH*GVAL*(2.0 - (1/AA)) $This is a check used to determine H
!H = ALPH*AA                  $Initially set the step-size, H equal to alpha*AA.
$
$If SSYP > CHEK, H is given a new value; see following IF stmt.
$
*IF("SSYP" GT "CHEK"):!H = (ALPH*ALPH*GVAL)/(SSYP-SYS+(2.0*ALPH*GVAL))
$
$Calculate the modified parameter values using the obtained step-size (H).
!A1 = ASS1 + H*(AG1 - ASS1)   $Parameter estimates obtained using B-K method.
!A2 = ASS2 + H*(AG2 - ASS2)
$
$Calculate the following ratios, if RAT1 and RAT2 are < CRIT (0.0001), then
$the change in the estimated parameters is insignificant and the iterative
$process is terminated.
$
!RAT1 = (A1 - ASS1)/(ASS1 + EPS)
```

```
!RAT1 = ABS(RAT1)
!RAT2 = (A2 - ASS2)/(ASS2 + EPS)
!RAT2 = ABS(RAT2)
$
!LOOP=LOOP+1    $Next iteration
*XQT AUS
$
$ Updates the table of the sequential estimates
 TABLE,U(TYPE=-2): 4 CONV HIST 1 1
 J="LOOP": "A1","A2","AG1","AG2"
$
$Set this iterations final estimates equal to the initial estimates for
$the next iteration.
!AS1 = A1
!AS2 = A2
$
*IF("RAT1" LE "CRIT"):!IT1 = 1
*IF("RAT2" LE "CRIT"):!IT2 = 1
!ITER = IT1 + IT2          $Determines if the change in both ests. is insignf
*IF("ITER" EQ 2):*JUMP 4001 $If ests. no longer change, stop iterating.
!NEPS=NEPS+1               $Goes to next iteration
*IF("NEPS" GE "NEMX"):*JUMP 4001
$If the parameters don't converge before the max. No. of iters., end process
*XQT DCU
 PRINT 2 TS AUS 2 1
 PRINT 2 N1 AUS 1 1        $Prints out the residuals for each iteration.
 PACK 1
 ERASE 2
*JUMP 4000                 $Est. haven't converged yet, go to next iteration
*LABEL 4001                $To end iteration process
*XQT DCU
 PRINT 4 TS AUS 1
 PRINT 4 CONV HIST 1 1
$ PRINT 1 TRAN TEMP 1 1
$ PRINT 1 TRAN TIME 1 1
$The above libraries are only printed for the final iteration. (4 TS AUS 1
$is the for each iteration; experimental temperatures).
*RETURN
* INVH
$
$*************************************************************************
$
$  Subroutine TRAN - Solves direct problem using TRTB processor
$
$*************************************************************************
$
*(29 TRAN ANAL)TRAN
*DCALL(29 NODE GENE) $Generate the nodes used in the mesh
*DCALL(29 TABL GENE) $Generate tables needed in analysis
*DCALL(29 TABL UPDA) $Update the thermal properties (estimates)
```

```
*DCALL(29 ELEM DEFI) $Defines the elements (Cond.,Conv., Heat Source, etc
$
*XQT TGEO            $Element geometry processor; it computes local coordinates
$                  and performs element geometry checks.  The user MUST
$                  execute TGEO after each execution of ELD.
*XQT TRTB            $Transient analysis processor - Implicit with C.N. code
 RESET PTV=0.00001 T1="TIMI" T2="TIMF" DT= "DELT" PRINT=0 MXNDT=100000
 TEMP="TEMI"
 TSAVE="DELT"
$
*XQT AUS
!NCOU=NTS-1
!NBLO=1
*DCALL (29 BILD TS)
$
*XQT DCU             $Processor that performs an array of database utility
$                  functions (see Manual, Section 12-1)
 DISABLE 1 EKS B
*RETURN
*TRAN
$
$*************************************************************************
$
$  Main program
$
$*************************************************************************
$
*DCALL (29 VARB DEFI)
*DCALL (29 INV HEAT)
*XQT EXIT
```

APPENDIX G

Uncertainty Due to Experimental Measurements

The uncertainty in the estimated thermal properties due to experimental measurement errors can be found from

$$\delta R = \left[\sum_{i=1}^{N} \left(\frac{\partial R}{\partial X_i} \delta X_i \right)^2 \right]^{1/2} \tag{G.1}$$

where δR is the uncertainty in the thermal property being analyzed, δX_i is the uncertainty in the experimental variable, and the partial derivative of R with respect to X_i is the sensitivity coefficient with respect to the measurement, X_i. In the experiments conducted in this investigation, error could be associated with the temperature (X_T), voltage (X_V), or current (X_I) measurements. Therefore, the uncertainty in the effective thermal conductivity perpendicular to the fibers ($k_{x\text{-}eff}$) would be given by

$$\delta k_{x\text{-}eff} = \left[\left(\frac{\partial k_{x\text{-}eff}}{\partial T} \delta X_T \right)^2 + \left(\frac{\partial k_{x\text{-}eff}}{\partial V} \delta X_V \right)^2 + \left(\frac{\partial k_{x\text{-}eff}}{\partial I} \delta X_I \right)^2 \right]^{1/2} \tag{G.2}$$

Using this equation, a $\delta k_{x\text{-}eff}$ of ±0.035 W/m°C was calculated. In Chapter 5, the mean value for $k_{x\text{-}eff}$ was estimated as 0.518 ± 0.028 W/m°C. This uncertainty of ±0.028 W/m°C, associated with the 95% confidence region, is approximately 20% smaller than $\delta k_{x\text{-}eff}$, found from the measurement errors. This result implies that the actual error associated with $k_{x\text{-}eff}$ may be larger than estimated.